UNIVERSITÄT BERN

Graduate School for Health Sciences

Effects of exposure to colored light on cerebral and systemic physiology in humans

PhD Thesis submitted by

Hamoon Zohdi
from **Iran**

for the degree of PhD in Health Sciences (Neurosciences)

Thesis advisor
Prof. Dr. med. Ursula Wolf
Institute of Complementary and Integrative Medicine, Faculty of Medicine, University of Bern

Thesis co-advisor
Dr. sc. nat. Felix Scholkmann
Institute of Complementary and Integrative Medicine, Faculty of Medicine, University of Bern

Thesis co-referee
Prof. Dr. Tobias Nef
ARTORG Center for Biomedical Engineering Research, Faculty of Medicine, University of Bern

Original document saved on the web server of the University Library of Bern

This work is licensed under a
Creative Commons Attribution-Non-Commercial-No-Derivative works 2.5 Switzerland License.
To see the license go to http://creativecommons.org/licenses/by-nc-nd/2.5/ch/
or write to Creative Commons, 171 Second Street, Suite 300, San Francisco, California 94105, USA.

source: https://doi.org/10.48549/10 | downloaded: 26.4.2024

Copyright Notice

This document is licensed under the Creative Commons Attribution-Non-Commercial-No derivative works 2.5 Switzerland. http://creativecommons.org/licenses/by-nc-nd/2.5/ch/

You are free:

to copy, distribute, display, and perform the work

Under the following conditions:

Attribution. You must give the original author credit.

Non-Commercial. You may not use this work for commercial purposes.

No derivative works. You may not alter, transform, or build upon this work.

For any reuse or distribution, you must take clear to others the license terms of this work.

Any of these conditions can be waived if you get permission from the copyright holder.

Nothing in this license impairs or restricts the author's moral rights according to Swiss law.

The detailed license agreement can be found at:
http://creativecommons.org/licenses/by-nc-nd/2.5/ch/legalcode.de

Figure 2 and 3 in chapter 1 reprinted from NeuroImage, Volume 85, Part 1, Scholkmann, F., Kleiser, S., Metz, A.J., Zimmermann, R., Pavia, J.M., Wolf, U. and Wolf, M. "A review on continuous wave functional near-infrared spectroscopy and imaging instrumentation and methodology", 6-27, Copyright (2014), with permission from Elsevier.

Accepted by the Faculty of Medicine and the Faculty of Human Sciences of the University of Bern

Bern, Dean of the Faculty of Medicine

Bern, Dean of the Faculty of Human Sciences

Dedication

This dissertation is dedicated

To my brilliant and supportive wife "Fatemeh"
for her constant love and encouragements

To my loving parents "Shahin & Morteza"
for their care and support

Abstract

Humans in industrialized societies have become independent of the natural day and night cycle due to the invention and use of artificial light. Colored light is an element of everyday life, which affects various human functions. The main aim of this PhD thesis is to comprehensively investigate the effects of exposure to colored light on cerebral and human physiology. To achieve this goal, 201 healthy right-handed adults were recruited for 20 different colored light conditions. By using systemic physiology augmented functional near-infrared spectroscopy (SPA-fNIRS) neuroimaging, each subject was measured 2-4 times on different days resulting in 676 single measurements. The SPA-fNIRS approach combines the measurement of brain activity and systemic physiological changes. fNIRS is a non-invasive neuroimaging technique employed to measure changes in cerebral hemodynamics and oxygenation. There is an interaction between these and changes in systemic physiology: consequently, the SPA-fNIRS generally enables us to identify and understand these interactions. We simultaneously assessed the effects of colored light exposure (CLE) in the visual cortex (VC), prefrontal cortex (PFC) and systemic physiology. Such a comprehensive study has not been carried out yet, and an integrative view of how the color of light affects the brain and the systemic physiology is lacking. In general, CLE has relatively long-lasting effects on cerebral and systemic physiology in humans, and yellow light leads to a higher brain activation in the PFC than the other colored lights. Yellow CLE is associated with more active and positive emotions, including happiness, joy, hope and cheerfulness. We also show that long-term colored light exposures induce wavelength-dependent modulations of brain responses in the VC. Violet and blue lights elicit higher changes in cerebral parameters compared to the other colored lights during the CLE and recovery phase. Our results show that CLE affects individual humans differently. In particular, blue light leads to eight different hemodynamic response patterns, while the typical hemodynamic response pattern (increase in oxygenated ([O_2Hb]) and decrease in deoxygenated ([HHb]) hemoglobin) is still observed and valid at the group-level analysis. The SPA-fNIRS approach is able to show that systemic and cerebral physiology interact.

Experimental findings in most parts of this research display that inter-subject variability of hemodynamic responses is partially explained by systemic physiological changes. The finding of this research that blue light has an activating effect in the VC should be taken into consideration when assessing the impact of modern light sources such as screens and light-emitting diodes (LEDs) on the human body. Our findings that yellow light leads to higher PFC activation be tested as a potentially beneficial tool in chromotherapy, i.e., a complementary medicine method, to balance “energy” lacking in physical, emotional, and mental levels. Although yellow light, i.e., CLE in general term, influences humans in several positive ways, it should be noted that each individual reacts differently to the CLE, implying that colored light therapy has to be also adjusted to each individual. Therefore, further research should clarify which color in CLE benefits whom. In a civilization that is rapidly exposed to new and increasing lighting, the findings of this research are relevant for the scientific community, medical professionals, and society.

Acknowledgements

As a student at the University of Bern, I had a great opportunity to work at the Institute of Complementary and Integrative Medicine (IKIM), a place where I was introduced to novel concepts in neuroscience and physiology. The contributions of many people have helped me to make my time at IKIM a rewarding experience.

First and foremost, I would like to express my sincere gratitude and appreciation to my advisor, Prof. Dr. Ursula Wolf, for her heartfelt support, encouragement, and patient guidance. Without her continued support, I would not have been able to complete the current work. I am particularly grateful to her for always providing me the opportunities to attend national and international conferences and to meet scientists from the global research community. I owe special thanks to my co-advisor, Dr. Felix Scholkmann, for his great support, continuous discussion and helpful inputs during all stages of my PhD. I am deeply thankful to my co-referee, Prof. Dr. Tobias Nef, for his constructive comments and conversations that were always helpful and inspiring.

I would like to thank all my colleagues and friends at IKIM for their friendship, help, support, and numerous inputs and comments from which I greatly benefited. Special thanks go to our students for their contribution to the measurements and our subjects for participating in this study.

Finally, I would like to express my sincere gratitude to my family. I owe all of my accomplishments to my loving parents, Shahin and Morteza; without their care and confidence, I would not be where I am today. Most of all, I am deeply grateful to my lovely wife, Fatemeh, who has been with me all these years and has made them the best years of my life. Her support, encouragement, and love have always given me the strength to attain my goals.

Table of contents

Abstract…… 6

Acknowledgements 8

List of Abbreviations 11

Chapter 1 Introduction 13

1.1. Colored light and human physiology 13

1.2. Functional near-infrared spectroscopy (fNIRS) 15

1.3. Systemic physiology augmented functional near-infrared spectroscopy (SPA-fNIRS) 19

1.4. Objectives of the thesis 21

1.5. Hypotheses 22

1.6. Summary of chapters 23

Chapter 2 Pulse-respiration quotient (PRQ) as an indicator of human activity and human health state 24

Peer reviewed publication 1 25

The resting-state pulse-respiration quotient of humans: lognormally distributed and centred around a value of four

Chapter 3 SPA-fNIRS: A promising tool to investigate cerebral and physiological changes 32

Peer reviewed publication 2 33

Right-left asymmetry of prefrontal cerebral oxygenation: does it depend on systemic physiological activity, absolute tissue oxygenation or hemoglobin concentration?

Peer reviewed publication 3 42

Frontal cerebral oxygenation asymmetry: inter-subject variability and dependence on systemic physiology, season, and time of day

Peer reviewed publication 4 62

Impact of changes in systemic physiology on fNIRS/NIRS signals: analysis based on oblique subspace projections decomposition

Chapter 4 Individual changes in optical properties of cerebral tissue during and after colored light exposure 70

Peer reviewed publication 5 71

Absolute values of optical properties (μ_a , μ_s', μ_{eff} and DPF) of human head tissue: dependence on head region and individual

Peer reviewed publication 6 78

Long-term changes in optical properties (μ_a , μ_s', μ_{eff} and DPF) of human head tissue during functional neuroimaging experiments

Chapter 5 Yellow and short-wavelength light lead to higher brain activation in the PFC and VC, respectively 86

Peer reviewed publication 7 95

Long-term blue light exposure changes frontal and occipital cerebral hemodynamics: not all subjects react the same

Chapter 6 CLE-VFT: Differences in hemodynamic response patterns for the blue and red light exposure 102

Peer reviewed publication 8 103

Color-dependent changes in humans during a verbal fluency task under colored light exposure assessed by SPA-fNIRS

Peer reviewed publication 9 117

Individual differences in hemodynamic responses measured on the head due to a long-term stimulation involving colored light exposure and a cognitive task: a SPA-fNIRS study

Chapter 7 Discussion 134

Chapter 8 Conclusion 138

Chapter 9 Outlook 140

References.. 142

List of Abbreviations

ANS	Autonomic nervous system
AUC	Area under the curve
CBF	Cerebral blood flow
CLE	Colored light exposure
CW-NIRS	Continuous wave domain near-infrared spectroscopy
EEG	Electroencephalography
FCOA	Frontal cerebral oxygenation asymmetry
FD-NIRS	Frequency domain near-infrared spectroscopy
fMRI	Functional magnetic resonance imaging
fNIRS	Functional near-infrared spectroscopy
HF	High frequency
HHB	Deoxygenated hemoglobin
HR	Heart rate
HRV	Heart rate variability
ipRGCs	Intrinsically photosensitive retinal ganglion cells
LED	Light emitting diodes
LF	Low frequency
MAP	Mean arterial pressure
MEG	Magnetoencephalography
NVC	Neurovascular coupling

μ_a	Absorption coefficient
μ_s'	Reduced scattering coefficient
O_2Hb	Oxygenated hemoglobin
PET	Positron emission tomography
$P_{ET}CO_2$	Partial pressure End-tidal carbon dioxide
PFC	Prefrontal cortex
PP	Pulse pressure
PRQ	Pulse-respiration quotient
RR	Respiration rate
SCL	Skin conductance level
SPA-fNIRS	Systemic physiology augmented functional near-infrared spectroscopy
SpO_2	Arterial oxygen saturation
StO_2	Tissue oxygen saturation
TD-NIRS	Time domain near-infrared spectroscopy
tHb	Total hemoglobin
VC	Visual cortex
VFT	Verbal fluency task

Chapter 1 Introduction

1.1. Colored light and human physiology

Color and colored light have always attracted human attention and played vital roles in daily human life. How colored light is formed and how human color vision works have been topics widely discussed throughout various fields, from physics to medicine and from art to psychology. Colored light exposure is an experience of everyday life. It is used in public areas to gain customers' attention or within private settings as functional or decorative lighting. Specifically, in our modern society, we are increasingly exposed to various colored light sources, from advertisements to computers and from energy-saving light bulbs to smartphones. Therefore, the effects of colored light on human physiology are of rising interest in both the research community and society. Colored light may influence what we appear to see, our emotions and moods, and even performance, but do we really understand colored light and its effects on human physiology? While there are a number of known interactions between colored light and the human body, still many other physiological effects of colored light are unexplored.

In order to understand the impact of colored light on human physiology, it is essential to differentiate between visual and non-visual effects. Visual effects deal with the incident light's processing by photoreceptor cells in the retina transmitting the signals to bipolar cells, then onto ganglion cells, and ultimately by the optic nerve to the visual cortex (VC) [1]. Non-visual effects, mediated by the non-image forming system, have increasingly generated interest during the last decades and started with the discovery of the light-sensitive protein "melanopsin" [2,3]. Non-visual effects are based on different photoreceptors, mainly the intrinsically photosensitive retinal ganglion cells (ipRGCs), which contain melanopsin. These photoreceptors transmit signals to the hypothalamus, epithalamus, limbic system, and the midbrain, i.e., areas involved in regulating the autonomic nervous system (ANS) and oscillatory physiological processes [1]. The high sensitivity of this non-visual pathway to blue light recently led to an increasing number of studies investigating the potential disease-promoting effect

of blue light exposure on human physiology [4,5]. This research is of particular significance since blue light is increasingly prevalent in our environment due to energy-saving LEDs and screens.

Light striking on the ipRGCs has been shown to modulate brain responses during attention and cognitive tasks [6–8]. This knowledge has been transferred to several applications, e.g., office lighting [9] or clinical interventions such as the treatment of seasonal affective disorder [10,11]. In particular, white and blue light were used for the treatment of seasonal affective disorder and depression [12–14]. Blue light especially suppresses melatonin secretion, a hormone important for initiating sleep [8,15–19], while white light interacts with the plasma cortisol, a hormone associated with stress [20]. In close relation to the effect of blue light on melatonin, blue light altered the core body temperature [21], and the heart rate (HR) [22–24]. However, these variables were only directly affected by light in the late evening before sleep, when the melatonin concentration in the blood is rising. During the day, only a few studies measured the interaction of light with human physiology, and most studies did not show the effects of colored light on heart rate [25–29] or body temperature [30].

Indeed effects of many physiological parameters were reported in the literature. Colored light influenced heart rate variability (HRV) within a short period of time and affected the ANS depending on the color as well as the emotional status of subjects [29,31–34]. It has also been shown in humans that during red light exposure, cardiorespiratory coordination was confined to 4:1 [29]. HR was reported to decrease [32,34] and to increase [21] under blue light exposure. Under red light exposure HR decreased [34,35], increased [29] or remained unchanged [32]. Under green light exposure, HR decreased and did not change under white light exposure [34]. No significant color effect was found for the respiration rate (RR) [25]. Mean arterial pressure (MAP) increased under blue light. Skin conductance response was increased under red and decreased under blue, orange, and green light [25,34]. Although some studies show specific effects, these studies do not point towards a clear and reproducible effect of colored light on the respective variable.

Although each light stimulus evokes both visual and non-visual effects, also involving systemic physiology, basic research on the visual and non-visual effects on the human brain and systemic physiological evoked by colored light exposure are surprisingly scarce. What is lacking is an integrative view of how the color of a light stimulus affects the brain and the systemic physiology.

The role of the VC in visual color perception and processing is well investigated [36–38]. For example, similar responses in the VC for different visual color (red, green, yellow, blue) stimuli were found [36]. Thus, we expect color effects are more likely to evolve from the non-visual pathway. Research on the brain regions involved in the processing of ipRGC-mediated non-visual effects is increasing [39,40]. One brain region of particular interest is the prefrontal cortex (PFC). The PFC is not only functionally connected to the VC, enabling higher-order cognitive processing of visual/color information [41], but also to the suprachiasmatic nucleus in the hypothalamus receiving information from the ipRGCs [1]. These facts indicate that investigating the role of the PFC in the processing of colored light stimuli is warranted.

1.2. Functional near-infrared spectroscopy (fNIRS)

The activity of the VC and PFC can easily be investigated by functional near-infrared spectroscopy (fNIRS), which is an optical, non-invasive, easy-to-use, and portable neuroimaging technique that enables imaging of cerebral hemodynamics and oxygenation from cortical layers in the human brain [42,43]. The fNIRS technique relies on the light in the near-infrared spectral range (650-950 nm) emitted from either laser diodes or LEDs [44]. Near-infrared light relatively deeply penetrates into biological tissue following a characteristic Gaussian profile. The probability function of the traveling light detected by a detector has a typical banana-shaped path (Figure 1) [44,45]. The most important chromophore absorbing light at this spectral window is hemoglobin, which can be found in two forms, i.e., oxygenated (O_2Hb) and deoxygenated (HHb) hemoglobin. O_2Hb absorption is mainly above 800 nm, while HHb absorption is mainly below 800 nm [46,47]. Human tissues are relatively transparent to light in the optical window; hence, when near-infrared light is shone onto tissue, the light penetrates the

tissue and undergoes absorption and scattering, which both contribute to light attenuation [46,48–50]. By measuring the attenuation and time of flight (or phase) of the light re-emerging from the tissue for at least two appropriate wavelengths, concentrations of O_2Hb and HHb as well as total hemoglobin (tHb = O_2Hb+HHb) and tissue oxygen saturation (StO_2 = ([O_2Hb]/[tHb]) × 100) can be determined.

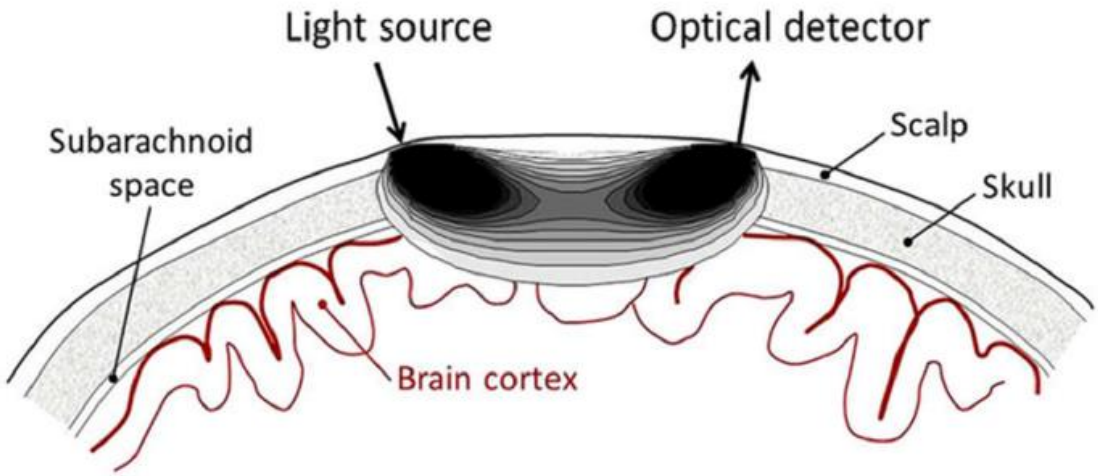

Figure. 1 Schematic illustration of the optical region of sensitivity (banana-shaped region) in the human brain. The illumination (light source) and collection (optical detector) points are located on the scalp with a source-detector distance of 3 cm. The sensitivity of the optical signal to the tissue is not spatially uniform and decreases with depth. But, there are methods to increase the sensitivity to the brain, e.g., by a multidistance approach. Figure reprinted from [51] with permission from the journal.

Brain activity leads to an increase in oxygen consumption, causing a decrease in [O_2Hb] and an increase in [HHb]. This triggers regional changes, inducing an increased cerebral blood flow (CBF), which is characteristic of neurovascular coupling (NVC). Since the regional supply of oxygen increases more than its consumption, i.e., an over-compensation, an increase in [O_2Hb] and a decrease in [HHb] is observed. This is measured by fNIRS (Figure 2) [44,46,52].

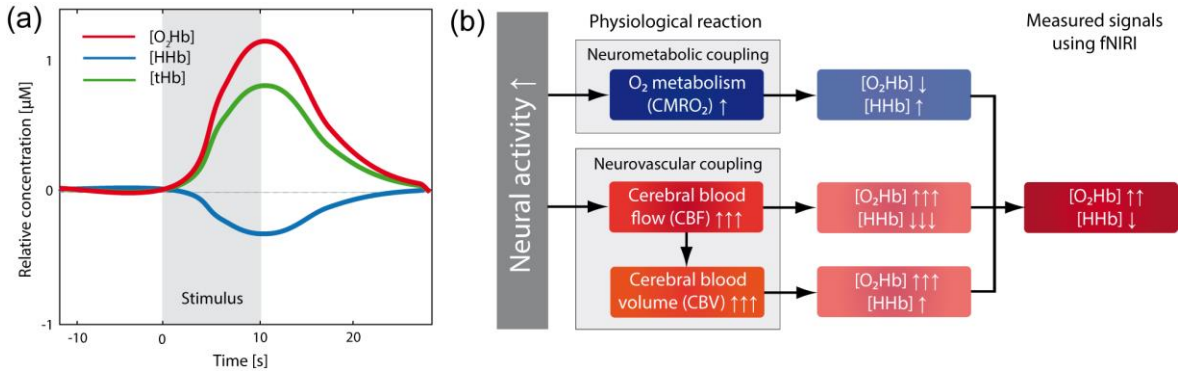

Figure. 2 (a) Typical hemodynamic response pattern and (b) the effects of cerebral hemodynamics and oxygenation changes on the fNIRS signals caused by an increase in neural activity. Figure reprinted from [44] with permission from Elsevier (see copyright information on page 2).

Non-invasive neuroimaging techniques measure either the activation related to the electrical activity (e.g., electroencephalography (EEG), Magnetoencephalography (MEG)) or to the hemodynamic response (e.g., positron emission tomography (PET), functional magnetic resonance imaging (fMRI), and fNIRS of the brain [53]. Compared to the other methods, fNIRS is relatively inexpensive, simple to use, portable, and enables continuous and long-term measurements (monitoring). This method is also more tolerant to movement artifacts, which make it particularly suitable for populations and procedures for which other techniques are limited, including the applications in small infants and children as well as procedures involving mobility and interactivity even outside of the clinical and research setting [49,50]. However, disadvantages of fNIRS are the efforts needed to fix optodes in hairy regions, which is similar to EEG, and the limited penetration depth; yet the cortex can well be reached [52]. Moreover, the possibility of mistakably measuring fNIRS signals contaminated by systemic changes can be considered as another significant aspect of fNIRS [54] (but also affect fMRI). Table 1 shows in detail the comparison of fNIRS with other neuroimaging techniques.

Table. 1 Comparison of different neuroimaging techniques

	fNIRS	**fMRI**	**EEG**	**MEG**	**PET**
Signal	O_2Hb & HHb	HHb (BOLD)	Electromagnetic	Electromagnetic	CBF
Hemodynamic	Yes	Yes	No	No	Yes
Neural activity	No	No	Yes	Yes	No
Penetration depth	Cortex	Whole head	Cortex	Deep structures	Whole head
Temporal resolution	>millisecond	second	milliseconds	milliseconds	minute
Spatial resolution	10-20 mm	~ 5 mm	50-90 mm	50-90 mm	5 mm
Robustness to motion	Moderate	Limited	Limited	Limited	Limited
Populations	All	Limited	All	All	Limited
Portability	Yes	No	Yes	No	No
Sounds	Silent	Noisy	Silent	Silent	Silent
Price	Low	High	Low	High	High

From a methodological point of view, three main modes of NIRS-based optical tissue spectroscopy techniques, including continuous wave (CW), frequency domain (FD), and time domain (TD) have been developed. The principle of these modes is summarized in Figure 3. In brief, CW-NIRS is based on light intensity measurement and relies on a few assumptions (e.g., constant differential pathlength factor and light scattering). Since there are two unknowns (light absorption and light scattering) and only one measurement, this type of NIRS is able to determine only changes in [O_2Hb] and [HHb], but not absolute values. On the other hand, FD-NIRS and TD-NIRS measure not only the light intensity but also the time of flight of photons through tissue, which makes them suitable devices to quantify absolute values of [O_2Hb] and [HHb] [44,55–57]. This enables also to calculate the total hemoglobin concentration ([tHb] = [O_2Hb] + [HHb]), a measure reflection the blood volume and blood flow, and the tissue oxygen saturation (StO_2=[O_2Hb]/[tHb]), a measure of the oxygenation. In this project, the FD-NIRS system (Imagent, ISS Inc., Champaign, IL, USA) with a multi-distance approach was used. A multi-distance approach enables to minimize the influence of superficial layers, e.g., skin. FD-NIRS enables to measure the absolute optical properties, namely, the absorption coefficient (μ_a) and the reduced scattering coefficient (μ_s'), and consequently the absolute concentrations of O_2Hb and HHb in

human head tissue [58,59]. The determination of optical properties are of great importance in practical applications. It also provides valuable information about the status and composition of the tissue. Moreover, knowledge of optical properties is essential for the accuracy of the fNIRS procedures [60,61]. The FD-NIRS system quantifies the optical properties by measuring the amplitude and phase of the near-infrared light passing through the tissue and fitting the transmitted phase and amplitude in accordance with the diffusion approximation [58,62].

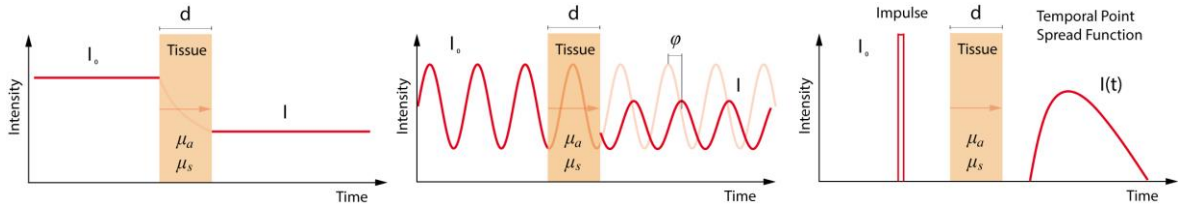

Figure. 3 Schematic of the three NIRS modes. CW-NIRS (left): a continuous light is shone onto the tissue and the intensity of the re-emitted light is measured. FD-NIRS (middle): a modulated continuous light is shone onto the tissue and the intensity of the re-emitted light, as well as the phase shift, are measured. TD-NIRS (right): an ultra-short light impulse is shone onto the tissue and the arrival times of the photons that emerge from the tissue are measured. Figure reprinted from [44] with permission from Elsevier (see copyright information on page 2).

1.3. Systemic physiology augmented functional near-infrared spectroscopy (SPA-fNIRS)

Our group pioneered the systemic physiology augmented functional near-infrared spectroscopy (SPA-fNIRS) approach [1,63], which enables to measure brain activity (with fNIRS) along with systemic physiological changes. This approach is based on measurements with a multichannel frequency-domain near-infrared spectroscopy system and simultaneous measurements of systemic physiological parameters. These parameters include, for example, the partial pressure end-tidal carbon dioxide ($P_{ET}CO_2$), HR, RR, pulse-respiration quotient (PRQ), MAP, pulse pressure (PP), arterial oxygen saturation (SpO_2), skin conductance level (SCL), high-frequency (HF; 0.15–0.4 Hz), and low-frequency (LF; 0.04–0.15 Hz) component of the HRV. These systemic physiological variables

are measured by three devices, including SOMNOtouch NIBP (SOMNOmedics GmbH, Randersacker, Germany), NONIN LifeSense (NONIN Medical, Plymouth, MN, USA), and an electrodermal activity measurement system (Verim Mind-Reflection GSR, Poland). Figure 4 displays the positions of the devices and sensors used in the SPA-fNIRS approach on the subject.

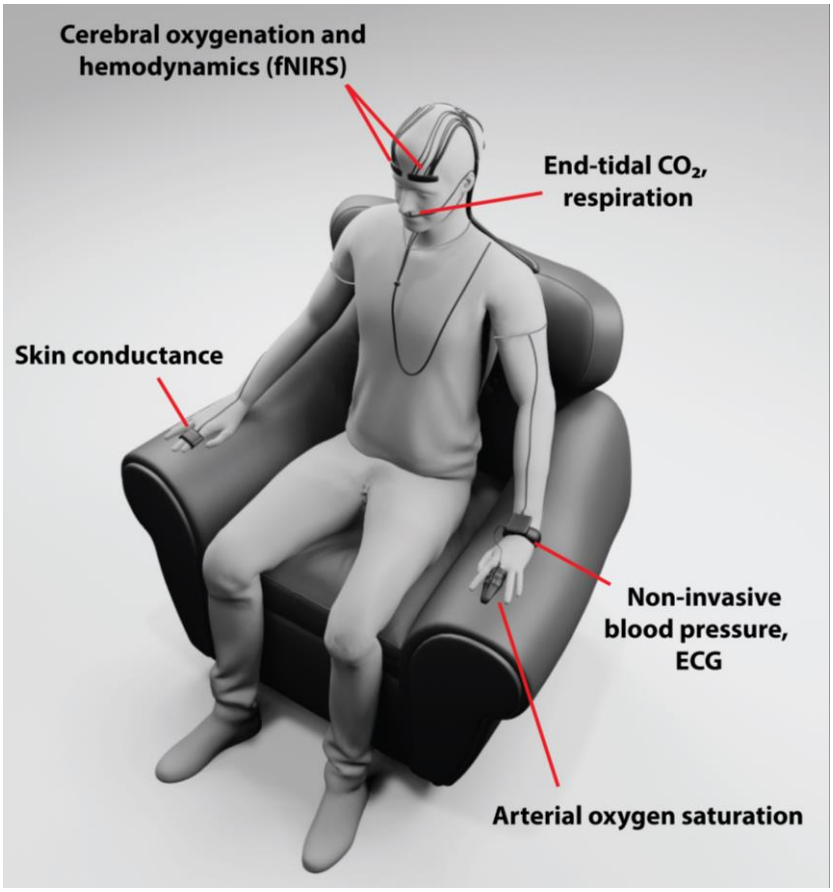

Figure. 4 Schematic illustration of the placement of the sensors on the subject. The SPA-fNIRS approach consists of a combination of fNIRS system (Imagent, ISS Inc., Champaign, IL, USA) with devices to measure systemic physiology: The SOMNOtouch NIBP measured MAP, PP, HR, SpO_2, and HRV. Verim Mind-Reflection GSR was employed to determine the SCL. $P_{ET}CO_2$ and RR were non-invasively measured by NONIN LifeSense [64]. *Picture credit: Daniel Guthruf*

This approach is ideally suited to enable a better understanding and a reliable interpretation of the changes in the fNIRS signals. In our previous studies, we

showed that changes in $P_{ET}CO_2$ have strong effects on cerebral hemodynamics [62,65]. We particularly demonstrated that changes in breathing, i.e., hyperventilation during speech tasks caused hypocapnia resulting in decreased StO_2 [62]. It has also been shown that MAP and SpO_2 correlate with the changes in the fNIRS signals at the PFC and the motor cortex [64,66]. Caldwell et al. designed a model providing valuable information regarding the possible confounding factors of fNIRS measurements [67]. They showed that depending on the degree of the changes in $P_{ET}CO_2$ and MAP, it is possible to induce misleading hemodynamic responses [67]. Systemic physiological changes may mask (false negative) or mimic (false positive) neuronally induced hemodynamic responses [54]. Therefore, using the SPA-fNIRS approach enables to identify, remove and understand the effects of systemic physiological changes on fNIRS signals.

1.4. Objectives of the thesis

The main aim of this PhD thesis was to comprehensively investigate effects of colored light on cerebral and systemic physiology in healthy adult humans and to implement an integrative approach: the SPA-fNIRS. Therefore, besides fNIRS parameters, several physiological parameters were measured concurrently. To reliably extract the respective brain and systemic physiological activity, expanding and enhancing biomedical signal analysis methods is essential. In the measurements, subjects were exposed to the light of different colors and intensities.

Colors and colored lights, in addition to space, texture and interior form, are major design elements of the physical learning environment. It has been demonstrated that colored lights (or colors) have significant effects on students, influencing their emotions, mood, performance and systemic physiology [35,68–70]. In addition, students are nowadays exposed to a considerable amount of artificial light when they have to do their tasks using smartphones and tablets, known as modern light-emitting devices. Selecting an optimal desktop background for such screens may enhance cognitive performance in contexts of education.

Picking specific colored light for educational purposes may also affect systemic physiology in positive or negative ways. Therefore, the second main objective of this PhD is to investigate in detail a mixed-effect of colored light exposure (CLE) and a cognitive task (verbal fluency task; VFT) on cerebral hemodynamics, oxygenation, and systemic physiology.

The results of this research facilitate a better understanding of the CLE effects on the underlying neuroscientific mechanisms in the brain and body, which in turn will pave the way for safe and advantageous applications of colored light in daily life and therapeutic settings. Moreover, in a society that is rapidly exposed to new and increasing lighting, the findings of this PhD project are relevant and beneficial for the scientific community, medical professionals, and society.

1.5. Hypotheses

The following hypotheses are explored in this PhD thesis.

Hypothesis 1: Colored light evokes an activation of the VC, which is independent of the color.

Hypothesis 2: Colored light evokes an activation of the PFC, which is dependent on the color.

Hypothesis 3: Colored light has intensity-dependent effects.

Hypothesis 4: Colored light affects individual humans differently.

Hypothesis 5: Colored light has relatively long-lasting effects.

Hypothesis 6: The interaction of cerebral and systemic physiology is distinguished by the SPA-fNIRS approach.

1.6. Summary of chapters

This thesis consists of nine chapters in which nine peer-reviewed publications are presented. It starts with an introduction and explanation of the objectives of this PhD thesis in Chapter 1. A review of the pulse respiration quotient (PRQ) is presented in Chapter 2. Chapter 3 shows the SPA-fNIRS approach, and the impact of changes in systemic physiology on fNIRS signals is revealed. In Chapter 4, optical properties and the effect of CLE on changes in optical properties is explained. Effects of six CLE and two-colored light intensities on cerebral hemodynamics, oxygenation, and systemic physiology are reported in Chapter 5. Long-term blue light exposure effects on the PFC and VC are also studied in this chapter at both group and subgroup analysis. Chapter 6 includes a detailed investigation of the effects of long-term stimulation involving CLE and VFT, on cerebral and human physiology. The findings of this PhD thesis are generally discussed in Chapter 7. Finally, conclusions are drawn (Chapter 8), and recommendations for future works are given (Chapter 9).

Chapter 2

Pulse-respiration quotient (PRQ) as an indicator of human activity and human health state

This chapter aims to give a succinct introduction to acquaint the readers with one of the systemic physiological parameters, *pulse-respiration quotient* (PRQ), investigated in this PhD thesis. One specific type of cardiorespiratory coupling is the interrelation between the HR and the RR. This relationship can be analyzed by dividing the HR by the RR, resulting in the PRQ (= HR/RR). The PRQ is a useful parameter that reflects basic and emergent properties of the complex interaction between the cardiac and respiratory systems, attaining the overall state of human physiology [71]. This parameter represents the ANS state and can be used as a measure of cardiorespiratory coordination [72]. It is known that during the day, various PRQs in the range of 2 to 15 can be observed, while during sleep, the PRQ has a peak at around 4, i.e., corresponding to 4:1 HR and RR ratio values, in healthy subjects [73]. Our group recently reviewed a detailed description and medical characteristics of the PRQ regarding applications for disease classification and monitoring [71]. In brief, they showed that PRQ, which is time- and sex-dependent, changes during human development, physical activity, and body posture with specific patterns during sleep [71].

Publication 1 focuses on understanding the reference values of the PRQ during resting-state at day. The PRQ of 134 healthy subjects were measured 2 to 4 times on different days resulting in 482 single PRQ values, which is, to the best of the author's knowledge, the most extensive PRQ study conducted in human adults so far. This publication shows that the PRQ follows a lognormal distribution (is not normally distributed). Moreover, experimental findings in Publication 1 confirm that the PRQ during resting-state at day on a group-level has a high probability of having a value of around 4, i.e., where the heart beats four times during one breathing cycle. A state of PRQ ~ 4 relates to an ideal functioning of the cardiovascular system, a balanced state of the ANS, and the human's healthy physiological state.

Peer reviewed publication 1

The resting-state pulse-respiration quotient of humans: lognormally distributed and centred around a value of four

Felix Scholkmann, **Hamoon Zohdi**, Ursula Wolf

Physiological Research (2019) 68, 1027-1032.

DOI: 10.33549/physiolres.934232

URL: https://www.biomed.cas.cz/physiolres/pdf/2019/68_1027.pdf

Own contributions:

- Contribute to carrying out measurements
- Signal processing
- Data analysis
- Review and editing of the manuscript

Physiol. Res. 68: 1027-1032, 2019 *https://doi.org/10.33549/physiolres.934232*

SHORT COMMUNICATION

The Resting-State Pulse-Respiration Quotient of Humans: Lognormally Distributed and Centered Around a Value of Four

F. SCHOLKMANN[1,2], H. ZOHDI[1], U. WOLF[1]

[1]University of Bern, Institute of Complementary and Integrative Medicine, Bern, Switzerland, [2]Biomedical Optics Research Laboratory, Department of Neonatology, University Hospital Zurich, University of Zurich, Zurich, Switzerland

Received June 13, 2019
Accepted July 31, 2019
Epub Ahead of Print October 25, 2019

Summary

The pulse-respiration quotient (heart rate divided by the respiration rate, PRQ = HR/RR) is a parameter capturing the complex state of cardiorespiratory interactions. We analysed 482 single PRQ values obtained from measurement on 134 healthy adult subjects (49 men, 85 women, age: 24.7 ± 3.4, range: 20–46 years) during rest. We found that the distribution of PRQ values (i) has a global maximum at around a value of 4 (median: 4.19) and (ii) follows a lognormal distribution function. A multimodality of the distribution, associated with several PRQ attractor states was not detected by our group-level based analysis. In summary, our analysis shows that in healthy humans the resting-state PRQ is around 4 and lognormally distributed. This finding supports claims about the special role of the 4 to 1 cardiorespiratory coupling in particular and the PRQ in general for physiological and medical views and applications. To the best of our knowledge, our study is the largest conducted so far in healthy adult humans about reference values of the PRQ during a resting-state at day.

Key words

Pulse-respiration quotient • PRQ • Cardiorespiratory interaction • Cardiorespiratory coupling

Corresponding author

F. Scholkmann, University of Bern, Institute of Complementary and Integrative Medicine, Fabrikstrasse 8, 3012 Bern, Switzerland. E-mail: Felix.Scholkmann@ikim.unibe.ch

Two intrinsic oscillatory processes accompany each moment of a living human being: cardiac activity and respiration. Both oscillations are locally triggered but regulated in a complex way as best represented by a non-linear dynamical system based on two weakly coupled oscillators that are coupled by several structural and functional types of cardiorespiratory interactions, leading to emergent cardiorespiratory coupling phenomena (Benarroch 2018, Dick *et al*. 2014, Elstad *et al*. 2018, Krause *et al*. 2017, Lotrič and Stefanovska 2000, Moser *et al*. 2008, Schulz *et al*. 2013, Valenza *et al*. 2016). Such a cardiorespiratory coupling phenomenon is that the heart rate (HR) and the respiration rate (RR) have a specific frequency relationship. As recently reviewed by our group (Scholkmann and Wolf 2019), this relationship is given by dividing the heart rate (HR) by the respiration rate (RR), resulting in the *pulse-respiration quotient* (PRQ = HR/RR). The PRQ in humans is of physiological relevance and depends mainly on the age, sex and individual physiological constitution of the subject, as well as on the time-of measurement (linked to the chronobiological state), physical activity, psychophysical and cognitive activity, and body posture (Scholkmann and Wolf 2019).

Two special features of the PRQ are that (i) in the resting-state of a healthy human (preferably during night, or during resting-periods at day), the PRQ tends to have a value of 4, i.e. a state where the heart beats four times during one breathing cycle (Bettermann *et al*. 2000, Gutenbrunner and Hildebrandt 1998, Steiner 1989), and

© 2019 Institute of Physiology of the Czech Academy of Sciences, Prague, Czech Republic

that (ii) the PRQ is not normally distributed but seems to follow a lognormal distribution (Scholkmann and Wolf 2019). Furthermore, there are reports indicating that the PRQ tends to favour integer values (a quantization) due to an in-phase cardiorespiratory coupling effect (termed cardiorespiratory coordination) with preferred values of the harmonic ratios n/m with $n = 3–6$ and $m = 1$ while n and m represent the numerator and denominator of the equation PRQ = HR/RR = n/m (Bettermann *et al*. 2000, Bettermann *et al*. 2001, Bettermann *et al* 2002, Scholkmann and Wolf 2019). The relationship between the HR and RR is thus not random but is an emergent property as a result of complex cardiorespiratory interactions. A PRQ of 4 can be regarded as an attractor state that is approached during resting-conditions, while other attractor states are at other harmonic ratios (but less pronounced).

The aim of the present work was to evaluate these three assertions, i.e. the preference of the resting-state PRQ showing values around 4, being lognormally distributed and also exhibiting a quantization of values with preferences around integers. To this end, a large data set of own measurements has been analysed that was obtained during a systemic physiology augmented functional near-infrared spectroscopy (SPA-fNIRS) study conducted at our institute. The data set comprised of resting-state measurement of HR and RR of subjects sitting on a chair in a darkened room and wearing a SPA-fNIRS setup to measure brain and physiological activity. HR was measured with a device registering cardiac activity as well as continuous blood pressure (SOMNOtouch NIBP, SOMNOmedics GmbH, Randersacker, Germany; sampling rate: 4 Hz). RR was measured with a patient monitor with a capnography module (LifeSense, Nonin Medical, Plymouth, MN, USA; sampling rate: 1 Hz). The capnograph was connected to a small tube with an open end attached below the nostrils of the subject. The tube attached did not influence the breathing of the subject nor caused any discomfort. The PRQ was determined by averaging the HR and RR measurement for each experiment for a recording period of 5 min (i.e. last 5 min of the baseline phase). It was ensured that the subjects were in an awake resting-state during the measurements. Measurements were conducted in 134 healthy subjects (49 men, 85 women, age: 24.7 ± 3.4, range: 20–46 years) and were repeated 2–4 times for each subject (on different days) resulting in 482 single measurements and thus single resting-state PRQ values. The subjects did not have an acute disease nor a chronic disease affecting the cardiovascular, cardiorespiratory or neuronal system. The body mass index of the population was 22.08 ± 2.42 (range: 17.54–31.22) showing that the population consisted of subjects of normal weight.

The measured raw signals were processed in Matlab (R2017a, MathWorks, Inc., MA, USA) and the statistical analysis was conducted in R (version 3.4.4) (R Core Team 2019). For the analysis of the data distribution, the R package "fitdistrplus" (Delignette-Muller and Dutang 2015) was employed.

In order to investigate *assertion 1* (i.e. the prevalence of the resting-state PRQ showing values around 4) and *assertion 2* (i.e. the lognormal distribution of the data), the PRQ data were analysed with a Cullen and Frey plot (skewness-kurtosis plot) (Cullen and Frey 1999) involving a nonparametric bootstrap procedure (number of bootstraps: 5000) to take into account the uncertainty in estimating the kurtosis and skewness (Efron and Tibshirani 1994). The empirical distribution of PRQ values was compared with the following distributions: normal, uniform, exponential, logistic, beta, lognormal and gamma. Fig. 1a shows that the lognormal distribution is the most suitable one explaining the empirical PRQ distribution. To further corroborate this finding, the goodness-of-fit was evaluated by fitting a lognormal distribution to the data, comparing the empirical and theoretical cumulative density functions (CDFs), creating a Q-Q plot (theoretical vs. empirical quantiles) and a P-P plot (fitted distribution function vs. empirical distribution function). Because the Cullen and Frey plot analysis found the lognormal distribution representing the empirical PRQ distribution at best, and since the Weibull distribution is similar to the lognormal one (Cain 2002, Kundu and Manglick 2004), the goodness-of-fit was evaluated for the lognormal and Weibull distribution. The analysis showed that the lognormal distribution fits the PRQ data better than the Weibull distribution (loglikelihood: -627.7287, Akaike information criterion (AIC): 1259.457, Bayesian information criterion (BIC): 1267.813 vs. -684.2619, AIC: 1372.524, BIC: 1380.88). The fit with the lognormal distribution (Fig. 2c) gave a median PRQ value of 4.19 with a skewness of the distribution of 1.00 and a kurtosis of 5.30, respectively. That the lognormal distribution fits the data well can be also inferred by visually comparing the empirical fit (density estimate) with the lognormal fit (Fig. 2a, c). Also the comparison with the empirical and theoretical CDFs (Fig. 2d), the

Q-Q plot (Fig. 2e) and the P-P plot (Fig. 2f) support the finding that the PRQ data follow a lognormal distribution.

To evaluate *assertion 3* (i.e. the quantization of PRQ values with preferences of integers), the following procedure was performed: each single PRQ value of the data set was compared to the next integer and the difference was calculated, resulting in ΔPRA values (ΔPRA = PRQ – [PRQ], with [·] the round-to-nearest integer operator), and the distribution of ΔPRQ values was analysed.

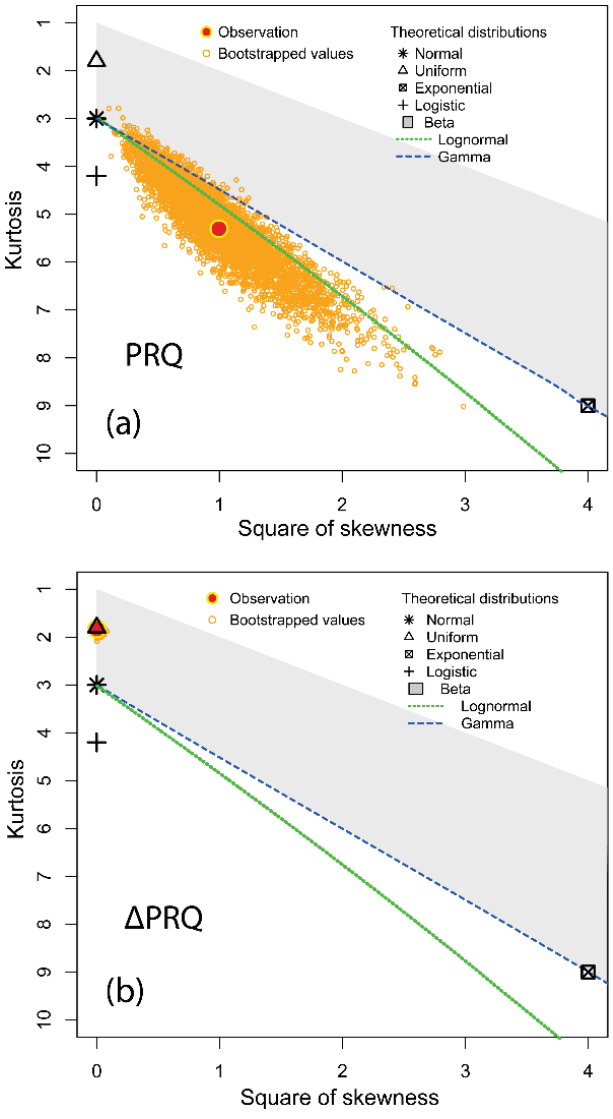

Fig. 1. Cullen and Frey plots for the PRQ (**a**) and ΔPRQ (**b**) data. The analysis revealed that the distribution of PRQ data is approximated at best by a lognormal distribution and the ΔPRQ data by a uniform one.

Since a quantization of PRQ values results in a distribution with preferred values of integers, the resulting ΔPRQ distribution should have a clear maxima around 0 and should follow approximately a normal distribution. As Fig. 2b shows, no preferred ΔPRQ value was evident from the distribution. The Cullen and Frey plot of the data (Fig. 1b) further showed that the data can be approximated at best with a uniform distribution and that a normal distribution does not fit the data well. Both results support the conclusion that no quantization of PRQ values was evident.

Our analysis thus confirmed assertion 1 and 2 that the resting-state PRQ on a group-level has a high probability of having a value of around 4 and being lognormally distributed. Our analysis thus agrees with the previous publications stating assertions 1 and 2, indicating the occurrence of cardiorespiratory coupling in the resting-state. Assertion 3 about the quantization of PRQ values (which would indicate a cardiorespiratory coordination) was not supported by our analysis. There are three main reasons for not finding the PRQ quantization according to our reasoning. First, it could be that the PRQ quantization is more/less pronounced in individual subjects and that a group-level analysis (as we did) is not able to detect it since the effect is weakened by our analysis approach. This aspect is especially significant since we calculated the PRQ value by dividing the median of the HR by the median of the PR (from the 5 min time-series) and not by calculating the instantaneous PRQ (from the 5 min time-series) and then taking the median of it. The second approach might be better characterizing the individual quantized PRQ states. Further research is needed to investigate this reasoning. Second, the PRQ quantization could be mainly better detected by analysing the PRQ values of an individual subject during a specific time-interval (during this interval, there might be a cardiorespiratory coupling preference, i.e. cardiorespiratory coordination, with integer PRQ values, as indicated by previous works). Calculating an average over all PRQ values for the interval (as we did) might weaken the PRQ quantization effect in the data since only the average of the PRQ is taken into account in the final group-level analysis and not possible additional maxima of the PRQ distribution. This conclusion is supported for example by the study of Bettermann *et al.* (2001) who detected a PRQ quantization when first analysing the individual PRQ distributions for each experiment and then performing the group-average; with this approach, the presence of local maxima in the PRQ distribution at values of 4, 3, 2 and 5 in nightly resting-stated PRQ values of women with metastasized breast cancer was detected. According to this finding, the PRQ quantization thus might

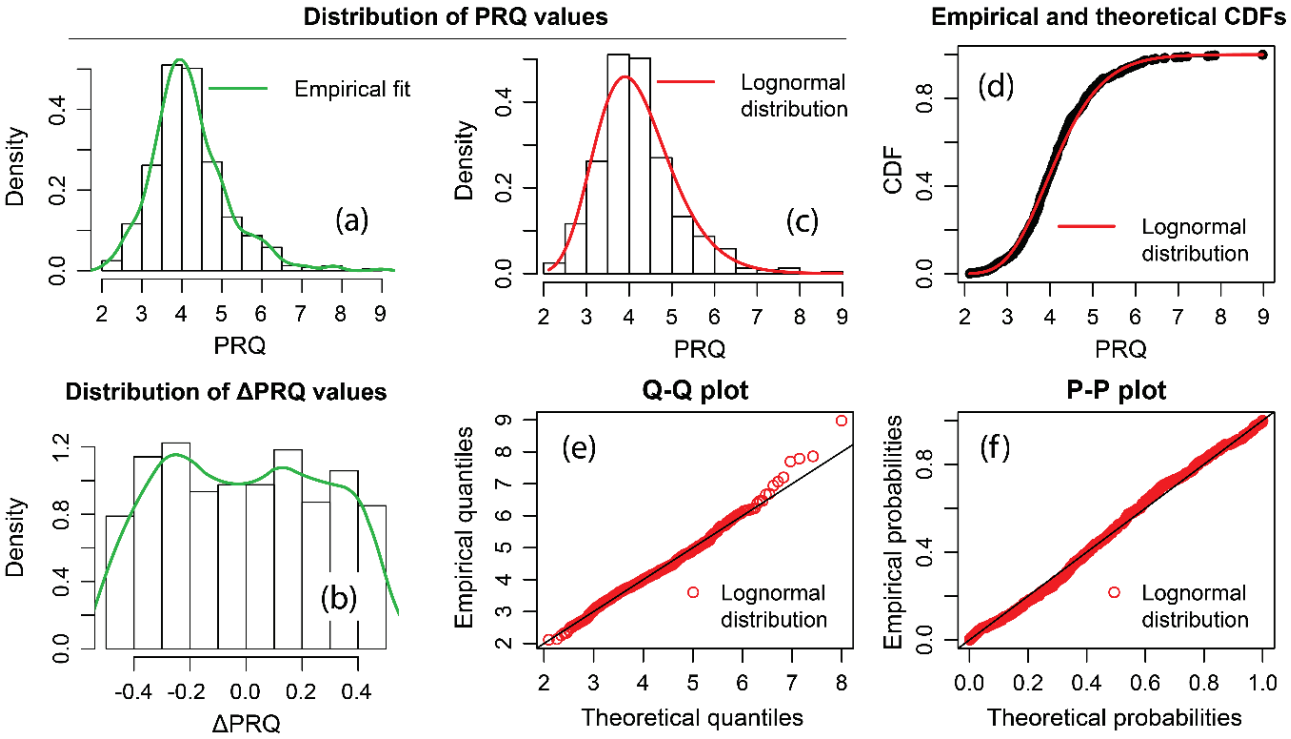

Fig. 2. (**a, b**) Comparison of histograms of PRQ and ΔPRQ values with density estimations. (**c-f**) Evaluation of the goodness-of-fit for fitting the PRQ distribution with a lognormal distribution. CDFs: cumulative density functions.

be also related to the health state of a subject, and since our study included healthy young subjects, the occurrence of this effect might be less likely. Third, the PRQ quantization might be only an artefact or phenomena that is happening only occasionally so that a generalization is unjustified. According to our assessment, the most likely conclusions seem to be the first and second ones. Further research is needed, and will be conducted by us, to clarify this aspect.

Our finding that the resting-state PRQ of human adults is indeed around 4 is not only of interest for basic human physiology but has also medical relevance since deviations from this norm might be associated with pathophysiological processes. Indeed, the usefulness of evaluating the resting-state PRQ in patients for diagnosis and disease monitoring has been already shown (Bettermann *et al*. 2001, Göbels 2014, Heckmann 2001, Hildebrandt 1960, 1980, 1985, 2009, Kümmell and Heckmann 1987, Suchantke 1951, Weckenmann 1975, 1981). For example, a tendency of resting-state PRQ to be closer to 4 during the course of an influenza disease has been documented (Müller 1972). A state of PRQ ≈ 4 has been termed "PRQ normalization", associated with an optimal functioning of the cardiovascular system a balanced state of the autonomic nervous system, being relevant for and being correlated with a healthy physiological state of a human (Hildebrandt 1997, Scholkmann and Wolf 2019). The significance of PRQ ≈ 4 is highlighted by the fact that the resting-state PRQ is also around 4.5 for all mammals and thus is not following an algometric scaling law as the HR or RR (Schmidt-Nielsen 1984, Stahl 1967).

The finding about the lognormality of the PRQ distribution is important for future studies using the PRQ since the statistical analysis of PRQ values thus needs to be treated accordingly, i.e. taking the log of the PRQ value is necessary to transform the data to a normal distribution so that the requirements of the classical statistical test are fulfilled.

To the best of our knowledge, our study is the largest conducted so far in healthy adult humans about reference values of the PRQ during a resting-state at day.

Conflict of Interest

There is no conflict of interest.

Acknowledgements

This work was supported by the grant CST grants 253 CST (2016, 2017) and 355 CST (2018), and the SAGST grant P12117. The authors wish to thank John Folkes for his kind assistance in English language revision and proofreading.

References

BENARROCH EE: Brainstem integration of arousal, sleep, cardiovascular, and respiratory control. *Neurology* **91**: 958-966, 2018.

BETTERMANN H, CYSARZ D, VAN LEEUWEN P: Detecting cardiorespiratory coordination by respiratory pattern analysis of heart period dynamics-the musical rhythm approach. *Int J Bif Chaos* **10**: 2349-2360, 2000.

BETTERMANN H, KRÖZ M, GIRKE M, HECKMANN C: Heart rate dynamics and cardiorespiratory coordination in diabetic and breast cancer patients. *Clinical Physiol* **21**: 411-420, 2001.

BETTERMANN H, VON BONIN D., FRÜHWIRTH M, CYSARZ D, MOSER M. Effects of speech therapy with poetry on heart rate rhythmicity and cardiorespiratory coordination. *Int J Cardiol* **84**: 77-88, 2002.

CAIN SR: Distinguishing between lognormal and Weibull distributions [time-to-failure data]. *IEEE Transactions on Reliability* **51**: 32-38, 2002.

CULLEN AC, FREY HC: Probabilistic techniques in exposure assessment. Springer, USA, 1999.

DELIGNETTE-MULLER ML, DUTANG C: Fitdistrplus: An R package for fitting distributions. *J Stat Software* **64**: 1-34, 2015.

DICK TE, HSIEH YH, DHINGRA RR, BAEKEY DM, GALAN RF, WEHRWEIN R, MORRIS KF: Cardiorespiratory coupling: common rhythms in cardiac, sympathetic, and respiratory activities. *Prog Brain Res* **209**: 191-205, 2014.

EFRON B, TIBSHIRANI RJ: An Introduction to the Bootstrap (Chapman & Hall), 1994.

ELSTAD M, O'CALLAGHAN EL, SMITH AJ, BEN-TAL A, RAMACHANDRA R: Cardiorespiratory interactions in humans and animals: rhythms for life. *Am J Physiol Heart Circ Physiol* **315**: H6-H17. 2018.

GÖBELS R, ALLMEER C: Die Behandlung mit Rhythmischer Massage bei einer Patientin mit Mammakarzinom. (in German) *Der Merkurstab* **67**: 126-135, 2014.

GUTENBRUNNER C., HILDEBRANDT G: Handbuch der Balneologie und medizinischen Klimatologie. (in German) Springer, Berling, Heidelberg, 1998.

HECKMANN C: Zur Frage der klinischen Bedeutung des Puls-Atem-Quotienten (QP/A). (in German) *Der Merkurstab* **54**: 13-24, 2001.

HILDEBRANDT G: Die rhythmische Funktionsordnung von Puls und Atmung. (in German) *Z. angew. Bäder-Klimaheilkunde* **7**: 533-615, 1960.

HILDEBRANDT G: Chronobiological aspects of cure treatment. *J Jpn Soc Balneol Climatol Phys Med* **44**: 1-37, 1980.

HILDEBRANDT G: Die Bedeutung rhythmischer Phänomene für Diagnose und Therapie. (in German) *Beitr. Erweit. Heilkunst geisteswiss. Erkenntnissen* **38**: 8-24, 1985.

HILDEBRANDT G: Rhythmusforschung als Aufgabe einer anthroposophisch-goetheanischen Naturwissenschaft. (in German) *Der Merkurstab* **50**: 329-336, 1997.

HILDEBRANDT G: Untersuchungen über die rhythmische Funktionsordnung von Pule und Atem. *Acta Medica Scandinavica* **152**: 175-184, 2009.

KRAUSE H, KRAEMER JF, PENZEL T, KURTHS J, WESSEL N: On the difference of cardiorespiratory synchronisation and coordination. *Chaos* **27**: 093933, 2017.

KÜMMELL HC, HECKMANN C: Herzinfarkt und rhythmisches System. (in German) *Der Merkurstab* **40**: 15-27, 1987.

KUNDU D, MANGLICK A. Discriminating between the Weibull and log-normal distributions. *Naval Research Logistics* **51**: 893-905, 2004.

LOTRIČ MB, STEFANOVSKA A: Synchronization and modulation in the human cardiorespiratory system. *Physica A* **283**: 451-461, 2000.

MOSER M, LEHOFER M, HILDEBRANDT G, VOICA M, EGNER S, KENNER T: Phase- and frequency coordination of cardiac and respiratory function. *Biol Rhytm Res* **26**: 100-111, 2008.

MÜLLER H: Der Puls-Atem-Quotient. Beobachtungen über die Verwendbarkeit in der Praxis. *Beitr. Erweit. Heilkunst geisteswiss. Erkenntnissen* **25**: 1-10, 1972.

SCHMIDT-NIELSEN K: Scaling: Why is animal size so important? Cambridge University Press, Cambridge, UK, 1984.

SCHOLKMANN F, WOLF U: The pulse-respiration quotient: A powerful but untapped parameter for modern studies about human physiology and pathophysiology. *Front Physiol* **10**: 371, 2019,

SCHULZ S, ADOCHIEI F-C, EDU I-R, SCHROEDER R, CORSTIN H, BÄR, K-J, VOSS A: Cardiovascular and cardiorespiratory coupling analyses: a review. *Philos Trans A Math Phys Eng Sci* **371**: 20120191-91, 2013.

STAHL WR: Scaling of respiratory variables in mammals. *J Appl Physiol* **22**: 453-460, 1967.

STEINER R: Physiologisch-therapeutisches auf Grundlage der Geisteswissenschaft. Zur Therapie und Hygiene. (in German) Rudolf Steiner Verlag, Dornach, Schweiz, 1989.

SUCHANTKE G: Puls und Atem; Versuch einer Funktions-Erkenntnis des rhythmischen Menschen in Klinik und Praxis. *Der Merkurstab* **4**: 105-112, 1951.

R CORE TEAM: A language and environment for statistical computing. R Foundation for Statistical Computing, Vienna, Austria, 2018. https://www.R-project.org/.

VALENZA G, TOSCHI N, BARBIERI R: Uncovering brain-heart information through advanced signal and image processing. *Philos Trans A Math Phys Eng Sci* **374**: 2067, 2016.

WECKENMANN M: Der Puls-Atem-Quotient der orthostatisch Stabilen und Labilen im stehen'. (in German) *Basic Res Cardiol* **70**: 339-349, 1975.

WECKENMANN M: Blutdruck und rhythmische Parameter als abhängige Größen im Grenzbereich zwischen orthostatischer Stabilität und Labilität. (in German) *Basic Res Cardiol* **76**: 211-223, 1981.

Chapter 3

SPA-fNIRS: A promising tool to investigate cerebral and physiological changes

In the previous chapter, the PRQ was introduced, and two special features of it were explained. This parameter, along with numerous cerebral and physiological parameters, can be measured by the SPA-fNIRS approach. This chapter comprises three peer-reviewed publications that aim to investigate with SPA-fNIRS whether changes in cerebral parameters, namely StO_2 and [tHb], can be associated with (or influenced by) systemic physiology. Publication 2 and 3 focus on the investigation of frontal cerebral oxygenation asymmetry (FCOA) at rest. SPA-fNIRS was employed to assess whether FCOA depends on systemic physiology. Results in Publication 2 show that there is no significant linear correlation between FCOA and systemic physiology, i.e., $P_{ET}CO_2$, HR, and PRQ. However, comprehensive investigations on a large number of healthy humans confirm that FCOA is nonlinearly associated with RR and PRQ, as explained in Publication 3. It is also shown in this publication that StO_2 correlates significantly with $P_{ET}CO_2$, while [tHb] is dependent on HR, RR, and PRQ. In Publication 4, the contribution of systemic physiology (HR, RR and $P_{ET}CO_2$) to StO_2 and [tHb] was investigated with a novel signal-processing method, i.e., *oblique subspace projections signal decomposition*. Experimental findings in Publication 4 display that cerebral parameters contain components related to changes in systemic physiology, and the contribution from systemic physiology varies strongly between subjects.

Peer reviewed publication 2

Right-left asymmetry of prefrontal cerebral oxygenation: does it depend on systemic physiological activity, absolute tissue oxygenation or hemoglobin concentration?

Felix Scholkmann, **Hamoon Zohdi**, Ursula Wolf

Advances in Experimental Medicine and Biology (2020) 1232, 105-112.

DOI: 10.1007/978-3-030-34461-0_15

URL: https://link.springer.com/chapter/10.1007%2F978-3-030-34461-0_15

Own contributions:

- Data analysis
- Review and editing of the manuscript

Right-Left Asymmetry of Prefrontal Cerebral Oxygenation: Does it Depend on Systemic Physiological Activity, Absolute Tissue Oxygenation or Hemoglobin Concentration?

Felix Scholkmann, Hamoon Zohdi, and Ursula Wolf

Abstract Background: We have repeatedly observed a right-left asymmetry (RLA) of prefrontal cerebral oxygenation of subjects during the resting state. Aim: To clarify if the RLA is a reliably observable phenomenon at the group level and whether it is associated with systemic physiology, absolute tissue oxygen saturation (StO_2) or total hemoglobin concentration ([tHb]). Material and Methods: StO_2 and [tHb] values at the right and left prefrontal cortex (PFC) were calculated for two 5- min resting phases based on data from 76 single measurements (24 healthy adults, aged 22.0 ± 6.4 years). StO_2 and [tHb] were measured with an ISS OxiplexTS frequency domain near-infrared spectroscopy device. In addition, end-tidal CO_2 ($P_{ET}CO_2$), heart rate (HR), respiration rate (RR) and the pulse-respiration quotient (PRQ = HR/RR) were measured and analyzed for the two phases. Results: On the group level it was found that i) StO_2 was higher at the right compared to the left PFC (for both phases), ii) RLA of StO_2 (ΔStO_2 = StO_2 (right)–StO_2 (left) was independent of $P_{ET}CO_2$, HR and PRQ, and iii) ΔStO_2 was associated with absolute StO_2 and [tHb] values (positively and negatively, respectively). Discussion and Conclusion: This study shows that i) RLA of StO_2 at the PFC is a real phenomenon, and that ii) ΔStO_2 at the group level does not depend on $P_{ET}CO_2$, HR, RR or PRQ, but on absolute StO_2 and [tHb]. We conclude that the RLA is a real effect, independent of systemic physiology, and most likely reflects genuine properties of the brain, i.e. different activity states of the two hemispheres.

Keywords Cerebral oxygenation · Near-infrared spectroscopy · Cardiorespiratory system · Capnography

F. Scholkmann (✉)
Institute of Complementary and Integrative Medicine, University of Bern, Bern, Switzerland

Biomedical Optics Research Laboratory, Department of Neonatology, University Hospital Zurich, University of Zurich, Zurich, Switzerland
e-mail: Felix.Scholkmann@ikim.unibe.ch

H. Zohdi · U. Wolf
Institute of Complementary and Integrative Medicine, University of Bern, Bern, Switzerland

© Springer Nature Switzerland AG 2020

P.-D. Ryu et al. (eds.), *Oxygen Transport to Tissue XLI*, Advances in Experimental Medicine and Biology 1232, https://doi.org/10.1007/978-3-030-34461-0_15

1 Introduction

In several functional near-infrared spectroscopy (NIRS) studies performed by our group in recent years, we observed a tendency of a right-left asymmetry (RLA) of prefrontal cerebral oxygenation during the resting-state phases of the subjects. Since the aims of the studies were to investigate task and stimulus evoked cerebral brain activity [1–5], we did not analyze RLA in detail. Therefore, this study aimed to investigate these phenomena in detail based on a large dataset from one of our previous studies. In particular, we aimed to clarify if the RLA is a reliably observable phenomenon on the group level and if it is associated with cardiorespiratory activity, absolute tissue oxygenation (StO_2) or total hemoglobin concentration ([tHb]).

2 Materials and Methods

Resting-state StO_2 and [tHb] values were calculated for two baseline phases from a dataset of our previous study [1] comprising 76 single measurements performed on 24 healthy subjects (aged 22.0 ± 6.4 years). Median StO_2 and [tHb] values at the right and left prefrontal cortex (PFC) were calculated for two 5-min resting-state phases (one during the pre-task baseline and the other from the post-task phase). Only data of high signal quality (i.e. StO_2 in the range of 40–100%, no movement artifacts) were included.

StO_2 and [tHb] were measured with an ISS OxiplexTS frequency domain NIRS device enabling StO_2 measurements relatively immune against oxygenation and hemodynamics in the superficial tissue layers. In addition, systemic physiology variables were assessed by measuring end-tidal CO_2 ($P_{ET}CO_2$) (N1000 gas analyzer, Nellcor, Boulder, CO, USA), heart rate (HR) (Medilog AR12, Schiller AG, Baar, Switzerland), respiration rate (RR) and the pulse-respiration quotient (PRQ = HR/RR). The RR was determined from the capnography signal by extracting the instantaneous frequency based on wavelet time-frequency decomposition.

Data were analyzed with Bayesian statistics (JASP, v.0.8.6) to assess whether i) RLA of StO_2 was detectable (Bayesian *t*-test, Cauchy scale: 0.4, hypothesis: StO_2 (right) > StO_2 (left), and whether ii) ΔStO_2 was correlated with HR, RR, PRQ, $P_{ET}CO_2$, mean of absolute StO_2 ($\langle StO_2 \rangle$) or the mean of absolute [tHb] ($\langle [tHb] \rangle$) (Bayesian linear regression; Cauchy prior width 1; tested hypothesis: correlated, correlated positively, or correlated negatively, depending on visual inspection of the scatter plot). Furthermore, it was assessed how well the ΔStO_2 values from both phases agreed (Bayesian linear regression).

3 Results

The distributions of StO_2 values for the left and right PFC and for both phases are depicted in Fig. 1. Also shown is the correlation between StO_2 (phase 1) and StO_2 (phase 2) as well as the distribution of ΔStO_2 values for both phases. The results of the correlation analysis are shown in Figs. 2 and 3.

The results of the analysis can be summarized as follows:

- At the group level, StO_2 measured on the right PFC was higher compared to the left PFC. This was true for both measurement times (median, interquartile range (IQR), phase 1 StO_2 (right) = 68.9% (63.7–72.3%), StO_2 (left) = 57.5% (52.7–62.9%); phase 2 StO_2 (right) = 68.3% (63.1–73.3%), StO_2 (left) = 56.8% (53.4–63.8%), as well as for the combined data set (i.e., phase 1 and 2 combined): StO_2 (right) = 68.6% (63.5–72.4%) vs. StO_2 (left) = 56.8% (52.9–63.4%). All three right-left comparisons yielded Bayes factors (BF_{10}) higher than 100 (with a Cauchy prior width of 0.4), i.e. indicating extreme evidence for the hypothesis StO_2 (right) > StO_2 (left).
- ΔStO_2 (phase 1) and ΔStO_2 (phase 2) were correlated to a high degree ($r = 0.949$ (% confidence interval, CI 0.916–0.967), $BF_{10} = 4.29 \times 10^{34}$ for the hypothesis of a positive correlation), indicating that the RLA of StO_2 is a stable phenomenon for each subject during the whole experiment.
- For both phases, the correlation analysis between ΔStO_2 and HR, RR, PRQ and $P_{ET}CO_2$ ($|r| < 0.2$) delivered BF_{10} values associated with strong to substantial

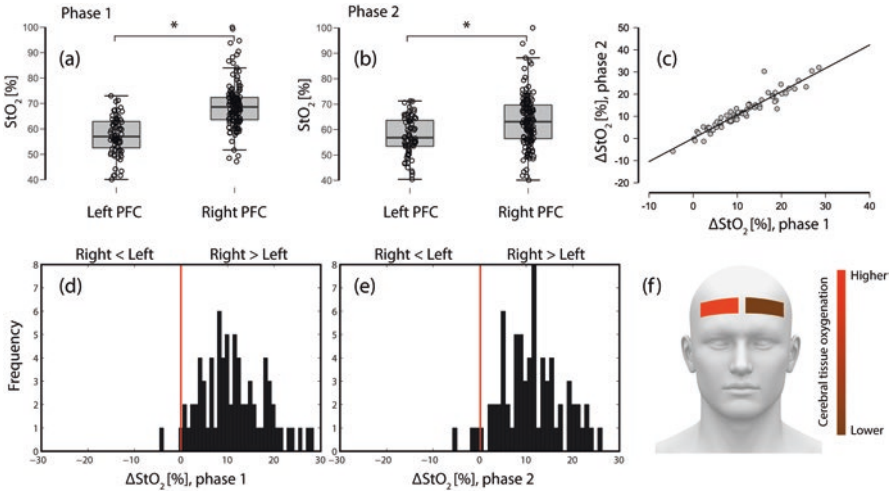

Fig. 1 (**a**, **b**) StO_2 for the right and left PFC measured at two different times (phase 1 and 2). (**c**) Correlation between ΔStO_2 (phase 1) with ΔStO_2 (phase 2). (**d**, **e**) Distribution of ΔStO_2 for both phases. (**f**) Visualization of the RLA of StO_2 observed in this study

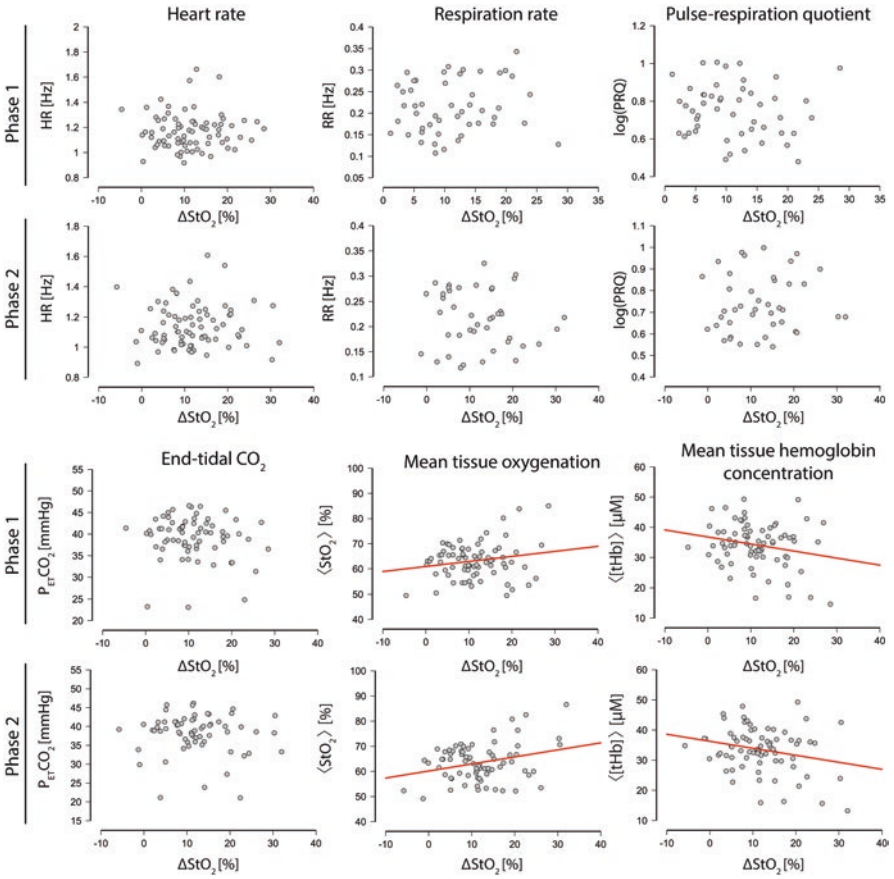

Fig. 2 Scatter plots showing ΔStO_2 vs. HR, RR, PRQ, $P_{ET}CO_2$, $\langle StO_2 \rangle$ and $\langle [tHb] \rangle$ for both phases of the resting-state time series. Correlations between the data are indicated by a linear fit

evidence (BF_{10} = 0.03–0.3) for the hypothesis of no correlation (see Table 1 for individual values and Fig. 2 for a visualization).

- ΔStO_2, was found to be correlated with absolute StO_2 and [tHb] (Table 1, Fig. 2). These correlations are most evident when analyzing the combined data (phase 1 and 2 combined), resulting in a positive correlation of ΔStO_2 with StO_2 ($r = 0.247$, BF_{10} = 19.40) and a negative correlation with [tHb] ($r = -0.230$, BF_{10} = 10.69) (Fig. 3). With $BF_{10} > 10$ there is strong evidence for the hypothesis that the variables are correlated. A Bayes factor robustness check (BF vs. Cauchy prior width) confirmed that the evidence of correlation does not change substantially when changing the Cauchy prior width from 0.25 to 1.5 (see Fig. 3).

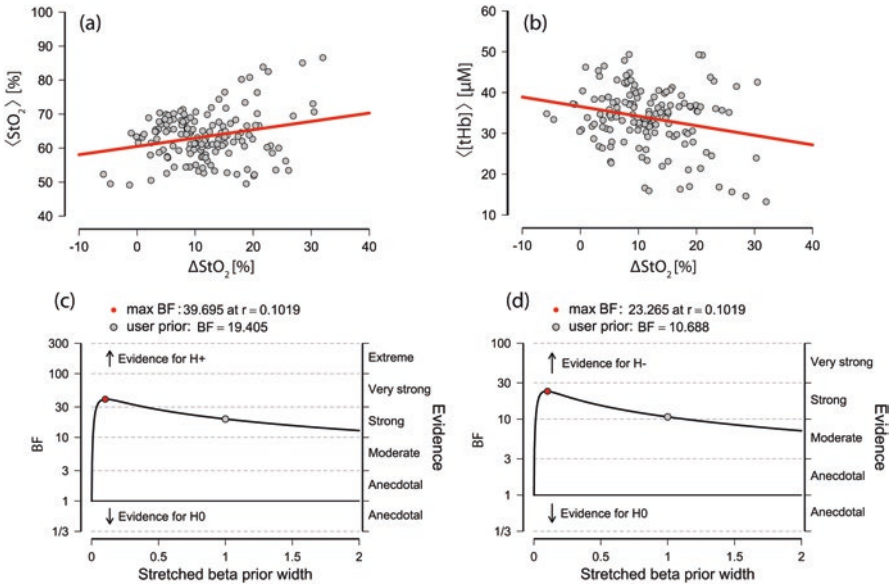

Fig. 3 Bayes factor robustness check (BF vs. Cauchy prior width) for the correlations ΔStO_2 vs. $\langle StO_2 \rangle$ and $\langle [tHb] \rangle$, respectively. For the analysis, the data from period 1 and 2 were combined to increase the robustness of the analysis

Table 1 Correlations between the right-left asymmetry of prefrontal cerebral oxygenation (ΔStO_2) and HR, RR, PRQ, $P_{ET}CO_2$, $\langle StO_2 \rangle$ and $\langle [tHb] \rangle$

Parameter 1	Parameter 1	Correlation coefficient (*r*), 95% CI	Bayes factor (BF_{10})
ΔStO_2 (phase 1)	HR (phase 1)	0.017 [-0.207, 0.238]	0.146
ΔStO_2 (phase 2)	HR (phase 2)	0.039 [-0.188, 0.260]	0.153
ΔStO_2 (phase 1)	RR (phase 1)	0.129 [-0.154, 0.385]	0.129
ΔStO_2 (phase 2)	RR (phase 2)	-0.084 [-0.367, 0.218]	0.220
ΔStO_2 (phase 1)	PRQ (phase 1)	-0.076 [-0.340, 0.204]	0.203
ΔStO_2 (phase 2)	PRQ (phase 2)	0.071 [-0.230, 0.355]	0.212
ΔStO_2 (phase 1)	$P_{ET}CO_2$ (phase 1)	-0.124 [-0.352, -0.10]	0.420
ΔStO_2 (phase 2)	$P_{ET}CO_2$ (phase 2)	-0.077 [-0.326, -0.007]	0.271
ΔStO_2 (phase 1)	$\langle StO_2 \rangle$ (phase 1)	0.196 [0.023, 0.400]	1.107
ΔStO_2 (phase 2)	$\langle StO_2 \rangle$ (phase 2)	0.289 [0.073, 0.478]	6.171
ΔStO_2 (phase 1)	$\langle [tHb] \rangle$ (phase 1)	-0.218 [-0.418, -0.031]	1.570
ΔStO_2 (phase 2)	$\langle [tHb] \rangle$ (phase 2)	-0.240 [-0.437, -0.040]	2.257
ΔStO_2 (combined)	$\langle StO_2 \rangle$ (combined)	0.247 [0.090, 0.389]	19.40∗
ΔStO_2 (combined)	$\langle [tHb] \rangle$ (combined)	-0.230 [-0.374, -0.074]	10.69∗

∗$BF_{10} > 10$

4 Discussion and Conclusion

This study shows that i) RLA of StO_2 at the PFC is a real phenomenon, and that ii) ΔStO_2 at the group level does not depend on $P_{ET}CO_2$, HR, RR or PRQ, but on absolute StO_2 and [tHb].

The absolute StO_2 values at the human PFC measured in our study (StO_2 (right) = 68.6 (IQR 63.5–72.4), StO_2 (left) = 56.8% (IQR 52.9–63.4%), combined values for both phases) are in the range of values reported by previous studies, e.g. 64.5 ± 10% (Invos 3100; measurement avoiding contributions from the extracerebral layer, but obtained without using a frequency domain NIRS instrument) [6], or slightly lower, e.g., 75.19 ± 8.3% (Imagent, ISS; combined values for the right and left PFC; measurement avoiding contributions from the extracerebral layer) [7] and 75.5 ± 4.5% (NIRO300, 4 cm source-detector separation, average over 2 channels and left and right PFC) [8]. The reason for the differences in StO_2 values between studies might be a difference in the age or physiological state of the subjects and the measurement methodology. For example, according to the manufacturer, the Invos NIRS device is not intended for measuring absolute values, provides slightly lower values than the ISS instrument, and the StO_2 values depend on the tHb concentration [9].

Our finding that on the group level during rest the right PFC has a higher oxygenation than the left, i.e. a RLA of StO_2 at the PFC, has seldom been investigated with NIRS. The only NIRS studies that investigated this aspect found no difference (right vs. left PFC (extracerebral tissue): 71.7 ± 3.03% vs. 71.7 ± 3.86%, and right vs. left PFC (cerebral tissue): 74.8 ± 5.83% vs. 75.6 ± 5.86%; 15 subjects, aged 20–50 years, using an ISS Imagent device [7] and right vs. left PCF (cerebral and extracerebral tissue combined, 4 cm source-detector separation): 75.6 ± 4.2% vs. 75.4 ± 4.9%, 16 subjects, using a NIRO300 device [8]. In these studies, much larger distances were employed, which leads to a substantially lower SNR. The explanation for this difference may be that the SNR was not high enough to show the RLA. In addition, the measurements of Quaresima et al. [8] were also sensitive to the extracerebal tissue layer whereas our measurements avoided this confounding effect.

To exclude a simple artifact, we tested whether our NIRS measurements were dependent on the specific NIRS optode by switching the right optode with the left and vice versa. Since the StO_2 difference persisted (data not shown; for the test the ISS Imagent was used; also here the RLA was observed), we conclude that the StO_2 RLA measured is not simply due to a measurement error.

That task or stimulus evoked brain activity shows a laterality in the PFC has been shown by many electroencephalography (EEG) studies linking the asymmetry to side-specific activities of behavior regulation, especially reflecting the activity of a "moderator of emotional responding for both approach and withdrawal related emotions", as summarized in a recent review [10]. The right PFC in particular seems to be "crucially involved in a regulatory control system that supervises the motivational systems of approach and avoidance" [11].

Studies applying functional NIRS (fNIRS) to investigate the frontal asymmetry by Sakatani et al. are generally in line with these EEG studies and also with our finding of a RLA of StO_2: several studies showed a higher increase in the concentration of oxyhemoglobin ($[O_2Hb]$) in the right PFC during mental stress tasks, mediated by the individual psychological state (anxiety level) [12–14] and the age [15]. However, a decrease in $[O_2Hb]$ in the right PFC, and a decrease in EEG activity at the same side, during a mental arithmetic task was reported in an fNIRS-EEG by others [16]. A stronger response (increase) in the left compared to the right PFC to a continuous colored light exposure (10 min) of the subjects was observed in a study by our group [17]. From this it can be concluded that the activity-dependent RLA of frontal NIRS-signal changes was observed by several fNIRS studies, and the magnitude and sign varied, probably depending on the task, individual subjects and differences in methodology.

Our study is the first to investigate whether the RLA of StO_2 during the resting state was dependent on the state of the cardiorespiratory system of the subjects; however, such a dependence was not observed in our study. This finding supports the notion that the degree of RLA of frontal oxygenation does not simply reflect systemic physiological (i.e. cardiorespiratory) activity, but rather constitutes real frontal asymmetry of brain activity (neurovascular coupling). The reason for the observed ΔStO_2 depends on absolute StO_2 and [HHb] and needs further research.

References

1. Scholkmann F et al (2013) End-tidal CO_2: an important parameter for a correct interpretation in functional brain studies using speech tasks. NeuroImage 66:71–79
2. Scholkmann F, Wolf M, Wolf U (2013) The Effect of Inner Speech on Arterial CO_2 and Cerebral Hemodynamics and Oxygenation: A Functional NIRS Study. Adv Exp Med Biol 789:81–87
3. Scholkmann F et al (2014) Cerebral hemodynamic and oxygenation changes induced by inner and heard speech: a study combining functional near-infrared spectroscopy and capnography. J Biomed Opt 19(1):017002
4. Metz AJ et al (2017) Physiological effects of continuous Colored light exposure on Mayer wave activity in cerebral Hemodynamics: a functional near-infrared spectroscopy (fNIRS) study. Adv Exp Med Biol 977:277–283
5. Scholkmann F et al (2017) Effect of short-term colored-light exposure on cerebral hemodynamics and oxygenation, and systemic physiological activity. Neurophotonics 4(04):1
6. Germon TJ et al (1995) Extracerebral absorption of near infrared light influences the detection of increased cerebral oxygenation monitored by near infrared spectroscopy. J Neurol Neurosurg Psychiatry 58(4):477–479
7. Choi J et al (2004) Noninvasive determination of the optical properties of adult brain: near-infrared spectroscopy approach. J Biomed Opt 9(1):221–229
8. Quaresima V et al (2000) Noninvasive measurement of cerebral hemoglobin oxygen saturation using two near infrared spectroscopy approaches. J Biomed Opt 5(2):201–205
9. Kleiser S et al (2017) Comparison of tissue oximeters on a liquid phantom with adjustable optical properties: an extension. Biomed Opt Express 9(1):86
10. Reznik SJ, Allen JJB (2018) Frontal asymmetry as a mediator and moderator of emotion: an updated review. Psychophysiology 55(1):e12965

11. Allen JJB et al (2018) Frontal EEG alpha asymmetry and emotion: From neural underpinnings and methodological considerations to psychopathology and social cognition. Psychophysiology 55(1):e13028
12. Tanida M, Katsuyama M, Sakatani K (2007) Relation between mental stress-induced prefrontal cortex activity and skin conditions: a near-infrared spectroscopy study. Brain Res 1184:210–216
13. Tanida M, Katsuyama M, Sakatani K (2008) Effects of fragrance administration on stress-induced prefrontal cortex activity and sebum secretion in the facial skin. Neurosci Lett 432(2):157–161
14. Ishikawa W et al (2014) Correlation between asymmetry of spontaneous oscillation of hemodynamic changes in the prefrontal cortex and anxiety levels: a near-infrared spectroscopy study. J Biomed Opt 19(2):027005
15. Sakatani K, Tanida M, Katsuyama M (2010) Effects of Aging on Activity of the Prefrontal Cortex and Autonomic Nervous System during Mental Stress Task. Adv Exp Med Biol 662:473–478
16. Al-Shargie F, Tang TB, Kiguchi M (2017) Assessment of mental stress effects on prefrontal cortical activities using canonical correlation analysis: an fNIRS-EEG study. Biomed Opt Express 8(5):2583–2598
17. Metz AJ et al (2017) Continuous coloured light altered human brain haemodynamics and oxygenation assessed by systemic physiology augmented functional near-infrared spectroscopy. Sci Rep 7(1):10027

Peer reviewed publication 3

Frontal cerebral oxygenation asymmetry: inter-subject variability and dependence on systemic physiology, season, and time of day

Hamoon Zohdi, Felix Scholkmann, Ursula Wolf

Neurophotonics (2020) *7*, 025006.

DOI: 10.1117/1.NPh.7.2.025006

URL: https://www.spiedigitallibrary.org/journals/neurophotonics/volume-7/issue-02/025006/Frontal-cerebral-oxygenation-asymmetry--intersubject-variability-and-dependence-on/10.1117/1.NPh.7.2.025006.full?SSO=1

Own contributions:

- Co-design of the study
- Contribute to carrying out measurements
- Signal processing
- Data analysis
- Visualization (all figures)
- Writing of the first draft

Frontal cerebral oxygenation asymmetry: intersubject variability and dependence on systemic physiology, season, and time of day

Hamoon Zohdi,[a] Felix Scholkmann,[a,b,†] and Ursula Wolf[a,†,*]

[a]University of Bern, Institute of Complementary and Integrative Medicine, Bern, Switzerland
[b]University of Zurich, University Hospital Zurich, Biomedical Optics Research Laboratory, Department of Neonatology, Zurich, Switzerland

Abstract

Significance: Our study reveals that frontal cerebral oxygenation asymmetry (FCOA), i.e. a difference in the oxygenation between the right and left prefrontal cortex (PFC), is a real phenomenon in healthy human subjects at rest.

Aim: To investigate FCOA, we performed a study with 134 healthy right-handed subjects with the systemic physiology augmented functional near infrared spectroscopy (SPA-fNIRS) approach.

Approach: Subjects were measured 2 to 4 times on different days resulting in an unprecedented number of 518 single measurements of the absolute values of tissue oxygen saturation (StO_2) and total hemoglobin concentration ([tHb]) of the right and left PFC. Measurements were performed with frequency-domain functional near-infrared spectroscopy. In addition, the cardiorespiratory parameters were measured simultaneously.

Results: We found that (i) subjects showed an FCOA (higher StO_2 on the right PFC), but not for tHb; (ii) intrasubject variability was excellent for both StO_2 and tHb, and fair for FCOA; (iii) StO_2 correlated significantly with blood CO_2 concentration, [tHb] with heart rate, respiration rate (RR), and the pulse–respiration quotient (PRQ), and FCOA with RR and PRQ; (iv) FCOA and StO_2 were dependent on season and time of day, respectively; (v) FCOA was negatively correlated with the room temperature; and (vi) StO_2 and tHb were not correlated with the subjects mood but with their chronotype, whereas FCOA was not dependent on the chronotype.

Conclusion: Our study demonstrates that FCOA is real, and it provides unique insights into this remarkable phenomenon.

© *The Authors. Published by SPIE under a Creative Commons Attribution 4.0 Unported License. Distribution or reproduction of this work in whole or in part requires full attribution of the original publication, including its DOI.* [DOI: 10.1117/1.NPh.7.2.025006]

Keywords: functional near-infrared spectroscopy; prefrontal cortex; right–left asymmetry; tissue oxygenation; systemic physiology.

Paper 20002R received Jan. 7, 2020; accepted for publication Jun. 8, 2020; published online Jun. 23, 2020.

1 Introduction

Our own preliminary measurements suggested that cerebral oxygenation differed between the right and left prefrontal cortex (PFC) in healthy human adults at rest.[1] This phenomenon, which we named frontal cerebral oxygenation asymmetry (FCOA), is characterized by higher tissue oxygenation over the right PFC compared to the left.

Hemispheric specialization has been reported for a wide range of cerebral functions.[2] For example, it is known that the regions in the left hemisphere are usually dominant for language and logical processing, whereas regions in the right hemisphere are specialized for spatial recognition and emotional control.[3,4] Lateralization of function was first reported in the domain of

*Address all correspondence to Ursula Wolf, E-mail: ursula.wolf@ikim.unibe.ch
†These authors share last authorship.

Downloaded From: https://www.spiedigitallibrary.org/journals/Neurophotonics on 24 Jun 2020
Terms of Use: https://www.spiedigitallibrary.org/terms-of-use

language functions, which is widely accepted as a fundamental feature of neural organization, where it was revealed that the left hemisphere is dominant in language processing.[5,6] Additionally, more than 90% of the population prefers the right hand for manual activities, with superior fine motor control and motor strength, which is controlled by the left hemisphere.[4] Research has demonstrated that neural organization exists for the control motor actions, where each brain hemisphere contributes exclusive control mechanisms to the movement of each arm.[7] Mutha et al.[7] suggested that the left hemisphere provides predictive control mechanisms, whereas the right one contributes positional control mechanisms during movement of either arm. In addition to lateralization of language and motor control, face processing has also been shown to have laterality to neural activity and connectivity. It has been demonstrated that areas in the right hemisphere are more anatomically connected, more synchronized during rest, and more actively communicating with each other during face perception compared to the left hemisphere.[8] Interestingly, numerous electroencephalography (EEG) studies have demonstrated a right–left asymmetry in brain activity during the resting state. Frontal EEG asymmetry (FEA) activity has been explained using the approach-withdrawal model suggesting that there are two different types of motivation.[9,10] The approach motivation signifies the propensity to move toward the desired stimulus and is associated with a higher left frontal activity, whereas the withdrawal/avoidance motivation indicates a propensity to move or stay away from an undesired stimulus and is associated with higher right frontal activity.[11–13] However, only a few studies on the asymmetry of brain tissue oxygenation and metabolism have been performed so far.[1,14] This prompted us to investigate this fascinating phenomenon in many subjects using functional near-infrared spectroscopy (fNIRS).

From a methodological point of view, three main types of NIRS-based optical tissue spectroscopy techniques have been developed so far: continuous wave (CW-NIRS), frequency domain (FD-NIRS), and time domain (TD-NIRS). CW-NIRS can provide information on concentration changes of oxyhemoglobin ($[O_2Hb]$) and deoxyhemoglobin ([HHb]) but cannot determine absolute baseline values. Therefore, it is appropriate for applications in cognitive neuroscience as absolute values are not crucial and functional activity is relatively assessed with respect to the baseline.[15] FD-NIRS and TD-NIRS measure not only the light intensity as CW NIRS but also the time of flight of photons through tissue. Therefore, time resolved techniques such as TD-NIRS and FD-NIRS are able to provide absolute $[O_2Hb]$, [HHb], and total hemoglobin ([tHb]) concentrations as well as absolute tissue oxygen saturation $[StO_2 = ([O_2Hb]/[tHb]) \times 100]$.[16,17] This is relevant additional information, e.g., the [tHb] is strictly proportional to cerebral blood volume by the hematocrit. Thus these systems have widely been used in many diverse fields and applications including clinical monitoring, traumatic brain injury, anesthesiology, neonatology, and psychiatry.[18] A comprehensive review on the history of fNIRS development, methodology, and imaging instrumentation has been published by Scholkmann et al.[19] In this study, we performed optical neuroimaging using multidistance FD-NIRS. This approach is also able to reduce the sensitivity to extracerebral tissue. It is known that the oxygenation of the brain depends on its activity state, and the metabolic changes in the brain are interrelated with systemic parameters.[20–22] Therefore, it is essential to employ the systemic physiology augmented (SPA) fNIRS approach, which additionally and simultaneously measures absolute values of cardiorespiratory parameters including the end-tidal carbon dioxide ($P_{ET}CO_2$), heart rate (HR), respiration rate (RR), and the pulse-respiration quotient (PRQ).

The main goal of this study was to investigate FCOA in a large number of healthy humans at rest to elucidate whether FCOA is a real and robust phenomenon. To facilitate a better understanding of this phenomenon, we employed SPA-fNIRS to assess whether FCOA depends on systemic physiological activity, absolute tissue oxygenation, or hemoglobin concentration. We also aimed to explore the effects of chronobiological and psychological variables on FCOA, as well as cerebral hemodynamics and oxygenation at the PFC during the resting state.

2 Subjects and Methods

2.1 *Subjects*

The study was carried out with 134 healthy subjects (85 female, 49 male, age 24.7 ± 3.4 years, and range 20 to 46 years). The subjects were all right-handed, according to the Edinburgh

Downloaded From: https://www.spiedigitallibrary.org/journals/Neurophotonics on 24 Jun 2020
Terms of Use: https://www.spiedigitallibrary.org/terms-of-use

Handedness Inventory.[23] Subjects were nonsmoking and indicated neither current nor previous history of neurological and psychiatric disorders or alcohol and drug abuse. Subjects were asked to refrain from consuming caffeine and eating 2 h prior to the experiment. The study protocol was approved by the Ethics Committee of the Canton of Bern. Informed consent was obtained from all subjects before the measurements. Subjects were also informed of their right to discontinue participation at any time.

2.2 *Experimental Protocol*

The resting state data were taken from a set of studies with different stimuli. Each measurement began with a baseline phase lasting 8 min, during which the subjects sat upright in a comfortable chair in a dark room. For this study, we examined only the last 5 min of this baseline period. Each subject was measured on four different days but at the same time of day to prevent chronobiological artifacts. They were asked to keep their eyes open throughout the entire measurement and to move their head or body as little as possible during the measurement to avoid movement artifacts. Additionally, the subjects were asked to fill out two questionnaires before and after each measurement in order to assess their mood: the positive affect negative affect schedule (PANAS)[24] and the self-assessment manikin test (SAM; five points scale).[25] The PANAS and SAM questionnaires are used as tools to measure state influence. Trait influence evaluation was not performed in our study. Additionally, we determined the chronotype by the Horne and Östberg morningness-eveningness questionnaire.[26] Measurements were performed between 7:00 am and 9:00 pm. The mean room temperature was $22.8°C \pm 0.6°C$.

2.3 *Measurement Setup*

The Imagent (ISS Inc., Champaign, Illinois, USA), a multichannel FD-NIRS system, which employs a multidistance approach, was used to determine absolute values of the $[O_2Hb]$, [HHb], [tHb], and StO_2 at a sampling rate of 2.5 Hz on the PFC. The Imagent's light source consists of 16 laser diodes at 760 nm and 16 laser diodes at 830 nm. Four highly sensitive photomultiplier tubes serve as detectors. The sensors were placed bilaterally on the left and right prefrontal cortex (L-PFC and R-PFC) of subjects at position Fp1 and Fp2, according to the international 10 to 20 system.[27] Each of the two ISS sensors had four light emitters and one light detector connected to an optical fiber delivering the light to the photomultiplier tube. The source–detector separations (d) were ~2.0, 2.5, 3.5, and 4.0 cm with the sources and detectors arranged collinearly.

HR was measured by SOMNOtouch™ NIBP (SOMNOmedics GmbH, Randersacker, Germany) with a sampling rate of 4 Hz. This device calculated the HR from the ECG data by calculating the $R-R$ intervals. RR and end-tidal carbon dioxide ($P_{ET}CO_2$) were measured noninvasively by a NONIN LifeSense (NONIN Medical, Plymouth, Minnesota, USA). Data were recorded at a sampling rate of 1 Hz. All data were recorded simultaneously.

2.4 *Signal Processing and Statistical Analysis*

One subject was excluded from data analysis due to the perceived discomfort of the fNIRS sensors. 126 subjects completed all four measurements; only for seven subjects, the number of experimental sessions was lower. Therefore, the entire data for the current analysis comprised 518 single measurements. All signal processing was performed in MATLAB (R2017a, MathWorks, Inc., Massachusetts, USA).

2.4.1 *Cerebral oxygenation and hemodynamics*

Prior to analysis, data with extremely low ($StO_2 < 40\%$) or improper high values ($StO_2 > 100\%$) were removed by visual inspection. Movement artifacts in the StO_2 and [tHb] signals were removed by the movement artifact reduction algorithm (MARA) based on moving standard deviation and piecewise-interpolation.[28] For 86% of the signal time series, no processing with MARA was necessary. To remove high-frequency noise, signals were low pass filtered using a

Downloaded From: https://www.spiedigitallibrary.org/journals/Neurophotonics on 24 Jun 2020
Terms of Use: https://www.spiedigitallibrary.org/terms-of-use

robust second-degree polynomial moving average (RLOESS) with a span of 2 min. This method assigns zero weight to data outside six mean absolute deviations (MAD). For each measurement, the 5-min median of the baseline phase was calculated for each cerebral parameter. Absolute values of StO_2 and [tHb] from the L-PFC and R-PFC were averaged to obtain a single value for the whole PFC. Moreover, the laterality index—defined as the difference between the absolute values for the R-PFC and L-PFC—was determined and is indicated by a "Δ." Finally, median values and the interquartile range (IQR) of StO_2 and [tHb] were calculated for each individual subject.

2.4.2 *Cardiorespiratory parameters*

All cardiorespiratory parameters, including HR, $P_{ET}CO_2$, and RR, were also denoised by the RLOESS method with a window length of 3, 1, and 2 min, respectively. Additionally, the PRQ (= HR/RR) was calculated to quantify the coupling between HR and RR. The 5-min median of the baseline phase was determined for all systemic physiology data. The IQR of parameters was calculated for each individual subject.

2.4.3 *Statistical analysis*

Outliers (defined as exceeding three scaled MAD from the median) of each dataset were removed prior to the correlation analysis. The best nonlinear curve fitting (from many models including line, poly, cubic, degree 4 and 5 polynomial, piecewise linear function with 2 segments, and exponential) was estimated with R statistical software (R 3.5.2, Performance Analytics package, r-project.org) and OriginPro (version 2018b, OriginLab Corporation, Northampton, Massachusetts, USA) for each pair of parameters (8 parameters and 28 pairs) and a robust nonlinear regression was then calculated with MATLAB using the least absolute residuals method in order to avoid false-positive correlation detection. *P*-values were then obtained from goodness-of-fit results of each parameter pair. A false discovery rate (FDR) correction was subsequently applied to the *p*-values in order to correct for the multiple comparison situation. The bootstrapped evidence (BSE) test was conducted to find bootstrapped correlations between all parameters (28 pairs). This nonparametric method is an actual resampling procedure that takes the precision with which both the experimental (H_1) and null (H_0) hypothesis can be estimated into account.[29] This test is also more robust compared to classical statistics by minimizing false positives while maintaining sensitivity. To investigate the dependence of cerebral parameters on seasonal changes, we applied the analysis of covariance (ANCOVA) by JASP (jasp-stats.org, version 0.9.2.0). ANCOVA is appropriate to test the main and interaction effects of categorical variables (covariates) on a continuous dependent variable. In this analysis, age and sex were selected as covariates, and a cerebral parameter and season were chosen as dependent and fixed factors, respectively. Since ANCOVA (Kruskal–Wallis nonparametric test; Dunn's *post hoc* comparisons; Holm correction) showed that the covariates (sex and age) have interaction effects on most cerebral variables, the effect of seasonal changes, time of day, and temperature on cerebral parameters were investigated separately for both female and male groups. For this analysis, eight subjects aged over 30 years were excluded from these evaluations in order to have a sample in a small age range (20 to 30 years of age). Finally, Cosinor analysis [Eq. (1)] and the sum of 2 cosine functions [Eq. (2)] were applied in order to find the best chronobiological fit model of the cerebral parameters:

$$f(t) = M + A\,\cos\left[\frac{2\pi(t+\varphi)}{24}\right], \tag{1}$$

where $f(t)$ denotes the value of the function at time t (e.g., a cerebral parameter), M is the midline estimating statistic of rhythm, A is the amplitude, t is measured in hours, and φ is the acrophase:

$$f(t) = \text{base} + A_1\,\cos\left[\frac{2\pi(t+\varphi)}{24}\right] + A_2\,\cos\left[\frac{2\pi(t+\varphi)}{12}\right]. \tag{2}$$

Downloaded From: https://www.spiedigitallibrary.org/journals/Neurophotonics on 24 Jun 2020
Terms of Use: https://www.spiedigitallibrary.org/terms-of-use

where $f(t)$ represents the value of the function at time t, base is the cerebral parameter baseline value, A_1 and A_2 are the amplitudes of the cosine functions, and φ is the acrophase.

2.4.4 *Reliability analysis*

The intrasubject variability of all data, including cerebral and cardiorespiratory parameters were analyzed by the intraclass correlation coefficient (ICC) using the R statistical software (R 3.5.2, ICC package, r-project.org). ICC is a more desirable measure of reliability, reflecting both degrees of correlation and agreement between measurements. According to Fleiss,[30] ICC values <0.4, between 0.4 and 0.6, in the range of 0.6 and 0.75, and >0.75 are indicative of poor, moderate, good, and excellent reliability, respectively.

3 Results

3.1 *Cerebral Oxygenation and Perfusion: Higher StO_2 of Right PFC*

For StO_2, we found right-dominant activity ($\Delta StO_2 > 0$), i.e., a highly significant ($p < 0.0001$) FCOA was detected in the resting state [Fig. 1(a)]. No significant ($p = 0.324$) asymmetry was found for [tHb] [Fig. 1(b)]. The intersubject mean value representing the normal value of StO_2 and [tHb] was (mean $\pm$ SD) $73.0\% \pm 5.9\%$ and 41.4 ± 9.3 μM, respectively [Figs. 1(c) and 1(d)]. For the right and left PFC the normal values of StO_2 were $73.7\% \pm 6.9\%$ (right) and $72.3\% \pm 6.1\%$ (left), and of [tHb] 41.4 ± 10.8 (right) and 41.4 ± 10.1 (left) [Figs. 2(a) and 2(b)]. The absolute values of StO_2 and [tHb] during the resting state are shown in Figs. 2(c) and 2(d). All data were normally distributed. From this point on, the outliers were removed and not considered for subsequent evaluations. After removal of the outliers, FCOA remained highly significant ($p < 0.0001$) [nonsignificant for [tHb] ($p = 0.218$)].

3.2 *Cardiorespiratory Activity*

Figures 1(e)–1(h) and 2(e), 2(h)–2(j) show the absolute values of $P_{ET}CO_2$, HR, RR, and PRQ for the individual subjects during resting state. On the group level, mean absolute and SD values of cardiorespiratory parameters were as follows (data were normally distributed): $P_{ET}CO_2$: 39.2 ± 4.4 mmHg, HR: 68 ± 11 beats/min (BPM), RR: 16.5 ± 2.9 breaths/min (BrPM), and PRQ: 4.2 ± 0.9. These values were all in the normal range for healthy adults at rest.

3.3 *Relationships with Systemic Physiology*

A correlation matrix of ΔStO_2, ΔtHb, StO_2, [tHb], $P_{ET}CO_2$, HR, RR, and log(PRQ) variables during the resting state is depicted in Fig. 3(a). In detail, Table S1 in the Supplementary Material shows curve fitted models, goodness-of-fit results, BSE parameter, and a significance level for each pair of variables. Statistically significant correlations were found between cerebral and cardiorespiratory parameters for six pairs of variables: ΔStO_2 versus RR ($p_{FDR} = 0.022$, $p = 0.010$), ΔStO_2 versus log(PRQ) ($p_{FDR} = 0.024$, $p = 0.012$), StO_2 versus $P_{ET}CO_2$ ($p_{FDR} < 0.0001$, $p < 0.0001$), [tHb] versus HR ($p_{FDR} = 0.001$, $p < 0.0004$), [tHb] versus RR ($p_{FDR} = 0.029$, $p = 0.016$), and [tHb] versus log(PRQ) ($p_{FDR} < 0.0001$, $p < 0.0001$).

Correlations were also observed between the cerebral parameters: ΔStO_2 versus ΔtHb ($p_{FDR} = 0.008$, $p = 0.003$), ΔStO_2 versus StO_2 ($p_{FDR} < 0.0001$, $p < 0.0001$), ΔStO_2 versus [tHb] ($p_{FDR} = 0.020$, $p = 0.008$), and StO_2 versus [tHb] ($p_{FDR} < 0.0001$, $p < 0.0001$). A relatively strong correlation between cardiorespiratory parameters was also present: $P_{ET}CO_2$ versus HR ($p_{FDR} < 0.0001$, $p < 0.0001$), $P_{ET}CO_2$ versus RR ($p_{FDR} = 0.039$, $p = 0.022$), $P_{ET}CO_2$ versus log(PRQ) ($p_{FDR} < 0.0001$, $p < 0.0001$), HR versus RR ($p_{FDR} = 0.001$, $p < 0.0005$), HR versus log(PRQ) ($p_{FDR} < 0.0001$, $p < 0.0001$), and RR versus log(PRQ) ($p_{FDR} < 0.0001$, $p < 0.0001$). Since PRQ was calculated from HR and RR, we expected a linear correlation of HR versus log(PRQ), and RR versus log(PRQ). Additionally, Fig. 3(b) illustrates the coefficient of correlation "r" and BSE parameter "ε" for each pair. The order of correlation starting

Downloaded From: https://www.spiedigitallibrary.org/journals/Neurophotonics on 24 Jun 2020
Terms of Use: https://www.spiedigitallibrary.org/terms-of-use

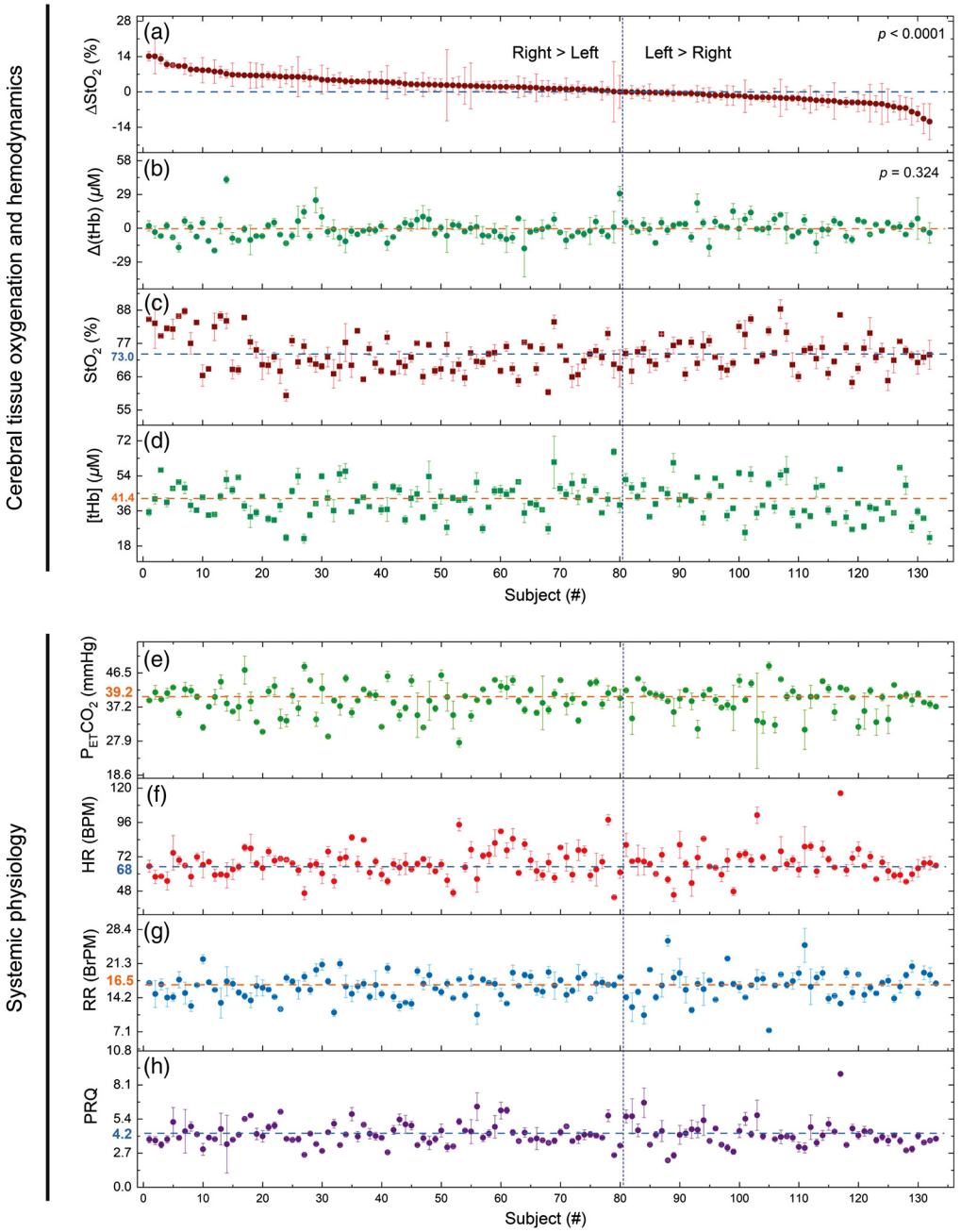

Fig. 1 (a) FCOA of StO_2 at the PFC sorted in descending order on the individual subjects. (b) Asymmetry of [tHb] and absolute values of (c) StO_2, (d) [tHb], (e) $P_{ET}CO_2$, (f) HR, (g) RR, and (h) PRQ displayed according to the ΔStO_2 sorting, at the PFC for individual subjects during resting state. The median and the IQR are shown for each subject.

from strongest (r-value close to 1 and $\varepsilon > 0.5$) is as follows: (1) StO_2 versus $P_{ET}CO_2$, (2) StO_2 versus [tHb], (3) $P_{ET}CO_2$ versus HR, (4) [tHb] versus log(PRQ), (5) $P_{ET}CO_2$ versus log(PRQ), (6) ΔStO_2 versus StO_2, (7) HR versus RR, and (8) [tHb] versus HR.

3.4 *Intrasubject Variability: ICC Values Indicate Good-to-Excellent Reliability of Most Parameters*

Figure 3(c) presents the ICC values of all variables. The ICC of StO_2, [tHb], StO_2 (left), [tHb] (right), [tHb] (left), $P_{ET}CO_2$, HR, and RR indicates excellent reliability. The ICC of

Downloaded From: https://www.spiedigitallibrary.org/journals/Neurophotonics on 24 Jun 2020
Terms of Use: https://www.spiedigitallibrary.org/terms-of-use

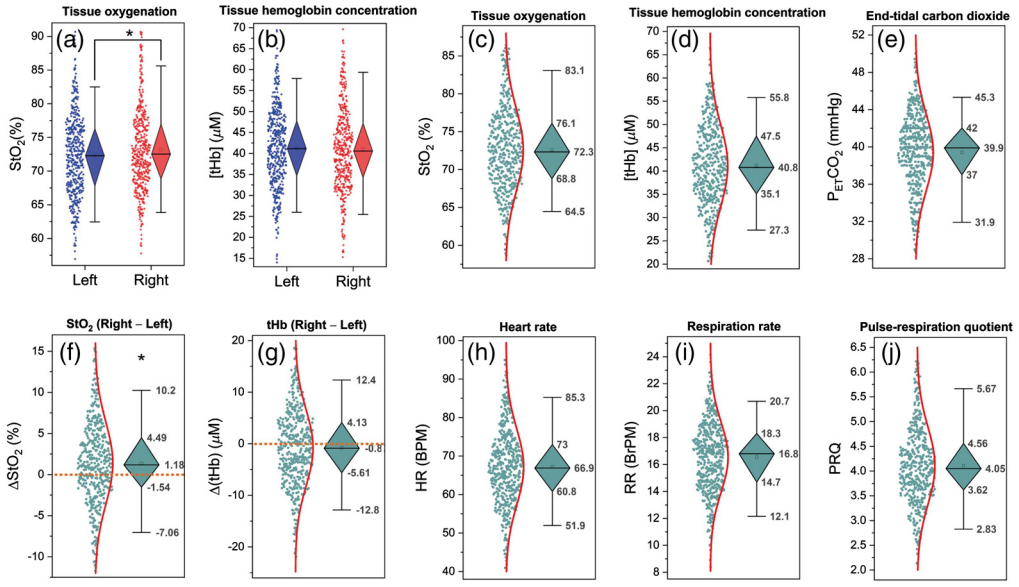

Fig. 2 Diamond box plots showing distributions of absolute (a) StO_2 and (b) [tHb] values at the R-PFC and L-PFC, (c) StO_2, (d) [tHb], (e) $P_{ET}CO_2$, (f) ΔStO_2, (g) ΔtHb, (h) HR, (i) RR, and (j) PRQ values in resting state. The diamond spans the first quartile to the third quartile (IQR). A segment inside the diamond shows the median and whiskers above and below the box plots represent the 95% prediction interval. The asterisks indicate the level of high significance between absolute StO_2 values of the R-PFC and L-PFC (*$p < 0.001$, Wilcoxon signed-rank test). Outliers are not displayed.

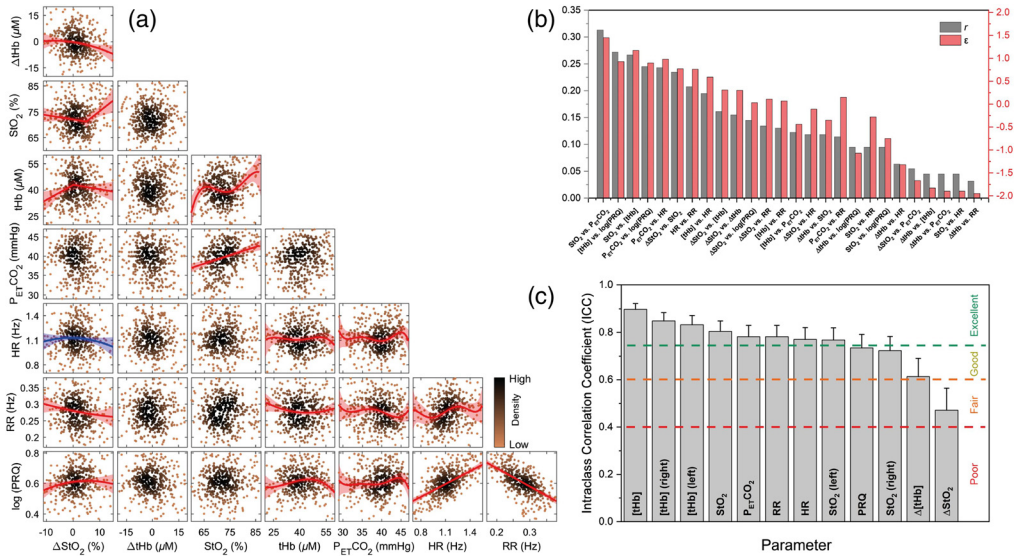

Fig. 3 (a) Correlation matrix of bivariate scatter plots of ΔStO_2, ΔtHb, StO_2, [tHb], $P_{ET}CO_2$, HR, RR, and log(PRQ). The best nonlinear fit is presented for pairs with a significant correlation (red: significant correlation proved by both FDR-corrected and uncorrected p values; blue: only uncorrected p value). The level of significance is calculated from goodness-of-fit results. The red and blue shaded areas show 95% of confidence intervals. Outliers are not displayed. (b) Bar chart of r- and ε values for each pair of ΔStO_2, ΔtHb, StO_2, [tHb], $P_{ET}CO_2$, HR, RR, and log(PRQ) parameters (sorted in descending order of r-values). ε values < -0.5, near-zero ($-0.5 < \varepsilon < 0.5$), between 0.5 and 1, and >1 are indicative of no, inconclusive, moderate, and strong correlation, respectively. (c) Bar chart of ICC values for all cerebral and cardiorespiratory parameters. Error bars represent the 95% confidence interval. The reliability of the ICC is indicated.

Downloaded From: https://www.spiedigitallibrary.org/journals/Neurophotonics on 24 Jun 2020
Terms of Use: https://www.spiedigitallibrary.org/terms-of-use

the PRQ, StO_2 (right), and ΔtHb shows good and the ICC of ΔStO_2 represents moderate reliability.

3.5 *Dependence of Cerebral Parameters on Sex and Seasonal Changes*

The impact of sex and seasons (infradian changes) on cerebral parameters is depicted in Fig. 4. A significant difference due to sex ($p < 0.0001$) was observed in both StO_2 and [tHb]. In addition, Δ[tHb] was higher for males compared to females ($p < 0.001$), but not for ΔStO_2 ($p = 0.635$). We found that FCOA showed the same trend of seasonal changes for both female and male groups and was higher in autumn and winter compared to spring and summer (spring versus autumn, $p = 0.001$; spring versus winter, $p < 0.001$; summer versus autumn, $p = 0.024$; summer versus winter, $p < 0.001$ and autumn versus winter, $p = 0.011$). Interestingly, a Cosinor model fitted to [tHb] data represents completely contrary patterns for male and female groups. Absolute [tHb] values of males were higher in spring and summer than that of in autumn and winter. Conversely, the [tHb] values of females were observed at higher levels in autumn and winter in comparison with spring and summer.

3.6 *Dependence of Cerebral Parameters on Time of Day*

The effect of time of day (circadian changes) on cerebral parameters is also shown in Fig. 4. A sum of 2 cosine functions was applied to fit the circadian rhythm of the data. The same trend of higher StO_2 values in the morning was observed for males and females ($p < 0.001$). Males demonstrated very high [tHb] values in the early morning and late evening ($p < 0.001$), but the trend was almost opposite in females ($p < 0.05$). The highest FCOA for [tHb] values were found at 10:00 and 14:00 for males and females, respectively. Regardless of sex, a highly significant difference was found between StO_2 values of morning and afternoon ($p < 0.001$). There was also a significant difference between StO_2 values of morning and evening ($p = 0.011$). No significant changes were found for [tHb] (morning versus afternoon: $p = 0.061$; morning versus evening: $p = 0.17$).

3.7 *Dependence of Cerebral Parameters on Temperature*

Figure 5 shows the changes in room temperature with respect to season 5(a) and time of day 5(b), and the temperature dependency of cerebral parameters [5(c)–5(f)]. The mean room temperature

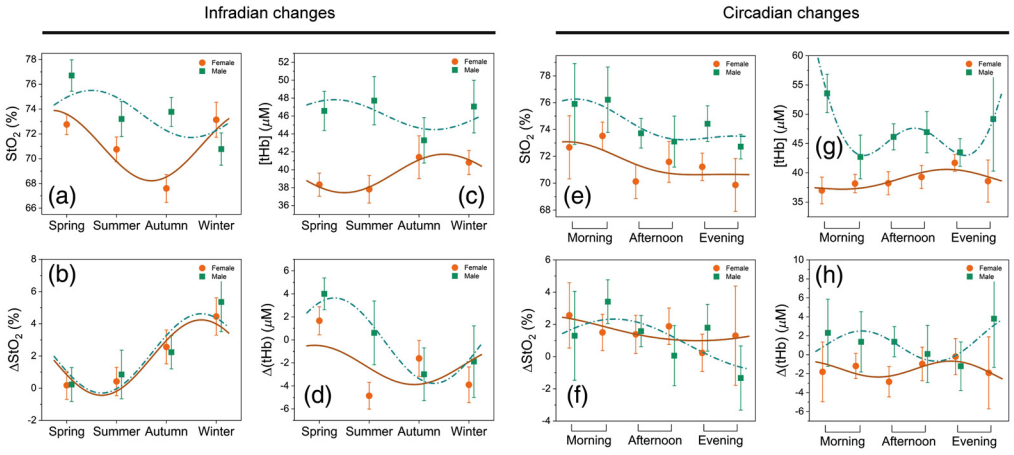

Fig. 4 Changes in StO_2, [tHb], ΔStO_2, and ΔtHb due to time of year [infradian changes (a)–(d)] and time of day [circadian changes (e)–(h); morning: 7:00–9:30 and 9:30–12:00; afternoon: 12:00–14:30 and 14:30–17:00; evening: 17:00–19:30 and 19:30–22:00] for females (orange) and males (green). Cosinor model and the sum of 2 cosines function are fitted to infradian and circadian changes, respectively (female, dark orange lines; male, dashed green lines). Error bars represent the 95% confidence interval.

Downloaded From: https://www.spiedigitallibrary.org/journals/Neurophotonics on 24 Jun 2020
Terms of Use: https://www.spiedigitallibrary.org/terms-of-use

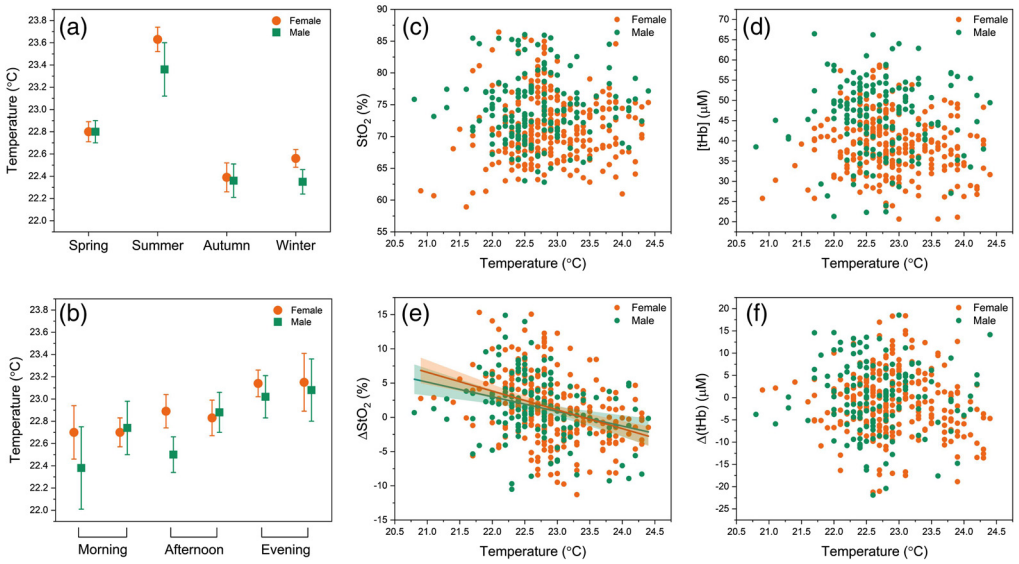

Fig. 5 Changes in temperature with (a) time of year and (b) time of day. Dependence of (c) StO_2, (d) [tHb], (e) ΔStO_2, and (f) ΔtHb on temperature. The lines represent a linear fit and the shaded areas and error bars show 95% confidence intervals. Outliers are not displayed.

was 22.8°C ± 0.6°C (range: 20.8°C to 24.8°C). Since the room was not air-conditioned, time of day and seasonal changes had an impact on the room temperature. As expected, the maximum room temperatures were recorded in summer and during the late evening. There was no significant linear correlation between room temperature and cerebral. The only exception was ΔStO_2, which decreased with increasing room temperature (females: $r = -0.35$, $p < 0.0001$; males: $r = -0.30$, $p < 0.0002$).

3.8 *Dependence of Cerebral Parameters on Mood and Chronotype*

The mean valence, arousal, and dominance ratings during resting state assessed by SAM scales (ranging from 1 to 5) was 4.02 ± 0.69, 2.92 ± 0.91, and 3.24 ± 0.77, respectively. The dependence of cerebral parameters on mood and chronotype is displayed in Fig. 6. No correlation was observed between the cerebral parameters and the positive affect scale of the PANAS

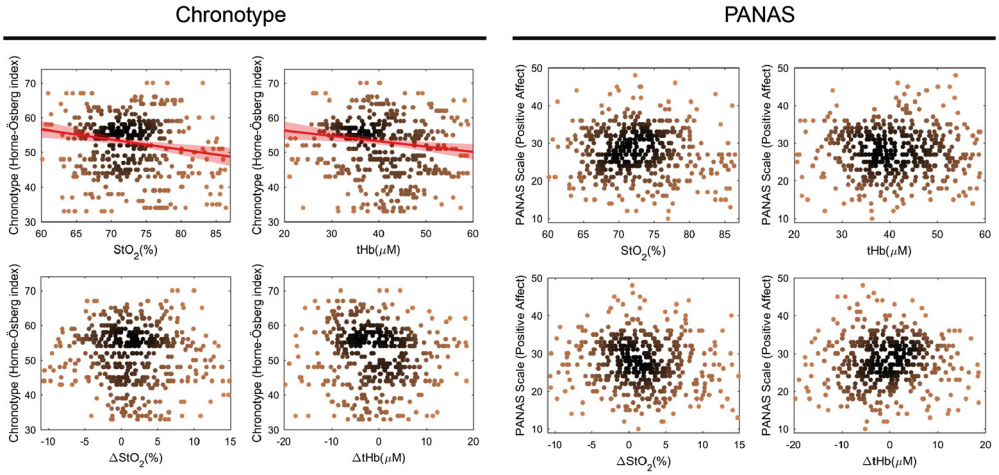

Fig. 6 The scatter plots show the dependence of StO_2, [tHb], ΔStO_2, and ΔtHb on chronotype (Horne-Östberg index) and mood (positive affect scale of PANAS). Correlations between the data are indicated by a linear fit, and the red shaded areas indicate 95% confidence intervals. Outliers are not displayed.

Downloaded From: https://www.spiedigitallibrary.org/journals/Neurophotonics on 24 Jun 2020
Terms of Use: https://www.spiedigitallibrary.org/terms-of-use

questionnaire. The Horne and Östberg index was calculated for each subject to measure the chronotype. The highest numbers (score: 59 to 86) indicate morningness and the lowest numbers (score: 16 to 41) eveningness. Scores from 42 to 58 indicate neither morningness nor eveningness. We found a linear correlation between StO_2 versus chronotype ($r = -0.1$, $p = 0.03$), and [tHb] versus chronotype ($r = -0.09$, $p = 0.04$).

4 Discussion

4.1 *Absolute Values of Tissue Oxygenation and Hemoglobin Concentration*

The normal range of StO_2 and [tHb] of the brain was investigated for medical applications. These absolute values are approximately in accordance with the literature.[31,32] The absolute StO_2 values of the PFC are in good agreement with Choi et al. (R-PFC: $74.75\% \pm 5.83\%$ versus. L-PFC: $75.63\% \pm 5.86\%$; $N = 30$, age: 20 to 50 years, device: Imagent, ISS Inc.).[33] However, our absolute [tHb] values at the PFC are lower in comparison with their findings (R-PFC: 79.68 ± 12.15 μM, L-PFC: 76.93 ± 14.98 μM). Our [tHb] values are similar to those of Vernieri et al. (left versus right frontal region: 46.2 ± 11.9 μM versus 44.0 ± 12.9 μM; 30 subjects, age: 63.9 ± 8.2, device: Oximeter, ISS Inc.).[34] Moreover, our StO_2 values are a bit higher compared to our previous study [StO_2 (right) = 68.6% (IQR: 63.5% to 72.4%), StO_2 (left) = 56.8% (IQR: 52.9% to 63.4%); 24 subjects, age: 22.0 ± 6.4 years, device: OxiplexTS, ISS Inc.].[1] The reasons for the difference between studies may be the age, physiological state of subjects, or methodology.

4.2 *Absolute Values of Cardiorespiratory Parameters*

Arterial partial pressure of carbon dioxide ($PaCO_2$) is one of the strongest parameters that affect CBF and [tHb].[19] Therefore, $PaCO_2$ has been included in functional brain studies to ensure a correct interpretation of the signals.[35–37] We measured $PaCO_2$ by the $P_{ET}CO_2$ method, which also provides continuous and noninvasive RR. Our $P_{ET}CO_2$ values were in agreement with the literature.[38–41]

Our findings showed that the mean value of HR was 68 ± 11 BPM (range: 41 to 116 BPM, females: 69 ± 11 BPM, males: 66 ± 11 BPM; $p = 0.036$). In 35,000 healthy subjects, a mean HR of 72 BPM (age: 20 and over, females: 74 ± 0.2 BPM, males: 71 ± 0.3 BPM; $p < 0.05$) was determined, which is close to our results.[42]

The mean RR value measured in our study was 16.5 ± 2.9 BrPM, which is within typical RR for adults (range: 6.9 to 27.1 BrPM, females: 16.8 ± 2.8 BPM, males: 16.1 ± 3.1 BPM; $p = 0.015$).

The PRQ is a parameter to attain the overall current state of human physiology.[43] PRQ represents the state of the ANS and is a measure of cardiorespiratory coordination. PRQ is time- and sex-dependent, and changes during human development, physical activity, and body posture with specific patterns during sleep.[43] The resting state PRQ distribution has a peak at ~4.[44–46] We also found a mean resting state PRQ of ~4 (4.2 ± 0.9, ranging from 2.1 to 9.0).

4.3 *Relationships with Systemic Physiology*

Although systemic physiological activity affects the absolute values of StO_2 and [tHb], FCOA was not influenced. The reason is that both R-PFC and L-PFC are affected in the same way by systemic physiology.[1,21] Although we generally confirmed this finding, we found nonlinear correlations between ΔStO_2 versus RR ($p = 0.022$) and ΔStO_2 versus PRQ ($p = 0.024$).

As expected, we found a highly significant ($R^2 = 0.10$, $p < 0.0001$) positive linear correlation between StO_2 and $P_{ET}CO_2$. Our finding is in agreement with the study carried out by Miller and Mitra.[47] and with the physiologically well-known CO_2-response, i.e., a decrease in $P_{ET}CO_2$ (hypocapnia) reduces the CBF by cerebral vasoconstriction.[48] This reduced oxygen supply leads to a lower StO_2.[35,36] Hence, $P_{ET}CO_2$ is positively correlated with StO_2

Downloaded From: https://www.spiedigitallibrary.org/journals/Neurophotonics on 24 Jun 2020
Terms of Use: https://www.spiedigitallibrary.org/terms-of-use

4.4 *Frontal Cortex Oxygenation Asymmetry*

In EEG studies, activity in left frontal regions is mostly associated with appetitive motivation and approach-related affect such as hope, happiness, and joy (positive affect). Conversely, the right frontal regions are related to vigilant attention and behavioral inhibition that regularly occurs during certain withdrawal-related affect such as depression and nervousness (negative affect).[11,12,49–51] In general, the right frontal cortex reflects motivational systems of approach and avoidance, whereas the left frontal cortex inhibits the amygdala and downregulates negative affect.[52,53] Higher right frontal activity is attributed to greater negative affect (e.g., film-induced fear and disgust), whereas positive affect (e.g., film-induced happiness) elicits a higher left frontal activity.[54,55]

We hypothesized that the FCOA reveals asymmetry of the PFC neuronal activity at rest. The StO_2 was higher at the R-PFC than the L-PFC, indicating that the R-PFC is more activated than the L-PFC and this indicates a higher inhibitory activity or withdrawal motivation. This is reasonable considering that the subjects were in the resting state. Such rightward lateralization has also been found in the literature.[56,57] Although our findings are in line with several studies indicating that the right cortices have a stronger response compared to the left ones, some studies have reported no hemispheric differences or even leftward regional lateralization.[33,58] Liu et al.[6] demonstrated that right or left regional laterality could be observed across different brain systems depending on multiple genetic or environmental mechanisms.

4.4.1 *FCOA as an indicator of human health*

The R-PFC plays a vital role in the brain's response to stress because this area is a primary part of both the emotion and vigilance networks. Neurons that are either the target or the releasing site of an array of stress mediators (neurotransmitter and hormone) have been recognized in this area.[59] Thus FCOA is associated with specific emotional responses to mental stress and personality traits (state influence versus trait influence).[14,52,60] High left frontal brain activity is more psychologically and physically healthy than relatively less left frontal brain activity.[53,61] Individuals with higher L-PFC activity have lower concentrations of the stress hormone cortisol and the corticotrophin-releasing hormone, higher activity of natural killer cells, and higher antibody concentration in response to influenza vaccines.[53,62] It was also demonstrated that subjects with higher L-PFC activity, recover more quickly from a negative occurrence with higher levels of psychological well-being.[53,63] Conversely, dominant R-PFC activity is associated with increased activation of the hypothalamic–pituitary–adrenal axis[59,64–66] and higher secretion of corticotrophin-releasing hormone and adrenal steroid hormones (e.g., glucocorticoids and adrenal androgens).[66–69] Higher R-PFC activity may occur during stressful situations, such as a test or job interview.[70] An EEG study showed that FEA was shifted from the left during an easy examination session to the right during a stressful examination session.[71] A higher change in FEA from the easy to the stressful session was associated with more adverse health conditions. Further research suggested that subjects with more R-PFC activity compared to L-PFC are sensitive to mental stress and prone to exhibit various stress-induced somatic disorders.[56,64] Moreover, it was found that higher levels of R-PFC activation predict a reduced immune response in humans.[59,62] The more an individual's FEA is changed during periods of stress, the more negative health consequences are likely to be experienced.[49]

We observed no correlation between cerebral parameters; in particular, FCOA and the positive affect scale of the PANAS questionnaire.

Depression is associated with an under-activation of the approach system and/or over-activation of the withdrawal system.[72] Research provides support for an association between FEA and depression[12,73,74] and may predict the emotional state in depression disorders.[72] Although there is a small number of studies linking FEA with psychopathology, the research suggests FEA may be a promising marker of depression vulnerability.[49] Decreased relative left-frontal activity during resting state was attributed to increased vulnerability to depression.[75] In adolescent boys without a history of depression, right-sided frontal activation predicted depressive symptoms 1 year later.[76] Many studies indicate that FEA is a valid marker for depression vulnerability. Regardless of whether anxiety was used as a covariate or not, frontal alpha

Downloaded From: https://www.spiedigitallibrary.org/journals/Neurophotonics on 24 Jun 2020
Terms of Use: https://www.spiedigitallibrary.org/terms-of-use

asymmetry indicative of relatively higher right frontal activity predicts depression, whereas the opposite is not true.[77]

Thus the measurement of such an FEA and FCOA may have considerable clinical value.

4.4.2 *Anatomic, physiologic, and genetic influences*

The corpus callosum provides a neuroanatomical correlation in the asymmetry of the frontal cortices.[78] Negative affect generally leads to activation in the R-PFC, amygdala, inferior frontal gyrus, and insula, whereas the L-PFC may play a role in the downregulation of amygdala and is associated with reward-related cortical regions.[53,65,79] The neural correlates of vigilance and sustained attention are primarily localized in the right prefrontal and parietal lobe and the thalamus.[80] The link between left frontal and left amygdala activity is crucial for emotional regulation.[73]

Genetic models have been proposed to account for cerebral dominance, and anatomical asymmetries are likely influenced by genetic factors. However, no gene or pathway has yet been identified as a determinant of lateralization, although there are a number of candidates including LMO4, STMN4, BAI1, and IGFBP5, which were highly expressed in the right regions.[3,81,82]

4.4.3 *FEA as a promising marker of subject characteristics and emotions*

It was demonstrated that asymmetry in PFC neuronal activity during the resting state, measured with EEG, predicts the emotional state.[72]

Table 1 shows a summary of the emotions and characteristics of individuals with FEA.

4.4.4 *Environment and certain situational variable*

Experimental, environmental, and situational factors that influence approach or withdrawal motivation may affect FCOA. These variables include body posture, experimental conditions, trait

Table 1 A summary of subject characteristics and emotions with left and right dominant activity

Left dominant activity	Right dominant activity	References
Anxious apprehension (e.g., worry)	Anxious arousal (e.g., panic)	72, 73, and 83–86
Maniacs	Phobias (social phobics)	50, 83, 87 and 88
Extrovert	Introvert (neuroticism)	89 and 90
Promotion (a need for growth and advancement)	Prevention (a need for safety and security)	91 and 92
Anger, joy, and jealousy	Disgust and depression	12 and 93–97
Hostility to social rejection	Isolation to social rejection	60 and 98
Higher socioeconomic status	Lower socioeconomic status	99
—	Defensiveness	100 and 101
—	Hopelessness	75 and 102
—	Less risk-taking	103
—	Ostracism	104
—	Obsessive-compulsive disorder	105
—	More concerned with making mistakes and punishment	106

Downloaded From: https://www.spiedigitallibrary.org/journals/Neurophotonics on 24 Jun 2020
Terms of Use: https://www.spiedigitallibrary.org/terms-of-use

variables, and timing. Thus the seasons and time of day play essential roles in FCOA scores. We found higher R-PFC activity (higher StO_2) associated with more depression in autumn and winter compared to spring and summer. These findings are in line with a previous study.[107] Indeed, it is known that the population experiences a worsening of their mood and stronger depressive symptoms (seasonal affective disorder) in winter.[108–110] This is also visible in the highly significant seasonal variation in cortisol levels in winter and autumn compared to spring and summer.[111] Thus it is reasonable that we found a significant influence of the seasons on FCOA.

We also found a significant dependence of the StO_2 on the time of day (Fig. 4). Higher StO_2 values were observed in the morning compared to the afternoon and evening. Since [tHb] was not significantly changed during the day, such an increase in StO_2 may imply that more oxygenated blood was present in the brain tissue during the morning hours compared to the evening and afternoon. We can interpret this increase as reduced oxygen consumption and, thus, energy metabolism in the morning, which would be in agreement with the synaptic homeostasis hypothesis.[112] This increase could also be linked to circadian effects, e.g., cortisol rhythm exerting its wake-promoting effect in the morning hours.[113,114] Moreover, the present findings indicated that the time of day has no significant influence on FCOA, which is in line with the literature.[115]

It was also shown in this study that FCOA in StO_2 decreased with increasing room temperature. In other words, we found that the lower the room temperature, the higher the R-PFC activation. Lower room temperature increased whole-body cooling sensation and reduced thermal comfort, especially after prolonged exposure.[116] Our findings are in line with the approach-motivational model, which links higher R-PFC activation to greater withdrawal-related affect (negative affect) such as uncomfortableness, nervousness, and depression. It is known that increasing the length of daylight and temperature results in a decrease in the depression score,[110,117] which indirectly confirms our findings in terms of the effects of both seasons and temperature on FCOA.

5 Conclusion

We found highly significant ($p < 0.0001$) FCOA, which was correlated to room temperature, RR, and PRQ but was not affected by mood or chronotype of the subject. This higher right PFC activity may be due to the more prominent inhibition activity during the resting state.

The absolute values of StO_2 and [tHb] were influenced by systemic physiological activity, such as $P_{ET}CO_2$, HR, RR, and PRQ, and gender.

FCOA and StO_2 were dependent on season and time of day, respectively. FCOA was higher in autumn/winter compared to spring/summer, whereas StO_2 was higher in the morning than in the afternoon/evening.

These relevant findings were only achievable using FD-fNIRS instrumentation that enabled the measurement of absolute values while using a SPA-fNIRS approach.

Our study demonstrates that FCOA is real, while providing unique insights to understand this remarkable phenomenon.

Disclosures

The authors declared no potential conflicts of interest with respect to the research, authorship, and/or publication of this article.

Acknowledgments

We would like to thank our students for their work and our subjects for participating in this study. The financial support of the Software AG Foundation (Grant No. P12117) and the Christophorus Foundation (Grant Nos. 253CST and 355CST) is gratefully acknowledged. We thank Oliver Kress, PhD for valuable comments and proofreading of the manuscript.

Downloaded From: https://www.spiedigitallibrary.org/journals/Neurophotonics on 24 Jun 2020
Terms of Use: https://www.spiedigitallibrary.org/terms-of-use

References

1. F. Scholkmann, H. Zohdi, and U. Wolf, "Right-left asymmetry of prefrontal cerebral oxygenation: does it depend on systemic physiological activity, absolute tissue oxygenation or hemoglobin concentration?" *Adv. Exp. Med. Biol.* **1232**, 105–112 (2020).
2. A. Hougaard et al., "Cerebral asymmetry of fMRI-BOLD responses to visual stimulation," *PLoS One* **10**, e0126477 (2015).
3. T. Sun and C. A. Walsh, "Molecular approaches to brain asymmetry and handedness," *Nat. Rev. Neurosci.* **7**, 655–662 (2006).
4. K. Hugdahl, "Symmetry and asymmetry in the human brain," *Eur. Rev.* **13**, 119–133 (2005).
5. F. Homae, "A brain of two halves: insights into interhemispheric organization provided by near-infrared spectroscopy," *Neuroimage* **85**, 354–362 (2014).
6. H. Liu et al., "Evidence from intrinsic activity that asymmetry of the human brain is controlled by multiple factors," *Proc. Natl. Acad. Sci. U. S. A.* **106**, 20499–20503 (2009).
7. P. K. Mutha, K. Y. Haaland, and R. L. Sainburg, "The effects of brain lateralization on motor control and adaptation," *J. Mot. Behav.* **44**, 455–469 (2012).
8. Y. Wang et al., "Multimodal mapping of the face connectome," *Nat. Hum. Behav.* **4**, 397–411 (2020).
9. R. J. Davidson, "Emotion and affective style: hemispheric substrates," *Psychol. Sci.* **3**, 39–43 (1992).
10. R. J. Davidson, "Affective style and affective disorders: perspectives from affective neuroscience," *Cognit. Emot.* **12**, 307–330 (1998).
11. P. A. Gable, L. B. Neal, and A. H. Threadgill, "Regulatory behavior and frontal activity: considering the role of revised-BIS in relative right frontal asymmetry," *Psychophysiology* **55**, e12910 (2018).
12. B. D. Nelson et al., "Depression symptom dimensions and asymmetrical frontal cortical activity while anticipating reward," *Psychophysiology* **55**, e12892 (2018).
13. P. C. Schmid et al., "Frontal cortical effects on feedback processing and reinforcement learning: relation of EEG asymmetry with the feedback-related negativity and behavior," *Psychophysiology* **55**, e12911 (2018).
14. W. Ishikawa et al., "New method of analyzing NIRS data from prefrontal cortex at rest," *Adv. Exp. Med. Biol.* **789**, 391–397 (2013).
15. P. Pinti et al., "The present and future use of functional near-infrared spectroscopy (fNIRS) for cognitive neuroscience," *Ann. N. Y. Acad. Sci.* **1464**(1), 5–29 (201820).
16. H. Zohdi et al., "Long-term changes in optical properties (μa, μ's, μeff and DPF) of human head tissue during functional neuroimaging experiments," *Adv. Exp. Med. Biol.* **1072**, 331–337 (2018).
17. F. Scholkmann et al., "Absolute values of optical properties (μa, μ's, μeff and DPF) of human head tissue: dependence on head region and individual," *Adv. Exp. Med. Biol.* **1072**, 325–330 (2018).
18. F. Lange and I. Tachtsidis, "Clinical brain monitoring with time domain NIRS: a review and future perspectives," *Appl. Sci.* **9**, 1612 (2019).
19. F. Scholkmann et al., "A review on continuous wave functional near-infrared spectroscopy and imaging instrumentation and methodology," *Neuroimage* **85**, 6–27 (2014).
20. F. Scholkmann et al., "Effect of short-term colored-light exposure on cerebral hemodynamics and oxygenation, and systemic physiological activity," *Neurophotonics* **4**, 045005 (2017).
21. N. Nasseri et al., "Impact of changes in systemic physiology on fNIRS/NIRS signals: analysis based on oblique subspace projections decomposition," *Adv. Exp. Med. Biol.* **1072**, 119–125 (2018).
22. H. Zohdi, F. Scholkmann, and U. Wolf, "Long-term blue light exposure changes frontal and occipital cerebral hemodynamics: not all subjects react the same," *Adv. Exp. Med. Biol.* **1269** (2020).
23. R. C. Oldfield, "The assessment and analysis of handedness: the Edinburgh inventory," *Neuropsychologia* **9**, 97–113 (1971).

Downloaded From: https://www.spiedigitallibrary.org/journals/Neurophotonics on 24 Jun 2020
Terms of Use: https://www.spiedigitallibrary.org/terms-of-use

24. D. Watson, L. C. Anna, and A. Tellegen, "Development and validation of brief measures of positive and negative affect: the PANAS scales," *J. Pers. Soc. Psychol.* **54**, 1063 (1988).
25. M. M. Bradley and P. J. Lang, "Measuring emotion: the self-assessment manikin and the semantic differential," *J. Behav. Ther. Exp. Psychiatry* **25**, 49–59 (1994).
26. J. A. Horne and O. Östberg, "A self-assessment questionnaire to determine morningness-eveningness in human circadian rhythms," *Int. J. Chronobiol.* **4**(2), 97–110 (1976).
27. H. H. Jasper, "The ten-twenty electrode system of the International Federation," *Electroencephalogr. Clin. Neurophysiol.* **10**, 370–375 (1958).
28. F. Scholkmann et al., "How to detect and reduce movement artifacts in near-infrared imaging using moving standard deviation and spline interpolation," *Physiol. Meas.* **31**, 649–662 (2010).
29. D. S. Schwarzkopf, "Non-dichotomous inference using bootstrapped evidence," bioRxiv, p. 017327 (2015).
30. J. Fleiss, *The Design and Analysis of Clinical Experiments*, Wiley, New York (1986).
31. V. Quaresima et al., "Bilateral prefrontal cortex oxygenation responses to a verbal fluency task: a multichannel time-resolved near-infrared topography study," *J. Biomed. Opt.* **10**, 011012 (2005).
32. Y. Murayama et al., "Relation between cognitive function and baseline concentrations of hemoglobin in prefrontal cortex of elderly people measured by time-resolved near-infrared spectroscopy," *Adv. Exp. Med. Biol.* **977**, 269–276 (2017).
33. J. Choi et al., "Noninvasive determination of the optical properties of adult brain: near-infrared spectroscopy approach," *J. Biomed. Opt.* **9**(1), 221–229 (2004).
34. F. Vernieri et al., "Transcranial Doppler and near-infrared spectroscopy can evaluate the hemodynamic effect of carotid artery occlusion," *Stroke* **35**, 64–70 (2004).
35. F. Scholkmann et al., "Cerebral hemodynamic and oxygenation changes induced by inner and heard speech: a study combining functional near-infrared spectroscopy and capnography," *J. Biomed. Opt.* **19**, 017002 (2014).
36. F. Scholkmann et al., "End-tidal CO_2: an important parameter for a correct interpretation in functional brain studies using speech tasks," *Neuroimage* **66**, 71–79 (2013).
37. F. Scholkmann, M. Wolf, and U. Wolf, "The effect of inner speech on arterial CO_2 and cerebral hemodynamics and oxygenation: a functional NIRS study," in *Oxygen Transport to Tissue XXXV*, S. Van Huffel et al., Eds., pp. 81–87, Springer, New York (2013).
38. C. J. Gauthier et al., "Absolute quantification of resting oxygen metabolism and metabolic reactivity during functional activation using QUO2 MRI," *Neuroimage* **63**, 1353–1363 (2012).
39. J. Hinkelbein et al., "Accuracy and precision of three different methods to determine Pco_2 ($P_a\,co_2$ vs. $P_{et}co_2$ vs. $P_{tc}co_2$) during interhospital ground transport of critically ill and ventilated adults," *J. Trauma* **65**, 10–18 (2008).
40. A. M. Golestani et al., "Mapping the end-tidal CO_2 response function in the resting-state BOLD fMRI signal: spatial specificity, test-retest reliability and effect of fMRI sampling rate," *Neuroimage* **104**, 266–277 (2015).
41. I. Lajoie, F. B. Tancredi, and R. D. Hoge, "Regional reproducibility of BOLD calibration parameter M, OEF and resting-state $CMRO_2$ measurements with QUO2 MRI," *PLoS One* **11**, e0163071–31 (2016).
42. Y. Ostchega et al., "Resting pulse rate reference data for children, adolescents, and adults: United States, 1999–2008," *Natl. Health Stat. Rep.* **41**, 1–16 (2011).
43. F. Scholkmann and U. Wolf, "The pulse-respiration quotient: a powerful but untapped parameter for modern studies about human physiology and pathophysiology," *Front. Physiol.* **10**, 1–18 (2019).
44. F. Scholkmann, H. Zohdi, and U. Wolf, "The resting-state pulse-respiration quotient of humans: lognormally distributed and centred around a value of four," *Physiol. Res.* **68**, 1027–1032 (2019).
45. M. Moser et al., "Phase and frequency coordination of cardiac and respiratory function," *Biol. Rhythm Res.* **26**, 100–111 (1995).
46. D. von Bonin et al., "Adaption of cardio-respiratory balance during day-rest compared to deep sleep-An indicator for quality of life?" *Psychiatry Res* **219**, 638–644 (2014).

Downloaded From: https://www.spiedigitallibrary.org/journals/Neurophotonics on 24 Jun 2020
Terms of Use: https://www.spiedigitallibrary.org/terms-of-use

47. S. Miller and K. Mitra, "NIRS-based cerebrovascular regulation assessment: exercise and cerebrovascular reactivity," *Neurophotonics* **4**, 041503 (2017).
48. K. Szabo et al., "Hypocapnia induced vasoconstriction significantly inhibits the neurovascular coupling in humans," *J. Neurol. Sci.* **309**, 58–62 (2011).
49. S. J. Reznik and J. J. B. Allen, "Frontal asymmetry as a mediator and moderator of emotion: an updated review," *Psychophysiology* **55**, e12965 (2018).
50. R. J. Davidson, D. C. Jackson, and N. H. Kalin, "Emotion, plasticity, context, and regulation: perspectives from affective neuroscience," *Psychol. Bull.* **126**, 890–909 (2000).
51. H. Fischer et al., "Right-sided human prefrontal brain activation during acquisition of conditioned fear," *Emotion* **2**, 233–241 (2002).
52. J. J. B. Allen et al., "Frontal EEG alpha asymmetry and emotion: from neural underpinnings and methodological considerations to psychopathology and social cognition," *Psychophysiology* **55**, e13028 (2018).
53. R. J. Davidson, "What does the prefrontal cortex 'do' in affect: perspectives on frontal EEG asymmetry research," *Biol. Psychol.* **67**, 219–234 (2004).
54. A. J. Tomarken, R. J. Davidson, and J. B. Henriques, "Resting frontal brain asymmetry predicts affective responses to films," *J. Pers. Soc. Psychol.* **59**, 791–801 (1990).
55. R. E. Wheeler, R. J. Davidson, and A. J. Tomarken, "Frontal brain asymmetry and emotional reactivity: a biological substrate of affective style," *Psychophysiology* **30**, 82–89 (1993).
56. W. Ishikawa et al., "Correlation between asymmetry of spontaneous oscillation of hemodynamic changes in the prefrontal cortex and anxiety levels: a near-infrared spectroscopy study," *J. Biomed. Opt.* **19**, 027005 (2014).
57. Y. Murayama, L. Hu, and K. Sakatani, "Relation between prefrontal cortex activity and respiratory rate during mental stress tasks: a near-infrared spectroscopic study," *Adv. Exp. Med. Biol.* **923**, 209–214 (2016).
58. A. J. Metz et al., "Continuous coloured light altered human brain haemodynamics and oxygenation assessed by systemic physiology augmented functional near-infrared spectroscopy," *Sci. Rep.* **7**, 10027 (2017).
59. J. Wang et al., "Perfusion functional MRI reveals cerebral blood flow pattern under psychological stress," *Proc. Natl. Acad. Sci. U. S. A.* **102**, 17804–17809 (2005).
60. E. Harmon-Jones and P. A. Gable, "On the role of asymmetric frontal cortical activity in approach and withdrawal motivation: an updated review of the evidence," *Psychophysiology* **55**, e12879 (2018).
61. E. Harmon-Jones, "Contributions from research on anger and cognitive dissonance to understanding the motivational functions of asymmetrical frontal brain activity," *Biol. Psychol.* **67**, 51–76 (2004).
62. M. A. Rosenkranz et al., "Affective style and in vivo immune response: neurobehavioral mechanisms," *Proc. Natl. Acad. Sci. U. S. A.* **100**, 11148–11152 (2003).
63. D. C. Jackson et al., "Now you feel it, now you don't: frontal brain electrical asymmetry and individual differences in emotion regulation," *Psychol. Sci.* **14**, 612–617 (2003).
64. K. Sakatani, "Optical diagnosis of mental stress: review," *Adv. Exp. Med. Biol.* **737**, 89–95 (2012).
65. R. M. Buijs and C. G. Van Eden, "The integration of stress by the hypothalamus, amygdala and prefrontal cortex: balance between the autonomic nervous system and the neuroendocrine system," *Prog. Brain Res.* **126**, 117–132 (2000).
66. M. Tanida, M. Katsuyama, and K. Sakatani, "Relation between mental stress-induced prefrontal cortex activity and skin conditions: a near-infrared spectroscopy study," *Brain Res.* **1184**, 210–216 (2007).
67. K. E. Habib, P. W. Gold, and G. P. Chrousos, "Neuroendocrinology of stress," *Endocrinol. Metab. Clin.* **30**, 695–728 (2001).
68. C. Tsigos and G. P. Chrousos, "Hypothalamic-pituitary-adrenal axis, neuroendocrine factors and stress," *J. Psychosom. Res.* **53**, 865–871 (2002).
69. M. Tanida, M. Katsuyama, and K. Sakatani, "Effects of fragrance administration on stress-induced prefrontal cortex activity and sebum secretion in the facial skin," *Neurosci. Lett.* **432**, 157–161 (2008).

Downloaded From: https://www.spiedigitallibrary.org/journals/Neurophotonics on 24 Jun 2020
Terms of Use: https://www.spiedigitallibrary.org/terms-of-use

70. B. S. McEwen and E. N. Lasley, *The End of Stress as We Know It*, Joseph Henry Press, Washington, D.C. (2002).
71. R. S. Lewis, N. Y. Weekes, and T. H. Wang, "The effect of a naturalistic stressor on frontal EEG asymmetry, stress, and health," *Biol. Psychol.* **75**, 239–247 (2007).
72. A. H. Kemp et al., "Disorder specificity despite comorbidity: resting EEG alpha asymmetry in major depressive disorder and post-traumatic stress disorder," *Biol. Psychol.* **85**, 350–354 (2010).
73. G. E. Bruder, J. W. Stewart, and P. J. McGrath, "Right brain, left brain in depressive disorders: clinical and theoretical implications of behavioral, electrophysiological and neuroimaging findings," *Neurosci. Biobehav. Rev.* **78**, 178–191 (2017).
74. N. van der Vinne et al., "Frontal alpha asymmetry as a diagnostic marker in depression: fact or fiction? A meta-analysis," *NeuroImage Clin.* **16**, 79–87 (2017).
75. R. Nusslock et al., "Cognitive vulnerability and frontal brain asymmetry: common predictors of first prospective depressive episode," *J. Abnorm. Psychol.* **120**, 497–503 (2011).
76. A. M. Mitchell and P. Pössel, "Frontal brain activity pattern predicts depression in adolescent boys," *Biol. Psychol.* **89**, 525–527 (2012).
77. P. Pössel et al., "A longitudinal study of cortical EEG activity in adolescents," *Biol. Psychol.* **78**, 173–178 (2008).
78. D. J. L. G. Schutter and E. Harmon-Jones, "The corpus callosum: a commissural road to anger and aggression," *Neurosci. Biobehav. Rev.* **37**, 2481–2488 (2013).
79. R. J. Davidson, "Darwin and the neural bases of emotion and affective style," *Ann. N. Y. Acad. Sci.* **1000**, 316–336 (2003).
80. M. Sarter, B. Givens, and J. P. Bruno, "The cognitive neuroscience of sustained attention: where top-down meets bottom-up," *Brain Res. Rev.* **35**, 146–160 (2001).
81. T. Sun et al., "Early asymmetry of gene transcription in embryonic human left and right cerebral cortex," *Science* **308**, 1794–1798 (2005).
82. C. Lai et al., "A forkhead-domain gene is mutated in a severe speech and language disorder," *Nature* **413**, 519–523 (2001).
83. R. J. Davidson et al., "While a phobic waits: regional brain electrical and autonomic activity in social phobics during anticipation of public speaking," *Biol. Psychiatry* **47**, 85–95 (2000).
84. G. Wiedemann et al., "Frontal brain hipoactivity as a biological substrate of anxiety in patients with panic disorders," *Arch. Gen. Psychiatry* **56**, 78–84 (1999).
85. W. Heller et al., "Patterns of regional brain activity differentiate types of anxiety," *J. Abnorm. Psychol.* **106**, 376–385 (1997).
86. E. E. Smith, L. Zambrano-Vazquez, and J. J. B. Allen, "Patterns of alpha asymmetry in those with elevated worry, trait anxiety, and obsessive-compulsive symptoms: a test of the worry and avoidance models of alpha asymmetry," *Neuropsychologia* **85**, 118–126 (2016).
87. K. Kano et al., "The topographical features of EEGs in patients with affective disorders Kunio," *Electroencephalogr. Clin. Neurophysiol.* **83**, 124–129 (1992).
88. D. A. Moscovitch et al., "Frontal EEG asymmetry and symptom response to cognitive behavioral therapy in patients with social anxiety disorder," *Biol. Psychol.* **87**, 379–385 (2011).
89. T. Canli et al., "An fMRI study of personality influences on brain reactivity to emotional stimuli," *Behav. Neurosci.* **115**, 33–42 (2001).
90. C. L. Smith and M. A. Bell, "Stability in infant frontal asymmetry as a predictor of toddlerhood internalizing and externalizing behaviors," *Dev. Psychobiol.* **52**, 158–167 (2010).
91. D. C. Molden, Y. L. Angela, and E. T. Higgins, "Motivations for promotion and prevention," in *Handbook of Motivation Science*, J. Shah and W. Gardner, Eds., pp. 169–187, Guilford Press, New York (2008).
92. D. M. Amodio et al., "Implicit regulatory focus associated with asymmetrical frontal cortical activity," *J. Exp. Soc. Psychol.* **40**, 225–232 (2004).
93. E. Harmon-Jones, C. K. Peterson, and C. R. Harris, "Jealousy: novel methods and neural correlates," *Emotion* **9**, 113–117 (2009).
94. N. J. Kelley et al., "Jealousy increased by induced relative left frontal cortical activity," *Emotion* **15**, 550–555 (2015).

Downloaded From: https://www.spiedigitallibrary.org/journals/Neurophotonics on 24 Jun 2020
Terms of Use: https://www.spiedigitallibrary.org/terms-of-use

95. N. A. Jones and N. A. Fox, "Electroencephalogram asymmetry during emotionally evocative films and its relation to positive and negative affectivity," *Brain Cognit.* **20**, 280–299 (1992).
96. L. A. Killeen and D. M. Teti, "Mothers' frontal EEG asymmetry in response to infant emotion states and mother-infant emotional availability, emotional experience, and internalizing symptoms," *Dev. Psychopathol.* **24**, 9–21 (2012).
97. C. S. Carver and E. Harmon-Jones, "Anger is an approach-related affect: evidence and implications," *Psychol. Bull.* **135**, 183–204 (2009).
98. J. E. Beeney et al., "EEG asymmetry in borderline personality disorder and depression following rejection," *Pers. Disord. Theory Res. Treat.* **5**, 178–185 (2014).
99. A. J. Tomarken et al., "Resting frontal brain activity: linkages to maternal depression and socio-economic status among adolescents," *Biol. Psychol.* **67**, 77–102 (2004).
100. J. P. Kline and S. Allen, "The failed repressor: EEG asymmetry as a moderator of the relation between defensiveness and depressive symptoms," *Int. J. Psychophysiol.* **68**, 228–234 (2008).
101. N. W. Crost, C. A. Pauls, and J. Wacker, "Defensiveness and anxiety predict frontal EEG asymmetry only in specific situational contexts," *Biol. Psychol.* **78**, 43–52 (2008).
102. J. A. Coan and J. J. B. Allen, "Frontal EEG asymmetry as a moderator and mediator of emotion," *Biol. Psychol.* **67**, 7–50 (2004).
103. L. R. R. Gianotti et al., "Tonic activity level in the right prefrontal cortex predicts individuals' risk taking," *Psychol. Sci.* **20**, 33–38 (2009).
104. T. Kawamoto, H. Nittono, and M. Ura, "Cognitive, affective, and motivational changes during ostracism: an ERP, EMG, and EEG study using a computerized cyberball task," *Neurosci. J.* **2013**, 1–11 (2013).
105. M. Ischebeck et al., "Altered frontal EEG asymmetry in obsessive-compulsive disorder," *Psychophysiology* **51**, 596–601 (2014).
106. K. Nash, M. Inzlicht, and I. McGregor, "Approach-related left prefrontal EEG asymmetry predicts muted error-related negativity," *Biol. Psychol.* **91**, 96–102 (2012).
107. C. K. Peterson and E. Harmon-Jones, "Circadian and seasonal variability of resting frontal EEG asymmetry," *Biol. Psychol.* **80**, 315–320 (2009).
108. L. Päeske et al., *EEG Functional Connectivity Detects Seasonal Changes*, Springer, Singapore (2019).
109. D. Armbruster, B. Brocke, and A. Strobel, "Winter is coming: seasonality and the acoustic startle reflex," *Physiol. Behav.* **169**, 178–183 (2017).
110. A. Magnusson, "An overview of epidemiological studies on seasonal affective disorder," *Acta Psychiatr. Scand.* **101**, 176–184 (2000).
111. J. A. King et al., "Sequence and seasonal effects of salivary cortisol," *Behav. Med.* **26**, 67–73 (2000).
112. G. Tononi and C. Cirelli, "Sleep function and synaptic homeostasis," *Sleep Med. Rev.* **10**, 49–62 (2006).
113. C. Cajochen, S. Chellappa, and C. Schmidt, "What keeps us awake?—the role of clocks and hourglasses, light, and melatonin," *Int. Rev. Neurobiol.* **93**, 57–90 (2010).
114. A. J. Metz et al., "Brain tissue oxygen saturation increases during the night in adolescents," in *Oxygen Transport to Tissue XXXV*, S. Van Huffel et al., Eds., pp. 113–119, Springer, New York (2013).
115. J. R. Velo et al., "Should it matter when we record? Time of year and time of day as factors influencing frontal EEG asymmetry," *Biol. Psychol.* **91**, 283–291 (2012).
116. K. W. Tham and H. C. Willem, "Room air temperature affects occupants' physiology, perceptions and mental alertness," *Build. Environ.* **45**, 40–44 (2010).
117. J. Molin et al., "The influence of climate on development of winter depression," *J. Affect. Disord.* **37**, 151–155 (1996).

Hamoon Zohdi received his MSc degree in biomedical engineering from the University of Bern in 2016. He is a PhD student at the Institute of Complementary and Integrative Medicine, University of Bern, Bern, Switzerland. His current research focuses on fNIRS with a special

Downloaded From: https://www.spiedigitallibrary.org/journals/Neurophotonics on 24 Jun 2020
Terms of Use: https://www.spiedigitallibrary.org/terms-of-use

interest in investigating changes in cerebral and systemic physiology in humans elicited by different colored light exposures.

Felix Scholkmann received his PhD from the University of Zürich, Zürich, Switzerland, in 2014. He is a research associate at the University of Bern and a postdoc and a research associate at the University of Zurich. His research focuses on biomedical signal processing, biophotonics/neurophotonics (development and application of NIRS), neuroscience, integrative physiology, and biophysics.

Ursula Wolf is a full professor at the Medical Faculty of the University of Bern and the director of the Institute of Complementary and Integrative Medicine. Her research interests focus on integrative medicine, in particular patient centered research, integrative physiology, and clinical studies.

Downloaded From: https://www.spiedigitallibrary.org/journals/Neurophotonics on 24 Jun 2020
Terms of Use: https://www.spiedigitallibrary.org/terms-of-use

Peer reviewed publication 4

Impact of changes in systemic physiology on fNIRS/NIRS signals: analysis based on oblique subspace projections decomposition

Nassim Nasseri, Alexander Caicedo, Felix Scholkmann, **Hamoon Zohdi**, Ursula Wolf

Advances in Experimental Medicine and Biology (2018) 1072, 119-125.

DOI: 10.1007/978-3-319-91287-5_19

URL: https://link.springer.com/chapter/10.1007%2F978-3-319-91287-5_19

Own contributions:

- Review and editing of the manuscript

Impact of Changes in Systemic Physiology on fNIRS/NIRS Signals: Analysis Based on Oblique Subspace Projections Decomposition

Nassim Nasseri, Alexander Caicedo, Felix Scholkmann, Hamoon Zohdi, and Ursula Wolf

Abstract

Measurements of cerebral and muscle oxygenation (StO_2) and perfusion ([tHb]) with functional near-infrared spectroscopy (fNIRS) and near infrared spectroscopy (NIRS), respectively, can be influenced by changes in systemic physiology. The aim of our study was to apply the oblique subspace projections signal decomposition (OSPSD) to find the contribution from systemic physiology, i.e. heart rate (HR), electrocardiography (ECG)-derived respiration (EDR) and partial pressure of carbon dioxide (pCO_2) to StO_2 and [tHb] signals measured on the prefrontal cortex (PFC) and calf muscle. OSPSD was applied to two datasets ($n_1 = 42$, $n_2 = 79$ measurements) from two fNIRS/NIRS speech studies. We found that (i) all StO_2 and [tHb] signals contained components related to changes in systemic physiology, (ii) the contribution from systemic physiology varied strongly between subjects, and (iii) changes in systemic physiology generally influenced fNIRS signals on the left and right PFC to a similar degree.

N. Nasseri (✉) · H. Zohdi · U. Wolf
Institute of Complementary Medicine, University of Bern, Bern, Switzerland
e-mail: nassim.nasseri@ikom.unibe.ch

A. Caicedo
Department of Electrical Engineering ESAT, STADIUS KU Leuven, Leuven, Belgium

imec, Leuven, Belgium

Research Foundation Flanders (FWO), Brussels, Belgium

F. Scholkmann
Biomedical Optics Research Laboratory, Department of Neonatology, University Hospital Zurich, University of Zurich, Zurich, Switzerland

Institute of Complementary Medicine, University of Bern, Bern, Switzerland

1 Introduction

When interpreting functional near infrared spectroscopy (fNIRS) signals, it is often assumed that the signal reflects an evoked/neural/cerebral response in the brain. However, it is known that at least 6 different components contribute to fNIRS signals [1, 2]. Among these components, evoked changes in systemic physiology make a considerable contribution to fNIRS signals. For example, task-evoked changes in partial pressure of carbon dioxide (pCO_2) can have a significant effect on fNIRS signals [3–6]. Despite several attempts to remove the influence of systemic physiology on

© Springer International Publishing AG, part of Springer Nature 2018

O. Thews et al. (eds.), *Oxygen Transport to Tissue XL*, Advances in Experimental Medicine and Biology 1072, https://doi.org/10.1007/978-3-319-91287-5_19

fNIRS signals, there is insufficient knowledge yet about the quantitative contribution of systemic physiology on fNIRS signals.

The aim of our study was to apply a novel signal-processing method to find the contribution of heart rate (HR), respiration (quantified by the electrocardiography (ECG)-derived respiration, EDR), and pCO_2 to cerebral and muscle oxygenation (StO_2) and perfusion ([tHb]). We aimed to investigate the inter-trial variabilities in the contribution of these parameters and at analyzing a possible laterality in the contributions with respect to the left and right prefrontal cortex (PFC).

2 Methods

Two datasets were employed for this analysis. Dataset 1 included fNIRS signals which were measured on the left PFC (LPFC), NIRS signals on the calf muscle as well as HR and EDR. In this dataset, a NIRO 300 continuous-wave NIRS device (Hamamatsu Photonics, Hamamatsu, Japan) was used to record fNIRS and NIRS signals. This dataset included data from 17 subjects (8 male, 9 female, age 36.6 ± 12.7 years). Each subject was measured a maximum of three times, performing three different speech tasks (Alliteration, Hexameter, Prose). The dataset comprised 42 measurements (not all subjects completed all measurement sessions) from which one was excluded because not all the fNIRS/NIRS and/or physiological signals were available. The measurement protocol of this dataset was: 5 min baseline, 10 min intervention (speech task), and 20 min recovery (for further details see [5]).

Dataset 2 included fNIRS signals of the LPFC and right PFC (RPFC), HR, EDR, and, additionally pCO_2. fNIRS signals were measured by an OxiplexTS frequency-domain NIRS device (ISS, USA). pCO_2 was measured by a Nellcor N1000 gas analyzer (Medtronic, USA). This dataset included data from 24 subjects (13 male, 11 female, age 22 ± 6.4 years). Each subject was measured a maximum of four times, performing three different speech tasks (Alliteration, Hexameter, Prose) and mental arithmetic. The dataset comprised 79 measurements (not all subjects completed all measurement sessions) from which 17 were excluded because not all the fNIRS and/or physiological signals were available. The measurement protocol was: 8 min baseline, 5 min intervention (speech or mental arithmetic task), 5 min recovery, 5 min intervention (speech or mental arithmetic task), and 20 min recovery (for further details see [3]).

We applied the oblique subspace projections signal decomposition (OSPSD) method [7] to decompose StO_2 and [tHb] on the LPFC, RPFC, and the calf muscle. Input signals for the decomposition were HR and EDR (dataset 1) as well as HR, EDR, and pCO_2 (dataset 2). From the computed contribution signals by OSPSD, we calculated a contribution factor (*CF*) for each physiological signal according to:

$$CF_n = \frac{\left|C_n - \mu_n\right|^2}{\sum_n \left|C_n - \mu_n\right|^2 + \left|E_{\text{decom}}\right|^2} \times 100,$$

$$\text{with } E_{\text{decom}} = \left(\left|S_{\text{NIRS}} - \mu_{\text{NIRS}}\right|\right) - \sum_n \left(\left|C_n - \mu_n\right|\right),$$

S_{NIRS} the fNIRS/NIRS signal, C_n the contribution of each physiological signal computed by OSPSD, CF_n the contribution factor of each physiological signal (0–100%), n the number of physiological signals, and μ_n the mean value of C_n.

Both NIRS oximeters applied a multi-distance approach to calculate StO_2 and [tHb] and were, therefore, sensitive to deep tissue. Signal processing and statistical analysis were performed using Matlab (version 2017a, The Mathworks, USA). Dataset 1 and 2 were preprocessed as described in [3, 5]. We tested the significance of the difference between the contribution factors due to different tasks by a Kruskal-Wallis test. The significance of the correlation between the contribution factors was quantified by the linear correlation coefficient (r) and the p-value for testing the hypothesis of no correlation. For the brain (dataset 2), we defined laterality as the difference between the contribution factor of physiological parameters

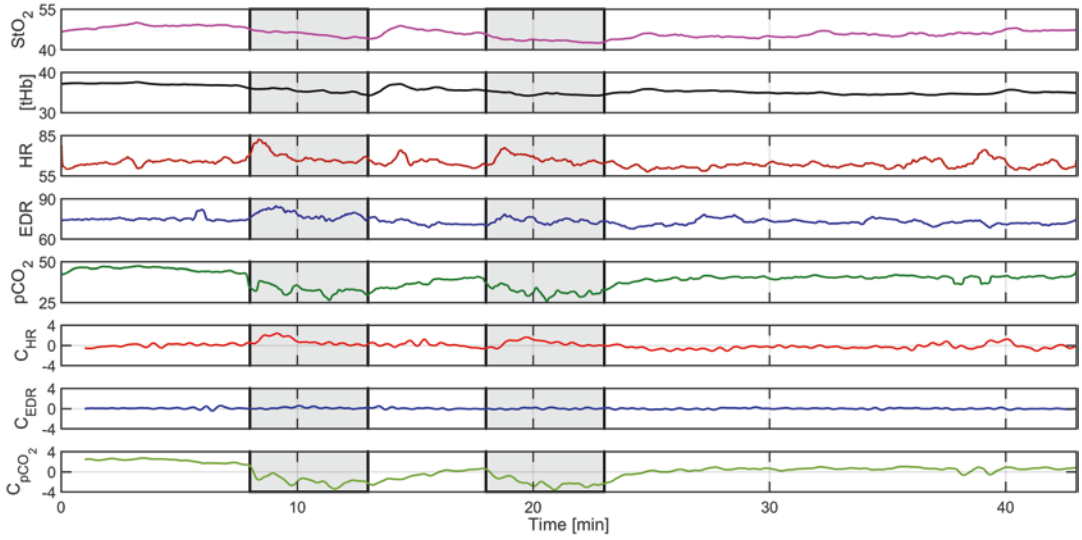

Fig. 1 Example of an fNIRS signal (StO_2 in %, [tHb] in µM) during a speech task (alliteration task; period marked with gray area) and the corresponding HR [BPM], EDR [a.u.], and pCO_2 [mmHg]) and contribution signals (C_{HR} HR contribution, C_{EDR} EDR contribution, C_{pCO2} pCO_2 contribution). For better readability, the StO_2 signal was smoothed by a Savitzky-Golay smoothing filter of order 2 and a window length (w) of 100 s. C_{HR}, C_{EDR}, and C_{pCO2} are smoothed with $w = 25$ s

in the LPFC and RPFC: CF Laterality = $CF_{n,\text{left}} - CF_{n,\text{right}}$, with $CF_{n,\text{left}}$ and $CF_{n,\text{right}}$ the contribution factors of systemic physiology to fNIRS signals measured on the LPFC and RPFC. For the CF laterality analysis, we applied a t-test to calculate the p-value for the null hypothesis that the CF laterality results from a normal distribution with mean value (μ) of 0.

3 Results and Discussion

An exemplary fNIRS signal from the LPFC and the corresponding contributions from HR, EDR, and pCO_2 are shown in Fig. 1. Here, the C_{EDR} and C_{pCO2} signals changed during the stimulation and returned to baseline after the stimulation. All StO_2 and [tHb] signals measured on the LPFC, RPFC, and the calf muscle contained components related to systemic physiology, and the contributions of these components varied strongly between trials. The standard deviations of the contribution factors are shown in Table 1.

Figure 2 visualizes the inter-trial variability of the contribution factors from systemic physiology on StO_2 and [tHb] measured on LPFC and separately for different speech tasks. This shows that the inter-trial variability of the contribution factors is not solely due to the type of the task. No significant difference, due to the type of task, was found between the contribution factors ($p > 0.05$).

The contributions from systemic physiology correlated significantly between LPFC and RPFC ($p < 0.01$). Figure 3 presents scatter plots of the contribution factors (CF_{HR}, CF_{EDR}, CF_{pCO2}) in LPFC vs. RPFC and Fig. 4 scatter plots of the contribution factors (CF_{HR}, CF_{EDR}) in LPFC vs. calf muscle.

Figure 5 shows that there was no significant laterality in the brain ($p > 0.01$). However, the p-value for laterality of CF_{HR} in [tHb] was much lower than the other 5 CFs and was shifted towards negative values. This indicates that HR contributed on average more in [tHb] in RPFC compared to LPFC. The reason for this difference needs to be clarified in future studies.

Table 1 The standard deviation (σ) of contribution factor of systemic physiology in StO_2 and [tHb] in the LPFC, RPFC, and calf muscle. $\sigma_{HR} = \sigma(\log(CF_{HR}))$, $\sigma_{EDR} = \sigma(\log(CF_{EDR}))$, $\sigma_{pCO2} = \sigma(\log(CFp_{CO2}))$

		StO_2			[tHb]		
Dataset 1		σ_{HR}	σ_{EDR}		σ_{HR}	σ_{EDR}	
	LPFC	0.555	0.508		0.689	0.600	
	Calf	0.672	0.604		0.588	0.537	
Dataset 2		σ_{HR}	σ_{EDR}	σ_{pCO2}	σ_{HR}	σ_{EDR}	σ_{pCO2}
	LPFC	0.502	0.484	0.632	0.542	0.553	0.659
	RPFC	0.444	0.506	0.606	0.501	0.485	0.681

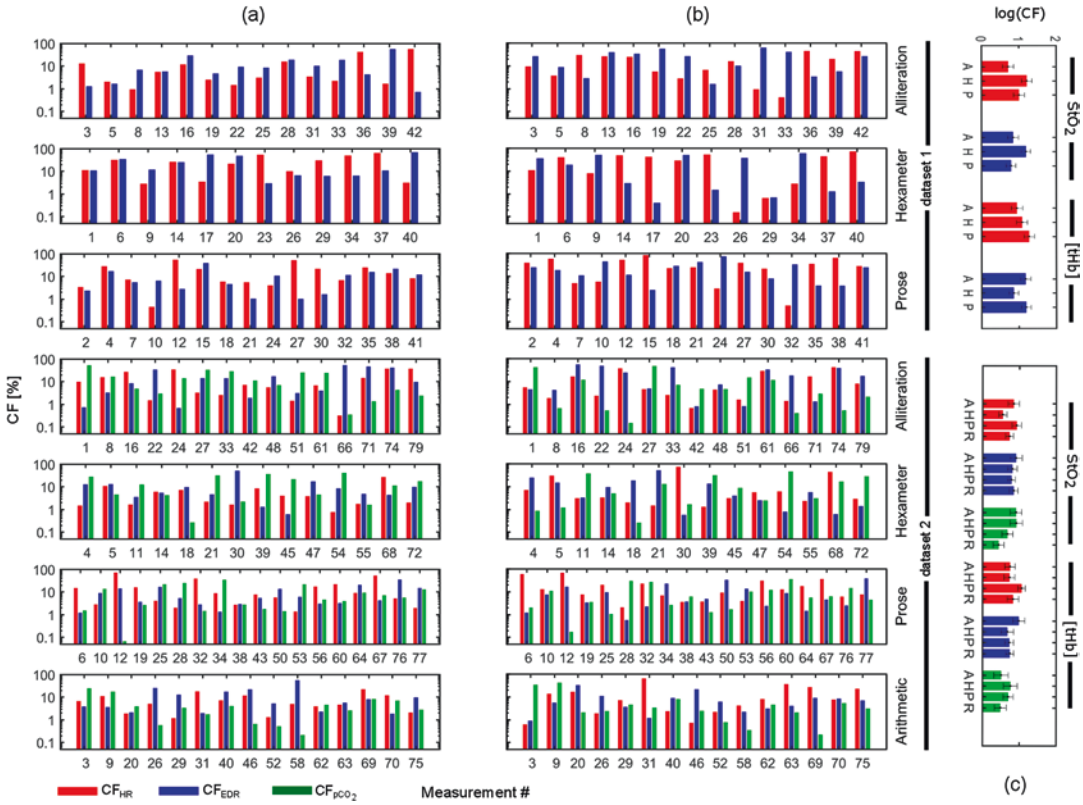

Fig. 2 Contribution factor (CF) of HR, EDR, and pCO_2, in (**a**) StO_2 and (**b**) [tHb], measured on LPFC for different speech (Alliteration, Hexameter, Prose) and Arithmetic tasks. (**c**) CF averaged over all subjects ± standard error of mean for different speech (Alliteration (A), Hexameter (H), Prose (P)) and Arithmetic (R) tasks. Results from measurements in which one or more of the signals (fNIRS or systemic physiology) were not available, are not shown

4 Conclusion

We conclude that (i) OSPSD is a valuable tool for multimodal fNIRS signal analysis and that (ii) changes in systemic physiology affect fNIRS/NIRS signals to a varying degree depending on the trial conditions, e.g. measurement paradigm, instrumentation and subjects. Recording physiological signals during fNIRS measurements enables better understanding and interpreting of fNIRS readings. We also conclude that (iii) systemic physiology may generally contribute differently to the NIRS signals recorded on the brain compared to the muscle tissue, and that (iv) the fNIRS recordings at the LPFC and RPFC may be influenced to a similar degree by changes in systemic physiology.

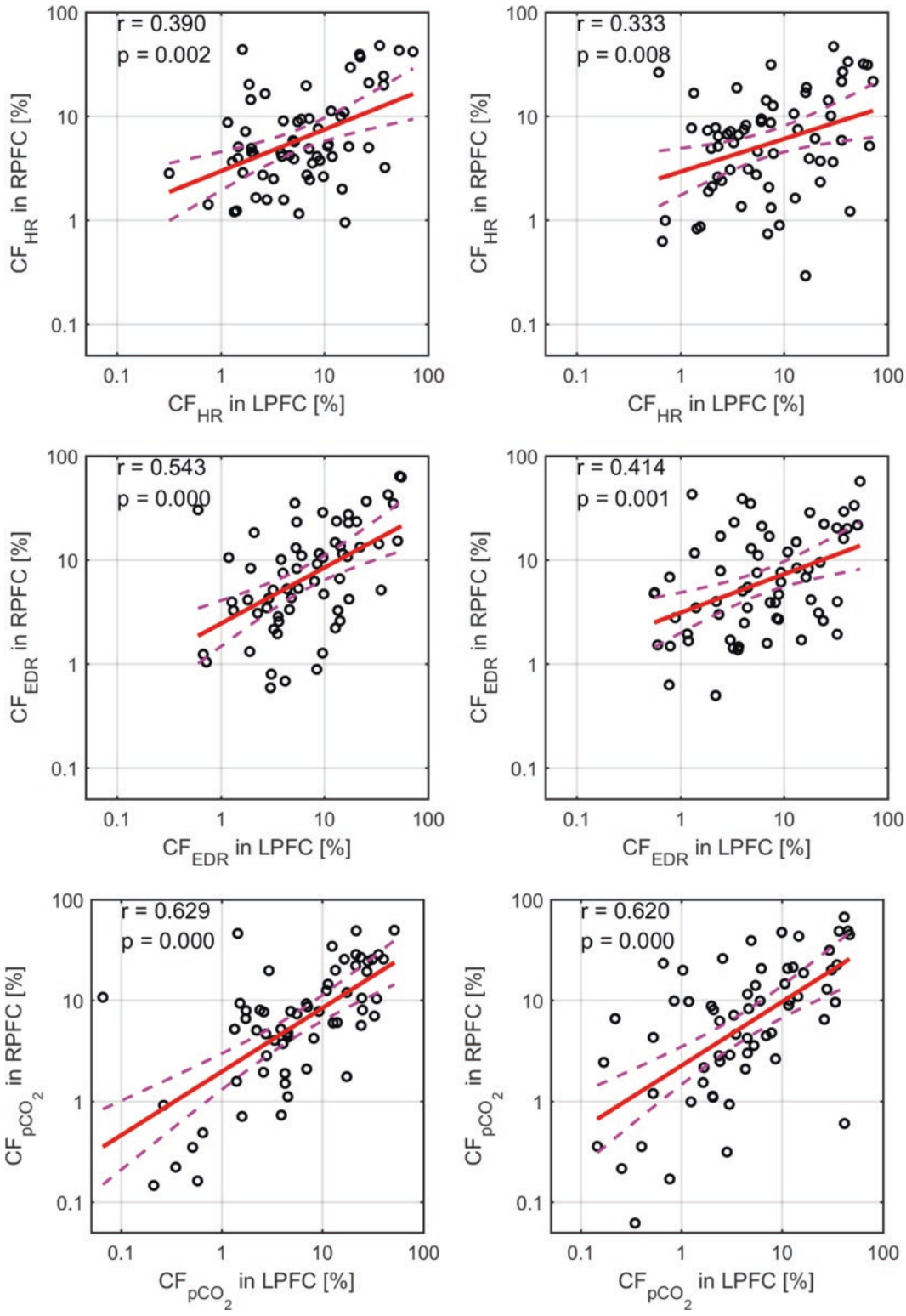

Fig. 3 Contribution factor (*CF*) of HR, EDR, and pCO_2 in RPFC vs. LPFC. Data points (rings), linear fits (solid lines), and 95% confidence intervals (dashed lines). Left column: StO_2, right column: [tHb]

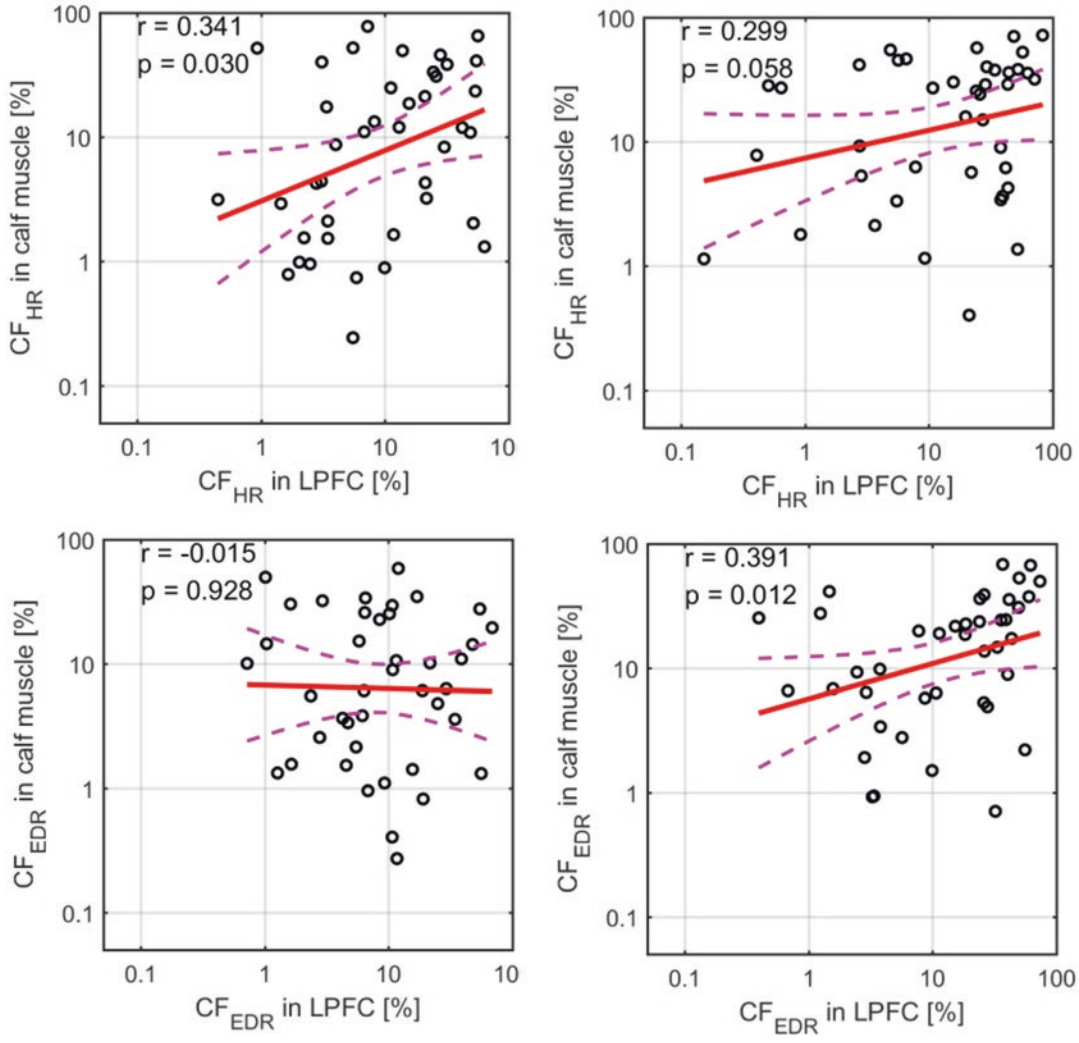

Fig. 4 Contribution factor (*CF*) of HR and EDR in calf muscle vs. LPFC. Data points (rings), linear fits (solid lines), and 95% confidence intervals (dashed lines). Left column: StO_2, right column: [tHb]

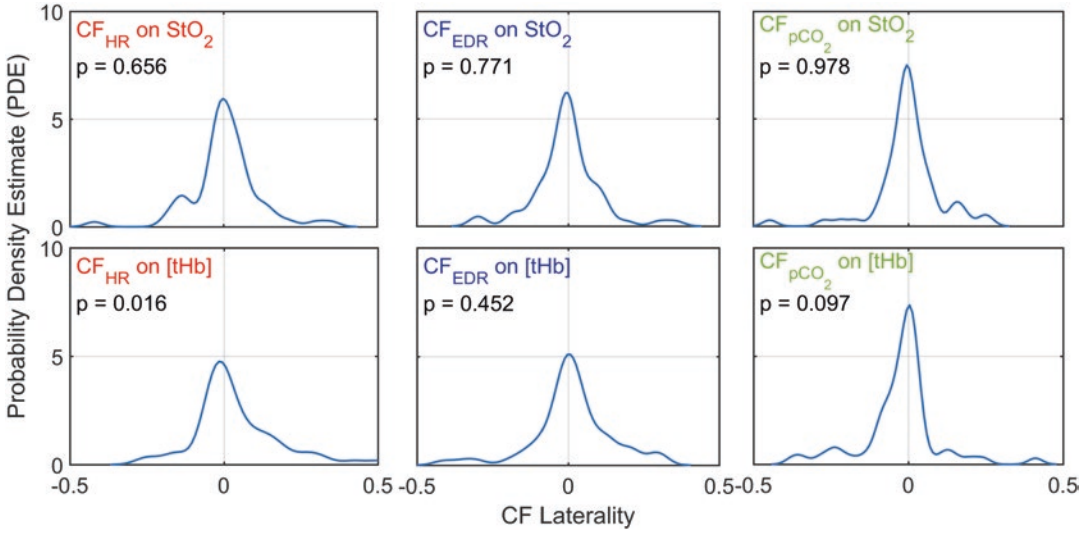

Fig. 5 Laterality of the contribution factors (*CF* Laterality) of systemic physiology in the LPFC and RPFC

References

1. Tachtsidis I, Scholkmann F (2016) False positives and false negatives in functional near-infrared spectroscopy: issues, challenges, and the way forward. Neurophotonics 3(3):031405
2. Scholkmann F, Kleiser S, Metz AJ et al (2014) A review on continuous wave functional near-infrared spectroscopy and imaging instrumentation and methodology. NeuroImage 1:6–27
3. Scholkmann F, Gerber U, Wolf M et al (2013) End-tidal CO_2: an important parameter for a correct interpretation in functional brain studies using speech tasks. NeuroImage 66:71–79
4. Scholkmann F, Klein S, Gerber U et al (2014) Cerebral hemodynamic and oxygenation changes induced by inner and heard speech: a study combining functional near-infrared spectroscopy and capnography. J Biomed Opt 19(1):17002
5. Wolf U, Scholkmann F, Rosenberger R et al (2011) Changes in hemodynamics and tissue oxygenation saturation in the brain and skeletal muscle induced by speech therapy – A near-infrared spectroscopy study. Sci World J 11:1206–1215
6. Scholkmann F, Wolf M, Wolf U (2013) The effect of inner speech on arterial CO_2 and cerebral hemodynamics and oxygenation: a functional NIRS study. Adv Exp Med Biol 789:81–87
7. Caicedo A, Varon C, Hunadi B et al (2016) Decomposition of near-infrared spectroscopy signals using oblique subspace projections: applications in brain hemodynamic monitoring. Front Physiol 7:515

Chapter 4

Individual changes in optical properties of cerebral tissue during and after colored light exposure

Identifying the optical properties of head tissue is the first step toward suitably designing devices, correctly interpreting measurements, and properly planning protocols [74]. Therefore, we were convinced to investigate the optical properties of human head tissue in this PhD project thoroughly. This chapter consists of two publications. Publication 5 describes that the optical properties of head tissue depend on the head region, individual subject, and age. It is also stated that the optical head tissue properties are like a “fingerprint” for the individual subject. In Publication 6, the effects of the CLE on changes in optical properties of human head tissue are shown. The findings demonstrate that all optical properties change during and after the CLE. Although no clear overall trend is visible at the group-level analysis, a clear long-term trend is obvious in almost all of the single measurements.

Peer reviewed publication 5

Absolute values of optical properties (μ_a , μ_s', μ_{eff} and DPF) of human head tissue: dependence on head region and individual

Felix Scholkmann, **Hamoon Zohdi**, Nassim Nasseri, Ursula Wolf

Advances in Experimental Medicine and Biology (2018) 1072, 325-330.

DOI: 10.1007/978-3-319-91287-5_52

URL: https://link.springer.com/chapter/10.1007%2F978-3-319-91287-5_52

Own contributions:

- Data analysis
- Review and editing of the manuscript

Absolute Values of Optical Properties (μ_a, μ'_s, μ_{eff} and DPF) of Human Head Tissue: Dependence on Head Region and Individual

Felix Scholkmann, Hamoon Zohdi, Nassim Nasseri, and Ursula Wolf

Abstract

Background: Absolute optical properties (i.e., the absorption coefficient, μ_a, and the reduced scattering coefficient, μ'_s) of head tissue can be measured with frequency-domain near-infrared spectroscopy (FD-NIRS). Aim: We investigated how the absolute optical properties depend on the individual subject and the head region. Materials and Methods: The data set used for the analysis comprised 31 single FD-NIRS measurements of 14 healthy subjects (9 men, 5 women, aged 33.4 ± 10.5 years). From an 8-min measurement (resting-state; FD-NIRS device: Imagent, ISS Inc.; bilateral over the prefrontal cortex, PFC, and visual cortex, VC) median values were calculated for μ_a and μ'_s as well as the effective attenuation coefficient (μ_{eff}) and the differential pathlength factor (DPF). The measurement was done for each subject one to three times with at least 24 h between the measurements. Results: (i) A Bayesian ANOVA analysis revealed that head region and subject were the most significant main effects on μ_a, μ'_s and μ_{eff}, as well as DPF, respectively. (ii) At the VC, μ_a, μ'_s and μ_{eff} had higher values compared to the PFC. (iii) The differences in the optical properties between PFC and VC were age-dependent. (iv) All optical properties also were age-dependent. This was strongest for the properties of the PFC compared to the VC. Discussion and Conclusion: Our analysis demonstrates that all optical head tissue properties (μ_a, μ'_s, μ_{eff} and DPF) were dependent on the head region, individual subject and age. The optical properties of the head are like a 'fingerprint' for the individual subject. Assuming constant optical properties for the whole head should be carefully reconsidered.

F. Scholkmann (✉)
University of Bern, Institute of Complementary Medicine, Bern, Switzerland

University Hospital Zurich, University of Zurich, Department of Neonatology, Biomedical Optics Research Laboratory, Zurich, Switzerland
e-mail: Felix.Scholkmann@ikom.unibe.ch

H. Zohdi · N. Nasseri · U. Wolf
University of Bern, Institute of Complementary Medicine, Bern, Switzerland

1 Introduction

Frequency-domain near-infrared spectroscopy (FD-NIRS) enables to measure absolute optical tissue properties (i.e., the absorption coefficient, μ_a, and the reduced scattering coefficient, μ'_s) of the human head non-invasively [1]. From those, two additional parameters can be calculated:

© Springer International Publishing AG, part of Springer Nature 2018

O. Thews et al. (eds.), *Oxygen Transport to Tissue XL*, Advances in Experimental Medicine and Biology 1072, https://doi.org/10.1007/978-3-319-91287-5_52

the effective attenuation coefficient ($\mu_{eff} = \sqrt{3\mu_a(\mu_a + \mu_s')}$) and differential pathlength factor ($DPF = 1/2\sqrt{3\mu_s'/\mu_a}$). In a previous study (also included in this volume, see [2]), we showed that the assumption of the time-independence of μ_s' and DPF values during a functional neuroimaging experiment is not necessarily valid – both parameters change substantially, which is evident especially when analyzing the time-course of individual subjects.

The aim of this study was to investigate how the absolute optical properties of the human head depend on the individual subject and the head region.

2 Material and Methods

The FD-NIRS data analyzed comprised 31 single datasets of μ_a, μ_s', μ_{eff} and DPF values (at wavelengths 760 and 834 nm) from the prefrontal cortex (PFC) and visual cortex (VC) obtained by resting-state measurements on 14 healthy subjects (9 male, 5 female, aged 33.4 ± 10.5 years, range 24–57 years); 1–3 single measurement were performed on each subject with at least 24 h between the measurements. A detailed description of the FD-NIRS data acquisition, experimental protocol and signal preprocessing can be found in [2].

Three data analyses were performed: (i) A 2×2×2×14 (head region × wavelength × gender × subject) Bayesian ANOVA (jasp-stats.org, version 0.8.1.1) was performed on the optical property values. Age was included in the analysis as a random factor. (ii) The dependence of the optical tissue properties on the head region was investigated further by testing whether the values were different for the PFC compared to those of the VC. To this end, for each single measurement the differences of the optical properties with respect to the head region were calculated ($\Delta\mu_a$ (PFC-VC), $\Delta\mu_s'$ (PFC-VC), $\Delta\mu_{eff}$ (PFC-VC) and ΔDPF (PFC-VC)) and it was tested if the mean was <0 (Bayesian *t*-test, Cauchy prior width: 0.3). Data from two wavelengths were averaged in this case. (iii) In the third analysis, it was evaluated whether the optical tissue parameters were dependent on the age of the subject. A regression analysis using linear or quadratic functions was employed. The regression was performed on combined data for both wavelengths.

3 Results

(i) The Bayesian ANOVA analysis revealed as the most significant main factors the head region (for μ_a, μ_s' and μ_{eff}) and subject (for DPF) (Table 1, Fig. 1a–d).

(ii) At the VC, μ_a, μ_s' and μ_{eff} had higher values compared to the PFC. The strongest difference between VC and PFC was seen for μ_{eff}. No difference was evident for the DPF (Table 2, Fig. 1e–h).

Table 1 Results of the Bayesian ANOVA

Variable	Head region	Wavelength	Gender	Subject
μ_a	**511.074**	0.196	6.971	20.071
μ_s'	**7.735×10^{11}**	0.816	0.550	0.287
μ_{eff}	**1.092×10^{12}**	0.253	0.472	0.274
DPF	3.394	0.673	14.082	**17.576**

The numbers refer to the Bayesian factors (BF_{10}) obtained. Bold numbers refer to the highest BF_{10} values for each variable

Note: A BF_{10} value of 10–30 represents moderate evidence for the alternative hypothesis (H_1), 10–30 strong evidence for H_1, 30–100 very strong evidence for H_1, and > 100 extreme evidence for H_1

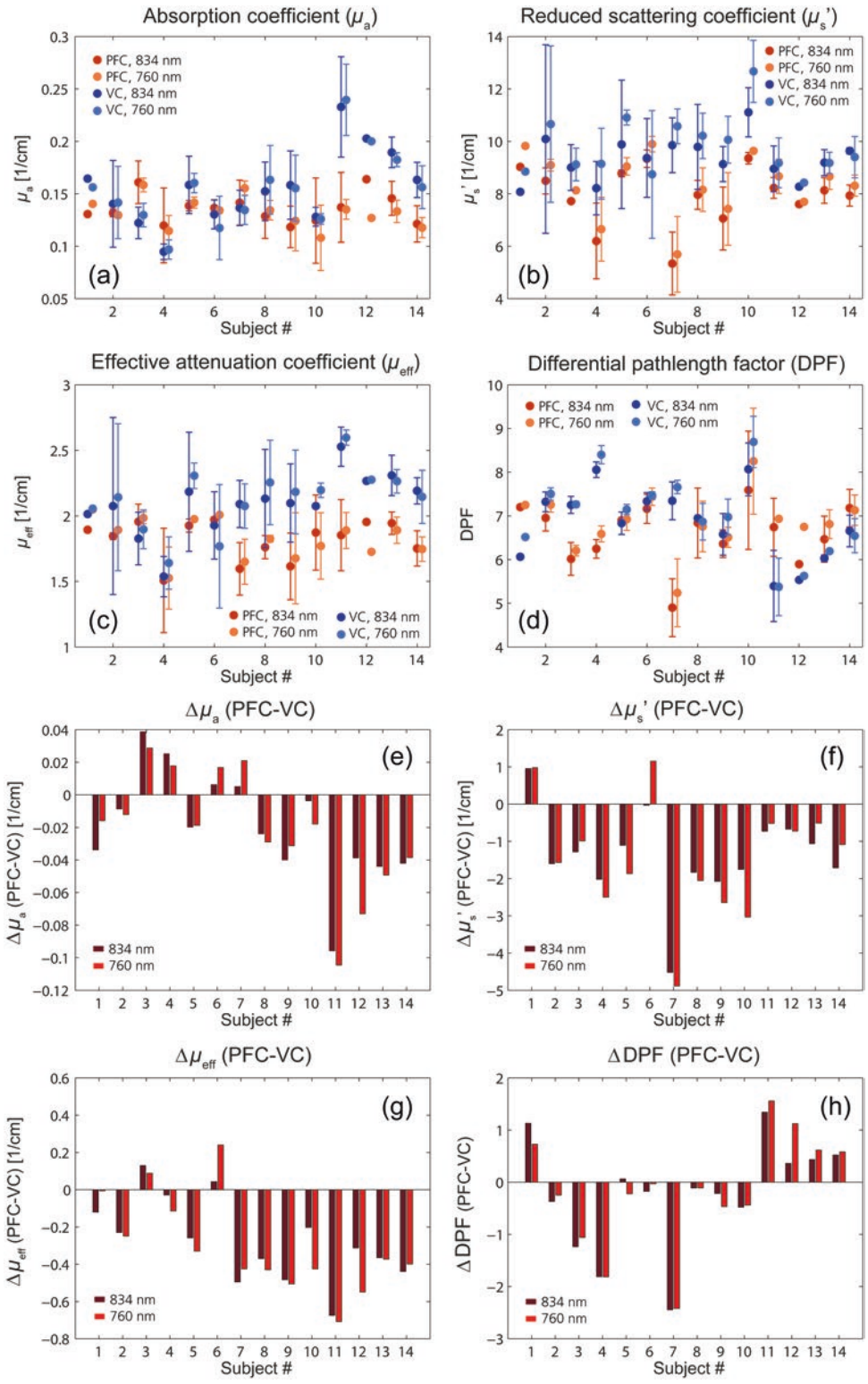

Fig. 1 (**a**–**d**) Dependence of the optical head properties on the individual subjects. The median and the IQR is shown. (**e**–**h**) Subject-specific difference in optical properties between the PFC and VC

Table 2 Results of the Bayesian *t*-test

	$\Delta\mu_a$ (PFC-VC)	$\Delta\mu_s'$ (PFC-VC)	$\Delta\mu_{eff}$ (PFC-VC)	ΔDPF (PFC-VC)
Mean ± SD	−0.021 ± 0.035	−1.416 ± 1.392	−0.286 ± 0.240	−0.185 ± 1.049
BF_{10}	18.86	2476.25	20342.87	0.834

Given are the mean and standard deviation (SD) value for each of the four datasets as well as the BF values (BF_{10})

(iii) The differences in the optical properties between PFC and VC were age-dependent. The dependency was linear ($\Delta\mu_a$ (PFC-VC) and ΔDPF (PFC-VC)) and U-shaped ($\Delta\mu_s'$ (PFC-VC) and $\Delta\mu_{eff}$ (PFC-VC)), respectively (Fig. 2e–h).

(iv) The absolute values of the optical properties were also age-dependent while this dependence was strongest for the properties of the PFC compared to the VC (Table 2, Fig. 1a–d). A strong U-shaped correlation was observed for μ_a, μ_s' and μ_{eff} for the PFC but not for the VC.

4 Discussion and Conclusions

Our finding that the optical properties depend on the head region, the individual subject as well as the age has also been shown by others [3–6]. In particular, differences in the optical properties of the PFC compared to the VC were also observed by Chiarelli et al. [3] (μ_{eff} (VC) > μ_{eff} (PFC)) and by Katagiri et al. [6] $\left(\mu_s'(\mathrm{VC}) > \mu_s'(\mathrm{PFC})\right)$, and correspond to our finding. A large inter-subject variability of the absolute μ_{eff} values of the head, as observed in our study, was also described in [3]. Structural anatomical differences (i.e., regional differences of vascularization and neuronal tissue composition, as well as the scalp and skull layer thickness [7]) between these two regions might be the reasons for this region-specific difference.

We observed that the DPF values were strongly dependent on the individual subject (Fig. 1d), yet with high reproduciblity as shown by the small error bars in (Fig. 1d) compared to (Fig. 1a–c).

Our finding that the absolute optical properties were age-dependent also confirms other investigations [4, 5]. In a previous analysis [5] based on multiple datasets, we found a positive relationship between DPF and age; this generally agrees with our present findings (increasing trend for DPF with age on the PFC, but not on the VC). This result may indicate that the age-dependence might be head region dependent. That the differences of the optical properties with respect to the PFC and VC are also age-dependent is a novel finding in the present study and (to the best of our knowledge) has not previously been reported. The reasons for this observation are not yet clear but are probably caused by different age-dependent changes in the optical properties of the head regions.

Our findings are not only of relevance from the perspective of basic research but also with regard to a proper interpretation of measured optical properties of the head due to changes in the neurovascular state of the brain, i.e. during stroke [8].

In conclusion, we found that all optical brain tissue properties (μ_a, μ_s', μ_{eff} and DPF) were dependent on the brain region, individual subject and age. These optical properties of the head are like a ‘fingerprint’ for the individual subject. The DPF depends strongly on the individual subject and the μ_{eff} on the head region. Further research should investigate the underlying physiological/anatomical reasons for these findings, and envisage potential medical diagnostic applications of optical tissue imaging (besides analyzing μ_a). The usual assumption of constant optical properties for the whole head should also be reconsidered.

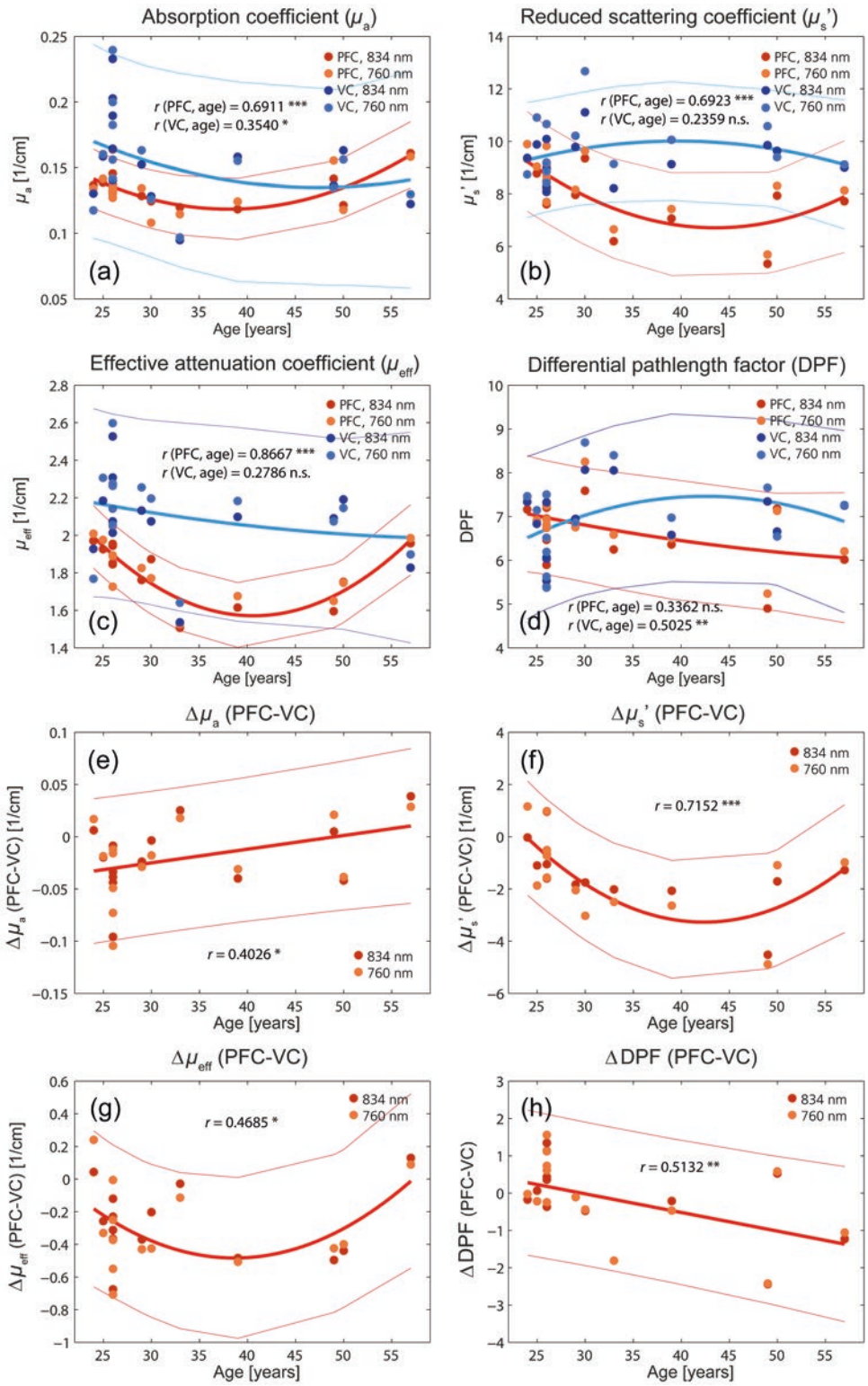

Fig. 2 Age-dependence of the absolute tissue optical properties (**a**–**d**) and the differences between the PFC and VC (**e**–**h**). Each plot shows also the regression lines, the confidence bounds, the correlation strength (r) and the result of the statistical testing (*n.s.* not statistically significant, * $p < 0.05$, ** $p < 0.01$, *** $p < 0.001$)

References

1. Toronov V, Webb A, Choi JH et al (2001) Study of local cerebral hemodynamics by frequency-domain near-infrared spectroscopy and correlation with simultaneously acquired functional magnetic resonance imaging. Opt Express 9(8):417–427
2. Zohdi H, Scholkmann F, Nasseri N et al (2018) Long-term changes in optical properties (μ_a, μ_s', μ_{eff} and DPF) of human head tissue during functional neuroimaging experiments. In: Advances in Experimental Medicine and Biology. Springer, Cham
3. Chiarelli AM, Maclin EL, Low KA, Fantini S et al (2017) Low-resolution mapping of the effective attenuation coefficient of the human head: a multidistance approach applied to high-density optical recordings. Neurophotonics 4(2):021103
4. Zhao H, Tanikawa Y, Gao F, Onodera Y et al (2002) Maps of optical differential pathlength factor of human adult forehead, somatosensory motor and occipital regions at multi-wavelengths in NIR. Phys Med Biol 47(12):2075–2093
5. Scholkmann F, Wolf M (2013) General equation for the differential pathlength factor of the frontal human head depending on wavelength and age. J Biomed Opt 18(10):105004
6. Katagiri A, Dan I, Tuzuki D et al (2010) Mapping of optical pathlength of human adult head at multi-wavelengths in near infrared spectroscopy. Adv Exp Med Biol 662:205–212
7. Strangman GE, Zhang Q, Li Z (2014) Scalp and skull influence on near infrared photon propagation in the Colin27 brain template. NeuroImage 85(1):136–149
8. Highton D, Tachtsidis I, Tucker A et al (2016) Near infrared light scattering changes following acute brain injury. Adv Exp Med Biol 876:139–144

Peer reviewed publication 6

Long-term changes in optical properties (μ_a , μ_s', μ_{eff} and DPF) of human head tissue during functional neuroimaging experiments

Hamoon Zohdi, Felix Scholkmann, Nassim Nasseri, Ursula Wolf

Advances in Experimental Medicine and Biology (2018) 1072, 331-337.

DOI: 10.1007/978-3-319-91287-5_53

URL: https://link.springer.com/chapter/10.1007%2F978-3-319-91287-5_53

Own contributions:

- Data analysis
- Writing of the first draft

Long-Term Changes in Optical Properties (μ_a, μ'_s, μ_{eff} and DPF) of Human Head Tissue During Functional Neuroimaging Experiments

Hamoon Zohdi, Felix Scholkmann, Nassim Nasseri, and Ursula Wolf

Abstract

Frequency-domain near-infrared spectroscopy (FD-NIRS) enables to measure absolute optical properties (i.e. the absorption coefficient, μ_a, and the reduced scattering coefficient, μ_s') of the brain tissue. The aim of this study was to investigate how the optical properties changed during the course of a functional NIRS experiment. The analyzed dataset comprised of FD-NIRS measurements of 14 healthy subjects (9 males, 5 females, aged: 33.4 ± 10.5 years, range: 24–57 years old). Each measurement lasted 33 min, i.e. 8 min baseline in darkness, 10 min intermittent light stimulation, and 15 min recovery in darkness. Optical tissue properties were obtained bilaterally over the prefrontal cortex (PFC) and visual cortex (VC) with FD-NIRS (Imagent, ISS Inc., USA). Changes in μ_a and μ_s' were directly measured and two parameters were calculated, i.e. the differential pathlength factor (DPF) and the effective attenuation coefficient (μ_{eff}). Differences in the behavior of the optical changes were observed when comparing group-averaged data versus single datasets: no clear overall trend was presented in the group data, whereas a clear long-term trend was visible in almost all of the single measurements. Interestingly, the changes in μ_s' statistically significantly correlated with μ_a, positively in the PFC and negatively in the VC. Our analysis demonstrates that all optical brain tissue properties (μ_a, μ_s', μ_{eff} and DPF) change during these functional neuroimaging experiments. The change in μ_s' is not random but follows a trend, which depends on the single experiment and measurement location. The change in the scattering properties of the brain tissue during a functional experiment is not negligible. The assumption $\mu_s' \approx$ const during an experiment is valid for group-averaged data but not for data from single experiments.

H. Zohdi · N. Nasseri · U. Wolf (✉)
Institute of Complementary Medicine, University of Bern, Bern, Switzerland
e-mail: ursula.wolf@ikom.unibe.ch

F. Scholkmann
Institute of Complementary Medicine, University of Bern, Bern, Switzerland

Department of Neonatology, Biomedical Optics Research Laboratory, University Hospital Zurich, University of Zurich, Zurich, Switzerland

© Springer International Publishing AG, part of Springer Nature 2018

O. Thews et al. (eds.), *Oxygen Transport to Tissue XL*, Advances in Experimental Medicine and Biology 1072, https://doi.org/10.1007/978-3-319-91287-5_53

1 Introduction

Functional near-infrared spectroscopy (fNIRS) is a non-invasive neuroimaging technique measuring cerebral blood oxygenation and perfusion [1]. An absolute quantitation of the concentration of oxyhemoglobin ([O_2Hb]) and deoxyhemoglobin ([HHb]) is possible applying the frequency-domain near-infrared spectroscopy (FD-NIRS) technique. The optical properties of tissue, namely the absorption coefficient (μ_a) and reduced scattering coefficient (μ_s'), provide information on the state and composition of the investigated tissue. Two additional parameters characterizing the optical properties of the tissue are the effective attenuation coefficient (μ_{eff}) and differential pathlength factor (DPF). While μ_{eff} is sufficient for determining light attenuation in the diffusion regime and is proportional to the geometric mean of μ_a and μ_s', DPF is defined as the scaling factor that relates source-detector separations (SDS) to the average path length light travels between the source and detector. To date, most fNIRS studies in humans using continuous-wave near-infrared spectroscopy (CW-NIRS) devices rely on an assumed constant DPF and μ_s' during the measurement, an assumption not necessarily true in reality. Any fNIRS quantification of tissue oxygen saturation and hemodynamics that assumes a constant DPF and μ_s' will be erroneous when the DPF and μ_s' change over time.

The aim of this study was to monitor changes in absolute optical properties in human head tissue during a neuroimaging experiment.

2 Material and Methods

The dataset for the present analysis comprised FD-NIRS measurements of 14 healthy subjects (9 males, 5 females, aged 33.4 ± 10.5 years, range 24–57 years old) obtained during a neuroimaging study recently conducted [2]. The study investigated stimulus-evoked changes in cerebral hemodynamics and oxygenation elicited by wide-field visual color stimulation with three different colors. Each measurement lasted 33 min (i.e. 8 min baseline in darkness, 10 min intermittent light stimulation, and 15 min recovery in darkness).

A multi-channel FD-NIRS system with multi-distance approach (Imagent, ISS Inc., Champaign, IL, USA) was employed to measure absolute μ_a and μ_s' of tissue bilaterally at the prefrontal cortex (PFC; Fp1 and Fp2) and the visual cortex (VC; RVC and LVC).

For the present analysis, data from the whole data set were selected that did not contain movement artifacts and had a high signal-to-noise ratio (indicated by the absolute light intensity values recorded at the detectors) of the μ_a and μ_s' signals for both measurements at the PFC and VC. A total of 31 single experiments were analyzed. For the analysis, the $\Delta\mu_a$ and $\Delta\mu_s'$ signals were downsampled to 1.25 Hz to reduce the high-frequency noise. From the μ_a and μ_s' signals, two additional signals were calculated afterward to quantify the tissue optical properties with two additional parameters: DPF and μ_{eff}, given as $\mathrm{DPF} = 1/2\sqrt{3\mu_s'/\mu_a}$ and $\mu_{eff} = \sqrt{3\mu_a\left(\mu_a + \mu_s'\right)}$.

All the subsequent processing steps were performed for μ_a, μ_s', μ_{eff} and DPF. Signals from the left and right PFC as well as VC were averaged to obtain signals for the whole PFC and VC, respectively. To analyze the long-term (i.e. minute) trend of the signals, the signals were first normalized (by subtracting the median value of the first 3 min from each time point), and then a group-average (median ± confidence intervals) of all experiments was calculated. The normalized signals are indicated by a 'Δ'. Changes in the signals were quantified (stimulus interval vs. baseline, recovery vs. stimulus interval, and recovery vs. baseline) by calculating the median values during the specific time intervals and by performing a statistical analysis (Wilcoxon signed-rank test, corrected for multiple comparisons). Individual changes in the signals were also analyzed.

Finally, the correlations of the long-term changes in the optical signals were determined (Spearman correlation) for the following signal combinations (for both PFC and VC and for both wavelengths): $\Delta\mu_s'$ vs. $\Delta\mu_a$, $\Delta\mu_s'$ vs. $\Delta\mu_{eff}$, $\Delta\mu_s'$ vs. ΔDPF, $\Delta\mu_a$ vs. ΔDPF, $\Delta\mu_a$ vs. $\Delta\mu_{eff}$, and $\Delta\mu_{eff}$ vs. ΔDPF.

3 Results

The group-averaged long-term changes of the optical signals, μ_a, μ_s', μ_{eff} and DPF, exhibited mainly three features (Fig. 1): (i) no clear overall trend was present (the analysis of the comparisons of signal intervals revealed no statistically significant trend; Fig. 3a–d), (ii) stimulus-evoked changes in μ_s' and μ_{eff} were visible at the onset of the visual stimulation block (increase in $\mu_s' \approx 0.02\,\mathrm{cm}^{-1}$ and increase in $\mu_{eff} \approx 0.01\ \mathrm{cm}^{-1}$, at 760 nm), and (iii) evoked changes were only visible in the signals from the PFC and not from the VC.

When looking at the changes in μ_a, μ_s', μ_{eff} and DPF in the single datasets the following features were evident (Fig. 2): (i) a clear long-term trend was visible in almost all of the datasets; (ii) non-random i.e., physiological changes were present in the data of the PFC and the VC; and (iii) the changes varied in a non-systematic manner between subjects.

Concerning the correlations of the long-term changes of optical parameters an interesting phenomenon was observed: (Fig. 3e–f): $\Delta\mu_s'$ and $\Delta\mu_a$ correlated statistically significantly positively in the PFC and negatively at the VC. The difference was statistically significant by itself for both wavelengths. The other correlations were positive ($\Delta\mu_s'$ vs. $\Delta\mu_{eff}$, $\Delta\mu_s'$ vs. ΔDPF, $\Delta\mu_a$ vs. $\Delta\mu_{eff}$) and negative ($\Delta\mu_a$ vs. ΔDPF, $\Delta\mu_{eff}$ vs. ΔDPF).

4 Discussion and Conclusions

The assumption that μ_s' as well as the DPF do not change systematically during a neuroimaging experiment with fNIRS is not valid. There is a large variability of μ_s' discernable when analyzing individual datasets from single experiments. The variability is greatly reduced by group-averaging of the data; however, stimulus-evoked changes in μ_s' and μ_{eff} were also clearly detected in this case at the PFC. Changes in μ_s' are not surprising during a period of increased tissue hemoglobin content (intermittent light stimulation) since the changes in the shape of the blood vessels (e.g. diameter) and the increased number of red blood cells lead to an increase in the scattering properties of the tissue [3]. But changes in scattering were not necessarily accompanied by significant changes in the absorption (Fig. 1). In addition, changes in glucose in the tissue may lead to changes in μ_s' [4]. Differences in μ_s' variability between PFC and VC (Fig. 1) may be attributed to differences in the brain activation and other physiological processes between these regions, structural anatomical differences (vessel density and skull thickness) and the smaller light intensity at the detector in the VC compared to the PFC due to hair, which leads to a lower signal-to-noise ratio and hence higher variability in the VC. The predominant error of the ISS Imagent is the shot noise and the error of measurement thus depends on the number of photons measured. The lower penetration depth of NIRS at the VC due to a higher μ_s' is expected to even reduce the variability in the VC. Fast transient increases in μ_s' at the onset of visual stimulation have been reported by various research groups [3]. The changes in μ_{eff} observed can be attributed to changes in μ_s' and μ_a. Concerning the variation of DPF, it has been reported that the DPF at 761 nm depends on oxygenation and is positively related to the arterial oxygen saturation (SaO_2) and sagittal sinus venous oxygen saturation (SvO_2) [5]. The finding in our study that μ_s' changes were positively correlated with μ_a changes at the PFC and negatively at the VC is unexpected and requires further investigation.

Concerning the question whether the magnitude of the changes in μ_s' is relevant for the correct determination of [O_2Hb] and [HHb], in CW-fNIRS studies it can be concluded that a stimulus-evoked changing of 0.02 in μ_s' (as observed in our study, Fig. 1a) corresponds to a 0.12 µM change in [O_2Hb] assuming an absolute O_2Hb concentration of 60 µM. Since a normal stimulus-evoked change of [O_2Hb] during a neuroimaging experiment is in the order of 0.1 µM, such a change in μ_s' is relevant. The long-term changes of μ_s', having an even

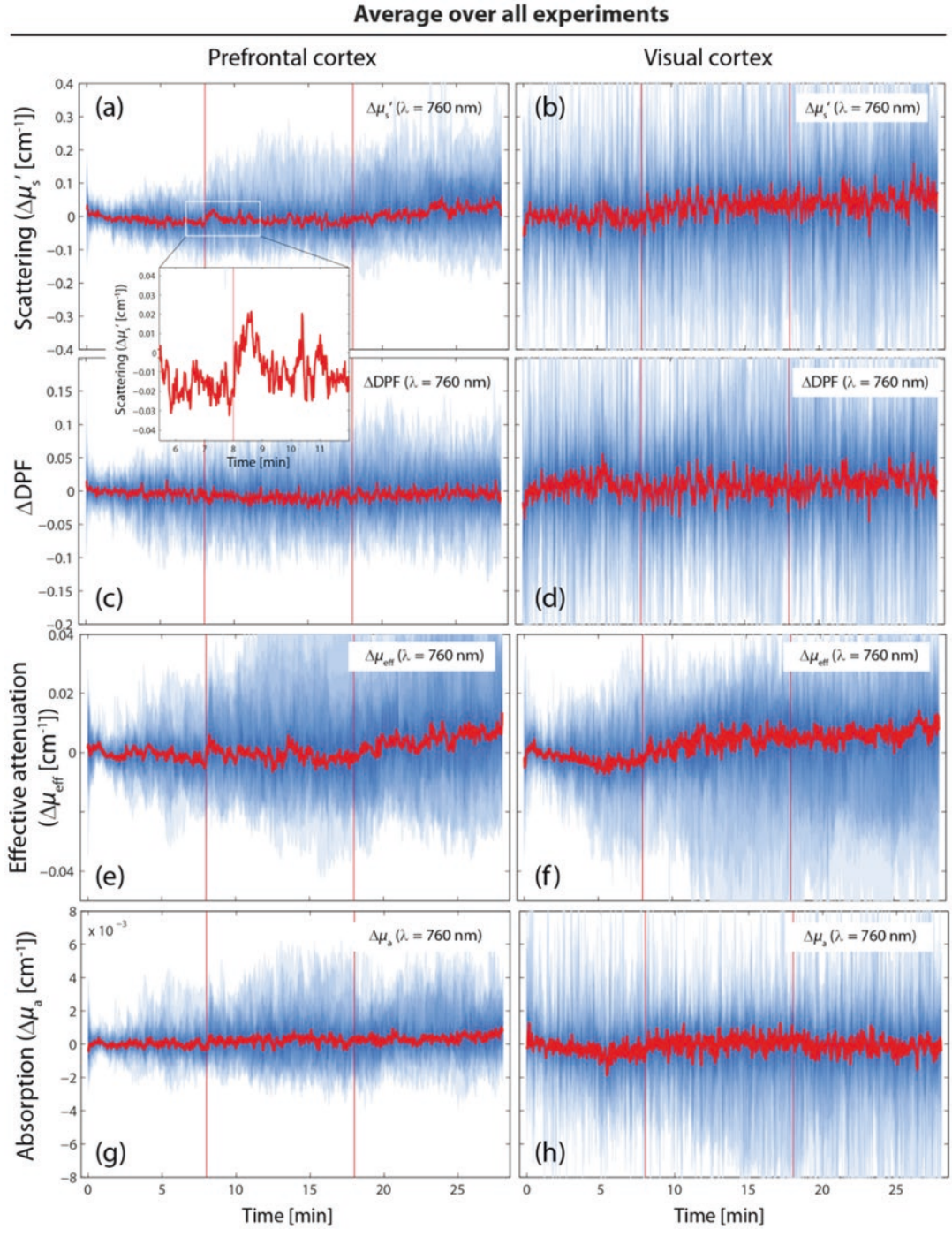

Fig. 1 Time-series of the group-averaged relative changes in the optical properties ($\Delta\mu_s'$, ΔDPF, $\Delta\mu_{eff}$, $\Delta\mu_a$) of the prefrontal cortex (PFC) and the visual cortex (VC) at 760 nm. Data are shown as median values and the 95% confidence interval (blue area). One segment of (**a**) is zoomed in, indicating a stimulus-evoked change in $\Delta\mu_s'$

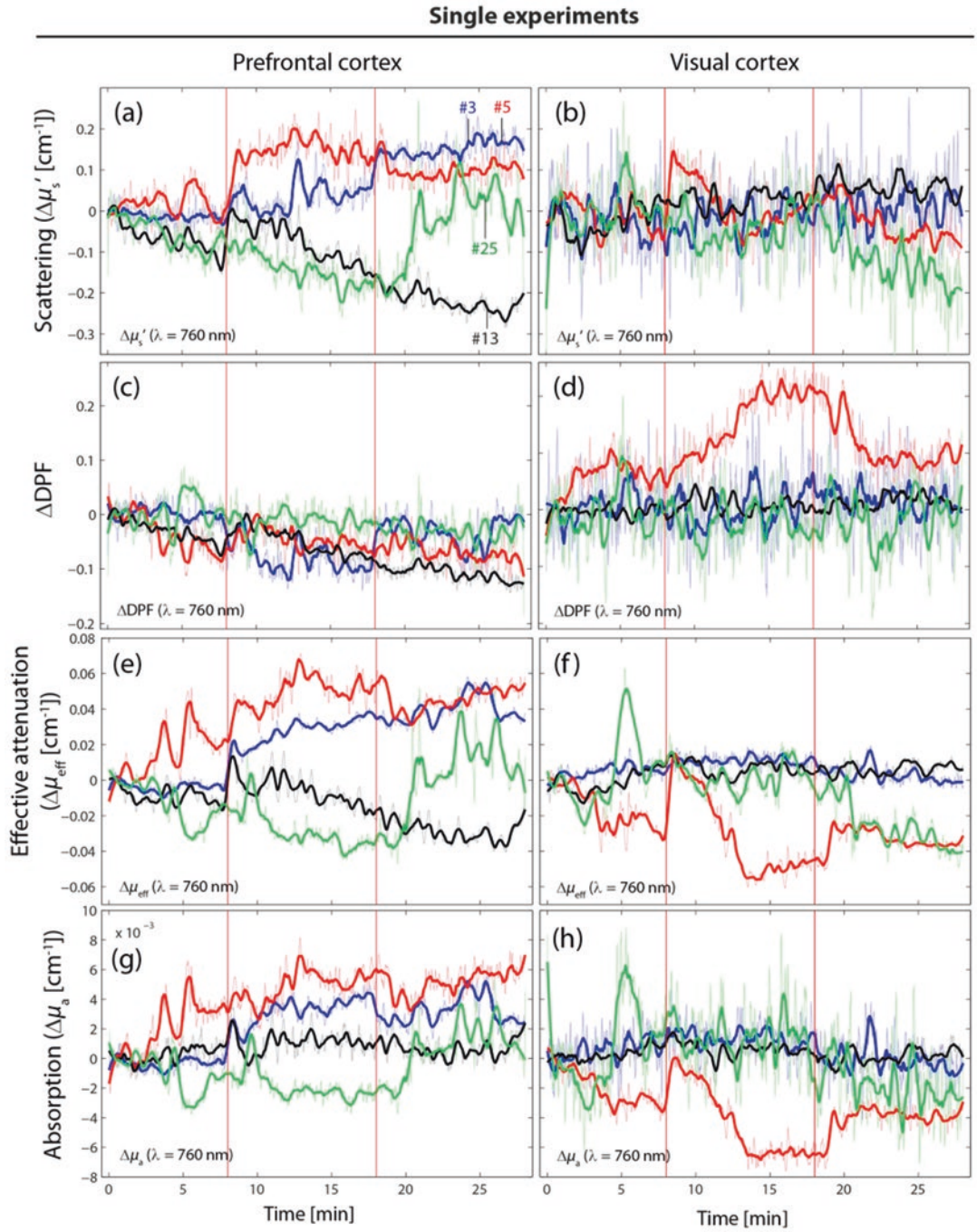

Fig. 2 Time series of the *single dataset* relative changes from four trials (with a different subject each; trials: #3, #5, #13, and #25) in the optical properties ($\Delta\mu_s', \Delta DPF, \Delta\mu_{eff}, \Delta\mu_a$) of the prefrontal cortex (PFC) and the visual cortex (VC) at 760 nm

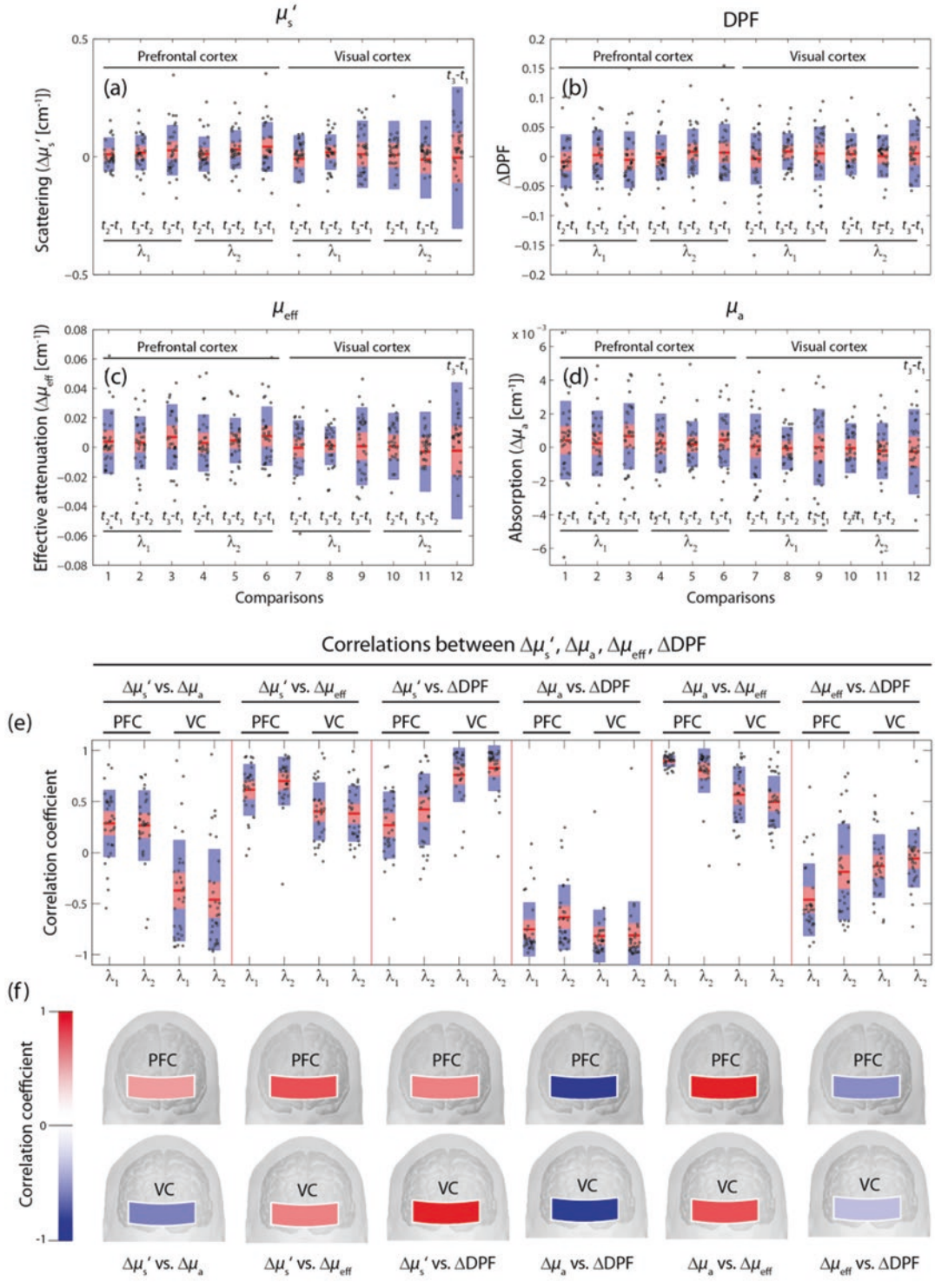

Fig. 3 Overview of the changes in the optical signals ($\Delta\mu_s', \Delta DPF, \Delta\mu_{eff}, \Delta\mu_a$) of the prefrontal cortex (PFC) and the visual cortex (VC) at two wavelengths (λ_1 = 760 nm, λ_2 = 830 nm) quantified by calculation of the median values during the specific time intervals (t_1: baseline; t_2: stimulus interval; t_3: recovery) (**a**–**d**). Correlations of the long-term changes in the optical parameters for both measurement locations (PFC and VC) and at two wavelengths (**e**–**f**)

higher magnitude (especially when looking on individual measurements), are relevant for CW-fNIRS studies that investigate the long-term changes in [O_2Hb] and [HHb] (i.e. resting-state fNIRS studies or NIRS-oximetry applications for patient monitoring). In conclusion, we found that changes in the scattering properties of the brain tissue during a functional experiment are not negligible, especially in single datasets; the assumption $\mu_s' \approx$ const during an experiment is valid for group-average data but not for data from single experiments. Moreover, in this particular type of functional NIRS experiments, we recommend using FD-NIRS or time-domain NIRS systems instead of CW-NIRS, since these techniques are able to measure the time-dependence of μ_s' directly. Finally, the authors believe that further research is warranted to understand the exact effects of changes in optical properties on the changes in [O_2Hb] and [HHb].

References

1. Scholkmann F, Kleiser S, Metz AJ et al (2014) A review on continuous wave functional near-infrared spectroscopy and imaging instrumentation and methodology. NeuroImage 85(1):6–27
2. Scholkmann F, Hafner T, Metz AJ et al (2017) Effect of short-term colored-light exposure on cerebral hemodynamics and oxygenation, and systemic physiological activity. Neurophotonics 4(4):045005
3. Hueber DM, Franceschini MA, Ma HY et al (2001) Non-invasive and quantitative near-infrared haemoglobin spectrometry in the piglet brain during hypoxic stress, using a frequency-domain multidistance instrument. Phys Med Biol 46:41–62
4. Maier JS, Walker SA, Fantini S et al (1994) Possible correlation between blood glucose concentration and the reduced scattering coefficient of tissues in the near infrared. Opt Lett 19:2062–2064
5. Kusaka T, Hisamatsu Y, Kawada K et al (2003) Measurement of cerebral optical pathlength as a function of oxygenation using near-infrared time-resolved spectroscopy in a piglet model of hypoxia. Opt Rev 10:466–469

Chapter 5

Yellow and short-wavelength light lead to higher brain activation in the PFC and VC, respectively

Light can be decomposed into a spectrum of six distinct colors, including violet, blue, green, yellow, orange and red. In this PhD thesis, the effects of the six types of aforementioned colored lights of two different intensities (illuminance: 30 lux and 120 lux at eye level) were investigated how they affect cerebral hemodynamics, oxygenation, and systemic physiology. To this end, the SPA-fNIRS approach was employed. The research was conducted with 141 (85 female, 56 male) healthy right-handed subjects. They were measured four times on different days for the abovementioned conditions resulting in 547 single measurements (seven subjects did not complete all four experimental sessions). Each subject was exposed to the light of different colors and intensities in a randomized crossover protocol for 15 minutes continuously. Before (baseline, 8 min) and after (recovery, 20 min) the CLE, subjects were in darkness.

In this chapter, the effects of light of different colors and intensities on cerebral and physiological parameters at the group level are shown. Then, the most promising findings of this research are presented, and the effects of specific colored light on some parameters are displayed and discussed. Finally, this chapter will close by showing the effects of the most disputable colored light − blue light − on the PFC and VC in the form of Publication 7.

Figures 5, 6, and 7 depict block-average changes in cerebral hemodynamics, oxygenation, and systemic physiology evoked by six colored light at two intensities (12 conditions). These conditions include blue 30 lux, blue 120 lux, red 30 lux, red 120 lux, green 30 lux, green 120 lux, yellow 30 lux, yellow 120 lux, violet 30 lux, violet 120 lux, orange 30 lux, and orange 120 lux.

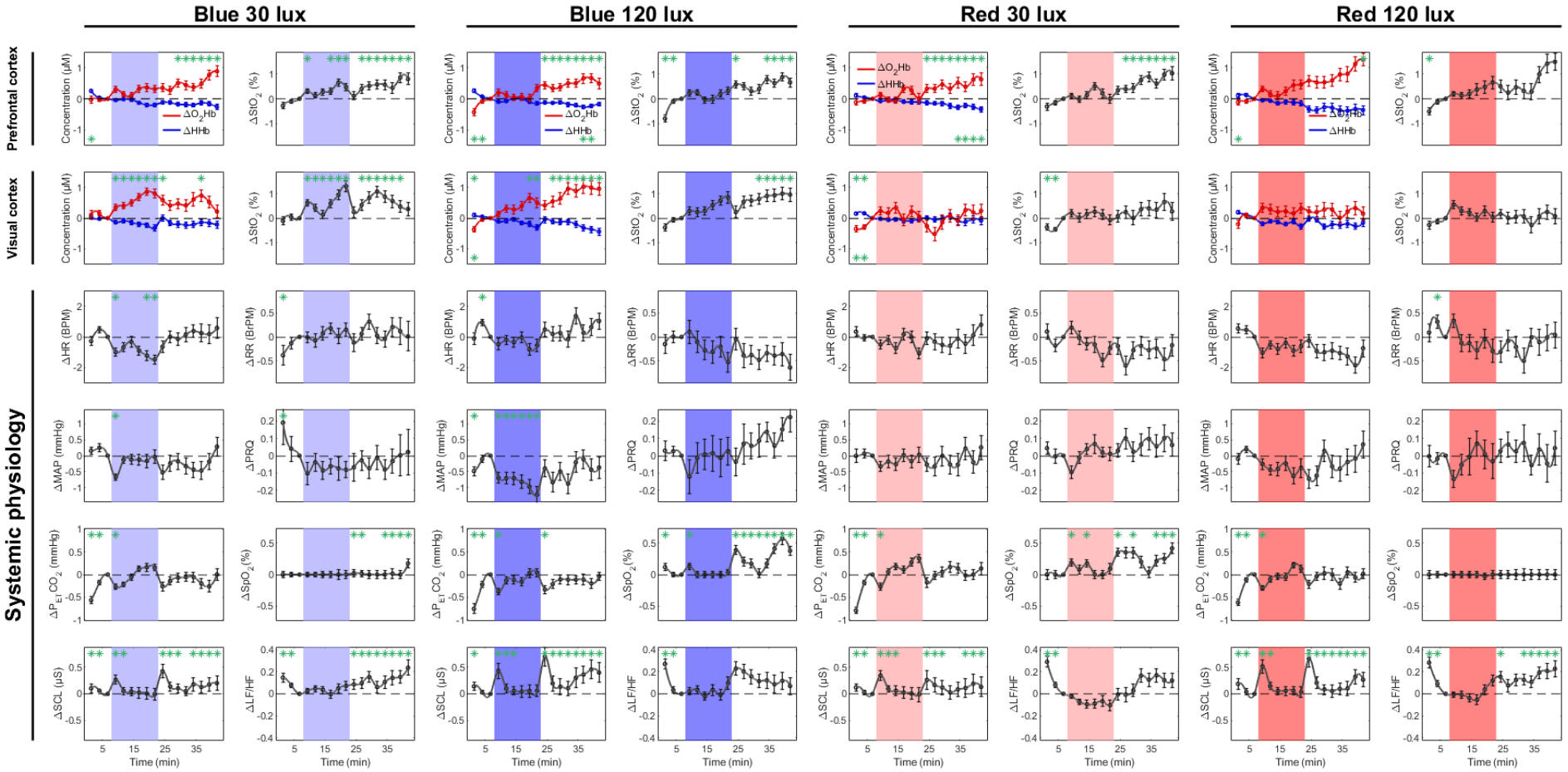

Figure. 5 Block-averaged (group-level) changes in cerebral hemodynamics, oxygenation and systemic physiology (median ± SEM) evoked by blue 30 lux, blue 120 lux, red 30 lux, and red 120 lux. The shaded areas represent time intervals during the stimulation period. The time series are sub-divided into 17 periods (2.5 min each). Then, they are normalized to the last time period of the baseline. Green asterisks indicate a significant change of the marked time point with respect to baseline ($p < 0.05$, Wilcoxon signed-rank test).

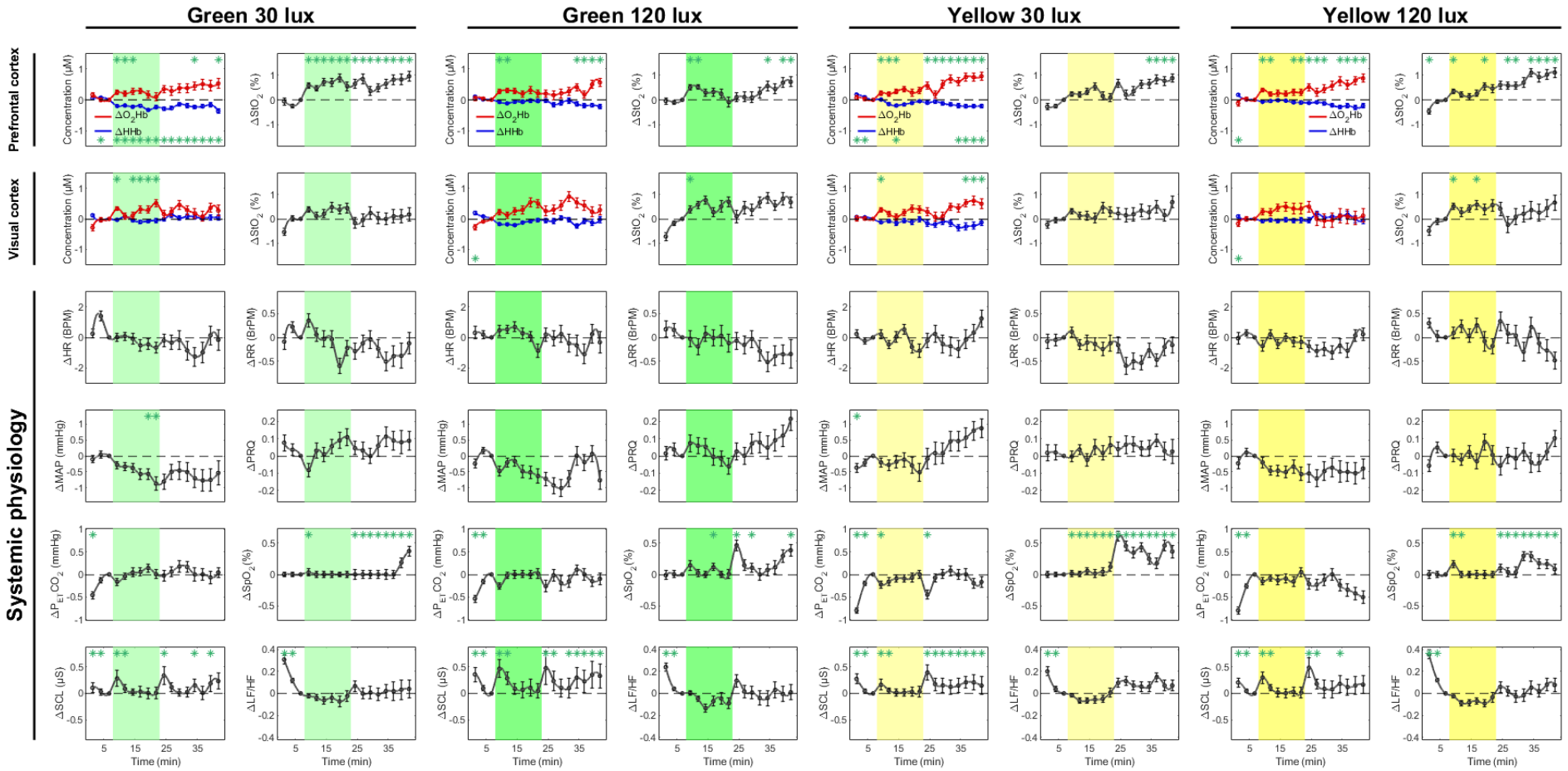

Figure. 6 Block-averaged (group-level) changes in cerebral hemodynamics, oxygenation and systemic physiology (median ± SEM) evoked by green 30 lux, green 120 lux, yellow 30 lux, and yellow 120 lux. The shaded areas represent time intervals during the stimulation period. The time series are sub-divided into 17 periods (2.5 min each). Then, they are normalized to the last time period of the baseline. Green asterisks indicate a significant change of the marked time point with respect to baseline ($p < 0.05$, Wilcoxon signed-rank test).

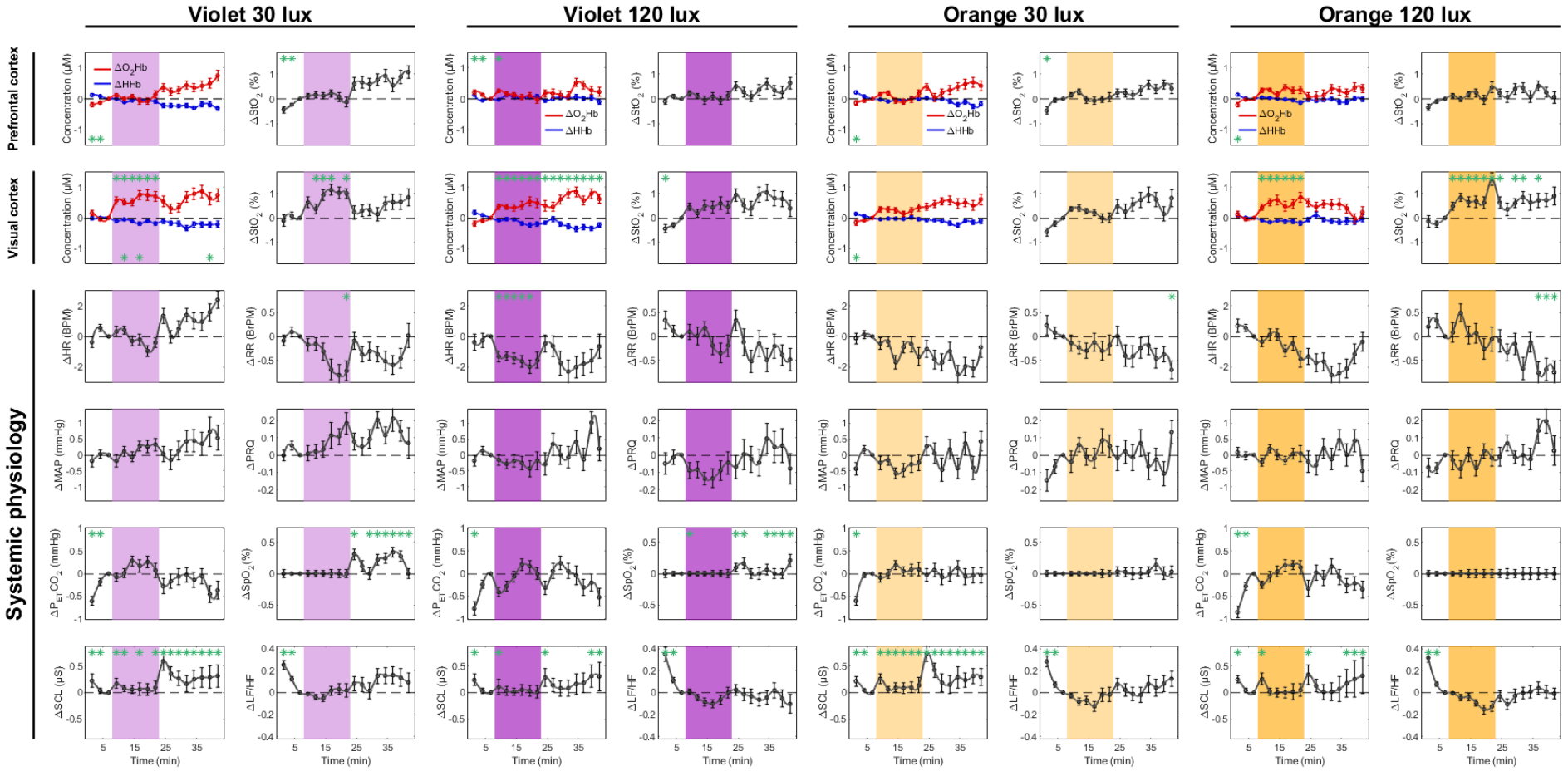

Figure. 7 Block-averaged (group-level) changes in cerebral hemodynamics, oxygenation and systemic physiology (median ± SEM) evoked by violet 30 lux, violet 120 lux, orange 30 lux, and orange 120 lux. The shaded areas represent time intervals during the stimulation period. The time series are sub-divided into 17 periods (2.5 min each). Then, they are normalized to the last time period of the baseline. Green asterisks indicate a significant change of the marked time point with respect to baseline ($p < 0.05$, Wilcoxon signed-rank test).

In order to better understand the effects of various types of colored light and to compare different conditions, 210 significance matrices were created. These include 70 (Size: 12 × 12) matrices for 35 cerebral and physiological parameters at two phases (CLE and recovery), and 140 (Size: 6 × 6) matrices (35 parameters × 2 phases × 2 intensities). An example of a 12 × 12 matrix for one of the physiological parameters (mean arterial pressure, MAP) during the CLE is shown in Figure 8. This matrix aims to show if there are any significant differences between different conditions. The matrix consists of three parts. All 12 conditions investigated in this study are depicted on the diagonal. The lower triangular portion of the matrix displays p values, and it can be found if there is a significant difference between the two specific conditions. The upper triangular portion of the matrix shows which condition leads to a higher activation. In other words, it illustrates which of the two conditions has a higher area under the curve value (AUC). For example, this figure presents that orange 120 lux evoked significantly higher changes in MAP during the CLE compared to almost all conditions except orange 30 lux and violet 30 lux. It means that no significant differences were observed between orang 120 lux and orange 30 lux (p = 0.49) as well as orange 120 lux and violet 30 lux (p = 0.60). In another example, it was found that there is a significant difference between blue and green colored light at 120 lux (p = 0.026), i.e., MAP changes during the CLE were significantly higher for the green in comparison with blue colored light. Such a significant difference was also obvious between blue and green colored light at 30 lux (p = 0.010), this time in favor of blue light.

The aim of this chapter is not to represent and discuss all the created matrices in detail. In the following, some findings of this research are shown. Figure 9 displays a significance matrix of [O_2Hb] in the PFC for six colored light conditions at low-intensity levels (30 lux) in both CLE and recovery phases. Yellow light leads to higher [O_2Hb] changes in the PFC compared to the other colored light. This effect was also found in other cerebral and oxygenation parameters, including [HHb], [tHb], and StO_2. In the VC, we found that, in general, the shorter wavelength, the higher brain activation, i.e., violet and blue evoked higher changes in [O_2Hb], [HHb], and StO_2 during the CLE and recovery phase (Figure 10).

Figure. 8 Significance matrix of MAP for 12 conditions during the CLE. Colored light conditions are shown on the diagonal of the matrix. The lower triangular part of the matrix displays *p* values (Wilcoxon signed-rank test). The upper triangular part of the matrix shows which of the two conditions leads to a higher activation.

Specific intensity-dependent effects and explicit order between different colors are hardly seen in this study for all parameters. For example, oxygenation changes in the VC were higher for orange and green and lower for blue and violet at 120 lux compared to the low intensity (30 lux). No significant differences were observed between 30 lux and 120 lux for red and yellow. On the other hand, activation of the PFC was higher for blue and green at low intensity in comparison with high intensity, and no differences between low and high intensity were found for the others (red, orange, yellow, violet). In another example, low intensity elicited higher changes in HR during the CLE for red, orange, and violet, while high intensity evoked HR only during the blue light exposure.

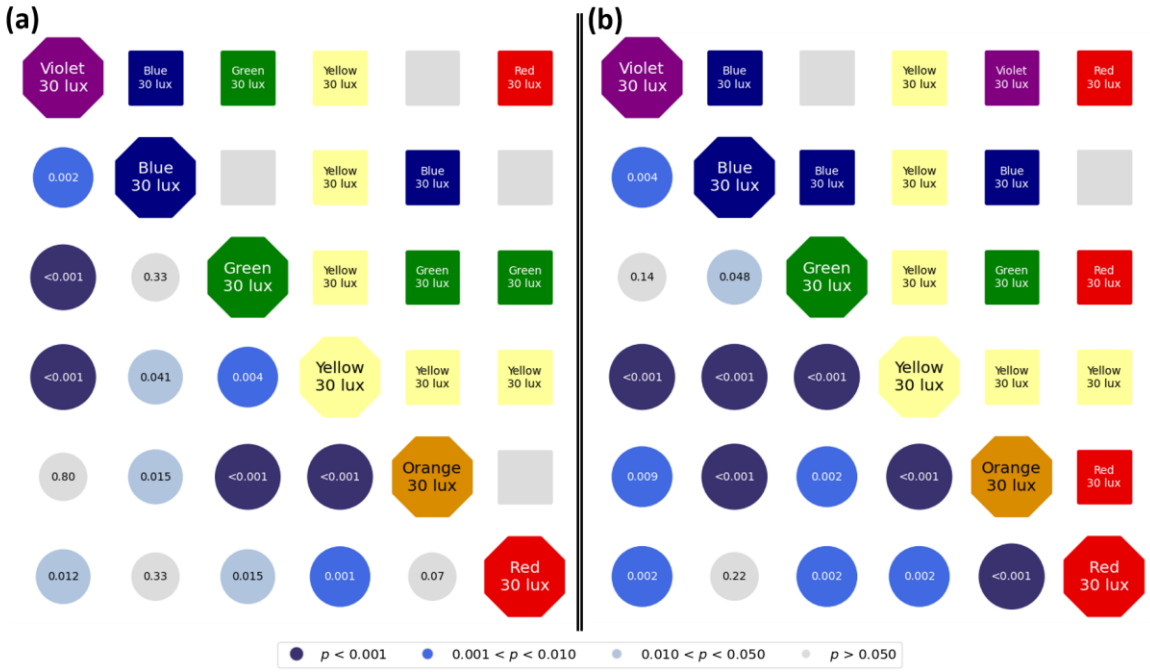

Figure. 9 Significance matrix of O_2Hb in the PFC for six conditions (30 lux) in both **(a)** CLE and **(b)** recovery phases. Colored light conditions are shown on the diagonal of the matrix. The lower triangular part of the matrix displays *p* values (Wilcoxon signed-rank test). The upper triangular part of the matrix shows which of the two conditions leads to a higher activation.

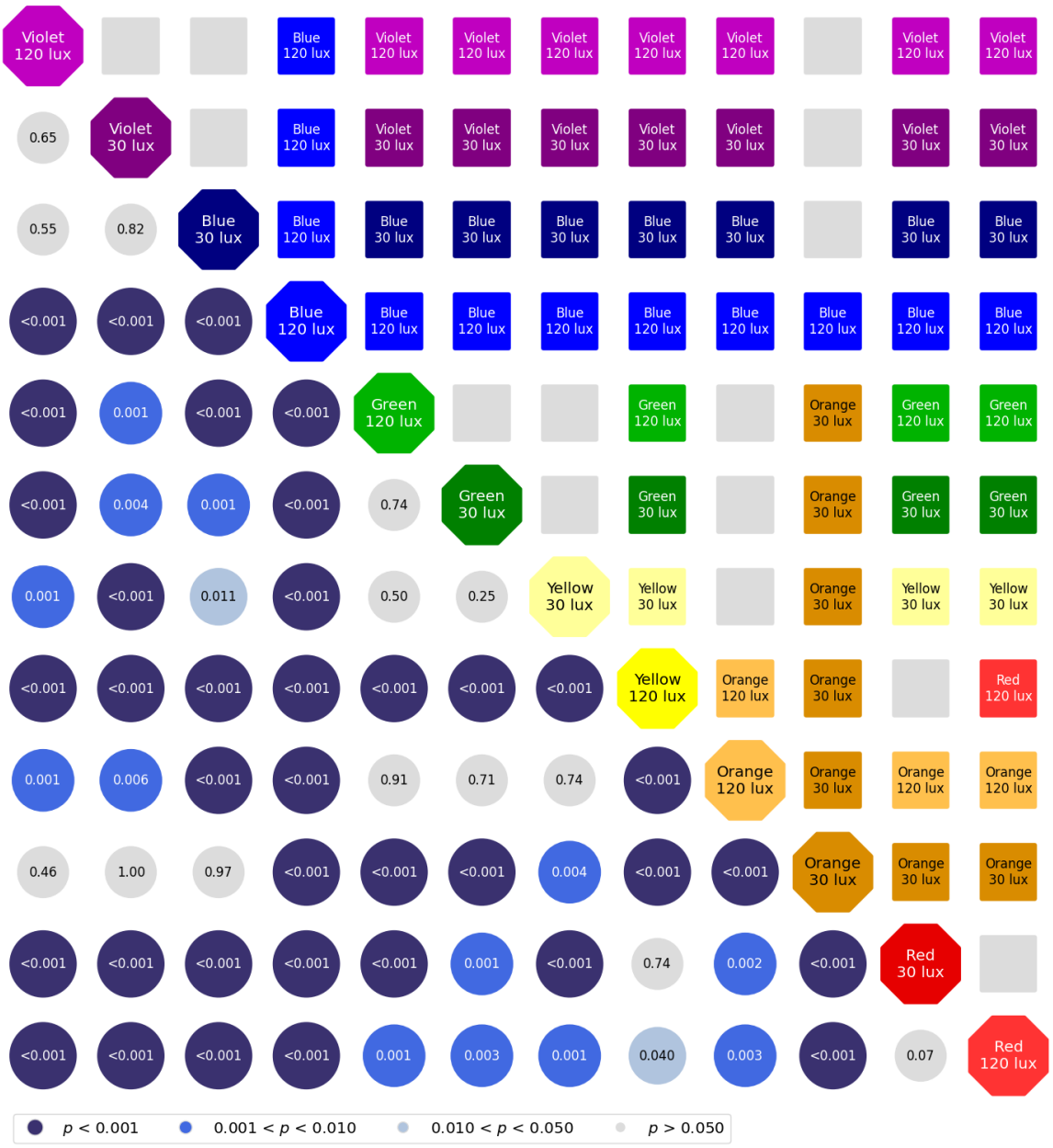

Figure. 10 Significance matrix of O_2Hb in the PFC for 12 conditions during the recovery. Colored light conditions are shown on the diagonal of the matrix. The lower triangular part of the matrix displays *p* values (Wilcoxon signed-rank test). The upper triangular part of the matrix shows which of the two conditions leads to a higher activation.

Exposure to blue light can influence many physiological functions, and it can be used to treat circadian and sleep dysfunctions and seasonal affective disorder as well as boosting alertness, helping cognitive function, and elevating mood [75,76]. In the following, Publication 7 focuses particularly on investigating the impact of blue light exposure on frontal and occipital human cerebral hemodynamics and oxygenation. Our findings depict that blue light affects individual humans differently. Despite the typical hemodynamic response pattern (an increase of [O_2Hb] and a decrease of [HHb]) observed at group-level analysis, this pattern was found in only 8 out of 32 cases. It is also observed that blue light exposure leads to eight different hemodynamic response patterns, which, in particular, should be taken into consideration when assessing the impact of blue light on society.

Peer reviewed publication 7

Long-term blue light exposure changes frontal and occipital cerebral hemodynamics: not all subjects react the same

Hamoon Zohdi, Felix Scholkmann, Ursula Wolf

Advances in Experimental Medicine and Biology (2020) 1269, 217-222.

DOI: 10.1007/978-3-030-48238-1_34

URL: https://link.springer.com/chapter/10.1007%2F978-3-030-48238-1_34

Own contributions:

- Co-design of the study
- Contribute to carrying out measurements
- Signal processing
- Data analysis
- Visualization (all figures)
- Writing of the first draft

Check for updates

34 Long-Term Blue Light Exposure Changes Frontal and Occipital Cerebral Hemodynamics: Not All Subjects React the Same

Hamoon Zohdi, Felix Scholkmann, and Ursula Wolf

Abstract

Background: In modern society, we are increasingly exposed to numerous sources of blue light, including screens (e.g., TVs, computers, laptops, smartphones, tablets) and light from fluorescent and LED lamps. Due to this wide range of applications, the effects of blue light exposure (BLE) on the human physiology need to be thoroughly studied. Aim: To investigate the impact of long-term BLE on frontal and occipital human cerebral hemodynamics and oxygenation using functional near-infrared spectroscopy (fNIRS) neuroimaging. Materials and Methods: 32 healthy right-handed subjects (20 females, 12 males; age: 23.8 ± 2.2 years) were exposed to blue LED light for 15 minutes. Before (baseline, 8 min) and after (recovery, 10 min) the BLE, subjects were in darkness. We measured the concentration changes of oxyhemoglobin ([O_2Hb]) and deoxyhemoglobin ([HHb]) at the prefrontal cortex (PFC) and visual cortex (VC) by fNIRS during the experiment. Subjects were then classified into different groups based on their hemodynamic response pattern of [O_2Hb] at the PFC and VC during BLE. Results: On the group level (32 subjects), we found an increase in [O_2Hb] and a decrease in [HHb] at both cortices during BLE. Evoked changes of [O_2Hb] were higher at the VC compared to the PFC. Eight different hemodynamic response patterns were detected in the subgroup analysis, while an increase of [O_2Hb] in both cortices was the most common pattern (8 out of 32 cases, 25%) during BLE. Discussion and Conclusion: Our study showed that the hemodynamic and oxygenation changes at the PFC and VC during BLE (i) were generally higher in the VC compared to the PFC, (ii) showed an intersubject variability with respect to their magnitudes and shapes, and (iii) can be classified into eight groups. We conclude that blue light affects humans differently. It is essential to consider this when assessing the impact of the BLE on society.

Keywords

Blue light exposure · Functional near-infrared spectroscopy · Different hemodynamic response patterns · Prefrontal cortex · Visual cortex

H. Zohdi (✉) · U. Wolf
University of Bern, Institute of Complementary and Integrative Medicine, Bern, Switzerland
e-mail: hamoon.zohdi@ikim.unibe.ch

F. Scholkmann
University of Bern, Institute of Complementary and Integrative Medicine, Bern, Switzerland

University Hospital Zurich, University of Zurich, Department of Neonatology, Biomedical Optics Research Laboratory, Zurich, Switzerland

© Springer Nature Switzerland AG 2021

E. M. Nemoto et al. (eds.), *Oxygen Transport to Tissue XLII*, Advances in Experimental Medicine and Biology 1269, https://doi.org/10.1007/978-3-030-48238-1_34

34.1 Introduction

Blue light is increasingly prevalent in our modern society due to modern light sources such as light-emitting diodes (LEDs) and fluorescent lamps and the omnipresence of screens (e.g., TVs, computers). The adverse effect of blue light exposure (BLE) on human physiology is increasingly recognized [1–3]. But BLE can also be beneficial, for example, treating circadian and sleep dysfunction and seasonal affective disorder, as well as boosting alertness, helping cognitive function, and elevating mood [4, 5].

Functional near-infrared spectroscopy (fNIRS) is a technology for cost-effective and noninvasive neuroimaging in research and clinical practice. This technique measures cerebral blood oxygenation and perfusion [6, 7]. Absolute quantitation of the concentration of oxyhemoglobin ([O_2Hb]) and deoxyhemoglobin ([HHb]) is possible by applying the frequency-domain near-infrared spectroscopy (FD-NIRS) technique [8].

The effects of BLE on the visual and nonvisual pathway can be distinguished by the measurement of the visual cortex (VC) and prefrontal cortex (PFC). We measured both cortices in parallel in order to investigate the effects of BLE in the visual and nonvisual pathways associated with the processing of visual information. Moreover, it is known that colors may affect the emotional status and mood, and thus, we expected modulation of PFC activation by BLE.

In this study, we aimed to investigate the impact of long-term wide-angle BLE on frontal and occipital human cerebral hemodynamics using fNIRS. The results of the current study are expected to facilitate a better understanding of the beneficial and detrimental effects of BLE on society.

34.2 Material and Methods

Thirty-two healthy right-handed subjects (20 females, 12 males; age: 23.8 ± 2.2 years, range: 20–28 years) were assessed in this study. They were asked to sit upright in a comfortable chair while their feet were on the ground and a white wall was in front of them (distance eyes-wall:160 ± 5 cm). The blue LED light (six LED PAR headlights: each has 12 × 35 mm RGBW LEDs; peak wavelength: 450 nm; illuminance: 120 lux at eye level) was continuously exposed to the white wall (width: 2.5 m, height: 3 m) for 15 minutes. Before (baseline, 8 min) and after (recovery, 10 min) the BLE, subjects were in darkness.

The focus of this study was on the intersubject variability of the hemodynamic responses.

The concentration changes of [O_2Hb] and [HHb] were measured bilaterally over the PFC and VC by FD-NIRS (Imagent, ISS Inc., Champaign, IL, USA). The PFC optodes were placed over the left (Fp_1) and right (Fp_2) PFC and over the right (O_2) and left (O_1) VC, respectively, according to the international 10–20 system. The source-detector separations of the optodes were 2.0, 2.5, 3.5, and 4.0 cm over the PFC and 2.0, 2.5, 3.0, and 3.5 cm over the VC. Movement artifacts in [O_2Hb] and [HHb] signals were detected and removed by the movement artifact reduction algorithm (MARA) [9]. To further remove high-frequency noise, signals were low pass filtered using a robust second-degree polynomial moving average (RLOESS) filter with a span of 4 min. Signals from the left and right PFC and VC were subsequently averaged to obtain signals for the whole PFC and VC, respectively. The signals were then normalized to the last 5 minutes of the baseline period to analyze the changes of [O_2Hb] and [HHb] for each subject. To compare the changes of [O_2Hb] and [HHb] between PFC and VC at the group level, the BLE phase was segmented into 60 parts, and the median of [O_2Hb] and [HHb] values for each segment was calculated for each subject. Then, the median value of each segment among all subjects was calculated. Finally, the median values obtained for all segments were averaged.

Subjects were finally classified into different groups based on their hemodynamic response pattern of [O_2Hb] at the PFC and VC during BLE. The BLE phase of normalized [O_2Hb] signal was segmented into 60 parts, and the median value for each segment was calculated. Then, the One-Sample Wilcoxon Signed Rank Test was

applied to all median values of segments. Inconclusive (−) pattern indicates a failure to reject the null hypothesis (median is zero) at the 5% significant level ($p > 0.05$), while increase (↑) and decrease (↓) patterns indicate a rejection of the null hypothesis ($p < 0.05$).

34.3 Results

Group-Level Analysis The group-averaged long-term changes of [O_2Hb] and [HHb] at the PFC and VC are depicted in Fig. 34.1. We found an increase in [O_2Hb] and a decrease in [HHb] at both cortices during BLE. Evoked changes of [O_2Hb] were higher at the VC compared to the PFC ($p < 0.001$; effect size (Cohen's d): $d = 1.03$), while [HHb] changes at the PFC were more prominent than that of the VC ($p < 0.001$; $d = 1.15$). This change was observed, especially after light exposure in the recovery period.

Subgroup Analysis We observed a large inter-subject variability of the hemodynamic responses. Nevertheless, the hemodynamic responses were assigned to eight groups according to the changes of [O_2Hb] at the VC and PFC, i.e., eight different response pattern could be defined. Figure 34.2 and Table 34.1 show the classification of stimulus-evoked hemodynamic responses based on [O_2Hb] pattern at the PFC and VC during BLE. The most common fNIRS response pattern during BLE was an increase of [O_2Hb] associated with a decrease of [HHb] in both cortices (8 out of 32 cases, 25%). An increase and a decrease in [O_2Hb] at the PFC and VC, respectively, were the second most common pattern (6 out of 32 cases, 19%). In contrast to the latter pattern, we found a decrease in [O_2Hb] at the PFC and an increase in [O_2Hb] at the VC as the third pattern (5 out of 32 cases, 16%). Although the number of males investigated in this study was lower than females (20 females, 12 males), the frequency of the third most common pattern in the male group was considerably higher compared to female group (Group 3: 1 female, 4 males).

34.4 Discussion and Conclusions

Neuronal activation generally leads to an increase in [O_2Hb] with a concurrent decrease in [HHb] due to changes in cerebral hemodynamics and metabolism. At the group level, we observed in our study the typical hemodynamic changes in the PFC and VC during BLE. The mean increases in [O_2Hb] during BLE were less pronounced in the PFC than that in the VC. That the BLE also led to a change in the PFC is indicative for an activity increase of higher cognitive processes related to increase in activity of the PFC [10]. The reasons for the continued increase in the recovery phase are not yet clarified. Our hypothesis is that the BLE leads to long-lasting effects. Nevertheless, it is a valuable observation because it may have implications on the applications of blue light.

In spite of the typical hemodynamic response pattern observed at the group-level analysis, this pattern ([O_2Hb] increase in both cortices) was found in only 8 out of 32 cases. Different patterns

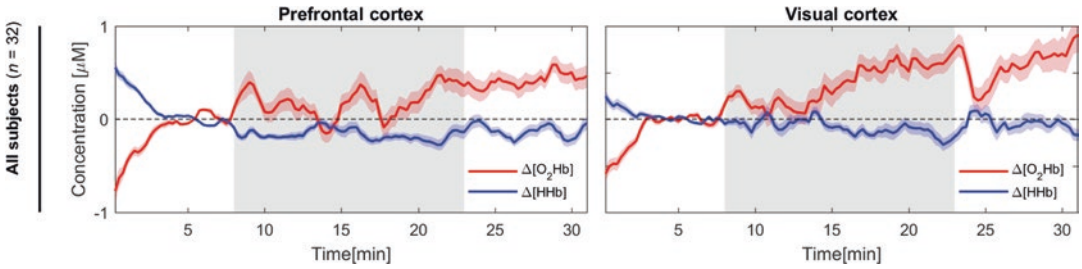

Fig. 34.1 Group-averaged changes in hemodynamic response ([O_2Hb] and [HHb]) of the PFC and VC. The gray-shaded areas represent the BLE. Median ± standard error of median (SEM) is shown

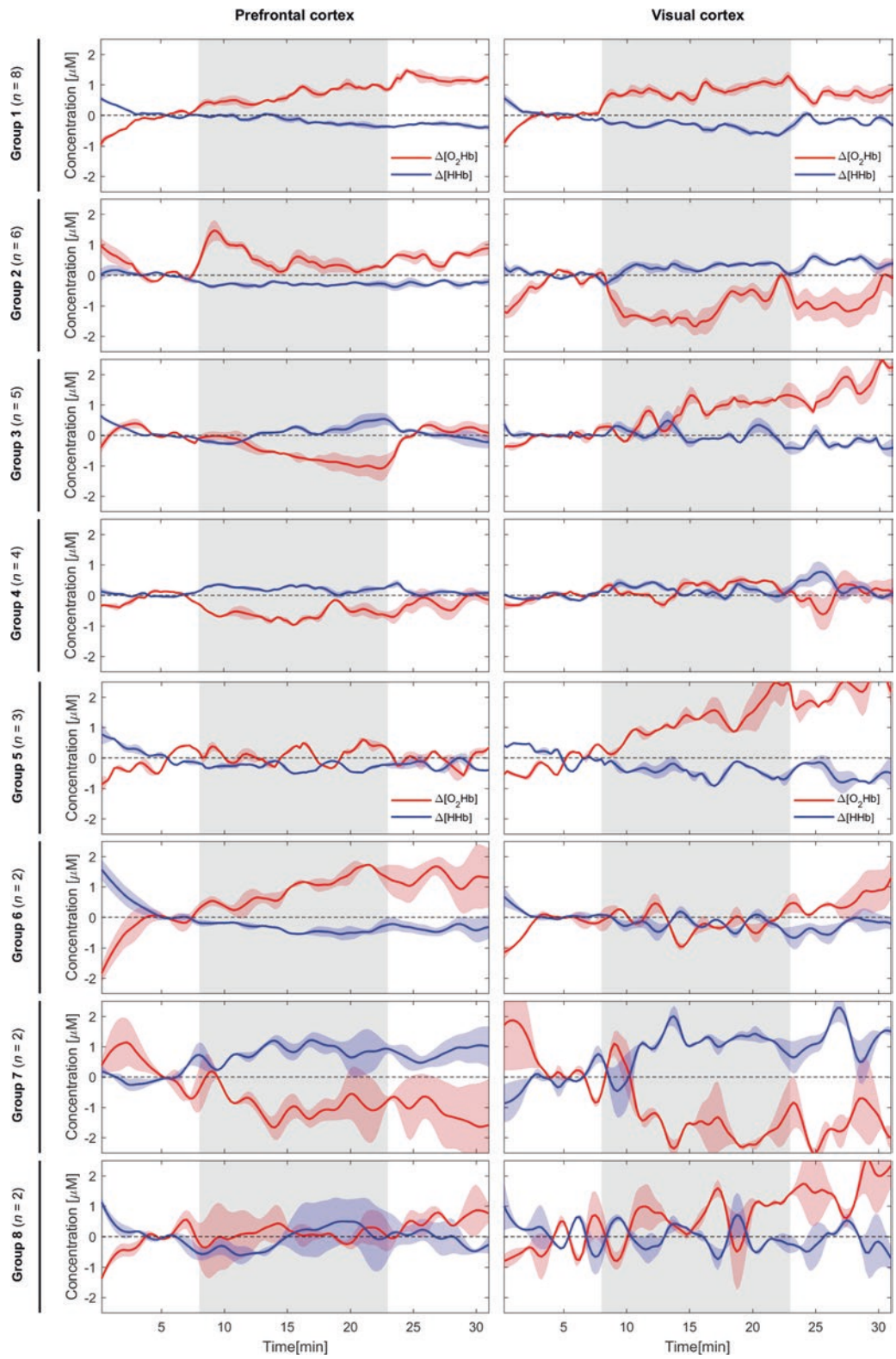

Fig. 34.2 Subgroup analysis (eight classes) of stimulus-evoked hemodynamic responses at the PFC and VC. The gray-shaded areas represent the BLE. Median ± SEM is shown

Table 34.1 Classification of hemodynamic response of [O_2Hb] patterns

	PFC	VC	Number of subjects within the group
Group 1	↑	↑	8 (5 females, 3 males); 63% female, 37% male
Group 2	↑	↓	6 (4 females, 2 males); 67% female, 33% male
Group 3	↓	↑	5 (1 female, 4 males); 20% female, 80% male
Group 4	↓	–	4 (4 females); 100% female
Group 5	–	↑	3 (1 female, 2 males); 33% female, 67% male
Group 6	↑	–	2 (2 females); 100% female
Group 7	↓	↓	2 (2 females); 100% female
Group 8	–	–	2 (1 female, 1 male); 50% female, 50% male

Decrease ↓, increase ↑, and inconclusive **–** at the PFC and VC during BLE

of cortical activation (characterized by the lack of [O_2Hb] increased or even decreased [O_2Hb]) were observed in the remaining subjects. In total, eight different hemodynamic response patterns were detected. Atypical changes in fNIRS signals can be triggered by systemic physiological noise, partial volume effects, or the presence of specific pathophysiological changes [11, 12]. Negative responses may also be explained by the interaction between neural activity, CBF, and cerebral metabolic rate of oxygen ($CMRO_2$). The decrease in [O_2Hb] may result from a further increase in oxygen consumption ($CMRO_2$) with a consequent mismatch between CBF and $CMRO_2$ increase, this time in favor of $CMRO_2$ [13]. Another possible reason for atypical patterns could be attributed to individual anatomical variability (e.g., diverse neuroanatomy) [12, 13]. Additionally, variations in CBF or arterial blood oxygenation, changes in intracranial pressure, hyper- or hypocapnia, and decreases of systemic blood pressure may alter the relationship between neuronal activity and fNIRS signals [14].

In conclusion, we found that blue light affects individual humans differently. Although a typical cortical activation pattern (an increase of [O_2Hb] associated with a decrease of [HHb]) was found for group-level analysis, such a pattern was observed in only eight subjects. However, we discovered eight different hemodynamic response patterns, which, in particular, should be taken into consideration when assessing the impact of BLE on society. We assume that the underlying reasons for the different patterns lie in individual changes in systemic physiology.

References

1. Hatori M, Gronfier C, Van Gelder RN et al (2017) Global rise of potential health hazards caused by blue light-induced circadian disruption in modern aging societies. NPJ Aging Mech Dis 3:9
2. O'Hagan JB, Khazova M, Price LLA (2016) Low-energy light bulbs, computers, tablets and the blue light hazard. Eye 30:230–233
3. Tosini G, Ferguson I, Tsubota K (2016) Effects of blue light on the circadian system and eye physiology Gianluca. Mol Vis 22:61–72
4. Vandewalle G, Maquet P, Dijk D-J (2009) Light as a modulator of cognitive brain function. Trends Cogn Sci 13:429–438
5. Viola AU, James LM, Schlangen LJM, Dijk D (2008) Blue-enriched white light in the workplace improves self-reported alertness, performance and sleep quality. Scand J Work Environ Health 34:297–306
6. Scholkmann F, Kleiser S, Metz AJ et al (2014) A review on continuous wave functional near-infrared spectroscopy and imaging instrumentation and methodology. NeuroImage 85:6–27
7. Zohdi H, Scholkmann F, Nasseri N, Wolf U (2018) Long-term changes in optical properties (μa, μ′s, μeff and DPF) of human head tissue during functional neuroimaging experiments. Adv Exp Med Biol 1072:331–337
8. Fantini S, Franceschini MA (2002) Frequency-domain techniques for tissue spectroscopy and imaging. Handb Opt Biomed Diag 7:405–453
9. Scholkmann F, Spichtig S, Muehlemann T, Wolf M (2010) How to detect and reduce movement artifacts in near-infrared imaging using moving standard deviation and spline interpolation. Physiol Meas 31:649–662
10. Scholkmann F, Hafner T, Metz AJ et al (2017) Effect of short-term colored-light exposure on cerebral hemodynamics and oxygenation, and systemic physiological activity. Neurophotonics 4:045005
11. Herold F, Wiegel P, Scholkmann F, Müller N (2018) Applications of functional near-infrared spectroscopy (fNIRS) neuroimaging in exercise–cognition science: a systematic, methodology-focused review. J Clin Med 7:466
12. Holper L, Shalóm DE, Wolf M, Sigman M (2011) Understanding inverse oxygenation responses during

motor imagery: a functional near-infrared spectroscopy study. Eur J Neurosci 33:2318–2328
13. Quaresima V, Ferrari M, Torricelli A et al (2005) Bilateral prefrontal cortex oxygenation responses to a verbal fluency task: a multichannel time-resolved near-infrared topography study. J Biomed Opt 10:011012
14. Lindauer U, Dirnagl U, Füchtemeier M et al (2010) Pathophysiological interference with neurovascular coupling – when imaging based on hemoglobin might go blind. Front Neuroenerg 2:25

Chapter 6

CLE-VFT: Differences in hemodynamic response patterns for the blue and red light exposure

The aim of this chapter is to thoroughly investigate a mixed-effect of CLE and VFT on behavioral performance as well as cerebral hemodynamics, oxygenation, and systemic physiology with the SPA-fNIRS approach. At the group-average analysis, Publication 8 was aimed to study how CLE-VFT interacts and affects cerebral hemodynamics, oxygenation, and systemic physiology. Subjects' VFT performance was also investigated during CLE. It is shown that SPA-fNIRS enables to understand of the interaction of cerebral and systemic parameters. No significant difference in the subjects' VFT performance was found between blue and red light exposure. In general, blue light exposure elicited stronger responses in cerebral hemodynamics and oxygenation in the VC. Additionally, significant differences between red and blue light exposure were observed in the recovery phase of systemic physiological parameters (namely, HRV). This shows that the CLE has relatively long-lasting effects (at least 15 min after cessation of the CLE), which underlines the importance of considering the persistent influence of colored light on brain function, cognition, and systemic physiology in everyday life. The group-average analysis, although commonly used, only displays the most prominent tendency between subjects. Therefore, the subgroup or subject-specific analysis is needed to completely understand the effects of the CLE-VFT. Thus, the aim of Publication 9 is to investigate a mixed-effect of CLE and VFT on hemodynamic and systemic physiological responses, this time at the subgroup level analysis. Our study finds that there is substantial intersubject-variability of cerebral hemodynamic responses, which is partially explained by subject-specific systemic physiological changes induced by the CLE-VFT. This publication shows that despite the typical hemodynamic response pattern normally observed at the group level (as shown in Publication 8), the subgroup analysis revealed that this pattern was found in only ~50% of the cases, and the number of patterns was different between red and blue light exposure.

Peer reviewed publication 8

Color-dependent changes in humans during a verbal fluency task under colored light exposure assessed by SPA-fNIRS

Hamoon Zohdi, Rahel Egli, Daniel Guthruf, Felix Scholkmann, Ursula Wolf

Scientific Reports (2021) 11, 9654

DOI: 10.1038/s41598-021-88059-0

URL : https://www.nature.com/articles/s41598-021-88059-0

Own contributions:

- Co-design of the study
- Contribute to carrying out measurements
- Signal processing
- Data analysis
- Visualization (Figures 3 & 4)
- Writing of the first draft

scientific reports

Check for updates

OPEN

Color-dependent changes in humans during a verbal fluency task under colored light exposure assessed by SPA-fNIRS

Hamoon Zohdi[1], Rahel Egli[1], Daniel Guthruf[1], Felix Scholkmann[1,2,3] & Ursula Wolf[1,3]✉

Light evokes robust visual and nonvisual physiological and psychological effects in humans, such as emotional and behavioral responses, as well as changes in cognitive brain activity and performance. The aim of this study was to investigate how colored light exposure (CLE) and a verbal fluency task (VFT) interact and affect cerebral hemodynamics, oxygenation, and systemic physiology as determined by systemic physiology augmented functional near-infrared spectroscopy (SPA-fNIRS). 32 healthy adults (17 female, 15 male, age: 25.5 ± 4.3 years) were exposed to blue and red light for 9 min while performing a VFT. Before and after the CLE, subjects were in darkness. We found that this long-term CLE-VFT paradigm elicited distinct changes in the prefrontal cortex and in most systemic physiological parameters. The subjects' performance depended significantly on the type of VFT and the sex of the subject. Compared to red light, blue evoked stronger responses in cerebral hemodynamics and oxygenation in the visual cortex. Color-dependent changes were evident in the recovery phase of several systemic physiological parameters. This study showed that the CLE has effects that endure at least 15 min after cessation of the CLE. This underlines the importance of considering the persistent influence of colored light on brain function, cognition, and systemic physiology in everyday life.

Light is essential not only for vision but also for the regulation of sleep and wakefulness, neurobehavioral, and neuroendocrine functions[1–7]. Among these nonvisual (i.e., non-image-forming) functions, light exposure has a direct impact on alertness and cognitive abilities[8,9]. Cognition is modulated by circadian rhythms and the nonvisual effects of light[10]. Short-wavelength (e.g. blue) monochromatic light affects the circadian rhythms of cognitive functions mediated by a melanopsin-based photoreceptor system[11]. One main class includes the intrinsically photosensitive retinal ganglion cells (ipRGCs), which are most sensitive to blue light (~460–480 nm)[1,12]. Thus, exposure to blue light influences many physiological functions, and it is applied to treat circadian and sleep dysfunctions, seasonal affective disorder as well as to boost alertness, help cognitive function, and elevate mood[13–15].

Whether exposure to colored light has an effect on cognition in humans is a current research question. Neuroimaging studies devoted to this topic employed electroencephalography (EEG)[11,16,17], positron emission tomography (PET)[18], and functional magnetic resonance imaging (fMRI)[1,12,19–22]. These human studies showed that light exposure affects cortical areas involved in the cognitive process and improves alertness and cognitive performance. In particular, the influence of brain responses (e.g., functional connectivity between hypothalamus and amygdala) and the cognitive performance were higher during blue light in comparison with longer wavelengths[1,20,22].

Among numerous cognitive tasks to assess cognitive functioning, the verbal fluency task (VFT) is a common neuropsychological test, which challenges the cognitive functioning during the arduous retrieval and verbal articulation of words[23]. In this test, subjects are instructed to produce as many words as possible within a restricted time, beginning with a certain letter (phonemic task) and/or belonging to a certain category of words (semantic task). The performance of these tasks is attributed to indicators of vocabulary size, lexical access speed, inhibition ability, and updating[24]. The performance of the test is mainly mediated by temporal, frontal, and parietal cortices[25–27].

[1]University of Bern, Institute of Complementary and Integrative Medicine, Fabrikstrasse 8, 3012 Bern, Switzerland. [2]Biomedical Optics Research Laboratory, Neonatology Research, Department of Neonatology, University Hospital Zurich, University of Zurich, 8091 Zurich, Switzerland. [3]These authors jointly supervised this work: Felix Scholkmann and Ursula Wolf. ✉email: ursula.wolf@ikim.unibe.ch

These cortices can easily be investigated by functional near-infrared spectroscopy (fNIRS), a neuroimaging technique, which measures changes in cerebral tissue hemodynamics and oxygenation related to alterations in neuronal activity[28–30]. One of the key advantages of fNIRS compared to fMRI is the relative insensitivity of this method to speech-related movement artefacts[31–33]. fNIRS is able to non-invasively and continuously determine concentrations of oxygenated ([O_2Hb]) and deoxygenated ([HHb]) hemoglobin of the cortical layers of the human brain[34,35]. It is known that cognitive activation leads to an increase in oxygen consumption, which is accompanied by an increase in cerebral blood flow (CBF) and total hemoglobin concentration ([tHb]) due to neurovascular coupling, resulting in an increase in [O_2Hb] with a concurrent decrease in [HHb][28,36,37]. Since [O_2Hb] and [HHb] are affected by factors not related to brain activity, i.e., changes in the systemic physiology, these factors need to be measured concurrently[38–40]. Therefore, it is crucial to employ the systemic physiology augmented (SPA) fNIRS approach, which relies on the measurement of brain activity with fNIRS along with the assessment of changes in systemic physiology—an approach our research group has been investigating for several years[38,39,41,42]. SPA-fNIRS is an ideal approach to avoid misinterpretations of fNIRS signals[43] as well as for a complete understanding of how the whole body reacts to task/stimulus paradigms.

The main goal of this study was to investigate by SPA-fNIRS how colored light exposure (CLE, red and blue light) and a VFT interact and affect cerebral hemodynamics and oxygenation, as well as systemic physiology. The findings of the current study are expected to facilitate a better understanding of the effect of colored light on cognition and behavior. The results have a broad range of implications for daily human life.

Subjects and methods

Subjects. 32 healthy subjects (17 female, 15 male, age 25.5 ± 4.3 years, range 19–45 years) participated in this study after they signed written informed consent. Subjects were all right-handed, non-smokers, medication-free, and with high education level (i.e., university students or university degree). They were asked to refrain from consuming caffeine and eating two hours prior to the experiment. The study was conducted in accordance with the World Medical Association Declaration of Helsinki, and the protocol and all methods were approved by the Ethics Committee of the canton of Bern (Project identifier: COLOR10; Basec-Nr. 2016-00674).

Experimental protocol. The subjects were asked to sit upright in a comfortable reclining chair in a dark room, while a white wall was in front of them (distance from the subject to the wall: 160 ± 5 cm). Following a randomized crossover design, each subject was exposed to two different light colors (red and blue). The spectrum of the light sources was measured by an Ocean Optics spectrometer and showed a peak wavelength of ~ 640 nm (full width at half maximum FWHM ~ 20 nm) for red and ~ 450 nm (FWHM ~ 20 nm) for blue. The illumination was adjusted to 120 lx (Digital Lux Meter, DT-1308, ATP) at the eye for both colors. The subjects were exposed to the colored light for 9 min on two different days but at the same time of day to minimize circadian variability of the responses. Before (baseline, 8 min) and after (recovery, 15 min) CLE, subjects were in darkness. The VFT, which contained three sessions, was carried out during CLE. Each session comprised three different trials in which the subjects had to produce as many words as possible within 30 s: (i) letter fluency task: producing nouns with a given letter (A, F, or M); (ii) control task: reciting weekdays in a consecutive manner; (iii) category fluency task: producing words from a specified category (flowers, fruits, or professions). The instruction of these tasks was given to the subjects by audiotaped voices. Figure 1a shows the schematic representation of the experimental VFT protocol used in this study. The order of the type of the trials (letter fluency, control, and category fluency) was fixed across all measurements, but the specific letters and categories were used in randomized order. Thus, each measurement period consisted of 9 trials of 30 s duration. The 1st, 4th, and 7th trials were letter fluency tasks with the letters A, F, or M in randomized order. The 2nd, 5th, and 8th trials were control tasks, where the subjects recited weekdays. The 3rd, 6th, and 9th trials were category fluency tasks with randomized categories. Each trial was followed by a resting phase of 30 s, where the subjects were asked to relax and stop mental engagement regarding previous tasks. The total duration of the VFT was 9 min and the period of the CLE was adjusted to this period. They were asked to keep their eyes open throughout the entire measurement and to move their head or body as little as possible during the measurement to avoid movement artifacts.

Measurement setup. With a multi-channel frequency-domain near-infrared spectroscopy (FD-NIRS) system (Imagent, ISS, Inc., Champaign, IL, USA), employing a multi-distance approach, changes of [O_2Hb], [HHb], [tHb] and tissue oxygen saturation (StO_2) were measured at a sampling rate of 2.5 Hz on the prefrontal cortex (PFC) and visual cortex (VC). The ISS optodes were positioned bilaterally over the PFC (left: Fp1 and right: Fp2) and the VC (left: O1 and right: O2), according to the international 10–20 system. The sensitivity profile of the optodes on the brain is shown in Fig. 1b. A detailed description of the FD-NIRS data acquisition and imaging instrumentation can be found in our previous studies[44,45].

Heart rate (HR) was measured with a SOMNOtouch NIBP device (SOMNOmedics GmbH, Randersacker, Germany) with a sampling rate of 4 Hz. SOMNOtouch calculated the HR from the ECG data by calculating the R-R intervals. This device also measured and determined the following parameters at a sampling rate of 1 Hz: Mean arterial pressure (MAP), pulse pressure (PP), arterial oxygen saturation (SpO_2), high-frequency (HF; 0.15–0.4 Hz), and low-frequency (LF; 0.04–0.15 Hz) component of the heart rate variability (HRV).

A NONIN LifeSense (NONIN Medical, Plymouth, MN, USA) was used to non-invasively measure end-tidal carbon dioxide ($P_{ET}CO_2$) and respiration rate (RR). Data were recorded at a sampling rate of 1 Hz.

An electrodermal activity measurement system (Verim Mind-Reflection GSR, Poland) was employed to determine the skin conductance (SC). Skin conductance level (SCL) and integrated skin conductance response (ISCR) were measured at 8 Hz sampling rate.

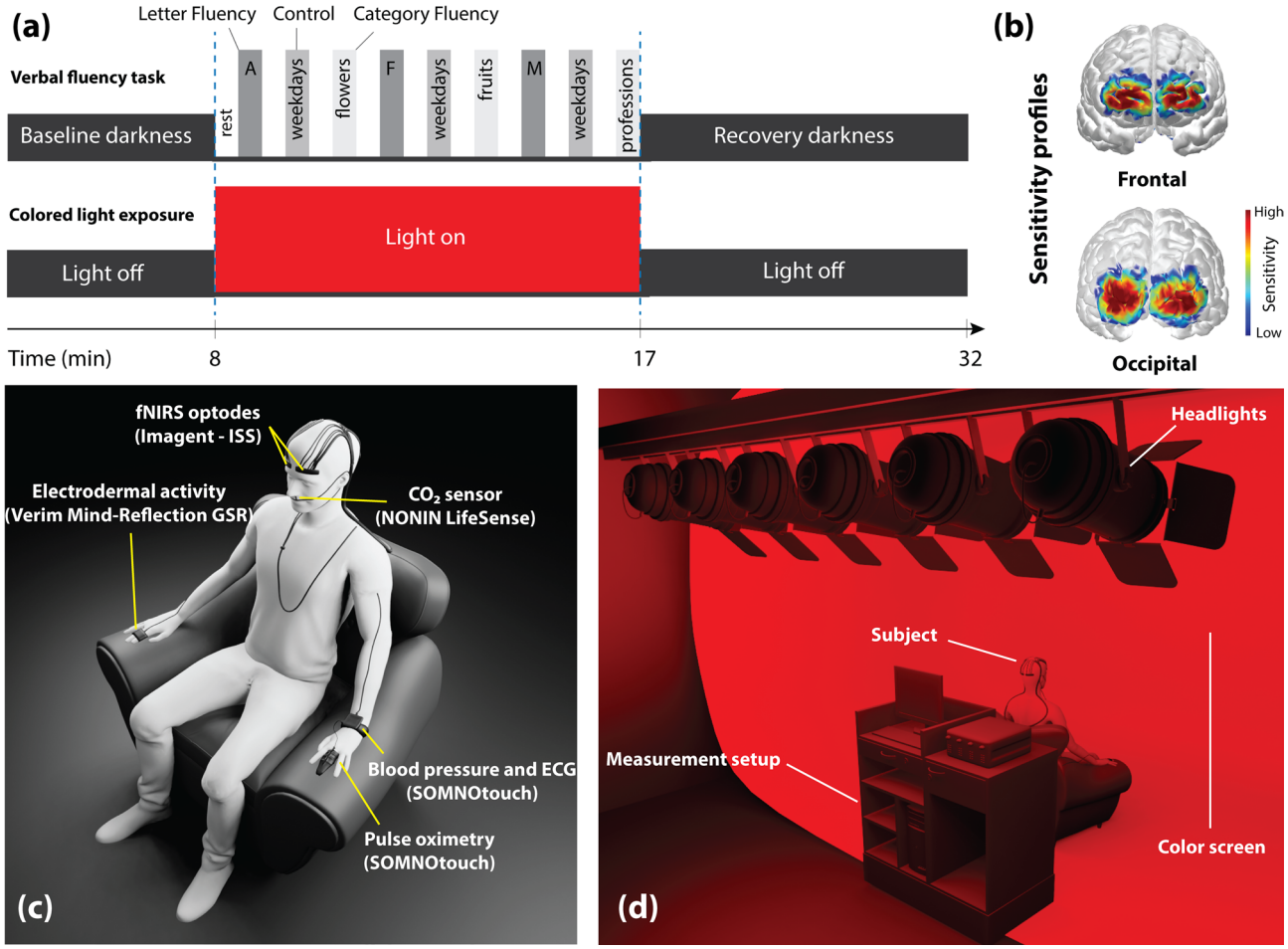

Figure 1. (**a**) Schematic illustration of the experimental protocol, including the VFT and CLE. (**b**) Sensitivity profile of ISS-sensors on the brain. The sensitivity profile shows which regions of the brain are measured with fNIRS. The higher the value, the more contribution of the fNIRS signal from the cerebral cortex layer. (**c**) Visualization of the placement of devices/sensors on the subject. (**d**) Experimental setup with the position of the subject and the color screen.

To quantify the coupling between HR and RR, the pulse-respiration quotient (PRQ) was calculated (PRQ = HR/RR)[46].

All data were recorded simultaneously. The position of devices and sensors on the subject is shown in Fig. 1c. Moreover, Fig. 1d presents the experimental setup with the position of the subject and the color screen. The 3D human model was constructed using the Blender 3D interface (http://www.blender.org, version 2.82).

Signal processing and statistical analysis. The data set of one subject was excluded from data analysis since the subject was not a German native speaker, which might have affected the VFT performance. All signal processing and statistical analysis were performed in MATLAB (R2017a, MathWorks, Inc., MA, USA).

Cerebral oxygenation and hemodynamics. Movement artefacts in fNIRS signals were detected and removed by the in-house developed movement artefact removal algorithm (MARA) based on moving standard deviation and piecewise-interpolation[47]. For 96.7% of the signal time series, no processing with MARA was required. When MARA was applied, it was ensured the overall trend of the time-series processed was not altered. To further remove high-frequency noise, signals were low pass filtered using a robust 2nd-degree polynomial moving average (RLOESS) filter with a span of 3 min. Signals from the left and right PFC and VC were subsequently averaged to obtain signals for the whole PFC and VC, respectively.

Systemic physiological parameters. All other biosignals, except the SC, were also denoised by the RLOESS method with a window length of 3 min. The SC data were processed with Ledalab toolbox (http://www.ledalab.de)[48,49]. This MATLAB toolbox is able to extract the phasic (high frequency) and tonic (low frequency) SC components by continuous decomposition analysis. In this study, the tonic component of the SC, known as skin conductance level (SCL), and the ISCR, which involved the integration (i.e., area under the curve) of the phasic driver signal, were used for the signal processing and statistical analysis.

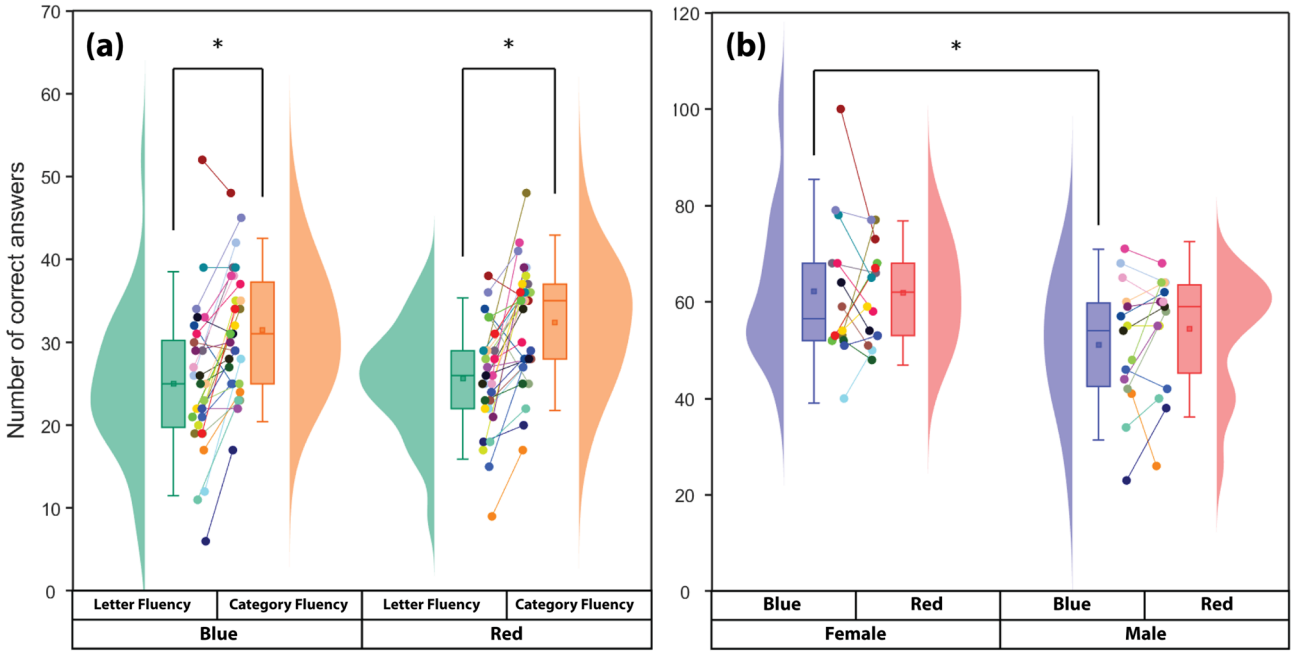

Figure 2. (**a**) Subjects' performance in the category and letter versions of the VFT during CLE. Asterisks show a significant difference between tasks ($p < 0.05$, Wilcoxon signed-rank test). (**b**) Effects of sex on the task performance of subjects who are exposed to two lighting conditions (blue vs. red). The asterisk shows a significant difference between male and female subjects during blue light exposure ($p < 0.05$, two-sample *t*-test). The same color data points and lines belong to an individual subject.

Statistical analysis. All bio-signals were segmented into ten parts (3 min each), and the median of each segment was calculated. Two segments were assigned to the baseline phase (2–8 min, time points (TP) 1–2), three to the CLE (TP 3–5), and five to the recovery phase (TP 6–10). The median of each segment was then normalized to the last TP of the baseline phase (TP2). Subsequently, to analyse and visualize the changes of the parameters at the group-level, the median and the standard error of the median (SEM) of each segment among all subjects were calculated. Additionally, a Wilcoxon signed-rank test for each TP in comparison with the last TP of the baseline (TP2) was calculated and a false discovery rate (FDR) correction was subsequently applied to the *p*-values in order to correct for the multiple comparison situation. In order to compare the effects of the two types of colored light (red vs. blue) on the changes of the bio-signals during the task/stimulation and recovery phases, each time point of red light was compared with the same time point in blue light using the Wilcoxon signed-rank test. Moreover, the number of correct words generated by each subject during the task period was determined as the subjects' task performance. Word repetitions and proper names of people and places were excluded from the data analysis. Synonyms and direct hypernyms/hyponyms were counted as one word. The effects of sex and type of cognitive task on subjects' performance were also investigated by the *t*-test and paired Wilcoxon signed-rank test, respectively. For the behavioral data, a $2 \times 2 \times 2$ analysis of variance (ANOVA) was applied with JASP (jasp-stats.org, version 0.11.0.0) to test for the main effects of sex, CLE, and VFT as well as for interaction effects. Investigating the effects of sex as well as the specific type of VFT on cerebral and physiological parameters is interesting, but it is beyond the scope of this article and will be analyzed in-depth in a future investigation.

Results

Task performance. Subjects were more successful in the category version of the VFT compared to the letter fluency version (blue: $p < 0.001$; effect size (Cohen's d): $d = 0.8$, red: $p < 0.001$; $d = 1.0$). No significant difference in the performance of both tasks was found between blue and red light. In more detail, subjects produced 25.0 ± 9.0 (mean ± SD) nouns in the letter fluency during the blue light condition, while they reached a number of 25.6 ± 6.5 nouns during the red light. In the category fluency, subjects produced 31.5 ± 7.4 and 32.3 ± 7.1 nouns during blue and red light exposure, respectively (Fig. 2a).

Sex effects. The total number of correct responses during the blue light condition for the female and male subjects was 62.2 ± 15.5 and 51.1 ± 13.2, respectively, whereas they produced 61.9 ± 10.0 (female) and 54.3 ± 12.1 (male) correct words during red light exposure. Females were generally better VFT performers compared to males. Although the difference was significant during the blue light condition ($p < 0.05$; $d = 0.8$) (Fig. 2b), no significant interaction effect was found for "Sex × Colored light" analyzed by ANOVA (Table 1).

Changes during the colored light exposure and verbal fluency tasks. Figures 3 and 4 depict block-averaged changes in cerebral hemodynamics, oxygenation, and systemic physiology evoked by CLE (blue vs.

	VFT correct responses	
	F-statistic	*p*-value
Main effects		
Sex (S)	**11.906**	**< 0.001**
Colored light (C)	0.278	0.599
VFT tasks (T)	**23.913**	**< 0.001**
Interaction effects		
S × C	0.435	0.511
S × T	0.064	0.800
C × T	0.005	0.942
S × C × T	0.222	0.639

Table 1. Summary of the ANOVA for subjects' performance. Values in bold indicate statistical significance at the $p < 0.05$ level.

red) and VFT. Independent of the color, CLE in combination with VFT elicited responses in the PFC and caused significant changes in systemic physiological parameters including MAP, $P_{ET}CO_2$, SCL, ISCR, and HRV (LF/HF).

Cerebral tissue hemodynamics and oxygenation. Both conditions (blue and red) elicited statistically significant changes in [O_2Hb] (increase), [HHb] (decrease), [tHb] (increase), and StO_2 (increase) in the PFC, while only the blue light exposure evoked significant changes in the VC, i.e., [O_2Hb] (increase), [HHb] (decrease), [tHb] (increase), and StO_2 (increase), throughout the whole CLE-VFT. In the VC, the red light caused only significant stimulus-evoked changes, i.e., [O_2Hb] (increase) and StO_2 (increase), at the onset of the CLE-VFT. Color-dependent effects were observed in [O_2Hb], [HHb], and StO_2 in the VC. Blue evoked stronger overall responses in cerebral hemodynamics and oxygenation in the VC. Additionally, higher [O_2Hb] and StO_2 changes at the beginning (TP3) of the blue light exposure were observed in the PFC compared to the red light exposure.

Systemic physiological activity. The following systemic physiological parameters showed statistically significant changes during the CLE-VFT: MAP, SpO_2, SCL, ISCR, and LF/HF (increase during blue and red); $P_{ET}CO_2$ (decrease during blue and red); HR and PP (increase during blue); HF (decrease during red). HR, MAP, and SCL changes were higher during blue light in comparison with red light, although the differences did not reach statistical significance. In addition, blue and red light exposure evoked no statistically significant changes in RR and PRQ after FDR correction. PRQ increased for both conditions, although the increase was less pronounced for the blue light.

Color-dependent changes in the recovery phase (post-light period) of some systemic physiological parameters were noticeable (e.g., $P_{ET}CO_2$: at the beginning of the recovery phase, SCL: at the end of the recovery phase). Changes in HF and LF/HF were color-dependent throughout the recovery phase.

Discussion

No significant difference in cognitive performance between blue and red. The VFT has been widely used as a tool to measure verbal ability and executive control. VFT performance also provides a possible predictor for prospective identification of diseases[24,50]. One of the main goals of this study was to investigate the effects of light of two colors (blue vs. red) on VFT performance. No significant difference in subjects' performance was found between blue and red light. One possible explanation for this finding is that the attention of the subjects was mainly focused on performing the VFT than actively perceiving and being aware of the CLE. This may have diminished the effect of the specific colored light on performance. The number of correct answers produced by the subjects in both versions of the VFT is in good agreement with Holper et al.[50] and higher compared to the previous studies[23,25,51]. All aforementioned VFT studies were conducted under normal lighting conditions. For the first time, the light of different colors was employed in our study to investigate its impacts on the subjects' performance. In addition to CLE, age, education level, physiological state of subjects, or even methodological variabilities may be possible reasons for the difference between studies in terms of VFT task performance. Herrman et al. showed that subjects ($n = 14$, middle to highly educated subjects, age: 31.4 ± 6.8 years) achieved an average of 33.0 ± 11.2 correct responses for the three letters (i.e., A, F, and S; each lasted 60 s) in the VFT[25]. In another study, subjects ($n = 325$, including right-handed, left-handed, and ambidextrous, age: 51–82 years) within 30 s produced 6.1 ± 2.0, and 9.9 ± 2.0 correct words in letter and category VFT, respectively[23]. Additionally, within both conditions (blue vs. red), performance in category fluency was significantly better than in letter fluency. These findings are in line with several studies[23,50,51]. The letter fluency is generally more challenging than the category fluency. In the category fluency, subjects can rely on existing links between related concepts or words, while the links between words in the letter fluency may be weaker or less accessible[24]. In other words, retrieval of a word (e.g., apple) automatically activates semantically associated words (e.g., orange, banana, peach, and mango) in the category fluency version of the VFT. By contrast, in the letter fluency, subjects must restrain the activation of associatively related concepts and employ different retrieval

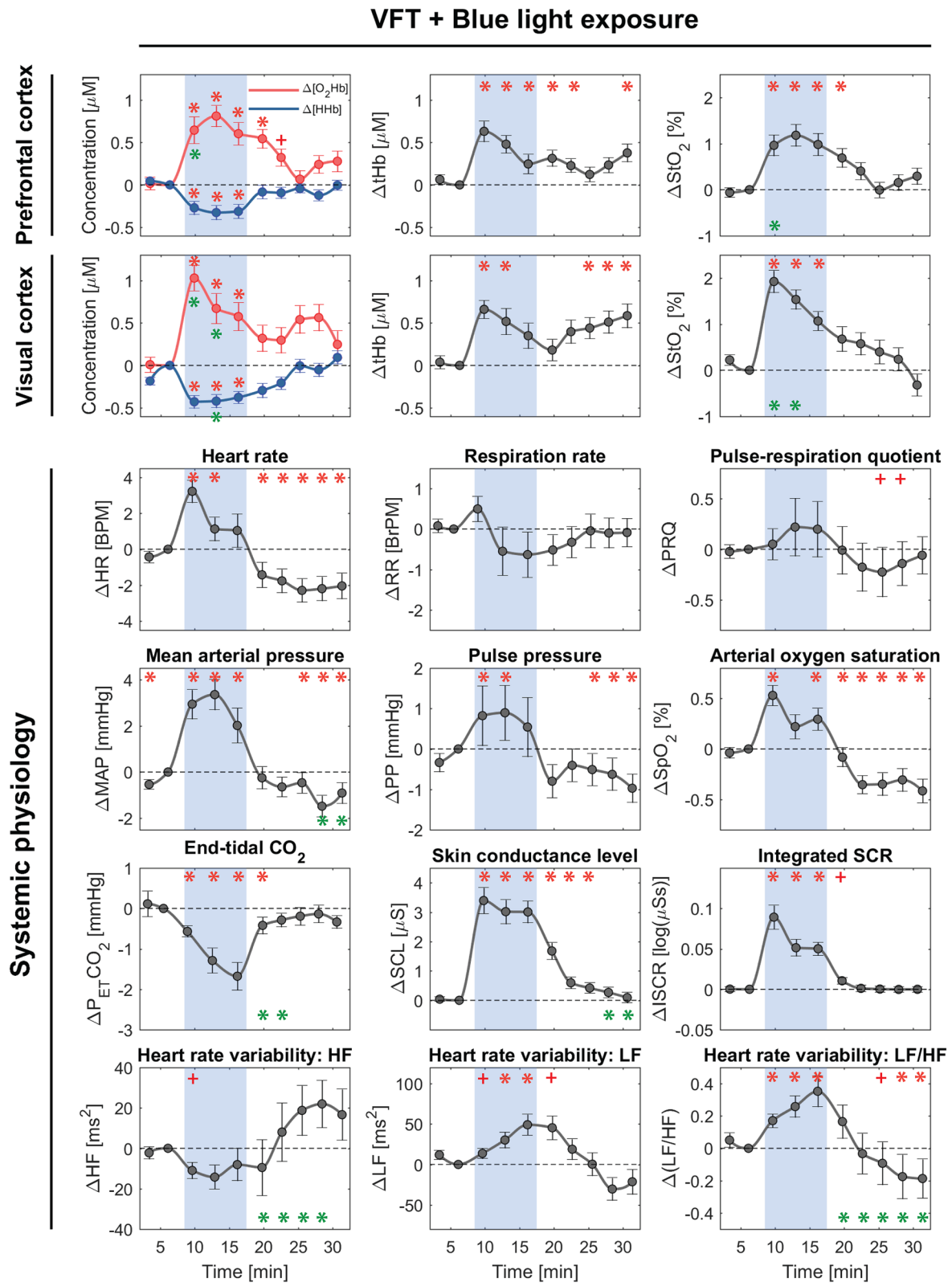

Figure 3. Block-averaged (group-level) changes in cerebral hemodynamics/oxygenation and systemic physiology (median ± SEM) evoked by blue light exposure and VFT. The blue shaded areas represent time intervals during the task/stimulation period. The time series are sub-divided into ten periods (3 min each). Then, they are normalized to the last time period of the baseline (TP2). Red symbols indicate a significant change of the marked time point with respect to baseline (asterisk *: proved by both FDR-corrected and uncorrected p values; plus +: only uncorrected p value, $p < 0.05$, Wilcoxon signed-rank test). Green asterisks present a color-difference (blue vs. red) of the marked time points ($p < 0.05$, Wilcoxon signed-rank test).

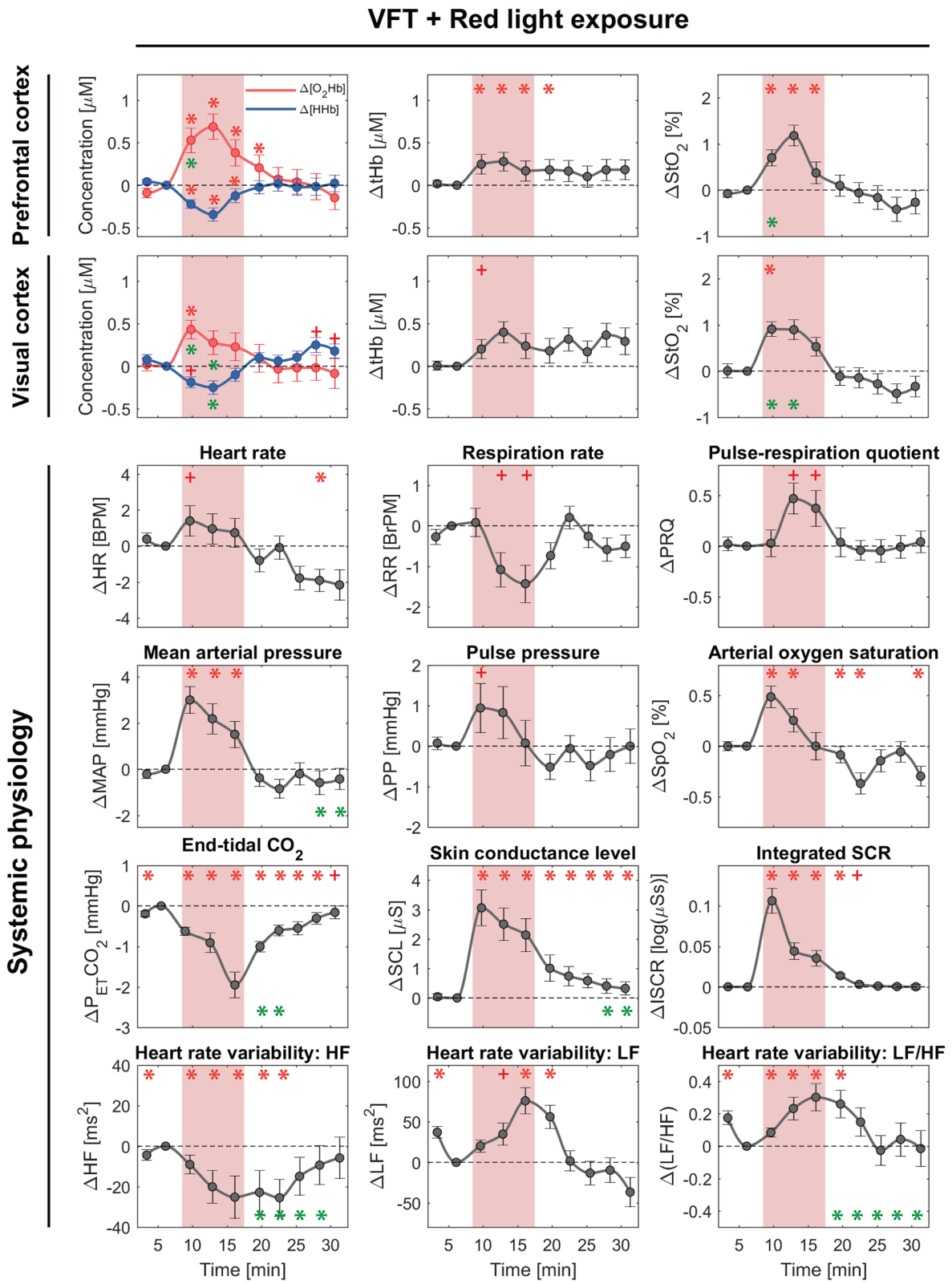

Figure 4. Block-averaged (group-level) changes in cerebral hemodynamics/oxygenation and systemic physiology (median ± SEM) evoked by red light exposure and VFT. The red shaded areas represent time intervals during the task/stimulation period. The time series are sub-divided into ten periods (3 min each). Then, they are normalized to the last time period of the baseline (TP2). Red symbols indicate a significant change of the marked time point with respect to baseline (asterisk *: proved by both FDR-corrected and uncorrected p values; plus +: only uncorrected p value, $p < 0.05$, Wilcoxon signed-rank test). Green asterisks present a color-difference (blue vs. red) of the marked time points ($p < 0.05$, Wilcoxon signed-rank test).

strategies[52,53]. In conclusion, we found a reasonable performance compared to previous studies but no effect of the CLE, which was tested for the first time.

Females were better VFT performers than males. Consistent with previous studies[23,54], we found that females generally performed VFT tasks more efficiently than males. This fact has become well-accepted, although some findings are inconsistent[55,56], where the task performance was equal between males and females. It has been proven that female subjects are better in the performance of verbal tasks, while male subjects are more successful in visual-spatial tasks[57,58]. The reason for sex differences at a behavioral level may be attributed to dissimilarities in the structure of the language-related cortex and the cerebral organization of language function[59]. It is known that language functions are more lateralized in males (i.e., to the left inferior frontal gyrus regions) than in females[60]. However, Weiss et al. proposed that such a difference in executive speech tasks is related to different processing strategies for lexical verbal fluency rather than sex-related hemispheric organization[59]. Additionally, the reasons for the significant difference between females and males in VFT performance during the blue light condition may be attributed to different color preferences and color perception between females and males or even fluctuations in sex hormones. Corticotropin-releasing hormone (CRH) plays key roles in the coordination of the stress response as a potential mediator of sex-related differences[61,62]. The presence of estrogen, a classical female sex hormone, has been proved in the CRH gene[61]. Therefore, sex differences at a behavioral performance may also be due to the role of estrogen in mediating stress response. It was demonstrated that a stressful experience caused a female's later ability to attain certain types of new memories and was dependent on changing levels of estrogen[63]. Shors and Leuner showed that performance of the classically conditioned eyeblink response was poor in the presence of very low and very high estrogen, whereas in the presence of moderate estrogen, performance was optimal[63]. It was also shown that females were better performers on spatial tests in low levels of estrogen and on articulatory-verbal tests in high levels of estrogen[64]. Coupled with the knowledge that estrogens in females and androgens in males are generally positively associated with the performance in verbal and spatial tasks, respectively, for our results, this implies that the ability of estrogen to enhance verbal performance in females can be taken as evidence for sex differences in cognitive functioning underlying the VFT.

Cerebral hemodynamics and oxygenation. In this study, we used FD-NIRS to investigate a mixed-effect of CLE and VFT on neural correlates of cognitive functioning. The FD-NIRS system is able to measure the absolute optical properties, namely the absorption coefficient and the reduced scattering coefficient, and consequently the absolute values of [O_2Hb], [HHb], [tHb] and StO_2. In contrast, continuous wave NIRS (CW-NIRS) can only provide information on changes of [O_2Hb] and [HHb] but cannot determine absolute values[44]. The CW-NIRS technique relies on assumed constant optical properties during the measurement, an assumption not necessarily true in reality[34]. Compared to CW-NIRS, the FD-NIRS technique is less sensitive to physiological noise from the extracerebral tissue compartment[45]. For further, more detailed information on NIRS-based techniques, we refer readers to Scholkmann et al.[28]. In our previous studies, we investigated how cerebral hemodynamics and oxygenation change during different short-term and long-term colored light exposures[13,38,41,65–67]. The impact of the VFT on human brain activity and cerebral perfusion was also investigated in several fNIRS studies[68–71]. We found in the current study that CLE in combination with VFT evoked responses in the PFC, while only blue light leads to significant changes in the VC throughout the CLE-VFT.

Color-independent prefrontal cortex responses. The PFC is involved in various higher-order cognitive functions, including memory, processing of language, selective attention, and task planning[70,71]. PFC activity can be evaluated by measuring changes in [O_2Hb], [HHb], [tHb], and StO_2. Our findings showed that, regardless of the color type, the CLE with a combination of the VFT leads to an increase in [O_2Hb], [tHb] and StO_2, and a concurrent decrease in [HHb], which corresponds to the typical pattern of cerebral activation. However, higher [O_2Hb] and StO_2 changes at the beginning (TP3) of the blue light exposure were evident compared to the red light.

Several studies using fNIRS have shown increases of [O_2Hb] and decreases of [HHb] in response to a VFT task[31,32,68,70]. A recent review concluded that cognitive tasks caused the [O_2Hb] increasing in more than 70% and [HHb] decreasing in 100% of the studies, which reported changes in hemoglobin concentrations in the PFC in response to the VFT or working memory tasks[72].

Concerning the CLE, we demonstrated in our previous study that short-term blue light led to a significantly different response in [O_2Hb], [tHb], and StO_2 in the PFC compared to red and green light[38]. A significant increase in StO_2 was indicated in the left PFC during blue but not red light in a long-term CLE study carried out by Weinzirl et al.[66]. In another study where we had investigated long-term CLE, cerebral hemodynamics and oxygenation in the PFC were significantly different for yellow compared to red and blue, but not between red and blue[41].

We showed that CLE accompanied by the VFT elicited significant changes in cerebral hemodynamics and oxygenation in the PFC. In parallel research performed with this study, we found that CLE alone did not significantly affect cerebral perfusion in the PFC (data not shown). Therefore, it seems that the impact of VFT was more prominent compared to CLE and the stimulating effect of CLE is low or even decreases when the brain is already involved in a challenging VFT task.

Color-dependent visual cortex responses. Compared to red light, we showed that blue light exposure evoked stronger overall responses in cerebral hemodynamics and oxygenation in the VC. In the literature, there are a few fNIRS reports investigating the effect of color and colored light on cerebral responses in the VC[13,38,73–75]. Even though Liu and Hong[75] showed that the left VC is more active during the blue-color stimulus, Scholkmann et al.[38], from our group, observed that the magnitude of the hemodynamic responses in the VC was independent

of color. In another fNIRS study, the authors found a significant increase in hemodynamics during the between-category (blue vs. green) changes, but not during the within-category (two different shades of green) changes[73]. The visual system response to blue light might be a marker for central nervous system dopamine tone[76], reported in an fMRI study. It was also proposed in other neuroimaging studies that colors in different categories are differently represented in the VC[77,78].

Systemic physiology responses. A higher increase in HR during exposure to blue light is in line with the research performed by Cajochen et al.[79] ($n = 10$ male subjects, age: 25.9 ± 3.8 years, exposure to 2 h of monochromatic lights in the evening). Contrary, a decrease was observed in one study under blue light in subjects with closed eyes ($n = 7$, age range: 23–55 years, exposure to 10 min color light panels (blue vs. red), illuminance: 140 lx, distance: 40 cm)[80]. All other studies presented no dependence of HR on CLE in sitting subjects[81–83]. The increase in HR during the blue light condition may be attributed to the autonomic nervous system (ANS) responding to blue light with an increase in sympathetic tone, i.e., a response that is predominantly susceptible to short-wavelength light[79].

In line with other research[83,84], in our study, colored light had no distinctive effects on RR based on FDR-corrected p values. This could be due to the large inter-subject variation caused by subjects having different RR responses. The absolute RR values measured in our previous study for healthy subjects at rest were within a large range (6.9–27.1 breaths per minute)[44].

The PRQ is a useful and unitless parameter to attain the overall state of human physiology[46]. This parameter is calculated as HR divided by RR and its resting-state distribution has a peak at ~ 4[85]. Although PRQ increase was more pronounced for the red light, we observed no statistically significant changes (FDR-corrected p values) in response to both conditions, which is in accordance with the literature[84]. In our previous study investigating short-term CLE effects with blue light, a decrease in PRQ was found[38].

We also found an increased MAP for both conditions and an increased PP only for blue light exposure. Increased diastolic blood pressure was reported for the light of higher color temperatures (i.e., 7500 °K vs. 3000 °K and 5000 °K) at high-intensity levels (> 320 lx)[86]. This indicates that light with an increased fraction of blue light increases blood pressure. In another study, MAP increased for blue light, but not for red at a high intensity (> 250 lx)[87].

The decrease in $P_{ET}CO_2$ during the CLE and VFT tasks is in line with the findings of Scholkmann et al.[40]. In that study, the effect of different speech tasks on $P_{ET}CO_2$ and cerebral hemodynamics and oxygenation was investigated. During all tasks, $P_{ET}CO_2$ was reduced with the strongest decrease during the alliteration task (~ 9 mmHg) and the smallest during the mental arithmetic task (~ 3 mmHg). In the present study, the $P_{ET}CO_2$ decrease was less than 2 mmHg for both blue and red light. In summary, typical patterns of the fNIRS data and $P_{ET}CO_2$ caused by a combination of the CLE and VFT are comparable to the mental arithmetic task of the aforementioned study. It is noteworthy that in the current study, the $P_{ET}CO_2$ decrease constitutes only weak hypocapnia induced by hyperventilation. In this case, the vasodilation caused by brain activity outweighed the vasoconstriction caused by hypocapnia.

Electrodermal activity (EDA) and HRV are two commonly used psychophysiological stress measures[88]. EDA reflects the variation of the electrical properties of the skin in response to sweat secretion[48,49]. In our study, both EDA parameters were significantly increased during blue and red light exposure. The increase in EDA is related to various factors such as mental stress or pain, owing to the stimulation of the sympathetic nervous system. Several studies have shown increasing of EDA parameters during mental load and cognitive stress, compared to baseline measurements[89–91]. In parallel research carried out with this study, we found that CLE alone (without VFT) affected EDA (data not shown; ΔSCL: $SCL_{CLE} - SCL_{base}$; Blue: 0.04 ± 0.08 µS; Red: 0.05 ± 0.07 µS) much lower than the CLE-VFT (this study; Blue: 3.08 ± 0.38 µS; Red: 2.98 ± 0.55 µS). Therefore, we conclude that the effect of the VFT on EDA changes was more noticeable than the CLE. In our previous study, we showed that short-term blue, red, and green light (without any cognitive tasks) triggered changes in SCL with large intersubject variability and only a marginal change in the group-average[38]. Other studies showed an increase in EDA under short-term (1 min) red light[83] and a decrease under long-term (20 min) blue, orange, and green light exposure[92].

HRV is an index of the ANS, providing a measure of ANS through parasympathetic and sympathetic modulation of cardiac function[93]. It is known that the LF component of HRV is modulated by both the parasympathetic nervous system (PNS) and the sympathetic nervous system (SNS), while HF is mainly controlled by the PNS[94]. Although it is widely believed that the LF/HF ratio reflects the sympathovagal balance, Billman showed that this assumption is not accurate and greatly oversimplifies the complex non-linear relations between the sympathetic and the parasympathetic divisions of the ANS[95]. In line with this new statement, von Rosenberg et al. proposed a simultaneous consideration of the LF and HF within a 2D scatter diagram, improving the discrimination ability in the physical and mental stress analysis[96]. HRV is considered as a marker of stress. In both conditions, we found a decrease of the HF and an increase of the LF during the CLE-VFT, although only the HF was significantly decreased during red light exposure. An increased LF and a decreased HF observed in both conditions are attributed to the mental stress that subjects experienced during VFT tasks[94,97]. This emphasizes once again the point that the influence of VFT is more prominent compared to CLE during the CLE-VFT and the stimulating effect of CLE is low or even decreases when the brain is already involved in a challenging VFT task. In line with the research carried out by Posada-Quintero and Chon[98], we found an increase in the LF component of HRV as well as the EDA in the presence of stressors (VFT tasks), which are known to be controlled by the SNS. In several studies, red light decreases HF power[84,99,100]. Even though blue light caused no significant HF changes in our study, an increase in the HF was observed due to blue light in other studies[81,101,102]. We did not observe any significant difference between red and blue during the CLE. However, changes in HF and LF/HF were interestingly color-dependent throughout the recovery phase. This may be indicative that brief exposure to colored light

has effects on HRV parameters that may persist for at least 15 min after cessation of the light. Higher HF changes and lower LF/HF ratio after blue light compared to red light may indicate an increase of the parasympathetic response during the recovery phase after blue light exposure. In other words, higher HF changes accompanied by insignificant changes in the LF after blue in comparison with red represent a more relaxed state for this condition based on the 2D scatter diagram proposed by von Rosenberg et al.[96].

Limitations. The study has the following limitations: (1) The size of the sample was calculated with power analysis to detect substantial effects (effect size: $d = 0.59$) at a $p < 0.05$ and a power of > 0.8. A large number of subjects may have shown further physiological or behavioral color-dependent responses. But, these effects would have been small and probably not very relevant. (2) Only blue and red light were analyzed. Different colors may have other effects. (3) The intensity of the CLE may evoke different effects. We selected a relatively high intensity (120 lx) that was the same for both colors. (4) The ISS optodes do not yet cover the entire head, and hence not the complete brain was analysed. (5) Depending on the nature of the task, different colored lights might affect cognitive tasks differently. It has been revealed that red improves performance on a detailed-oriented task, while blue enhances performance on a creative task[103]. Therefore, it would be worthwhile to include other cognitive tasks in future studies. (6) The VFT protocol can be simplified for future studies. The control task, which normally does not evoke brain activation and may reduce the effect, can be removed from the VFT protocol.

Conclusions and outlook

In conclusion, our study is the first employing SPA-fNIRS to investigate a mixed-effect of CLE and VFT on cerebral hemodynamics, oxygenation, and systemic physiology. Our new approach (SPA-fNIRS) enabled to understand the interaction of cerebral and systemic parameters. No significant difference in the subjects' VFT performance was found between blue and red light exposure, while sex and type of VFT (category versus letter) affected the subjects' performance significantly. Overall, blue light exposure evoked stronger responses in cerebral hemodynamics and oxygenation in the VC. We found several color-independent changes in cerebral and physiological signals due to the VFT. Moreover, significant differences between red and blue light exposure were observed in the recovery phase (post-exposure period) of systemic physiological parameters (namely, $P_{ET}CO_2$, SCL, HF, and LF/HF ratio). Therefore, it is essential to consider the relatively long-lasting (15 min) effects of CLE in humans. This underlines the importance of considering the persistent influence of colored light on brain function, cognition, and systemic physiology in everyday life.

In this study, SPA-fNIRS was used to assess a mixed-effect of CLE and VFT on human physiology. The results imply that the reaction of the brain and the systemic physiology is different or in some cases similar, depending on the physiological parameter and color of the light (with equal perceived brightness). In our previous study, with SPA-fNIRS, we were also able to demonstrate that MAP and SpO_2 were positively correlated with $[O_2Hb]$ at the PFC during the CLE-VFT[45]. Therefore, SPA-fNIRS should become a standard approach for fNIRS studies to enable a comprehensive understanding and the correct interpretation of changes in cerebral hemodynamics and oxygenation. This tool enables to understand the underlying reasons for a variety of stimulus-evoked changes and cognitive task performances.

Our findings contribute to a better understanding of CLE effects on human physiology. Although no significant difference in the performance of VFT tasks was found between blue and red light, the physiological color-dependent responses are potentially of high relevance in the process of choosing colors and colored lights for related objectives (e.g., room lighting and workplaces). Specifically, our findings about a mixed-effect of CLE and VFT on human physiology offer a broad range of implications for educational purposes and facilitate a better responding of the following questions: *Do colored lights (or colors) play a role in enhancing cognitive task performances as well as learning and nurturing concepts? What colored light improves motivation and creativity in the workplace?* Additionally, since exposure to colored light expeditiously increases in our modern society due to modern light sources such as screens and LEDs, investigation of colored light and its impact on human physiology are of rising interest. Especially at the present time, when students have to do their homework using smartphones and tablets, known as modern light-emitting devices, more than before due to the Covid-19 pandemic, another question might be raised: *What desktop background color do we pick for educational facilities?* The results of this research are expected to facilitate a better understanding of the CLE effects on the underlying neuroscientific mechanisms in the brain and body, which in turn would pave the way for safe and advantageous applications of colored light in daily life and even therapeutic settings. Moreover, in a society that is rapidly exposed to new and increasing lighting, it is expected that the findings of this research are being relevant and beneficial for the scientific community, medical professionals and the society.

Received: 22 September 2020; Accepted: 1 April 2021
Published online: 06 May 2021

References

1. Vandewalle, G., Maquet, P. & Dijk, D. J. Light as a modulator of cognitive brain function. *Trends Cogn. Sci.* **13**, 429–438 (2009).
2. Daneault, V. *et al.* Aging reduces the stimulating effect of blue light on cognitive brain functions. *Sleep* **37**, 85–96 (2014).
3. Duffy, J. F. & Czeisler, C. A. Effect of light on human circadian physiology. *Sleep Med. Clin.* **4**, 165–177 (2009).
4. Blume, C., Garbazza, C. & Spitschan, M. Effects of light on human circadian rhythms, sleep and mood. *Somnologie* **23**, 147–156 (2019).
5. Prayag, A. *et al.* Light modulation of human clocks, wake, and sleep. *Clocks Sleep* **1**, 193–208 (2019).
6. Souman, J. L. *et al.* Acute alerting effects of light: A systematic literature review. *Behav. Brain Res.* **337**, 228–239 (2018).
7. Russart, K. L. G. & Nelson, R. J. Light at night as an environmental endocrine disruptor. *Physiol. Behav.* **190**, 82–89 (2018).
8. Chellappa, S. L. *et al.* Photic memory for executive brain responses. *Proc. Natl. Acad. Sci. USA* **111**, 6087–6091 (2014).

9. Hartstein, L. E. *et al.* A comparison of the effects of correlated colour temperature and gender on cognitive task performance. *Light Res. Technol.* **50**, 1057–1069 (2018).
10. Fisk, A. S. *et al.* Light and cognition: Roles for circadian rhythms, sleep, and arousal. *Front. Neurol.* **9**, 1–18 (2018).
11. An, M. *et al.* Time-of-day-dependent effects of monochromatic light exposure on human cognitive function. *J. Physiol. Anthropol.* **28**, 217–223 (2009).
12. Vandewalle, G. *et al.* Brain responses to violet, blue, and green monochromatic light exposures in humans: Prominent role of blue light and the brainstem. *PLoS ONE* **2**, e1247 (2007).
13. Zohdi, H., Scholkmann, F. & Wolf, U. Long-term blue light exposure changes frontal and occipital cerebral hemodynamics: Not all subjects react the same. *Adv. Exp. Med. Biol.* 1269. In Press.
14. Viola, A. U. *et al.* Blue-enriched white light in the workplace improves self-reported alertness, performance and sleep quality. *Scand. J. Work Environ. Health* **34**, 297–306 (2008).
15. Tosini, G., Ferguson, I. & Tsubota, K. Effects of blue light on the circadian system and eye physiology Gianluca. *Mol. Vis.* **22**, 61–72 (2016).
16. Katsuura, T. *et al.* Effects of monochromatic light on time sense for short intervals. *J. Physiol. Anthropol.* **26**, 95–100 (2007).
17. Okamoto, Y. & Nakagawa, S. Effects of daytime light exposure on cognitive brain activity as measured by the ERP P300. *Physiol. Behav.* **138**, 313–318 (2015).
18. Perrin, F. *et al.* Nonvisual responses to light exposure in the human brain during the circadian night. *Curr. Biol.* **14**, 1842–1846 (2004).
19. Vandewalle, G. *et al.* Blue light stimulates cognitive brain activity in visually blind individuals. *J. Cogn. Neurosci.* **25**, 2072–2085 (2013).
20. Vandewalle, G. *et al.* Spectral quality of light modulates emotional brain responses in humans. *Proc. Natl. Acad. Sci. USA* **107**, 19549–19554 (2010).
21. Vandewalle, G. *et al.* Wavelength-dependent modulation of brain responses to a working memory task by daytime light exposure. *Cereb. Cortex* **17**, 2788–2795 (2007).
22. Vandewalle, G. *et al.* Effects of light on cognitive brain responses depend on circadian phase and sleep homeostasis. *J. Biol. Rhythms* **26**, 249–259 (2011).
23. Heinzel, S. *et al.* Aging-related cortical reorganization of verbal fluency processing: A functional near-infrared spectroscopy study. *Neurobiol. Aging* **34**, 439–450 (2013).
24. Shao, Z. *et al.* What do verbal fluency tasks measure? Predictors of verbal fluency performance in older adults. *Front. Psychol.* **5**, 772 (2014).
25. Herrmann, M. J., Ehlis, A. C. & Fallgatter, A. J. Frontal activation during a verbal-fluency task as measured by near-infrared spectroscopy. *Brain Res. Bull* **61**, 51–56 (2003).
26. Poor Zamany Nejat Kermany, M. *et al.* Early childhood exposure to short periods of sevoflurane is not associated with later, lasting cognitive deficits. *Paediatr. Anaesth.* **26**, 1018–1025 (2016).
27. Baldo, J. V. *et al.* Role of frontal versus temporal cortex in verbal fluency as revealed by voxel-based lesion symptom mapping. *J. Int. Neuropsychol. Soc.* **12**, 896–900 (2006).
28. Scholkmann, F. *et al.* A review on continuous wave functional near-infrared spectroscopy and imaging instrumentation and methodology. *Neuroimage* **85**, 6–27 (2014).
29. Lange, F. & Tachtsidis, I. Clinical brain monitoring with time domain NIRS: A review and future perspectives. *Appl. Sci.* **9**, 1612 (2019).
30. Pinti, P. *et al.* The present and future use of functional near-infrared spectroscopy (fNIRS) for cognitive neuroscience. *Ann. N. Y. Acad. Sci.* **1464**, 5 (2020).
31. Schecklmann, M. *et al.* Diminished prefrontal oxygenation with normal and above-average verbal fluency performance in adult ADHD. *J. Psychiatr. Res.* **43**, 98–106 (2009).
32. Tupak, S. V. *et al.* Differential prefrontal and frontotemporal oxygenation patterns during phonemic and semantic verbal fluency. *Neuropsychologia* **50**, 1565–1569 (2012).
33. Schecklmann, M. *et al.* Influence of muscle activity on brain oxygenation during verbal fluency assessed with functional near-infrared spectroscopy. *Neuroscience* **171**, 434–442 (2010).
34. Zohdi, H. *et al.* Long-term changes in optical properties (μa, μ′s, μeff and DPF) of human head tissue during functional neuroimaging experiments. *Adv. Exp. Med. Biol.* **1072**, 331–337 (2018).
35. Herold, F. *et al.* New directions in exercise prescription: Is there a role for brain-derived parameters obtained by functional near-infrared spectroscopy ?. *Brain Sci.* **10**, 342 (2020).
36. Matsuo, K. *et al.* Hypoactivation of the prefrontal cortex during verbal fluency test in PTSD: A near-infrared spectroscopy study. *Psychiatry Res. Neuroimaging* **124**, 1–10 (2003).
37. Wolf, M. *et al.* Different time evolution of oxyhemoglobin and deoxyhemoglobin concentration changes in the visual and motor cortices during functional stimulation: A near-infrared spectroscopy study. *Neuroimage* **16**, 704–712 (2002).
38. Scholkmann, F. *et al.* Effect of short-term colored-light exposure on cerebral hemodynamics and oxygenation, and systemic physiological activity. *Neurophotonics* **4**, 045005 (2017).
39. Nasseri, N. *et al.* Impact of changes in systemic physiology on fNIRS/NIRS signals: Analysis based on oblique subspace projections decomposition. *Adv. Exp. Med. Biol.* **1072**, 119–125 (2018).
40. Scholkmann, F. *et al.* End-tidal CO_2: An important parameter for a correct interpretation in functional brain studies using speech tasks. *Neuroimage* **66**, 71–79 (2013).
41. Metz, A. J. *et al.* Continuous coloured light altered human brain haemodynamics and oxygenation assessed by systemic physiology augmented functional near-infrared spectroscopy. *Sci. Rep.* **7**, 10027 (2017).
42. Caldwell, M. *et al.* Modelling confounding effects from extracerebral contamination and systemic factors on functional near-infrared spectroscopy. *Neuroimage* **143**, 91–105 (2016).
43. Tachtsidis, I. & Scholkmann, F. False positives and false negatives in functional near-infrared spectroscopy: Issues, challenges, and the way forward. *Neurophotonics* **3**, 031405 (2016).
44. Zohdi, H., Scholkmann, F. & Wolf, U. Frontal cerebral oxygenation asymmetry: Intersubject variability and dependence on systemic physiology, season, and time of day. *Neurophotonics* **7**, 025006 (2020).
45. Zohdi, H., Scholkmann, F. & Wolf, U. Individual differences in hemodynamic responses measured on the head due to a long-term stimulation involving colored light exposure and a cognitive task: A SPA-fNIRS study. *Brain Sci.* **11**, 54 (2021).
46. Scholkmann, F. & Wolf, U. The pulse-respiration quotient: A powerful but untapped parameter for modern studies about human physiology and pathophysiology. *Front. Physiol.* **10**, 1–18 (2019).
47. Scholkmann, F. *et al.* How to detect and reduce movement artifacts in near-infrared imaging using moving standard deviation and spline interpolation. *Physiol. Meas.* **31**, 649–662 (2010).
48. Benedek, M. & Kaernbach, C. Decomposition of skin conductance data by means of nonnegative deconvolution. *Psychophysiology* **47**, 647–658 (2010).
49. Benedek, M. & Kaernbach, C. A continuous measure of phasic electrodermal activity. *J. Neurosci. Methods* **190**, 80–91 (2010).
50. Holper, L. *et al.* Brain correlates of verbal fluency in subthreshold psychosis assessed by functional near-infrared spectroscopy. *Schizophr. Res.* **168**, 23–29 (2015).

51. Fallgatter, A. J. *et al.* Loss of functional hemispheric asymmetry in Alzheimer's dementia assessed with near-infrared spectroscopy. *Cogn. Brain Res.* **6**, 67–72 (1997).
52. Luo, L., Luk, G. & Bialystok, E. Effect of language proficiency and executive control on verbal fluency performance in bilinguals. *Cognition* **114**, 29–41 (2010).
53. Roca, M. *et al.* The relationship between executive functions and fluid intelligence in Parkinson's disease. *Psychol. Med.* **42**, 2445–2452 (2012).
54. Herrmann, M. J. *et al.* Cerebral oxygenation changes in the prefrontal cortex: Effects of age and gender. *Neurobiol. Aging* **27**, 888–894 (2006).
55. Papousek, I. & Schulter, G. Manipulation of frontal brain asymmetry by cognitive tasks. *Brain Cogn.* **54**, 43–51 (2004).
56. Kameyama, M. *et al.* Sex and age dependencies of cerebral blood volume changes during cognitive activation: A multichannel near-infrared spectroscopy study. *Neuroimage* **22**, 1715–1721 (2004).
57. Halpern, D. F. *Sex Differences in Cognitive Abilities* (Psychology Press, 2000).
58. Collins, D. W. & Kimura, D. A large sex difference on a two-dimensional mental rotation task. *Behav. Neurosci.* **111**, 845–849 (1997).
59. Weiss, E. M. *et al.* Brain activation pattern during a verbal fluency test in healthy male and female volunteers: A functional magnetic resonance imaging study. *Neurosci. Lett.* **352**, 191–194 (2003).
60. Shaywitz, B. A. *et al.* Sex differences in the functional organization of the brain for language. *Nature* **373**, 607–609 (1995).
61. Vamvakopoulos, N. C. & Chrousos, G. P. Evidence of direct estrogenic regulation of human corticotropin-releasing hormone gene expression: Potential implications for the sexual dimorphism of the stress response and immune/inflammatory reaction. *J. Clin. Investig.* **92**, 1896–1902 (1993).
62. Tsigos, C. & Chrousos, G. P. Hypothalamic-pituitary-adrenal axis, neuroendocrine factors and stress. *J. Psychosom. Res.* **53**, 865–871 (2002).
63. Shors, T. J. & Leuner, B. Estrogen-mediated effects on depression and memory formation in females. *J. Affect. Disord.* **74**, 85–96 (2003).
64. Kimura, D. Sex, sexual orientation and sex hormones influence human cognitive function. *Curr. Opin. Neurobiol.* **6**, 259–263 (1996).
65. Weinzirl, J. *et al.* Effects of changes in colored light on brain and calf muscle blood concentration and oxygenation. *Sci. World J.* **11**, 1216–1225 (2011).
66. Weinzirl, J., Wolf, M., Nelle, M. *et al.* Colored light and brain and muscle oxygenation. In *Oxygen Transport to Tissue XXXIII* 3–36 (2012).
67. Metz, A. J., Klein, S. D., Scholkmann, F. *et al.* Physiological effects of continuous colored light exposure on mayer wave activity in cerebral hemodynamics: a functional near-infrared spectroscopy (fNIRS) study. In *Oxygen Transport to Tissue XXXIX*, 277–283 (Springer, 2017).
68. Matsuo, K. *et al.* Prefrontal hemodynamic response to verbal-fluency task and hyperventilation in bipolar disorder measured by multi-channel near-infrared spectroscopy. *J. Affect. Disord.* **82**, 85–92 (2004).
69. Watanabe, A. *et al.* Cerebrovascular response to cognitive tasks and hyperventilation measured by multi-channel near-infrared spectroscopy. *J. Neuropsychiatry Clin. Neurosci.* **15**, 442–449 (2003).
70. Toichi, M. *et al.* Hemodynamic differences in the activation of the prefrontal cortex: Attention vs. higher cognitive processing. *Neuropsychologia* **42**, 698–706 (2004).
71. Quaresima, V. *et al.* Bilateral prefrontal cortex oxygenation responses to a verbal fluency task: A multichannel time-resolved near-infrared topography study. *J. Biomed. Opt.* **10**, 011012 (2005).
72. Bonetti, L. V. *et al.* Oxyhemoglobin changes in the prefrontal cortex in response to cognitive tasks: A systematic review. *Int. J. Neurosci.* **129**, 195–203 (2019).
73. Yang, J. *et al.* Cortical response to categorical color perception in infants investigated by near-infrared spectroscopy. *Proc. Natl. Acad. Sci. USA* **113**, 2370–2375 (2016).
74. Liu, X. & Hong, K. S. fNIRS based color detection from human visual cortex. In *2015 54th Annu Conf Soc Instrum Control Eng Japan, SICE 2015*, 1156–1161 (2015).
75. Liu, X. & Hong, K. S. Detection of primary RGB colors projected on a screen using fNIRS. *J. Innov. Opt. Health Sci.* **10**, 1750006 (2017).
76. Cowan, R. L. *et al.* Sex differences in response to red and blue light in human primary visual cortex: A bold fMRI study. *Psychiatry Res. Neuroimaging* **100**, 129–138 (2000).
77. Lueck, C. J. *et al.* The colour centre in the cerebral cortex of man. *Nature* **340**, 386–389 (1989).
78. Allison, T. *et al.* Electrophysiological studies of color processing in human visual cortex. *Electroencephalogr. Clin. Neurophysiol. Evoked Potentials* **88**, 343–355 (1993).
79. Cajochen, C. *et al.* High sensitivity of human melatonin, alertness, thermoregulation, and heart rate to short wavelength light. *J. Clin. Endocrinol. Metab.* **90**, 1311–1316 (2005).
80. Litscher, D., Wang, L. & Gaischek, I. *et al.* The influence of new colored light stimulation methods on heart rate variability, temperature, and well-being: results of a pilot study in humans. *Evidence-Based Complement Altern. Med.* **2013** Article ID 674183 (2013).
81. Mukae, H. & Sato, M. The effect of color temperature of lighting sources on the autonomic nervous functions. *Ann. Physiol. Anthropol.* **11**, 533–538 (1992).
82. Abbas, N., Kumar, D. & Mclachlan, N. The psychological and physiological effects of light and colour on space users. In *2005 IEEE Engineering in Medicine and Biology 27th Annual Conference*, 1228–1231 (2005).
83. Jacobs, K. W. & Hustmyer, F. E. Jr. Effects of four psychological primary colors on GSR, heart rate and respiration rate. *Percept. Mot. Skills* **38**, 763–766 (1974).
84. Edelhäuser, F., Hak, F., Kleinrath, U. *et al.* Impact of colored light on cardiorespiratory coordination. *Evid.-Based Complement Altern. Med.* **2013** (2013).
85. Scholkmann, F., Zohdi, H. & Wolf, U. The resting-state pulse-respiration quotient of humans: Lognormally distributed and centred around a value of four. *Physiol. Res.* **68**, 1027–1032 (2019).
86. Kobayashi, H. & Sato, M. Physiological responses to llluminance and color temperature of lighting. *Ann. Physiol. Anthropol.* **11**, 45–49 (1992).
87. Xia, Y., Shimomura, Y. & Katsuura, T. Comparison of the effects of wavelength and intensity of monochromatic light on cardiovascular responses during task and in recovery periods. *J. Hum. Environ. Syst.* **14**, 41–48 (2012).
88. Bhoja, R. *et al.* Psychophysiological stress indicators of heart rate variability and electrodermal activity with application in healthcare simulation research. *Simul. Healthc.* **15**, 39–45 (2020).
89. Posada-Quintero, H. F. & Bolkhovsky, J. B. Machine learning models for the identification of cognitive tasks using autonomic reactions from heart rate variability and electrodermal activity. *Behav. Sci.* **9**, 45 (2019).
90. Visnovcova, Z. *et al.* The complexity of electrodermal activity is altered in mental cognitive stressors. *Comput. Biol. Med.* **79**, 123–129 (2016).
91. Wickramasuriya, D. S., Qi, C. & Faghih, R. T. A state-space approach for detecting stress from electrodermal activity. In *Proc Annu Int Conf IEEE Eng Med Biol Soc EMBS*, 3562–3567 (2018).

92. Ross, M. J., Guthrie, P. & Dumont, J. C. The impact of modulated, colored light on the autonomic nervous system. *Adv. Mind Body Med.* **27**, 7–16 (2013).
93. Kloter, E. *et al.* Heart rate variability as a prognostic factor for cancer survival—A systematic review. *Front. Physiol.* **9**, 623 (2018).
94. Shaffer, F. & Ginsberg, J. P. An overview of heart rate variability metrics and norms. *Front. Public Health* **5**, 258 (2017).
95. Billman, G. E. The LF/HF ratio does not accurately measure cardiac sympatho-vagal balance. *Front. Physiol.* **4**, 26 (2013).
96. von Rosenberg, W. *et al.* Resolving ambiguities in the LF/HF ratio: LF-HF scatter plots for the categorization of mental and physical stress from HRV. *Front. Physiol.* **8**, 360 (2017).
97. Malik, M. *et al.* Heart rate variability: Standards of measurement, physiological interpretation, and clinical use. *Eur. Heart J.* **17**, 354–381 (1996).
98. Posada-Quintero, H. F. & Chon, K. H. Innovations in electrodermal activity data collection and signal processing: A systematic review. *Sensors* **20**, 479 (2020).
99. Elliot, A. J. *et al.* A subtle threat cue, heart rate variability, and cognitive performance. *Psychophysiology* **48**, 1340–1345 (2011).
100. Schäfer, A. & Kratky, K. W. The effect of colored illumination on heart rate variability. *Complement Med. Res.* **13**, 167–173 (2006).
101. Moharreri, S., Rezaei, S., Dabanloo, N. J. *et al.* Study of induced emotion by color stimuli: Power spectrum analysis of heart rate variability. In *Computing in Cardiology Conference (CinC), 2014*, 977–980 (IEEE, 2014).
102. Laufer, L. *et al.* Psychophysiological effects of coloured lighting on older adults. *Light Res. Technol.* **41**, 371–378 (2009).
103. Mehta, R. & Zhu, R. J. Blue or red? Exploring the effect of color on cognitive task performances. *Science* **323**, 1226–1229 (2009).

Acknowledgements

We would like to thank our students for their work and our subjects for participating in this study. The financial support of the Software AG Foundation (Grant No P12117) and the Christophorus Foundation (Grant Nos 253CST, 355CST) is gratefully acknowledged.

Author contributions

U.W., H.Z., and F.S. designed the study. R.E. performed the experiments. H.Z. and D.G. performed data preprocessing and data visualization. H.Z., F.S., D.G. and U.W. contributed to data analysis and interpretation. H.Z. and R.E. wrote the first draft of the manuscript. F.S. and U.W. reviewed and edited the manuscript.

Competing interests

The authors declare no competing interests.

Additional information

Correspondence and requests for materials should be addressed to U.W.

Reprints and permissions information is available at www.nature.com/reprints.

Publisher's note Springer Nature remains neutral with regard to jurisdictional claims in published maps and institutional affiliations.

Open Access This article is licensed under a Creative Commons Attribution 4.0 International License, which permits use, sharing, adaptation, distribution and reproduction in any medium or format, as long as you give appropriate credit to the original author(s) and the source, provide a link to the Creative Commons licence, and indicate if changes were made. The images or other third party material in this article are included in the article's Creative Commons licence, unless indicated otherwise in a credit line to the material. If material is not included in the article's Creative Commons licence and your intended use is not permitted by statutory regulation or exceeds the permitted use, you will need to obtain permission directly from the copyright holder. To view a copy of this licence, visit http://creativecommons.org/licenses/by/4.0/.

© The Author(s) 2021

Peer reviewed publication 9

Individual differences in hemodynamic responses measured on the head due to a long-term stimulation involving colored light exposure and a cognitive task: a SPA-fNIRS study

Hamoon Zohdi, Felix Scholkmann, Ursula Wolf

Brain Sciences (2021) 11, 54

DOI: 10.3390/brainsci11010054

URL: https://www.mdpi.com/2076-3425/11/1/54

Own contributions:

- Co-design of the study
- Contribute to carrying out measurements
- Signal processing
- Data analysis
- Visualization (all figures)
- Writing of the first draft

brain sciences

MDPI

Article

Individual Differences in Hemodynamic Responses Measured on the Head Due to a Long-Term Stimulation Involving Colored Light Exposure and a Cognitive Task: A SPA-fNIRS Study

Hamoon Zohdi [1], Felix Scholkmann [1,2,†] and Ursula Wolf [1,*,†]

[1] Institute of Complementary and Integrative Medicine, University of Bern, 3012 Bern, Switzerland; hamoon.zohdi@ikim.unibe.ch (H.Z.); felix.scholkmann@ikim.unibe.ch (F.S.)
[2] Biomedical Optics Research Laboratory, Neonatology Research, Department of Neonatology, University Hospital Zurich, University of Zurich, 8091 Zurich, Switzerland
* Correspondence: ursula.wolf@ikim.unibe.ch; Tel.: +41-31-631-8141
† These authors contributed equally as the senior authors.

Abstract: When brain activity is measured by neuroimaging, the canonical hemodynamic response (increase in oxygenated hemoglobin ([O_2Hb]) and decrease in deoxygenated hemoglobin ([HHb]) is not always seen in every subject. The reason for this intersubject-variability of the responses is still not completely understood. This study is performed with 32 healthy subjects, using the systemic physiology augmented functional near-infrared spectroscopy (SPA-fNIRS) approach. We investigate the intersubject variability of hemodynamic and systemic physiological responses, due to a verbal fluency task (VFT) under colored light exposure (CLE; blue and red). Five and seven different hemodynamic response patterns were detected in the subgroup analysis of the blue and red light exposure, respectively. We also found that arterial oxygen saturation and mean arterial pressure were positively correlated with [O_2Hb] at the prefrontal cortex during the CLE-VFT independent of the color of light and classification of the subjects. Our study finds that there is substantial intersubject-variability of cerebral hemodynamic responses, which is partially explained by subject-specific systemic physiological changes induced by the CLE-VFT. This means that both subgroup analyses and the additional assessment of systemic physiology are of crucial importance to achieve a comprehensive understanding of the effects of a CLE-VFT on human subjects.

Keywords: systemic physiology augmented functional near-infrared spectroscopy; SPA-fNIRS; colored light exposure; verbal fluency task; cerebral hemodynamics; systemic physiology; laterality

check for updates

Citation: Zohdi, H.; Scholkmann, F.; Wolf, U. Individual Differences in Hemodynamic Responses Measured on the Head Due to a Long-Term Stimulation Involving Colored Light Exposure and a Cognitive Task: A SPA-fNIRS Study. *Brain Sci.* **2021**, *11*, 54. https://doi.org/10.3390/brainsci11010054

Received: 27 November 2020
Accepted: 30 December 2020
Published: 5 January 2021

Publisher's Note: MDPI stays neutral with regard to jurisdictional claims in published maps and institutional affiliations.

Copyright: © 2021 by the authors. Licensee MDPI, Basel, Switzerland. This article is an open access article distributed under the terms and conditions of the Creative Commons Attribution (CC BY) license (https://creativecommons.org/licenses/by/4.0/).

1. Introduction

Colored light modulates a wide range of functions in human physiology, including the sleep-wake cycle via melatonin secretion, alertness, cognition, and thermoregulation [1,2]. Since the discovery of the photopigment melanopsin nearly two decades ago, non-image-forming (NIF) vision has been focused on as a potential explanation for a number of effects of colored light on human physiology [3,4]. This light-sensitive protein is expressed in a subclass of intrinsically photosensitive retinal ganglion cells and is most sensitive to narrowband blue light (~460−480 nm) [5,6]. It has become apparent that NIF vision responses to colored light, especially short-wavelength light, affect the cognitive process and enhance alertness and cognitive performance [7–12]. However, the effects of colored light on alertness and cognitive performance beyond the scope of NIF vision responses are not yet well understood. Previous studies demonstrated that improvements in cognitive performance via colors or colored light depend not only on the environment and certain situational variables, but also on the individual subject, as well as the type of cognitive task [13–16].

The verbal fluency task (VFT) is among the most widely applied neuropsychological tests for the assessment of cognitive function. The VFT is a classical method of language

production in which subjects are instructed to produce as many words as possible within a restricted time and following specific rules [17–21]. To assess the brain correlates of cognitive functioning underlying the VFT, several studies have been conducted using functional near-infrared spectroscopy (fNIRS) [22–31]. fNIRS is an optical neuroimaging technique enabling significant advances in the understanding of functional brain activity and higher cognitive functions [32,33]. This non-invasive technique is based on optical spectroscopy and detecting correlates of brain activity mediated by neurovascular coupling (NVC) [34]. A typical NVC response, due to increased neuronal activity, consists of an increase in oxygenated ([O_2Hb]) and total ([tHb]) hemoglobin and a simultaneous decrease in deoxygenated hemoglobin ([HHb]) [35,36]. fNIRS measurements have demonstrated that the VFT evokes symmetrical cerebral oxygenation responses within different brain regions, primarily in the prefrontal cortex (PFC) and lateral areas [37–40]. So far, only some studies have reported hemispheric differences in the frontal and temporal cortices, i.e., a more pronounced left compared to right hemispheric activation [41–44].

Although increases in [O_2Hb] and decreases in [HHb] serve as indicators for brain activity, other patterns of cortical activation were also found in various cognitive studies [45–47]. Such atypical fNIRS patterns can be attributed to different reasons, including individual differences in vascular regulation and measurement positions, as well as influences from changes in systemic physiology [46,48–50]. The effects of the latter on changes in [O_2Hb] and [HHb] can be detected by applying systemic physiology augmented functional near-infrared spectroscopy (SPA-fNIRS), which additionally and concurrently with fNIRS measures systemic physiological parameters [51–53].

Since the topic of intersubject variability of hemodynamic responses and changes in systemic physiology is not yet well investigated, we aimed in this study to further explore this topic in detail. In particular, two main goals were pursued: First, we investigated with SPA-fNIRS whether the CLE-VFT causes different reaction patterns in cerebral hemodynamics and systemic physiology. Second, we explored the effects of two light exposure conditions (blue and red) during the CLE-VFT on lateralization of cerebral cortices.

2. Materials and Methods

2.1. Subjects

The study was conducted with 32 healthy subjects (17 female, 15 male, age 25.5 $\pm$ 4.3 years). Subjects were all right-handed with high education level and without any acute or chronic disease affecting the neuronal or cardiorespiratory system. All subjects had normal color vision as assessed by the Ishihara's Tests for color blindness and color deficiency (Kanehara and CO., LTD., Tokyo, Japan).

2.2. Experimental Protocol

The subjects sat upright in a comfortable chair in front of a white wall (distance from the subject to the wall: 160 $\pm$ 5 cm). Each subject participated in two days of trials: One while being exposed to blue light, and the other while being exposed to red light (illuminance: 120 lux at eye level), the order of which was randomized. On each day, the subjects were exposed to the colored light for a duration of 9 min. The subjects were instructed to keep their eyes open during the entire experiment. Other than during periods of the CLE, the experimental room remained dark. The VFT, which included three sessions, was performed during the CLE. Each session comprised three different trials (phonemic, control, and semantic tasks) in which subjects had to produce as many words as possible for a given letter or category within 30 s. Each trial was followed by a resting phase of 30 s. These periods were set similar to previous VFT protocols in the literature [27,41,44]. Thus, the total duration of the task was 9 min and the period of the CLE was adjusted to this period. Figure 1a presents the schematic representation of the CLE-VFT protocol.

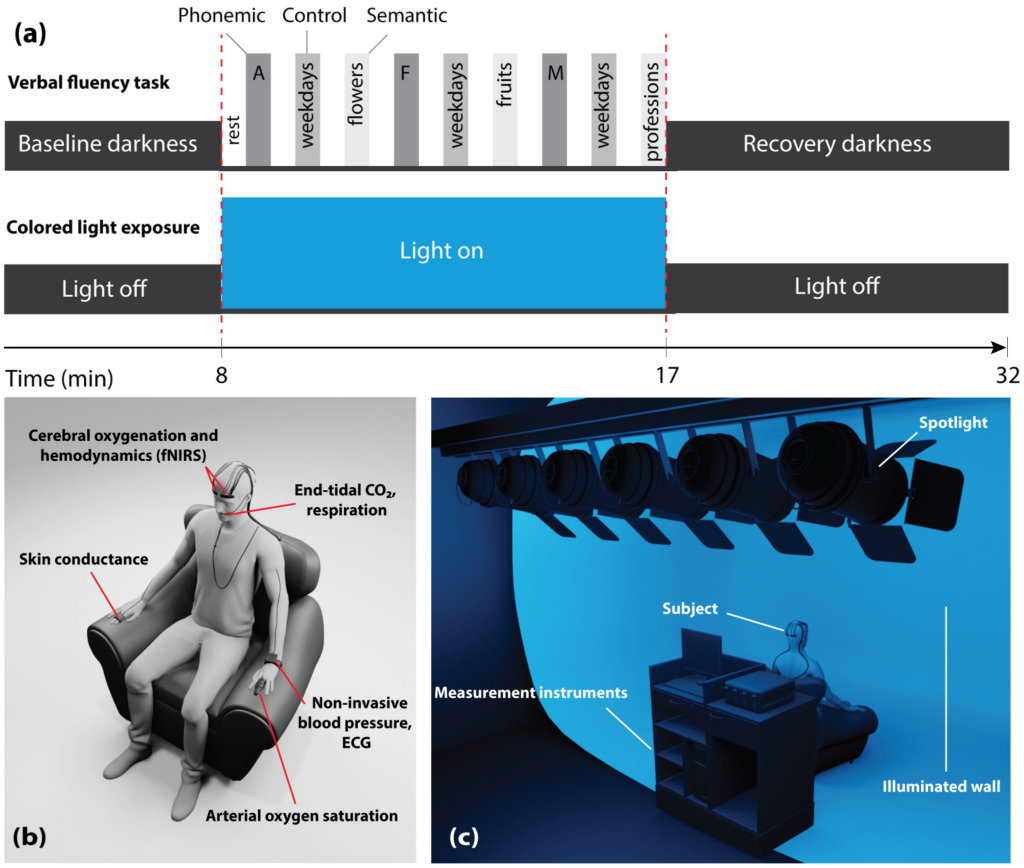

Figure 1. (**a**) Schematic illustration of the measurement protocol; (**b**) visualization of the placement of devices and sensors on the subject; (**c**) experimental setup with the position of the subject, illuminated screen, and spotlights. Two colors, i.e., either red or blue were used for the light exposure; in (**a**,**c**), the case of blue light exposure is visualized.

2.3. Measurement Setup

The SPA-fNIRS approach includes a multichannel frequency-domain near-infrared spectroscopy (FD-NIRS) system (Imagent, ISS Inc., Champaign, IL, USA) and devices to measure systemic physiological parameters: The SOMNOtouch^{TM} NIBP (SOMNOmedics GmbH, Randersacker, Germany) measured heart rate (HR) with a sampling rate of 4 Hz and mean arterial pressure (MAP) and arterial oxygen saturation (SpO_2) at a sampling rate of 1 Hz. End-tidal carbon dioxide ($P_{ET}CO_2$) and respiration rate (RR) were non-invasively measured by NONIN LifeSense (NONIN Medical, Plymouth, MN, USA) at a sampling rate of 1 Hz. An electrodermal activity measurement system (Verim Mind-Reflection GSR, Poland) was employed to determine the skin conductance level (SCL). SCL data were recorded at a sampling rate of 8 Hz. To measure the coupling between HR and RR, the pulse-respiration quotient (PRQ) [54,55] was calculated (PRQ = HR/RR).

The Imagent has 16 laser diodes at 760 nm and 16 laser diodes at 830 nm. Four highly sensitive photo-multiplier tubes are employed as detectors. Each of the four ISS optodes has four light emitters and one light detector, each connected to the instrument by optical fibers. The ISS optodes were placed bilaterally over the prefrontal cortex (PFC) (left: Fp1 and right: Fp2) and the visual cortex (VC) (left: O1 and right: O2) according to the international EEG 10–20 system [56]. The optodes were covered with two layers of dark cloth to prevent ambient light interference. ISS detectors were also shielded against visible light by acrylic long-pass filters with a cut-on wavelength of 685 nm (Knight Optical, Kent, UK) to prevent stray light from affecting the measurement. Moreover, since the light from the ISS instrument is frequency modulated at 110 MHz, exposure light, which is of other frequencies, is removed automatically. The source-detector separations of the optodes were

2.0, 2.5, 3.5, and 4.0 cm over the PFC and 2.0, 2.5, 3.0, and 3.5 cm over the VC. The FD-NIRS system, employing the multi-distance approach, measured absolute [O_2Hb], [HHb], and tissue oxygen saturation (StO_2) at a sampling rate of 2.5 Hz on the PFC and VC. The ISS instrument is based on multi-distance frequency domain measurement—which, based on the diffusion approximation, determines the absorption coefficient and the reduced scattering coefficient, and hence, absolute values of [O_2Hb], [HHb], and StO_2 [57]. These are calculated online by the software of the instrument.

Figure 1b,c display the positions of the devices and sensors on the subject, as well as the measurement setup showing the position of the subject, the (illuminated) screen, and the spotlights (six LED PAR spotlights—each has 12 × 35 mm RGBW LEDs).

2.4. Signal Processing and Statistical Analysis

One subject was excluded from data analysis because she was not a native German/Swiss German speaker. Two subjects aged over 30 years were excluded from the analysis to have a sample in a small age range (20 to 30 years). By removing these two subjects, we avoid the need to correct for an age when performing the statistical analysis, i.e., avoiding to have age-related effects as a confounder. It also helped us to have a quite homogenous sample with respect to the general ability of the subjects (e.g., language proficiency in the VFT task). The language proficiency of the older subjects deviated from the other group. Signal processing was performed in MATLAB (R2017a, MathWorks, Inc., Natick, MA, USA), and statistical analysis in OriginPro (version 2019b, OriginLab Corporation, Northampton, MA, USA)

2.4.1. Signal Processing

Too noisy data were first rejected by manual inspection (e.g., StO_2 outside the range of 50–100%). At this stage, data with a lower signal-to-noise ratio was mostly found at the VC, due to poor scalp-optode coupling. In total, 80% of the fNIRS signals were accepted for the next data pre-processing step. Then, movement artifacts were removed by the in-house developed movement artifact reduction algorithm based on moving standard deviation and piecewise-interpolation [58]. fNIRS signals were low pass filtered by a robust 2^{nd}-degree polynomial moving average (RLOESS) with a window length of 3 min. RLOESS filtering with a window length of > 1 min has been used as a smoothing filter in data processing of the fNIRS signals [51,59,60]. This method was able to remove high-frequency physiological noise (e.g., heart rate and respiratory rate) of the fNIRS signals. The effectiveness of this method has also been shown in the literature [61–63]. Furthermore, the FD-NIRS system enabled the measurements to be less sensitive to physiological noise coming from the extracerebral tissue compartment [64]. Then, signals from the left and right PFC and the left and right VC were averaged (since the patterns in the two hemispheres were not significantly different) to obtain signals for the whole PFC and VC, respectively.

All other systemic physiological parameters, except the SCL, were also smoothed using the RLOESS method with a span of 3 min. The SCL data were processed with the Ledalab toolbox [65,66] by means of continuous decomposition analysis performing optimization of 6 initial values.

2.4.2. Data and Statistical Analysis

Type of functional activation: The subgroup data analysis was performed by classifying subjects into different groups based on their hemodynamic response pattern of [O_2Hb] in the PFC and VC during the CLE-VFT. Nine groups are in principle possible, i.e., three directions (increase, no change, decrease in [O_2Hb]) to the power of two cortices (PFC and VC). To determine the direction during the CLE-VFT phase, the normalized [O_2Hb] signal was segmented into 40 parts, and the median value for each segment was calculated, followed by applying the one-sample Wilcoxon signed-rank test to all median values of segments. An insignificant (−) pattern indicates a failure to reject the null hypothesis at the 5% significant level, whereas increase and decrease patterns indicate a rejection of the null

hypothesis ($p < 0.05$). After classifying each subject into one of the nine groups, all other physiological signals not used for grouping purposes were block-averaged for each group.

Cerebral functional asymmetry: The following steps were applied to investigate the functional cerebral oxygenation asymmetry during the CLE-VFT: (i) The time-dependent StO_2 signal was selected as a promising marker for evaluation of the cerebral laterality. (ii) four different StO_2 signals from the left and right PFC, and VC were taken into account for each measurement. (iii) each StO_2 signal was normalized to the last 5 min of the baseline period. (iv) ΔStO_2 median values during the CLE-VFT were calculated (i.e., Δ indicates the normalized parameter).

VFT performance: A total number of VFT correct responses was averaged for all measurements, comprising both the red and blue light exposure. Subjects with a below- and an above-average number of correct responses were allocated to the moderate and excellent performer groups, respectively.

3. Results

3.1. Subgroup Analysis

While most subjects showed the expected activity pattern in the hemodynamic responses (increase in [O_2Hb] and decrease in [HHb] at the PFC and VC), a significant number of subjects showed deviations from this pattern. Therefore, the hemodynamic responses were assigned to the nine groups of possible reaction patterns according to the changes of [O_2Hb] at the PFC and VC (Table 1). In fact, five and seven different hemodynamic response patterns were observed in the subgroup analysis for the blue and red light exposure, respectively.

Table 1. Classification of the hemodynamic response of [O_2Hb] patterns (significant increase ↑, insignificant change –, significant decrease ↓) at the PFC and VC.

	Cerebral Cortex		Number of Subjects	
	PFC	VC	Blue Light Exposure	Red Light Exposure
Group 1	↑	↑	14 (7 female, 7 male)	12 (4 female, 8 male)
Group 2	↑	–	2 (1 female, 1 male)	2 (1 female, 1 male)
Group 3	↑	↓	4 (3 female, 1 male)	1 (1 female, 0 male)
Group 4	–	↑	2 (0 female, 2 male)	2 (2 female, 0 male)
Group 5	–	–	3 (2 female, 1 male)	4 (2 female, 2 male)
Group 6	–	↓	-	3 (2 female, 1 male)
Group 7	↓	↑	-	2 (1 female, 1 male)
Group 8	↓	–	-	-
Group 9	↓	↓	-	-

Figure 2 depicts the overview of group-averaged changes in cerebral hemodynamics and systemic physiology based on the first three common [O_2Hb] patterns at the PFC and VC evoked by the CLE-VFT. Considering the first group (most common pattern) of both colors, the color-dependent changes were only found in HR, which increased during the blue light and was almost constant during the red light exposure.

An increase in SCL and a decrease in $P_{ET}CO_2$ were observed for almost all groups independent of the color of light. Apart from fNIRS signals, which were statistically significantly correlated with [O_2Hb] in the PFC, we found that SpO_2 and MAP were positively correlated with [O_2Hb] at the PFC (SpO_2: $r = 0.372$, $p = 0.005$; MAP: $r = 0.583$, $p < 0.001$) independent of the light's color and classification of the subjects (Figure 3). In the fifth group of both lighting conditions, color-dependent changes in HR and RR during the CLE-VFT could be observed. HR and RR increased and decreased, respectively, during blue light exposure, while both were constant during red light exposure. Blue light elicited a significant increase in PRQ compared to red light.

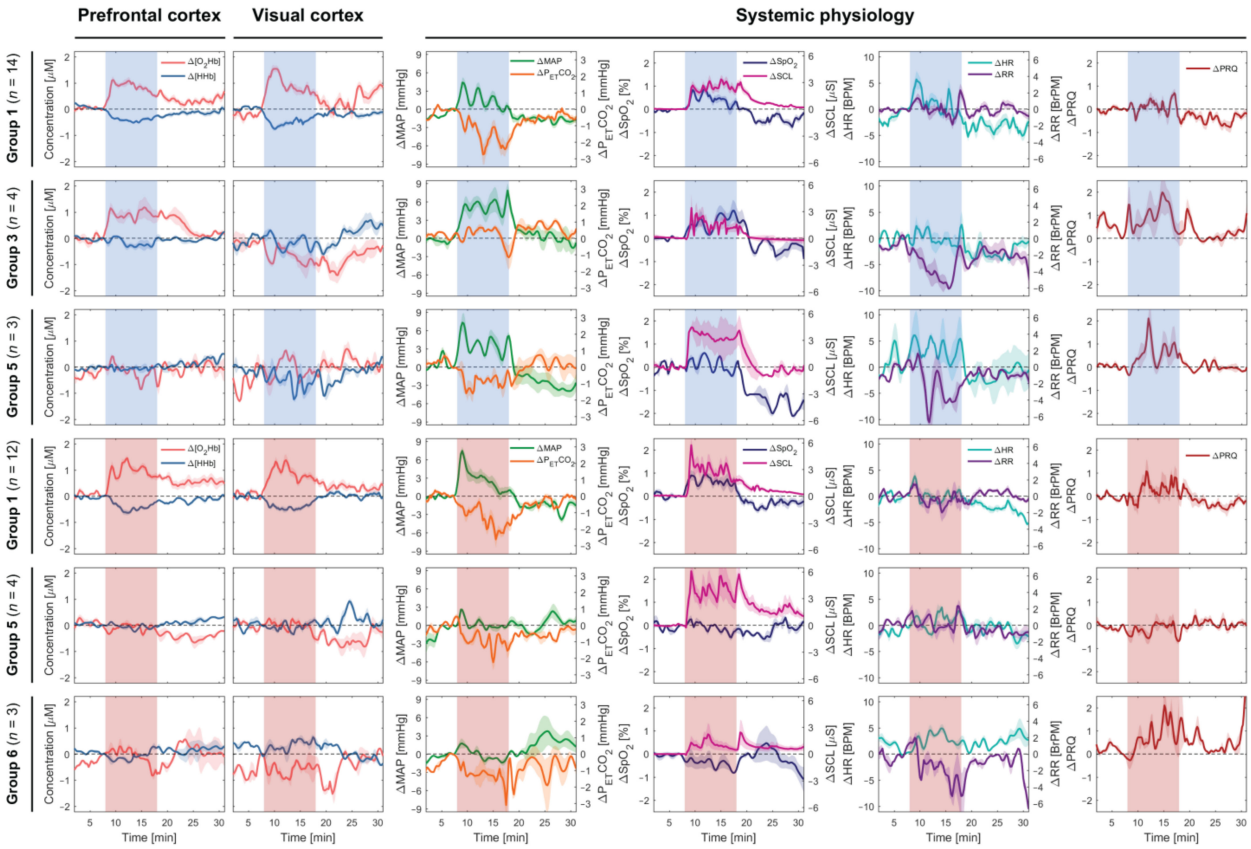

Figure 2. Subgroup analysis (the first three common patterns) of cerebral hemodynamics and systemic physiological parameters evoked by the CLE (blue vs. red light) and VFT. The red and blue shaded areas represent the task/stimulation periods during which the subjects were exposed to the respective colors. Median ± standard error of median (SEM) are shown.

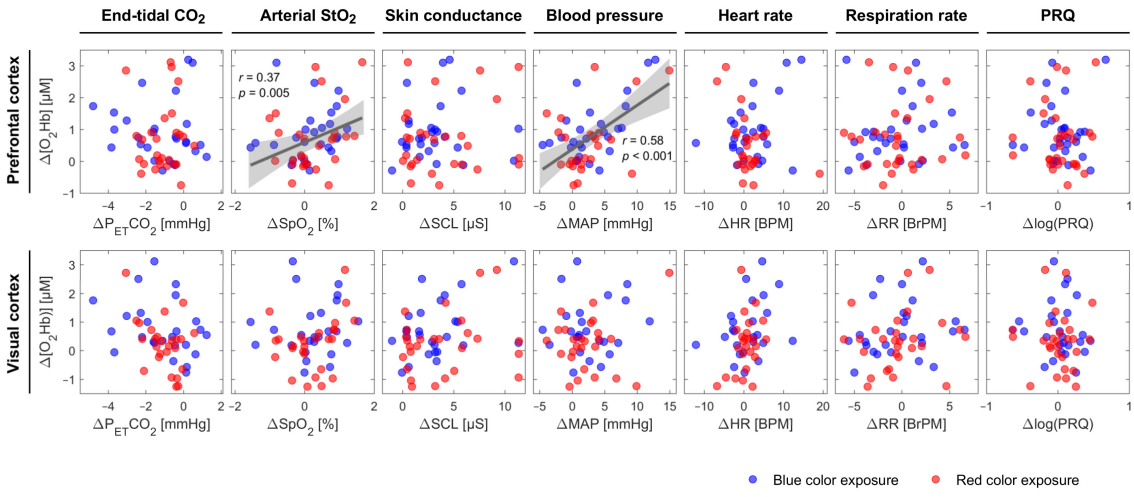

Figure 3. Scatter plots displaying $\Delta[O_2Hb]$ at the PFC and VC vs. other systemic physiological parameters during the CLE-VFT phase at the individual level independent of the color of light. The linear fit is presented for pairs with a significant correlation. The grey shaded areas show 95% of confidence intervals.

3.2. Laterality of Cerebral Activity Changes

Boxplots of ΔStO_2 values for the left and right VC and PFC and for both conditions (red and blue) during the CLE-VFT were depicted in Figure 4a,b. Evoked changes of StO_2

were generally higher for the blue light compared to the red light at the VC ($p < 0.05$; effect size (Cohen's d): $d = 0.4$). Oxygenation response to the CLE-VFT for blue light was bilateral and symmetrical at the PFC, while relatively greater left- than right-hemispheric activation was observed for the red light exposure ($p < 0.04$; $d = 0.3$).

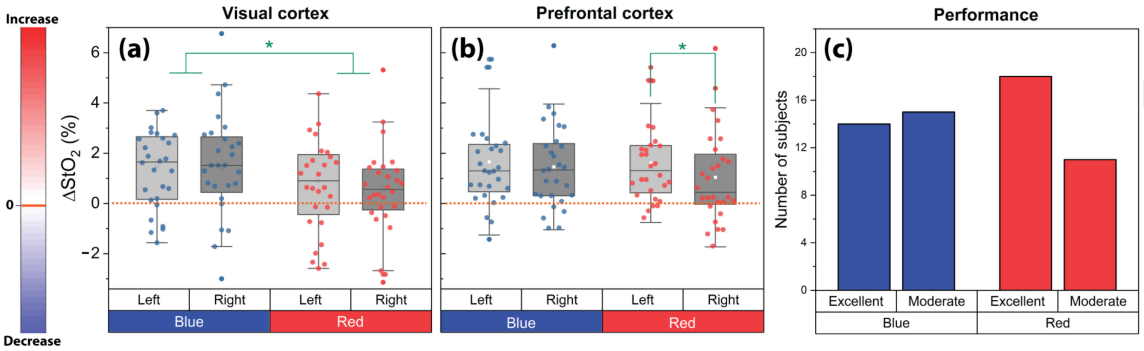

Figure 4. Evoked changes of StO_2 at the left and right (**a**) VC and (**b**) PFC for the blue and red light exposure during the CLE-VFT; (**c**) Effects of the CLE on the task performance of the subjects. The asterisks indicate the level of significance ($p < 0.05$, Wilcoxon signed-rank test).

3.3. Task Performance

Subjects articulated 56.5 ± 15.1 (mean ± SD; range: 23−100) correct nouns during the blue light exposure and 57.9 ± 11.6 (range: 26−77) during red light exposure. No significant difference in the task performance was found between the blue and red light exposure, and regardless of the color, subjects reached an average number of 57.2 ± 13.4 correct words. This number was taken as a threshold value to classify subjects into two groups (moderate vs. excellent performers). We found that the number of excellent performers during red light exposure was remarkably higher compared to the number of moderate performers, while no difference in the performance of both groups was observed during blue light (Figure 4c). Moreover, there was a significant difference between excellent performers during blue light versus red light conditions. In other words, the difference between the sample standard deviation of excellent performer groups under the influence of blue and red light is big enough to be statistically significant (F-Test: 3.72, $p = 0.015$).

4. Discussion

4.1. Prefrontal Cerebral Oxygenation Asymmetry during the Red Light Exposure

The lateralization of brain function is a propensity for some neural functions or cognitive processes specialized to one side of the cortex or the other. Numerous studies have provided valuable insights into the cerebral asymmetry of the human brain cortices [67–69]. In particular, the frontal lobe has increasingly become a special region of interest. Frontal cerebral asymmetry of resting-state brain activity has been explained using the approach-withdrawal model, where the higher relative leftward frontal activity is associated with appetitive motivation and approach-related affect (positive affect), while the rightward frontal activity is related to behavioral inhibition and withdrawal-related affect (negative affect) [51,70–72]. In the present study, we show that during the CLE-VFT, red light caused higher oxygenation in the left PFC compared to the right. The left relative to right frontal cortical activation during the red light might be attributed to greater positive affect, according to the approach-withdrawal model. Interestingly, we also found that the number of excellent performers during the red light exposure was remarkably higher than the number of moderate performers. In other words, red light led to better performance of subjects in the VFT, which showed its impact on leftward prefrontal lateralization. Our finding (that there is a positive correlation between the number of excellent performers and relative leftward PFC activity) is in accordance with previous research [42] which concluded that

during the VFT, subjects with excellent task performance showed a left-dominated dorsolateral frontal asymmetry, while moderate performers showed a right-dominated frontopolar asymmetry [42]. Moreover, slightly better VFT performance with red as compared to blue light exposure is in line with many color and colored light studies which have proposed that red improves task performance in comparison with other colors [73–77]. In particular, red enhances the performance for "overlearned motor", "proofreading", "target shooting", and "basic strength" tasks [76,78–80]. It has been demonstrated that red facilitates performance on detail-oriented tasks that require concentration and careful attention, while blue improves performance on creative tasks [80,81]. It was also presented that a low-demand task worsens performance in blue rather than red environments [75]. Beyond task type, other factors, including the subject's emotional state, subject's personality, subject's color preferences, and the subject's culture, may also influence cognitive performance. For example, better performances in color conditions lead to higher arousal [82]. In another study, the impact of color depended on personality [83]. For example, high screeners, i.e., people who have a natural tendency to effectively reduce the complexity of an environment, performed better in a red-painted office, whereas low screeners benefited from blue-green office spaces [83].

4.2. Other Patterns As the Typical Hemodynamic Response Pattern were Observed in Half of the Subjects

We selected [O_2Hb] as a marker to classify subjects into different groups. Compared to [HHb], this parameter is a more sensitive marker of cerebral blood flow (CBF) changes [49,84]. Besides, it has an acceptable high reproducibility, as well as a higher signal-to-noise ratio in comparison with the [HHb] signal [49,85,86].

Cognitive activation normally leads to an increase in [O_2Hb] and a decrease in [HHb], which is known as a typical hemodynamic response pattern. Despite this typical pattern normally observed at the group level, our subgroup analysis showed that this pattern was found in approximately 50% of cases (blue: 14 out of 25 cases, 56%; red: 12 out of 26 cases, 46%). The remaining subjects showed different cortical activation patterns. In total, five and seven different hemodynamic response patterns were detected in the subgroup analysis of the blue and red light exposure, respectively. We already reported in another study that the blue light exposure, without any cognitive test, led to 8 different hemodynamic response patterns (n = 32, age: 23.8 ± 2.2, 15 min blue light exposure at 120 lux illuminance) [47]. A possible explanation for the lower number of classified groups in this experiment (compared to the previous research [47]) could be that in this study, it is very likely that the attention of the subjects was mainly focused on the VFT and the stimulating impact of CLE decreases when the brain is already involved in a challenging VFT condition. Therefore, the more prominent impact of VFT compared to CLE caused less variety of hemodynamic response patterns.

We also found that an increase and a decrease in [O_2Hb] at the PFC and VC, respectively, was the second most common pattern during blue light, which is interestingly in line with our previous study [47]. Sakatani et al. also observed three different patterns of fNIRS parameter changes during a mental stress task [87]. They found that the frequency of the typical cortical activation response in a younger group (n = 24, age: 21.3 ± 0.9, 80% of subjects) was noticeably higher than in an older group (n = 11, age: 56.9 ± 4.2, 55% of subjects). Moreover, Quaresima and Ferrari reported that the typical hemodynamic response to the VFT was observed in only 4 out of 8 cases [45]. Consequently, based on the results of this research and the above-mentioned studies, it is clear that in spite of the typical cortical activation response (normally observed at the group-level), not all subjects react the same, and atypical changes in fNIRS signals can also be detected. One possible explanation for intersubject-variability of the responses is the fact that the environment and certain situational variables may influence cortical activation response. The dependence of cerebral parameters on several factors, including seasonal changes, time of day, temperature, mood, and chronotype, was investigated in detail in our recent paper [51]. Briefly, we showed that absolute values of StO_2 during the resting state were not correlated

with season and subjects' mood, but with the time of day and subjects chronotype [51]. Furthermore, we observed that frontal cerebral oxygenation asymmetry was correlated with the season and room temperature, but not dependent on subjects chronotype [51]. For this study, it was tried to keep all the experimental conditions constant. For example, two factors, including the date and time of participation, were precisely controlled for each subject's two participations. In terms of lighting conditions, all subjects experienced the same situation at least one h before the measurement. All measurements were also carried out in a time period from late August to early September, and the room temperature was almost constant (range: 22.4 °C to 22.9 °C). Therefore, in the current study, it seems that situational variables had minimal effects on the intersubject-variability of cerebral hemodynamic responses. However, atypical cortical activation responses can be triggered by diverse neuroanatomy, partial volume effects, variations in CBF, and systemic physiology [47–49]. For an in-depth explanation of the reasons for atypical pattern occurrence, the readers are kindly directed to Holper et al. [46].

4.3. SpO_2 and MAP are Positively Correlated with [O_2Hb] at the PFC

Different physiological sources may cause false-positives and false-negatives in fNIRS signals [88]. The recorded physiological signals, thus, can be used to regress out the components of systemic physiological signals from the brain signals measured by fNIRS. These include changes in blood pressure parameters, $P_{ET}CO_2$, SpO_2, and activity of the sympathetic nervous system [50]. It is also known that the systemic parameters are interrelated with the metabolic changes in the brain [51–53], and atypical changes in fNIRS signals can be triggered by systemic physiological factors [50,88,89]. Therefore, it is essential to employ the SPA-fNIRS approach to ensure the correct interpretation of changes in cerebral hemodynamics and oxygenation.

Considering the first group (i.e., the most common pattern) for both light colors (blue and red), we found color-dependent changes in HR, i.e., an increase during blue and no change during red. Although not all subjects showed an increase in HR during blue light, the increase found in most cases may be associated with the autonomous nervous system responding to light with an increase in sympathetic tone (short-wavelength light) [90]. Besides, independent of the color type and classification of the subjects, a decrease in $P_{ET}CO_2$ and an increase in SCL were observed for all groups, which once again shows that the effects of VFT on these two physiological signals were more dominant than the CLE effects. The decline in $P_{ET}CO_2$ during the CLE-VFT is in line with the research that the effect of different speech tasks on $P_{ET}CO_2$ was studied [91]. The lower CO_2 pressure is most likely attributed to the changes in breathing (hyperventilation) during the VFT. The increase in SCL can also be caused by various factors, namely, stress, which can be triggered by challenging VFT.

We found that SpO_2 was positively correlated with [O_2Hb] at the PFC independent of color type and classification of the subjects. Although several studies demonstrated a significant positive correlation between SpO_2 and cerebral (or somatic) tissue oxygen saturation [92–96], it is to the best of our knowledge that this is the first study showing a positive correlation between SpO_2 and [O_2Hb] at the PFC during a functional paradigm. [O_2Hb], measured by fNIRS, mainly reflects O_2Hb in small arteries, capillaries, and veins in brain tissue [97]. Lindauer et al. stated that variations in SpO_2, as well as other factors, including changes in CBF, intracranial pressure, and systemic pressure, may be the reasons for atypical cortical activation responses [48]. The MAP may also be accounted as a biomarker describing the [O_2Hb] changes at the PFC (positively correlated with [O_2Hb] at the PFC). This should be interpreted with care, since there is one exception for group 5 of the blue light (Figure 2), where [O_2Hb] was constant and MAP increased significantly. This can be attributed to the small number of subjects allocated to this group of blue light exposure. A large number of subjects may have revealed a correlation between MAP and [O_2Hb] in this group. MAP is an important parameter used to avoid false-positive results and to identify real cerebral hemodynamics and oxygenation changes [88]. A correlation between

MAP and [O_2Hb] (or StO_2) has been reported in various functional studies [89,98,99]. Tsubaki et al. investigated the relationships between NIRS signals and MAP during exercises on a bicycle ergometer [100]. They found highly significant correlations between MAP and [O_2Hb] during warm-up and at workloads corresponding to 30 and 50% of peak oxygen consumption [100]. In another recent study, in contrast, a non-significant association between StO_2 and MAP was observed in critically ill adults [101].

Considering the fifth group of both conditions, there were color-dependent changes in HR and RR during the CLE-VFT. HR and RR increased and decreased, respectively, during the blue light, while both were constant during the red light. It has been reported elsewhere that colored light had no effects on RR [102,103]. Because of the large intersubject variation caused by subjects having different RR, this parameter should always be interpreted with caution. We also found that the blue light exposure evoked a significant increase in the PRQ compared to red light in the fifth group of both conditions. This can be explained mostly by an increase in HR (or decrease in RR). The PRQ is a useful and unitless parameter to attain the overall state of human physiology [54]. No statistically significant changes in the PRQ in response to the CLE were observed at the group level of the study conducted by Edelhäuser et al. [102]. However, in a study of short-term CLE conducted by our group, blue light exposure caused a decrease in the PRQ [53].

In general, there are three possible explanations for the observed correlation between fNIRS signals, namely, [O_2Hb], and systemic physiology, such as SpO_2 and MAP. (i) The fNIRS signals of the brain are caused by changes in systemic physiology. (ii) The systemic physiological changes are caused by brain activity. (iii) The fNIRS signals reflect indeed NVC only, and the correlation we found between [O_2Hb] and systemic physiology has no causal relation.

One possibility for the first explanation is the fact that low-frequency changes (e.g., Mayer waves and task-evoked changes, due to systemic physiological activity) were not removed by the filtering, and hence, they are visible in both the systemic and cerebral variables. Although it is often assumed that fNIRS purely detects the cerebral-evoked-neural response in the brain, in reality, each fNIRS signal contains different components [88]. Still, in our opinion, the appropriate explanation relies probably on a mixture of the three above-mentioned effects, i.e., there is a complex interrelation of systemic physiology and brain activity. In our data, this is visible by—on the one hand—a slightly greater change in the VC compared to the PFC, indicating that fNIRS detects brain activity. On the other hand, the correlations between fNIRS and systemic physiological signals indicate that the fNRIS signals are also influenced by systemic changes.

4.4. How does [O_2Hb] Behave During Continuous Long-Term Stimulation?

Further investigating long-term colored light exposure is a crucial strategy needed to study and understand human physiology, especially in our modern society, when we are extensively exposed to different colored light. So far, few studies have investigated how brain activity changes during continuous long-term colored light stimulation [104,105]. It was shown that there is a habituation effect in the brain's activity, and this *habituation* is reflected as decreased oxygenation during the visual stimulation [106,107]. On the other hand, oxygenation may remain elevated (*plateau*) during long visual stimulation, decreasing only when the flow rate decreases, attributing to neuronal habituation effects [108]. One study using fNIRS also indicated that during continuous visual stimulation, [O_2Hb] increased during the first 19 s of stimulation and reached a *plateau*, and remained constantly elevated during the entire 5 min of the activation period [109]. In our study, both above-mentioned effects are visible, but they apply to different groups of subjects. For example, in the first group, during the blue CLE-VFT, the [O_2Hb] at both cortices decreased, therefore, indicating *habituation*. In the third group, during the same condition, [O_2Hb] reached a *plateau* during the CLE-VFT and even remained elevated at the beginning of the recovery phase. Similar trends are also visible during red CLE in group 1. The MAP shows similar trends during blue CLE, i.e., *habituation* in group1 and a *plateau* in group 3. Interestingly, $P_{ET}CO_2$ shows a decrease (away from baseline) in group 1 during blue

CLE, while it remains mostly unchanged in group 3. This may indicate that the *habituation* seen in group 1 is merely due to a CO_2 response. Thus, our study found changes in systemic physiology that impact the fNIRS signals and strongly enhance the understanding of changes in cerebral hemodynamics and oxygenation. Moreover, it is difficult to provide a concrete interpretation of previous fNIRS studies carried out without measurements of systemic physiology. Therefore, it is our opinion that measurements of systemic physiology along with cerebral hemodynamics are essential and should be carefully considered when performing neuroimaging studies.

5. Conclusions

We found that red light exposure led to better performance of subjects taking the VFT, while simultaneously showing a physiological response of higher oxygenation in the left PFC than the right.

Furthermore, we demonstrated that stimulus-evoked changes in cerebral hemodynamics, oxygenation, and systemic physiological activity generally show large intersubject variability. This means that each subject displayed individual responses to the experimental paradigm. A group-level analysis, although commonly used, only reveals the most prominent tendency between subjects: It is unable to account for the individual variability and consequently impedes a comprehensive and correct conclusion. Therefore, the subgroup or subject-specific analysis is needed to completely understand the effects of a CLE-VFT. Despite the typical hemodynamic response pattern (increase in [O_2Hb] and decrease in [HHb]) normally observed at the group level, the subgroup analysis showed that this pattern was found in only ~50% of the cases and the number of these typical hemodynamic response patterns was different between the red and blue light exposure. Our systemic physiology augmented fNIRS (SPA-fNIRS) approach enabled us to determine that SpO_2 and MAP correlate with the changes in [O_2Hb] at the PFC during the CLE-VFT, i.e., that systemic and cerebral physiology interact. This shows the importance of assessing systemic physiology in addition to neuroimaging to enable a comprehensive understanding of changes in cerebral hemodynamics and oxygenation. It also demonstrates that individuals respond differently to colored light not only on the cerebral, but also on the systemic level. This individual variability needs to be taken into account, in particular, when considering the influence of colored light on daily human life, e.g., at the workplace or in public places.

Author Contributions: U.W., H.Z., and F.S. designed the study. H.Z. performed data processing and data visualization. H.Z., F.S., and UW contributed to data analysis and interpretation. H.Z., F.S. and U.W. wrote the first draft of the manuscript. F.S. and U.W. All authors have read and agreed to the published version of the manuscript.

Funding: The financial support of the Software AG Foundation (grant no P12117) and the Christophorus Foundation (grant no 253CST, 355CST) is gratefully acknowledged.

Institutional Review Board Statement: The study was conducted in accordance with the World Medical Association Declaration of Helsinki, and the protocol was approved by the Ethics Committee of the Canton of Bern (Project identifier: COLOR10; Basec-Nr. 2016-00674)

Informed Consent Statement: Written informed consent was obtained prior to the measurements.

Data Availability Statement: The data that support the findings of this study are available from the corresponding author upon reasonable request.

Acknowledgments: We thank our students for their contribution to the measurements and our subjects for participating in this study. We also thank Oliver Kress, for his valuable comments and proofreading of the manuscript.

Conflicts of Interest: The authors declare no potential conflicts of interest with respect to the research, authorship, and/or publication of this article.

References

1. Vandewalle, G.; Maquet, P.; Dijk, D.J. Light as a modulator of cognitive brain function. *Trends Cogn. Sci.* **2009**, *13*, 429–438. [CrossRef] [PubMed]
2. Prayag, A.; Münch, M.; Aeschbach, D.; Chellappa, S.; Gronfier, C. Light Modulation of Human Clocks, Wake, and Sleep. *Clocks Sleep* **2019**, *1*, 193–208. [CrossRef] [PubMed]
3. Provencio, I.; Jiang, G.; Willem, J.; Hayes, W.P.; Rollag, M.D. Melanopsin: An opsin in melanophores, brain, and eye. *Proc. Natl. Acad. Sci. USA* **1998**, *95*, 340–345. [CrossRef] [PubMed]
4. Provencio, I.; Rodriguez, I.R.; Jiang, G.; Hayes, W.P.; Moreira, E.F.; Rollag, M.D. A novel human opsin in the inner retina. *J. Neurosci.* **2000**, *20*, 600–605. [CrossRef]
5. Bailes, H.J.; Lucas, R.J. Human melanopsin forms a pigment maximally sensitive to blue light (λmax ≈ 479 nm) supporting activation of Gq/11 and Gi/o signalling cascades. *Proc. R. Soc. B Biol. Sci.* **2013**, *280*, 20122987. [CrossRef]
6. Salari, V.; Scholkmann, F.; Vimal, R.L.P.; Császár, N.; Aslani, M.; Bókkon, I. Phosphenes, retinal discrete dark noise, negative afterimages and retinogeniculate projections: A new explanatory framework based on endogenous ocular luminescence. *Prog. Retin. Eye Res.* **2017**, *60*, 101–119. [CrossRef]
7. Vandewalle, G.; Archer, S.N.; Wuillaume, C.; Balteau, E.; Degueldre, C.; Luxen, A.; Dijk, D.-J.; Maquet, P. Effects of light on cognitive brain responses depend on circadian phase and sleep homeostasis. *J. Biol. Rhythm.* **2011**, *26*, 249–259. [CrossRef]
8. Vandewalle, G.; Schwartz, S.; Grandjean, D.; Wuillaume, C.; Balteau, E.; Degueldre, C.; Schabus, M.; Phillips, C.; Luxen, A.; Dijk, D.J.; et al. Spectral quality of light modulates emotional brain responses in humans. *Proc. Natl. Acad. Sci. USA* **2010**, *107*, 19549–19554. [CrossRef]
9. An, M.; Huang, J.; Shimomura, Y.; Katsuura, T. Time-of-day-dependent Effects of Monochromatic Light Exposure on Human Cognitive Function. *J. Physiol. Anthropol.* **2009**, *28*, 217–223. [CrossRef]
10. Katsuura, T.; Yasuda, T.; Shimomura, Y.; Iwanaga, K. Effects of monochromatic light on time sense for short intervals. *J. Physiol. Anthropol.* **2007**, *26*, 95–100. [CrossRef]
11. Killgore, W.D.S.; Dailey, N.S.; Raikes, A.C.; Vanuk, J.R.; Taylor, E.; Alkozei, A. Blue light exposure enhances neural efficiency of the task positive network during a cognitive interference task. *Neurosci. Lett.* **2020**, *735*, 135242. [CrossRef] [PubMed]
12. Yang, W.; Jeon, J.Y. Effects of correlated colour temperature of LED light on visual sensation, perception, and cognitive performance in a classroom lighting environment. *Sustainability* **2020**, *12*, 4051. [CrossRef]
13. Hartstein, L.E.; Durniak, M.T.; Karlicek, R.F.; Berthier, N.E. A comparison of the effects of correlated colour temperature and gender on cognitive task performance. *Light. Res. Technol.* **2018**, *50*, 1057–1069. [CrossRef]
14. Chellappa, S.L.; Steiner, R.; Blattner, P.; Oelhafen, P.; Götz, T.; Cajochen, C. Non-visual effects of light on melatonin, alertness and cognitive performance: Can blue-enriched light keep us alert? *PLoS ONE* **2011**, *6*, e16429. [CrossRef] [PubMed]
15. Huiberts, L.M.; Smolders, K.C.H.J.; de Kort, Y.A.W. Shining light on memory: Effects of bright light on working memory performance. *Behav. Brain Res.* **2015**, *294*, 234–245. [CrossRef] [PubMed]
16. Rautkylä, E.; Puolakka, M.; Tetri, E.; Halonen, L. Effects of correlated colour temperature and timing of light exposure on daytime alertness in lecture environments. *J. Light Vis. Environ.* **2010**, *34*, 59–68. [CrossRef]
17. Amunts, J.; Camilleri, J.A.; Eickhoff, S.B.; Heim, S.; Weis, S. Executive functions predict verbal fluency scores in healthy participants. *Sci. Rep.* **2020**, *10*, 1–11. [CrossRef] [PubMed]
18. Holmlund, T.B.; Cheng, J.; Foltz, P.W.; Cohen, A.S.; Elvevåg, B. Updating verbal fluency analysis for the 21st century: Applications for psychiatry. *Psychiatry Res.* **2019**, *273*, 767–769. [CrossRef] [PubMed]
19. McDonnell, M.; Dill, L.; Panos, S.; Amano, S.; Brown, W.; Giurgius, S.; Small, G.; Miller, K. Verbal fluency as a screening tool for mild cognitive impairment. *Int. Psychogeriatr.* **2020**, *32*, 1055–1062. [CrossRef]
20. Sokołowski, A.; Tyburski, E.; Sołtys, A.; Karabanowicz, E. Sex Differences in Verbal Fluency among Young Adults. *Adv. Cogn. Psychol.* **2020**, *16*, 92–102. [CrossRef]
21. Shao, Z.; Janse, E.; Visser, K.; Meyer, A.S. What do verbal fluency tasks measure? Predictors of verbal fluency performance in older adults. *Front. Psychol.* **2014**, *5*, 772. [CrossRef] [PubMed]
22. Udina, C.; Avtzi, S.; Durduran, T.; Holtzer, R.; Rosso, A.L.; Castellano-Tejedor, C.; Perez, L.M.; Soto-Bagaria, L.; Inzitari, M. Functional Near-Infrared Spectroscopy to Study Cerebral Hemodynamics in Older Adults During Cognitive and Motor Tasks: A Review. *Front. Aging Neurosci.* **2020**, *11*, 367. [CrossRef] [PubMed]
23. Bonetti, L.V.; Hassan, S.A.; Lau, S.T.; Melo, L.T.; Tanaka, T.; Patterson, K.K.; Reid, W.D. Oxyhemoglobin changes in the prefrontal cortex in response to cognitive tasks: A systematic review. *Int. J. Neurosci.* **2019**, *129*, 195–203. [CrossRef] [PubMed]
24. Husain, S.F.; Tang, T.B.; Yu, R.; Tam, W.W.; Tran, B.; Quek, T.T.; Hwang, S.H.; Chang, C.W.; Ho, C.S.; Ho, R.C. Cortical haemodynamic response measured by functional near infrared spectroscopy during a verbal fluency task in patients with major depression and borderline personality disorder. *EBioMedicine* **2020**, *51*, 102586. [CrossRef] [PubMed]
25. Onishi, A.; Furutani, H.; Hiroyasu, T.; Hiwa, S. An fNIRS study of brain state during letter and category fluency tasks. *J. Robot. Netw. Artif. Life* **2019**, *5*, 228–231. [CrossRef]
26. Schecklmann, M.; Ehlis, A.C.; Plichta, M.M.; Romanos, J.; Heine, M.; Boreatti-Hümmer, A.; Jacob, C.; Fallgatter, A.J. Diminished prefrontal oxygenation with normal and above-average verbal fluency performance in adult ADHD. *J. Psychiatr. Res.* **2009**, *43*, 98–106. [CrossRef]

27. Tupak, S.V.; Badewien, M.; Dresler, T.; Hahn, T.; Ernst, L.H.; Herrmann, M.J.; Fallgatter, A.J.; Ehlis, A.C. Differential prefrontal and frontotemporal oxygenation patterns during phonemic and semantic verbal fluency. *Neuropsychologia* **2012**, *50*, 1565–1569. [CrossRef]
28. Matsuo, K.; Watanabe, A.; Onodera, Y.; Kato, N.; Kato, T. Prefrontal hemodynamic response to verbal-fluency task and hyperventilation in bipolar disorder measured by multi-channel near-infrared spectroscopy. *J. Affect. Disord.* **2004**, *82*, 85–92. [CrossRef]
29. Takahashi, T.; Takikawa, Y.; Kawagoe, R.; Shibuya, S.; Iwano, T.; Kitazawa, S. Influence of skin blood flow on near-infrared spectroscopy signals measured on the forehead during a verbal fluency task. *Neuroimage* **2011**, *57*, 991–1002. [CrossRef]
30. Hock, C.; Villringer, K.; Muller-Spahn, F.; Wenzel, R.; Heekeren, H.; Schuh-Hofer, S.; Hofmann, M.; Minoshima, S.; Schwaiger, M.; Dirnagl, U.; et al. Decrease in parietal cerebral hemoglobin oxygenation during performance of a verbal fluency task in patients with Alzheimer's disease monitored by means of near-infrared spectroscopy NIRS—Correlation with simultaneous rCBF-PET measurements. *Brain Res.* **1997**, *755*, 293–303. [CrossRef]
31. Tsujii, T.; Masuda, S.; Yamamoto, E.; Ohira, T.; Akiyama, T.; Takahashi, T.; Watanabe, S. Effects of sedative and nonsedative antihistamines on prefrontal activity during verbal fluency task in young children: A near-infrared spectroscopy (NIRS) study. *Psychopharmacology* **2009**, *207*, 127–132. [CrossRef]
32. Scholkmann, F.; Kleiser, S.; Metz, A.J.; Zimmermann, R.; Mata Pavia, J.; Wolf, U.; Wolf, M. A review on continuous wave functional near-infrared spectroscopy and imaging instrumentation and methodology. *Neuroimage* **2014**, *85*, 6–27. [CrossRef] [PubMed]
33. Pinti, P.; Tachtsidis, I.; Hamilton, A.; Hirsch, J.; Aichelburg, C.; Gilbert, S.; Burgess, P.W. The present and future use of functional near-infrared spectroscopy (fNIRS) for cognitive neuroscience. *Ann. N. Y. Acad. Sci.* **2020**, *1464*, 5. [CrossRef] [PubMed]
34. Herold, F.; Gronwald, T.; Scholkmann, F.; Zohdi, H.; Wyser, D.; Müller, N.G.; Hamacher, D. New Directions in Exercise Prescription: Is There a Role for Brain-Derived Parameters Obtained by Functional Near-Infrared Spectroscopy? *Brain Sci.* **2020**, *10*, 342. [CrossRef] [PubMed]
35. Scholkmann, F.; Klein, S.D.; Gerber, U.; Wolf, M.; Wolf, U. Cerebral hemodynamic and oxygenation changes induced by inner and heard speech: A study combining functional near-infrared spectroscopy and capnography. *J. Biomed. Opt.* **2014**, *19*, 017002. [CrossRef]
36. Thranitz, J.; Knauth, M.; Heldmann, M.; Küchler, J.; Münte, T.F.; Royl, G. Elevation of intracranial pressure affects the relationship between hemoglobin concentration and neuronal activation in human somatosensory cortex. *Hum. Brain Mapp.* **2020**, *41*, 2702–2716. [CrossRef]
37. Schecklmann, M.; Ehlis, A.C.; Plichta, M.M.; Fallgatter, A.J. Functional near-infrared spectroscopy: A long-term reliable tool for measuring brain activity during verbal fluency. *Neuroimage* **2008**, *43*, 147–155. [CrossRef]
38. Herrmann, M.J.; Ehlis, A.C.; Fallgatter, A.J. Frontal activation during a verbal-fluency task as measured by near-infrared spectroscopy. *Brain Res. Bull.* **2003**, *61*, 51–56. [CrossRef]
39. Kameyama, M.; Fukuda, M.; Uehara, T.; Mikuni, M. Sex and age dependencies of cerebral blood volume changes during cognitive activation: A multichannel near-infrared spectroscopy study. *Neuroimage* **2004**, *22*, 1715–1721. [CrossRef]
40. Watanabe, A.; Matsuo, K.; Kato, N.; Kato, T. Cerebrovascular Response to Cognitive Tasks and Hyperventilation Measured by Multi-Channel Near-Infrared Spectroscopy. *J. Neuropsychiatry Clin. Neurosci.* **2003**, *15*, 442–449. [CrossRef]
41. Heinzel, S.; Metzger, F.G.; Ehlis, A.C.; Korell, R.; Alboji, A.; Haeussinger, F.B.; Hagen, K.; Maetzler, W.; Eschweiler, G.W.; Berg, D.; et al. Aging-related cortical reorganization of verbal fluency processing: A functional near-infrared spectroscopy study. *Neurobiol. Aging* **2013**, *34*, 439–450. [CrossRef] [PubMed]
42. Papousek, I.; Schulter, G. Manipulation of frontal brain asymmetry by cognitive tasks. *Brain Cogn.* **2004**, *54*, 43–51. [CrossRef]
43. Herrmann, M.J.; Walter, A.; Ehlis, A.C.; Fallgatter, A.J. Cerebral oxygenation changes in the prefrontal cortex: Effects of age and gender. *Neurobiol. Aging* **2006**, *27*, 888–894. [CrossRef] [PubMed]
44. Holper, L.; Aleksandrowicz, A.; Müller, M.; Ajdacic-Gross, V.; Haker, H.; Fallgatter, A.J.; Hagenmuller, F.; Rössler, W.; Kawohl, W. Brain correlates of verbal fluency in subthreshold psychosis assessed by functional near-infrared spectroscopy. *Schizophr. Res.* **2015**, *168*, 23–29. [CrossRef] [PubMed]
45. Quaresima, V.; Ferrari, M.; Torricelli, A.; Spinelli, L.; Pifferi, A.; Cubeddu, R. Bilateral prefrontal cortex oxygenation responses to a verbal fluency task: A multichannel time-resolved near-infrared topography study. *J. Biomed. Opt.* **2005**, *10*, 011012. [CrossRef]
46. Holper, L.; Shalóm, D.E.; Wolf, M.; Sigman, M. Understanding inverse oxygenation responses during motor imagery: A functional near-infrared spectroscopy study. *Eur. J. Neurosci.* **2011**, *33*, 2318–2328. [CrossRef]
47. Zohdi, H.; Scholkmann, F.; Wolf, U. Long-Term Blue Light Exposure Changes Frontal and Occipital Cerebral Hemodynamics: Not all Subjects React the Same. *Adv. Exp. Med. Biol.* **2021**, *1269*.
48. Lindauer, U.; Dirnagl, U.; Füchtemeier, M.; Böttiger, C.; Offenhauser, N.; Leithner, C.; Royl, G. Pathophysiological interference with neurovascular coupling—When imaging based on hemoglobin might go blind. *Front. Neuroenerg.* **2010**, *2*, 25. [CrossRef]
49. Herold, F.; Wiegel, P.; Scholkmann, F.; Müller, N. Applications of Functional Near-Infrared Spectroscopy (fNIRS) Neuroimaging in Exercise–Cognition Science: A Systematic, Methodology-Focused Review. *J. Clin. Med.* **2018**, *7*, 466. [CrossRef]
50. Zimeo Morais, G.A.; Scholkmann, F.; Balardin, J.B.; Furucho, R.A.; de Paula, R.C.V.; Biazoli, C.E.; Sato, J.R. Non-neuronal evoked and spontaneous hemodynamic changes in the anterior temporal region of the human head may lead to misinterpretations of functional near-infrared spectroscopy signals. *Neurophotonics* **2017**, *5*, 011002. [CrossRef]

51. Zohdi, H.; Scholkmann, F.; Wolf, U. Frontal cerebral oxygenation asymmetry: Intersubject variability and dependence on systemic physiology, season, and time of day. *Neurophotonics* **2020**, *7*, 025006. [CrossRef] [PubMed]
52. Nasseri, N.; Caicedo, A.; Scholkmann, F.; Zohdi, H.; Wolf, U. Impact of Changes in Systemic Physiology on fNIRS/NIRS Signals: Analysis Based on Oblique Subspace Projections Decomposition. *Adv. Exp. Med. Biol.* **2018**, *1072*, 119–125. [PubMed]
53. Scholkmann, F.; Hafner, T.; Metz, A.J.; Wolf, M.; Wolf, U. Effect of short-term colored-light exposure on cerebral hemodynamics and oxygenation, and systemic physiological activity. *Neurophotonics* **2017**, *4*, 045005. [CrossRef] [PubMed]
54. Scholkmann, F.; Wolf, U. The Pulse-Respiration Quotient: A Powerful but Untapped Parameter for Modern Studies about Human Physiology and Pathophysiology. *Front. Physiol.* **2019**, *10*, 1–18. [CrossRef]
55. Scholkmann, F.; Zohdi, H.; Wolf, U. The resting-state pulse-respiration quotient of humans: Lognormally distributed and centred around a value of four. *Physiol. Res.* **2019**, *68*, 1027–1032. [CrossRef]
56. Jasper, H.H. The ten-twenty electrode system of the International Federation. *Electroencephalogr. Clin. Neurophysiol.* **1958**, *10*, 370–375.
57. Fantini, S.; Sassaroli, A. Frequency-Domain Techniques for Cerebral and Functional Near-Infrared Spectroscopy. *Front. Neurosci.* **2020**, *14*, 300. [CrossRef]
58. Scholkmann, F.; Spichtig, S.; Muehlemann, T.; Wolf, M. How to detect and reduce movement artifacts in near-infrared imaging using moving standard deviation and spline interpolation. *Physiol. Meas.* **2010**, *31*, 649–662. [CrossRef]
59. Metz, A.J.; Klein, S.D.; Scholkmann, F.; Wolf, U. Physiological Effects of Continuous Colored Light Exposure on Mayer Wave Activity in Cerebral Hemodynamics: A Functional Near-Infrared Spectroscopy (fNIRS) Study. In *Oxygen Transport to Tissue XXXIX*; Springer: Berlin/Heidelberg, Germany, 2017; pp. 277–283.
60. Metz, A.J.; Klein, S.D.; Scholkmann, F.; Wolf, U. Continuous coloured light altered human brain haemodynamics and oxygenation assessed by systemic physiology augmented functional near-infrared spectroscopy. *Sci. Rep.* **2017**, *7*, 10027. [CrossRef]
61. Jahani, S.; Setarehdan, S.K.; Boas, D.A.; Yücel, M.A. Motion artifact detection and correction in functional near-infrared spectroscopy: A new hybrid method based on spline interpolation method and Savitzky–Golay filtering. *Neurophotonics* **2018**, *5*, 015003. [CrossRef]
62. Pinti, P.; Scholkmann, F.; Hamilton, A.; Burgess, P.; Tachtsidis, I. Current Status and Issues Regarding Pre-processing of fNIRS Neuroimaging Data: An Investigation of Diverse Signal Filtering Methods within a General Linear Model Framework. *Front. Hum. Neurosci.* **2019**, *12*, 505. [CrossRef] [PubMed]
63. Chen, W.L.; Wagner, J.; Heugel, N.; Sugar, J.; Lee, Y.W.; Conant, L.; Malloy, M.; Heffernan, J.; Quirk, B.; Zinos, A.; et al. Functional Near-Infrared Spectroscopy and Its Clinical Application in the Field of Neuroscience: Advances and Future Directions. *Front. Neurosci.* **2020**, *14*, 724. [CrossRef]
64. Franceschini, M.A.; Fantini, S.; Paunescu, L.A.; Maier, J.S.; Gratton, E. Influence of a superficial layer in the quantitative Spectroscopic Study of Strongly Scattering Media. *Appl. Opt.* **1998**, *37*, 7447–7458. [CrossRef] [PubMed]
65. Benedek, M.; Kaernbach, C. Decomposition of skin conductance data by means of nonnegative deconvolution. *Psychophysiology* **2010**, *47*, 647–658. [CrossRef] [PubMed]
66. Benedek, M.; Kaernbach, C. A continuous measure of phasic electrodermal activity. *J. Neurosci. Methods* **2010**, *190*, 80–91. [CrossRef]
67. Bryden, M.P. *Laterality Functional Asymmetry in the Intact Brain*; Elsevier: Amsterdam, The Netherlands, 2012.
68. Ocklenburg, S.; Güntürkün, O. *The Lateralized Brain: The Neuroscience and Evolution of Hemispheric Asymmetries*; Academic Press: Cambridge, MA, USA, 2017.
69. Güntürkün, O.; Ströckens, F.; Ocklenburg, S. Brain lateralization: A comparative perspective. *Physiol. Rev.* **2020**, *100*, 1019–1063. [CrossRef]
70. Gable, P.A.; Neal, L.B.; Threadgill, A.H. Regulatory behavior and frontal activity: Considering the role of revised-BIS in relative right frontal asymmetry. *Psychophysiology* **2018**, *55*, e12910. [CrossRef]
71. Reznik, S.J.; Allen, J.J.B. Frontal asymmetry as a mediator and moderator of emotion: An updated review. *Psychophysiology* **2018**, *55*, e12965. [CrossRef]
72. Allen, J.J.B.; Keune, P.M.; Schönenberg, M.; Nusslock, R. Frontal EEG alpha asymmetry and emotion: From neural underpinnings and methodological considerations to psychopathology and social cognition. *Psychophysiology* **2018**, *55*, e13028. [CrossRef]
73. Kwallek, N.; Lewis, C.M. Effects of environmental colour on males and females: A red or white or green office. *Appl. Ergon.* **1990**, *21*, 275–278. [CrossRef]
74. Kwallek, N.; Lewis, C.M.; Lin-Hsiao, J.W.D.; Woodson, H. Effects of nine monochromatic office interior colors on clerical tasks and worker mood. *Color Res. Appl.* **1996**, *21*, 448–458. [CrossRef]
75. Stone, N.J. Environmental view and color for a stimulated telemarketing task. *J. Environ. Psychol.* **2003**, *23*, 63–78. [CrossRef]
76. Elliot, A.J.; Aarts, H. Perception of the color red enhances the force and velocity of motor output. *Emotion* **2011**, *11*, 445–449. [CrossRef] [PubMed]
77. Von Castell, C.; Stelzmann, D.; Oberfeld, D.; Welsch, R.; Hecht, H. Cognitive performance and emotion are indifferent to ambient color. *Color Res. Appl.* **2018**, *43*, 65–74. [CrossRef]
78. Elliot, A.J.; Maier, M.A. Color Psychology: Effects of Perceiving Color on Psychological Functioning in Humans. *Annu. Rev. Psychol.* **2014**, *65*, 95–120. [CrossRef] [PubMed]
79. Küller, R.; Mikellides, B.; Janssens, J. Color, arousal, and performance—A comparison of three experiments. *Color Res. Appl.* **2009**, *34*, 141–152. [CrossRef]

80. Larionescu, V.M.; Pantelimona, M. The influence of colour on the efficiency of basketball throws. *Ann. "Dunarea Jos" Univ. Galati. Fascicle XV, Phys. Educ. Sport Manag.* **2012**, *1*, 82–86.
81. Mehta, R.; Zhu, R.J. Blue or red? Exploring the effect of color on cognitive task performances. *Science (80-)* **2009**, *323*, 1226–1229. [CrossRef]
82. Al-Ayash, A.; Kane, R.T.; Smith, D.; Green-Armytage, P. The influence of color on student emotion, heart rate, and performance in learning environments. *Color Res. Appl.* **2016**, *41*, 196–205. [CrossRef]
83. Kwallek, N.; Woodson, H.; Lewis, C.M.; Sales, C. Impact of three interior color schemes on worker mood and performance relative to individual environmental sensitivity. *Color Res. Appl.* **1997**, *22*, 121–132. [CrossRef]
84. Hoshi, Y. Functional near-infrared optical imaging: Utility and limitations in human brain mapping. *Psychophysiology* **2003**, *40*, 511–520. [CrossRef] [PubMed]
85. Strangman, G.; Culver, J.P.; Thompson, J.H.; Boas, D.A. A quantitative comparison of simultaneous BOLD fMRI and NIRS recordings during functional brain activation. *Neuroimage* **2002**, *17*, 719–731. [CrossRef] [PubMed]
86. Kumar, V.; Shivakumar, V.; Chhabra, H.; Bose, A.; Venkatasubramanian, G.; Gangadhar, B.N. Functional near infra-red spectroscopy (fNIRS) in schizophrenia: A review. *Asian J. Psychiatr.* **2017**, *27*, 18–31. [CrossRef] [PubMed]
87. Sakatani, K.; Tanida, M.; Katsuyama, M. Effects of Aging on Activity of the Prefrontal Cortex and Autonomic Nervous System during Mental Stress Task. *Adv. Exp. Med. Biol.* **2010**, *662*, 473–478. [PubMed]
88. Tachtsidis, I.; Scholkmann, F. False positives and false negatives in functional near-infrared spectroscopy: Issues, challenges, and the way forward. *Neurophotonics* **2016**, *3*, 031405. [CrossRef]
89. Caldwell, M.; Scholkmann, F.; Wolf, U.; Wolf, M.; Elwell, C.; Tachtsidis, I. Modelling confounding effects from extracerebral contamination and systemic factors on functional near-infrared spectroscopy. *Neuroimage* **2016**, *143*, 91–105. [CrossRef]
90. Cajochen, C.; Münch, M.; Kobialka, S.; Kräuchi, K.; Steiner, R.; Oelhafen, P.; Orgül, S.; Wirz-Justice, A. High Sensitivity of Human Melatonin, Alertness, Thermoregulation, and Heart Rate to Short Wavelength Light. *J. Clin. Endocrinol. Metab.* **2005**, *90*, 1311–1316. [CrossRef]
91. Scholkmann, F.; Gerber, U.; Wolf, M.; Wolf, U. End-tidal CO2: An important parameter for a correct interpretation in functional brain studies using speech tasks. *Neuroimage* **2013**, *66*, 71–79. [CrossRef]
92. Hueber, D.M.; Franceschini, M.A.; Ma, H.Y.; Zhang, Q.; Ballesteros, J.R.; Fantini, S.; Wallace, D.; Ntziachristos, V.; Chance, B. Non-invasive and quantitative near-infrared haemoglobin spectrometry in the piglet brain during hypoxic stress, using a frequency-domain multidistance instrument. *Phys. Med. Biol.* **2001**, *46*, 41–62. [CrossRef]
93. Weiss, M.; Dullenkopf, A.; Kolarova, A.; Schulz, G.; Frey, B.; Baenziger, O. Near-infrared spectroscopic cerebral oxygenation reading in neonates and infants is associated with central venous oxygen saturation. *Paediatr. Anaesth.* **2005**, *15*, 102–109. [CrossRef]
94. Li, T.; Duan, M.; Li, K.; Yu, G.; Ruan, Z. Bedside monitoring of patients with shock using a portable spatially-resolved near-infrared spectroscopy. *Biomed. Opt. Express* **2015**, *6*, 3431–3436. [CrossRef]
95. Benni, P.B.; MacLeod, D.; Ikeda, K.; Lin, H.M. A validation method for near-infrared spectroscopy based tissue oximeters for cerebral and somatic tissue oxygen saturation measurements. *J. Clin. Monit. Comput.* **2018**, *32*, 269–284. [CrossRef] [PubMed]
96. Ottestad, W.; Kåsin, J.I.; Høiseth, L.Ø. Arterial oxygen saturation, pulse oximetry, and cerebral and tissue oximetry in hypobaric hypoxia. *Aerosp. Med. Hum. Perform.* **2018**, *89*, 1045–1049. [CrossRef]
97. Scheeren, T.W.L.; Schober, P.; Schwarte, L.A. Monitoring tissue oxygenation by near infrared spectroscopy (NIRS): Background and current applications. *J. Clin. Monit. Comput.* **2012**, *26*, 279–287. [CrossRef]
98. Harms, M.P.M.; Colier, W.N.J.M.; Wieling, W.; Lenders, J.W.M.; Secher, N.H.; Lieshout, J.J. Van Orthostatic Tolerance, Cerebral Oxygenation, and Blood Velocity in Humans with Sympathetic Failure. *Stroke* **2000**, *31*, 1608–1614. [CrossRef]
99. Tisdall, M.M.; Taylor, C.; Tachtsidis, I.; Leung, T.S.; Elwell, C.E.; Smith, M. The effect on cerebral tissue oxygenation index of changes in the concentrations of inspired oxygen and end-tidal carbon dioxide in healthy adult volunteers. *Anesth. Analg.* **2009**, *109*, 906–913. [CrossRef] [PubMed]
100. Tsubaki, A.; Takai, H.; Oyanagi, K.; Kojima, S.; Tokunaga, Y.; Miyaguchi, S.; Sugawara, K.; Sato, D.; Tamaki, H.; Onishi, H. Correlation Between the Cerebral Oxyhaemoglobin Signal and Physiological Signals During Cycling Exercise: A Near- Infrared Spectroscopy Study. *Oxyg. Transp. to Tissue XXXVIII* **2016**, 159–166.
101. Wood, M.D.; Jacobson, J.A.; Maslove, D.M.; Muscedere, J.G.; Boyd, J.G. The physiological determinants of near-infrared spectroscopy-derived regional cerebral oxygenation in critically ill adults. *Intensive Care Med. Exp.* **2019**, *7*, 23. [CrossRef]
102. Edelhäuser, F.; Hak, F.; Kleinrath, U.; Lühr, B.; Matthiessen, P.F.; Weinzirl, J.; Cysarz, D. Impact of colored light on cardiorespiratory coordination. *Evid.-Based Complement. Altern. Med.* **2013**, *2013*, 7. [CrossRef]
103. Jacobs, K.W.; Hustmyer, F.E., Jr. Effects of four psychological primary colors on GSR, heart rate and respiration rate. *Percept. Mot. Skills* **1974**, *38*, 763–766. [CrossRef]
104. Krueger, G.; Granziera, C. The history and role of long duration stimulation in fMRI. *Neuroimage* **2012**, *62*, 1051–1055. [CrossRef]
105. Bandettini, P.A. Twenty years of functional MRI: The science and the stories. *Neuroimage* **2012**, *62*, 575–588. [CrossRef]
106. Krüger, G.; Kleinschmidt, A.; Frahm, J. Dynamic MRI sensitized to cerebral blood oxygenation and flow during sustained activation of human visual cortex. *Magn. Reson. Med.* **1996**, *35*, 797–800. [CrossRef]

107. Obrig, H.; Israel, H.; Kohl-Bareis, M.; Uludag, K.; Wenzel, R.; Müller, B.; Arnold, G.; Villringer, A. Habituation of the visually evoked potential and its vascular response: Implications for neurovascular coupling in the healthy adult. *Neuroimage* **2002**, *17*, 1–18. [CrossRef]
108. Bandettini, P.A.; Kwong, K.K.; Davis, T.L.; Tootell, R.B.H.; Wong, E.C.; Fox, P.T.; Belliveau, J.W.; Weisskoff, R.M.; Rosen, B.R. Characterization of cerebral blood oxygenation and flow changes during prolonged brain activation. *Hum. Brain Mapp.* **1997**, *5*, 93–109. [CrossRef]
109. Heekeren, H.R.; Obrig, H.; Wenzel, R.; Eberle, K.; Ruben, J.; Villringer, K.; Kurth, R.; Villringer, A. Cerebral haemoglobin oxygenation during sustained visual stimulation—A near-infrared spectroscopy study. *Philos. Trans. R. Soc. B Biol. Sci.* **1997**, *352*, 743–750. [CrossRef]

Chapter 7
Discussion

In this thesis, the effects of colored light on cerebral and human physiology were investigated with the SPA-fNIRS approach. First, the SPA-fNIRS was explained in more detail, and the PRQ was introduced as one of the systemic physiological parameters investigated in this research. Second, the impact of CLE on changes in optical properties was presented. Finally, effects of light of different colors and intensities as well as a mixed effect of CLE and VFT were shown. The aim of this chapter is to briefly discuss the hypotheses raised in the first chapter of this PhD thesis.

Realizing hypothesis 1: Colored light evokes an activation of the VC, which is independent of the color

This hypothesis was raised based on fMRI studies showing that different CLE have similar responses in the VC [36]. However, this was not found in our research. We demonstrated that long-term colored light exposures induce wavelength-dependent modulations of brain responses in the VC. Violet and blue lights elicit higher changes in cerebral parameters compared to the other colored lights during the CLE and recovery phase. The stronger response of the visual system to blue and violet light might be a marker for central nervous system dopamine tone [77]. It was also proposed that colors in different categories are differently represented in the VC. Wavelength information is carried by the parvocellular afferent system, which projects to the cytochrome oxidase-rich blobs of area V1. V1 blobs project to the thin strips of area V2 providing the wavelength selective input to area V4, located in the fusiform gyrus, as a vital site for color perception in the human brain [38,78]. In an fMRI study, color-dependent activation peaks were also found in spatially organized maps in the V2 area [37]. Since the spatial sensitivity of our fNIRS is 2-3 cm, this method is not able to reflect activation within a specific area but rather the whole VC activity. One possible explanation for wavelength-dependent cerebral changes in the VC may be associated with the role of Müller cells through the retina. These cells can be

considered as an integral part of the first step in the visual process and act as optical fibers, transferring light illuminating the retinal surface onto the cone photoreceptors [79]. Müller cells, known as wavelength-dependent wave-guides, concentrate the green-red part of the visible spectrum onto cones and the blue-violet part onto nearby rods [79,80]. It was also reported that light of short wavelengths is not captured in the straight guide, and most of the total power in these wavelengths leaks out to the surrounding high-sensitivity rods, most sensitive to short wavelengths [80].

Realizing hypothesis 2: Colored light evokes an activation of the PFC, which is dependent on the color

In this research, we found that yellow light causes higher brain activation in the PFC than the other colored lights. The finding of a higher brain activation due to the yellow light is in line with our previous research [63]. It is known that the hemodynamic response in the PFC is modulated by the emotional status. Al-Ayash et al. indicated that yellow elicited more active emotions and caused positive effects on motivation, as well as intellectual and physical activities [68]. Therefore, it seems that the yellow-colored light at low intensity influenced our subjects positively, and this impact was detectable by higher changes in hemodynamic responses and oxygenation compared to other colored lights. It was also reported by the subjects of the previous studies that yellow reminds them of the sun and summer; it reflects light and makes them happy, cheerful, active, and awake [68,81,82]. Color perception may produce physiological responses in the human body that become noticeable in humans' emotions and cognitive focus. Yellow was also postulated to be stimulating, to encourage an outward focus, and to produce forceful action [83].

Realizing hypothesis 3: Colored light has intensity-dependent effects

Although there were specific intensity-dependent effects for different colors and parameters, they appeared in such a way that it was not possible to discern an explicit order between different colors for any parameters in this study. Therefore, it is difficult to draw a firm conclusion about the effects of intensity on

cerebral and physiological parameters. Using higher brightness conditions (> 500 lux) instead of 120 lux may have elicited more pronounced and distinct physiological and cerebral intensity-dependent responses.

Realizing hypothesis 4: Colored light affects individual humans differently

Performing both a group-average analysis and a subgroup (subject-specific) analysis was one of the main goals of this research. This is vital to completely understand the effects of exposure to colored light in humans. Our findings in most parts of this research display that CLE affects individual humans differently. This should be taken into account when considering the impact of colored light on society. Such a different reaction of subjects to CLE was found in optical properties as well as hemodynamic responses, which is partially explained by systemic physiological changes.

Realizing hypothesis 5: Colored light has relatively long-lasting effects

Compared to the CLE, color-dependent changes are more evident in the recovery phase of most cerebral and physiological parameters. In other words, more significant differences can be found in the recovery phase in comparison with the CLE, which reiterated the point of the CLE having long-lasting effects in humans [84,85]. Alkozei et al. demonstrated that a relatively brief CLE has an enhancing effect on brain function that may persist for at least 40 minutes after cessation of the light [84]. This prolonged effect may be associated with sustained noradrenergic activation. They found that blue light exposure continues to affect brain functioning as well as optimizing neurocognitive performance after cessation of longer periods of exposure [84,85]. The relatively long-lasting effects of CLE highlights the importance of considering the persistent influence of colored light on brain function, cognition, and systemic physiology in everyday life.

Moreover, long-term stimulations have rarely been performed in functional neuroimaging studies [86,87]. Therefore, our studies are important, especially in terms of long-term changes in cerebral variables. Depending on each individual subject, we showed that habituation (decreased oxygenation during the visual

stimulation) or plateau (oxygenation remains elevated during the visual stimulation) effects are observed in cerebral parameters, namely [O_2Hb], which is partially explained by subject-specific systemic physiological changes [64]. Therefore, to identify and understand these impacts, it is strongly recommended to measure systemic physiology together with cerebral hemodynamics when performing fNIRS or even fMRI long-term studies.

Realizing hypothesis 6: The interaction of cerebral and systemic physiology is distinguished by the SPA-fNIRS approach

The SPA-fNIRS approach is able to show that systemic and cerebral physiology interact. Experimental findings in most parts of this research exhibit correlation between cerebral parameters and systemic physiology. The most relevant systemic physiological parameters that contributed to changes in the fNIRS signals are MAP, SpO_2, and $P_{ET}CO_2$. Such a correlation can be clarified by three possible explanations. (i) Changes in fNIRS signals are caused by changes in systemic physiology. (ii) Changes in systemic physiological parameters are caused by brain activity. (iii) fNIRS signals reflect neurovascular coupling only, and the correlation has no causal relation. Although it is often assumed that fNIRS purely detects the cerebral-evoked-neural response in the brain, in reality, each fNIRS signal contains different components. Thus, in our opinion, the appropriate explanation relies most probably on a mixture of the three above mentioned effects, i.e. there is a complex interaction of systemic physiology and brain activity.

Chapter 8
Conclusion

First and foremost, a group-level analysis along with an individual-level analysis are needed to completely understand the impacts of CLE in humans. Although a group-level analysis is commonly used in research, it is not enough for an inclusive and accurate conclusion. Therefore, using an individual-level (subject-specific) analysis is highly recommended for reliable interpretation of the effects of CLE in humans. In this research, it has been found that CLE affects individual humans differently. The individual-level analysis revealed that, in most cases, subjects have different reactions to the CLE. Among all subjects, i.e., 201 healthy adults, who participated in this research, it is almost impossible to find two matched subjects having the same reaction to the CLE in terms of cerebral and systemic physiological changes. The variety of CLE effects was even more noticeable in systemic physiological parameters compared to cerebral variables. Specifically, it is not easy to draw general conclusions about the effects of the light of different colors on systemic physiological changes during the CLE at the group-level. In contrast, the color-dependent changes are more evident in the recovery phase of most systemic physiological parameters reiterating the point of the CLE having long-lasting effects in humans. Such long-lasting effects, as well as color-dependent differences during the CLE, are also observed in cerebral variables of the VC and the PFC. Regardless of the impact of a cognitive task, blue light exposure leads to stronger effects in the VC compared to colors associated with longer wavelengths. This effect was proven in both studies with and without a VFT. The finding of this research that blue light has an activating effect in the VC should be taken into consideration when assessing the impact of modern light sources such as screens (e.g., smartphones and computers) and LEDs on the human body. Moreover, we showed that CLE (namely, yellow) affects the PFC. It is also known that the hemodynamic response in the PFC represents the emotional status and mood. Therefore, colored light affects the emotional status. Our findings that CLE leads to a PFC activation, i.e., yellow light causes a higher PFC activation, may be applied in complementary medicine, i.e., specifically

chromotherapy (color therapy), to create a balance and restore the health in emotional, mental, or even physical levels. Especially at present, when people are generally experiencing challenging times along with anxiety, depression, and nervousness due to the Covid-19 pandemic, yellow light can be applied as a healing tool to boost positive feelings like hope, daring, happiness, and optimism. Although CLE (e.g., yellow light) may generally influence humans in a number of beneficial ways, individuals may reacts differently to the CLE. Therefore, further research should clarify which color in CLE benefits whom.

Additionally, our findings of a mixed-effect of CLE and VFT on human physiology offer a broad range of implications for educational purposes. These days, students are exposed to a considerable amount of artificial light by using smartphones and tablets in order to do their homework. Although it may not be possible to improve their performance by selecting an optimal desktop background, it is possible to modify their systemic physiology in positive or negative ways based on the findings of this research.

It was also found that the SPA-fNIRS approach is ideally suited to enable a better understanding and a reliable interpretation of the changes in the fNIRS signals. This approach enabled us to show that systemic and cerebral physiology interact. In this research, we showed that the inter-subject variability of hemodynamic responses is partially explained by systemic physiological changes. Therefore, it is strongly recommended to measure systemic physiology together with cerebral hemodynamics when performing fNIRS studies. This enables to identify, remove and understand the effects of systemic physiological changes on fNIRS signals.

Finally, in the society that is rapidly exposed to new and increasing lighting, the findings of this research are relevant and beneficial for the scientific community, medical professionals, and society.

Chapter 9
Outlook

Based on the presented results, many objectives of this research were fulfilled in this dissertation. Looking to the future, there are a number of topics that should be addressed to further advance the understanding of CLE's effects on the human body and human's reactions:

- Since specific intensity-dependent effects and explicit order between different colors were merely seen in this study for all parameters, using higher brightness conditions (> 500 lux) instead of 120 lux may lead to more pronounced and distinct physiological and cerebral intensity-dependent responses.
- In this research, VFT was selected as a cognitive task, and its effects along with the CLE were studied on several parameters. Depending on the nature of the task, different colored lights might affect cognitive tasks differently. It has been revealed that red improves performance on a detailed-oriented task, while blue enhances performance on a creative task [69]. Therefore, it would be worthwhile to include other cognitive tasks in future studies.
- It would be worthwhile to also include white light exposure in different phases of measurement, for example, during the baseline phase.
- Since it has been reported by invasive methods that parietal regions of the human brain, i.e. an occipito-parietal attention network, are also involved in light processing [88], measuring the entire head non-invasively with SPA-fNIRS would be a next step.
- This research could be extended to other populations, including neonates, children, elderly subjects, and, ultimately, patients. This would allow a comparison of the results of this research with different groups of subjects.
- Since each individual reacts differently to the CLE, it would be worthwhile to generate an algorithm, which enables us to understand

how each individual responds to the CLE based on all cerebral and systemic physiological changes. Such an algorithm would enable to detect what benefits whom and thus be definitely beneficial for society and could also be used in personalized medicine. Using machine learning with informative and independent features would be the first and crucial step for an effective algorithm to classify patients into different groups. Based on that classification, patients who belong to a specific group would receive a specified treatment.

References

1. Scholkmann, F.; Hafner, T.; Metz, A.J.; Wolf, M.; Wolf, U. Effect of short-term colored-light exposure on cerebral hemodynamics and oxygenation, and systemic physiological activity. *Neurophotonics* **2017**, *4*, 045005.

2. Provencio, I.; Jiang, G.; Willem, J.; Hayes, W.P.; Rollag, M.D. Melanopsin: An opsin in melanophores, brain, and eye. *Proc. Natl. Acad. Sci.* **1998**, *95*, 340–345.

3. Provencio, I.; Rodriguez, I.R.; Jiang, G.; Hayes, W.P.; Moreira, E.F.; Rollag, M.D. A novel human opsin in the inner retina. *J. Neurosci.* **2000**, *20*, 600–605.

4. Erren, T.C.; Reiter, R.J. Light Hygiene: Time to make preventive use of insights - old and new - into the nexus of the drug light, melatonin, clocks, chronodisruption and public health. *Med. Hypotheses* **2009**, *73*, 537–541.

5. Emens, J.S.; Burgess, H.J. Effect of light and melatonin and other melatonin receptor agonists on human circadian physiology. *Sleep Med. Clin.* **2015**, *10*, 435–453.

6. Gaggioni, G.; Maquet, P.; Schmidt, C.; Dijk, D.-J.; Vandewalle, G. Neuroimaging, cognition, light and circadian rhythms. *Front. Syst. Neurosci.* **2014**, *8*.

7. Vandewalle, G.; Maquet, P.; Dijk, D.J. Light as a modulator of cognitive brain function. *Trends Cogn. Sci.* **2009**, *13*, 429–438.

8. Cajochen, C. Alerting effects of light. *Sleep Med. Rev.* **2007**, *11*, 453–464.

9. Van Bommel, W.J.M. Non-visual biological effect of lighting and the practical meaning for lighting for work. *Appl. Ergon.* **2006**, *37*, 461–466.

10. Bromundt, V.; Wirz-Justice, A.; Kyburz, S.; Opwis, K.; Dammann, G.; Cajochen, C. Circadian Sleep-Wake Cycles, Well-Being, and Light Therapy

in Borderline Personality Disorder. *J. Pers. Disord.* **2012**, *27*, 680–696.

11. Glickman, G.; Byrne, B.; Pineda, C.; Hauck, W.W.; Brainard, G.C. Light therapy for seasonal affective disorder with blue narrow-band light-emitting diodes (LEDs). *Biol. Psychiatry* **2006**, *59*, 502–507.

12. Even, C.; Schröder, C.M.; Friedman, S.; Rouillon, F. Efficacy of light therapy in nonseasonal depression: A systematic review. *J. Affect. Disord.* **2008**, *108*, 11–23.

13. Wirz-Justice, A.; Bader, A.; Frisch, U.; Stieglitz, R.D.; Alder, J.; Bitzer, J.; Hösli, I.; Jazbec, S.; Benedetti, F.; Terman, M.; et al. A randomized, double-blind, placebo-controlled study of light therapy for antepartum depression. *J. Clin. Psychiatry* **2011**, *72*, 986–993.

14. Strong, R.E.; Marchant, B.K.; Reimherr, F.W.; Williams, E.; Soni, P.; Mestas, R. Narrow-band blue-light treatment of seasonal affective disorder in adults and the influence of additional nonseasonal symptoms. *Depress. Anxiety* **2009**, *26*, 273–278.

15. Chellappa, S.; Gordijn, M.; Cajochen, C. Can light make us bright? Effects of light on cognition and sleep. In *Human Sleep and Cognition, Part II: Clinical and Applied Research*; 2011; Vol. 190, pp. 119–133.

16. Revell, V.L.; Skene, D.J. Impact of age on human non-visual responses to light. *Sleep Biol. Rhythms* **2010**, *8*, 84–94.

17. Lockley, S.W. *Circadian rhythms: Influence of light in humans*; Academic Press Oxford, England, 2009; Vol. 2;.

18. Hanifin, J.P.; Brainard, G.C. Photoreception for circadian, neuroendocrine, and neurobehavioral regulation. *J. Physiol. Anthropol.* **2007**, *26*, 87–94.

19. Yasukouchi, A.; Ishibashi, K. Non-visual effects of the color temperature of fluorescent lamps on physiological aspects in humans. *J. Physiol. Anthropol. Appl. Human Sci.* **2005**, *24*, 41–43.

20. Duffy, J.F.; Czeisler, C.A. Effect of Light on Human Circadian Physiology. *Sleep Med. Clin.* **2009**, *4*, 165–177.

21. Cajochen, C.; Münch, M.; Kobialka, S.; Kräuchi, K.; Steiner, R.; Oelhafen, P.; Orgül, S.; Wirz-Justice, A. High Sensitivity of Human Melatonin, Alertness, Thermoregulation, and Heart Rate to Short Wavelength Light. *J. Clin. Endocrinol. Metab.* **2005**, *90*, 1311–1316.

22. Morita, T.; Teramoto, Y.; Tokura, H. Inhibitory Effect of Light of Different Wabelengths on the Fall of Core Temperature during the Nighttime. *Jpn. J. Physiol.* **1995**, *45*, 667–671.

23. Morita, T.; Tokura, H. Effects of lights of different color temperature on the nocturnal changes in core temperature and melatonin in humans. *Appl. Hum. Sci.* **1996**, *15*, 243–246.

24. Münch, M.; Kobialka, S.; Steiner, R.; Oelhafen, P.; Wirz-Justice, A.; Cajochen, C. Wavelength-dependent effects of evening light exposure on sleep architecture and sleep EEG power density in men. *Am. J. Physiol. Integr. Comp. Physiol.* **2006**, *290*, R1421–R1428.

25. Jacobs, K.W.; Hustmyer Jr, F.E. Effects of four psychological primary colors on GSR, heart rate and respiration rate. *Percept. Mot. Skills* **1974**, *38*, 763–766.

26. Abbas, N.; Kumar, D.; Mclachlan, N. The Psychological and Physiological Effects of Light and Colour on Space Users. In Proceedings of the 2005 IEEE Engineering in Medicine and Biology 27th Annual Conference; 2005; pp. 1228–1231.

27. Laufer, L.; Láng, E.; Izsó, L.; Németh, E. Psychophysiological effects of coloured lighting on older adults. *Light. Res. Technol.* **2009**, *41*, 371–378.

28. Xia, Y.; Shimomura, Y.; Katsuura, T. Comparison of the Effects of Wavelength and Intensity of Monochromatic Light on Cardiovascular Responses during Task and in Recovery Periods. *J. Human-Environment*

Syst. **2012**, *14*, 41–48.

29. Edelhäuser, F.; Hak, F.; Kleinrath, U.; Lühr, B.; Matthiessen, P.F.; Weinzirl, J.; Cysarz, D. Impact of colored light on cardiorespiratory coordination. *Evidence-Based Complement. Altern. Med.* **2013**, *2013*, 7 pages.

30. Morita, T.; Tokura, H.; Wakamura, T.; Park, S.-J.; Teramoto, Y. Effects of the morning irradiation of light with different wavelengths on the behavior of core temperature and melatonin in humans. *Appl. Hum. Sci.* **1997**, *16*, 103–105.

31. Schäfer, A.; Kratky, K.W. The effect of colored illumination on heart rate variability. *Complement. Med. Res.* **2006**, *13*, 167–173.

32. Litscher, D.; Wang, L.; Gaischek, I.; Litscher, G. The influence of new colored light stimulation methods on heart rate variability, temperature, and well-being: results of a pilot study in humans. *Evidence-Based Complement. Altern. Med.* **2013**, *2013*, Article ID 674183, 7 pages.

33. Moharreri, S.; Rezaei, S.; Dabanloo, N.J.; Parvaneh, S. Study of induced emotion by color stimuli: Power spectrum analysis of heart rate variability. In Proceedings of the Computing in Cardiology Conference (CinC), 2014; IEEE, 2014; pp. 977–980.

34. Ross, M.J.; Guthrie, P.; Dumont, J.C. The impact of modulated, colored light on the autonomic nervous system. *Adv. Mind. Body. Med.* **2013**, *27*, 7–16.

35. Küller, R.; Mikellides, B.; Janssens, J. Color, arousal, and performance—A comparison of three experiments. *Color Res. Appl.* **2009**, *34*, 141–152.

36. Parkes, L.M.; Marsman, J.B.C.; Oxley, D.C.; Goulermas, J.Y.; Wuerger, S.M. Multivoxel fMRI analysis of color tuning in human primary visual cortex. *J. Vis.* **2009**, *9*, 1–13.

37. Xiao, Y.; Wang, Y.; Felleman, D.J. A spatially organized representation of colour in macaque cotical area V2. *Nature* **2003**, *421*, 535–539.

38. Allison, T.; Begleiter, A.; McCarthy, G.; Roessler, E.; Nobre, A.C.; Spencer, D.D. Electrophysiological studies of color processing in human visual cortex. *Electroencephalogr. Clin. Neurophysiol. Evoked Potentials* **1993**, *88*, 343–355.

39. Vandewalle, G.; Collignon, O.; Hull, J.T.; Daneault, V.; Albouy, G.; Lepore, F.; Phillips, C.; Doyon, J.; Czeisler, C.A.; Dumont, M. Blue light stimulates cognitive brain activity in visually blind individuals. *J. Cogn. Neurosci.* **2013**, *25*, 2072–2085.

40. Lockley, S.W.; Gooley, J.J. Circadian photoreception: spotlight on the brain. *Curr. Biol.* **2006**, *16*, R795–R797.

41. Gilbert, C.D.; Li, W. Top-down influences on visual processing. *Nat. Rev. Neurosci.* **2013**, *14*, 350–363.

42. Yücel, M.A.; von Lühmann, A.; Scholkmann, F.; Gervain, J.; Dan, I.; Ayaz, H.; Boas, D.; Cooper, R.J.; Culver, J.; Elwell, C.E.; et al. Best Practices for fNIRS publications. *Neurophotonics* **2021**, *8*, 012101.

43. Herold, F.; Gronwald, T.; Scholkmann, F.; Zohdi, H.; Wyser, D.; Müller, N.G.; Hamacher, D. New Directions in Exercise Prescription : Is There a Role for Brain-Derived Parameters Obtained by Functional Near-Infrared Spectroscopy ? *Brain Sci.* **2020**, *10*, 342.

44. Scholkmann, F.; Kleiser, S.; Metz, A.J.; Zimmermann, R.; Mata Pavia, J.; Wolf, U.; Wolf, M. A review on continuous wave functional near-infrared spectroscopy and imaging instrumentation and methodology. *Neuroimage* **2014**, *85*, 6–27, DOI: http://dx.doi.org/10.1016/j.neuroimage.2013.05.004).

45. Pan, Y.; Borragán, G.; Peigneux, P. Applications of Functional Near-Infrared Spectroscopy in Fatigue, Sleep Deprivation, and Social Cognition. *Brain Topogr.* **2019**, *32*, 998–1012.

46. Herold, F.; Wiegel, P.; Scholkmann, F.; Müller, N. Applications of Functional Near-Infrared Spectroscopy (fNIRS) Neuroimaging in Exercise–Cognition

Science: A Systematic, Methodology-Focused Review. *J. Clin. Med.* **2018**, *7*, 466.

47. Almajidy, R.J.; Mankodiya, K.; Abtahi, M.; Hofmann, U. A Newcomer's Guide to Functional Near Infrared Spectroscopy Experiments. *IEEE Rev. Biomed. Eng.* **2019**.

48. Bale, G.; Tachtsidis, I. The Use of Near - Infrared Spectroscopy to Monitor Tissue Oxygenation , Metabolism and Injury in Low Resource Settings. *Revolutionizing Trop. Med. Point-of-Care Tests, New Imaging Technol. Digit. Heal.* **2019**, 344–359.

49. Ferrari, M.; Quaresima, V. A brief review on the history of human functional near-infrared spectroscopy (fNIRS) development and fields of application. *Neuroimage* **2012**, *63*, 921–935.

50. Boas, D.A.; Elwell, C.E.; Ferrari, M.; Taga, G. Twenty years of functional near-infrared spectroscopy: Introduction for the special issue. *Neuroimage* **2014**, *85*, 1–5.

51. Fantini, S.; Frederick, B.; Sassaroli, A. Perspective: Prospects of non-invasive sensing of the human brain with diffuse optical imaging. *APL Photonics* **2018**, *3*, 110901.

52. Pinti, P.; Tachtsidis, I.; Hamilton, A.; Hirsch, J.; Aichelburg, C.; Gilbert, S.; Burgess, P.W. The present and future use of functional near-infrared spectroscopy (fNIRS) for cognitive neuroscience. *Ann. N. Y. Acad. Sci.* **2020**, *1464*, 5.

53. Lloyd-Fox, S.; Blasi, A.; Elwell, C.E. Illuminating the developing brain: The past, present and future of functional near infrared spectroscopy. *Neurosci. Biobehav. Rev.* **2010**, *34*, 269–284.

54. Tachtsidis, I.; Scholkmann, F. False positives and false negatives in functional near-infrared spectroscopy: issues, challenges, and the way forward. *Neurophotonics* **2016**, *3*, 031405.

55. Lange, F.; Tachtsidis, I. Clinical Brain Monitoring with Time Domain NIRS: A Review and Future Perspectives. *Appl. Sci.* **2019**, *9*, 1612.

56. Zohdi, H.; Scholkmann, F.; Wolf, U. Frontal cerebral oxygenation asymmetry: Intersubject variability and dependence on systemic physiology, season, and time of day. *Neurophotonics* **2020**, *7*, 025006.

57. Zohdi, H.; Scholkmann, F.; Nasseri, N.; Wolf, U. Long-Term Changes in Optical Properties (μa , μ′s , μeff and DPF) of Human Head Tissue During Functional Neuroimaging Experiments. *Adv. Exp. Med. Biol.* **2018**, *1072*, 331–337.

58. Wang, H.; Xia, F.; Han, G.; Zhao, Z.; Chen, H.; Wang, J. Optical parameters detection with multi-frequency modulation based on NIR DPDW. *Infrared Phys. Technol.* **2019**, *97*, 135–141.

59. Fantini, S.; Sassaroli, A. Frequency-Domain Techniques for Cerebral and Functional Near-Infrared Spectroscopy. *Front. Neurosci.* **2020**, *14*, 300.

60. Chiarelli, A.M.; Maclin, E.L.; Low, K.A.; Fantini, S.; Fabiani, M.; Gratton, G. Low-resolution mapping of the effective attenuation coefficient of the human head: a multidistance approach applied to high-density optical recordings. *Neurophotonics* **2017**, *4*, 021103.

61. Sandell, J.L.; Zhu, T.C. A review of in-vivo optical properties of human tissues and its impact on PDT. *J. Biophotonics* **2011**, *4*, 773–787.

62. Scholkmann, F.; Gerber, U.; Wolf, M.; Wolf, U. End-tidal CO2: An important parameter for a correct interpretation in functional brain studies using speech tasks. *Neuroimage* **2013**, *66*, 71–79.

63. Metz, A.J.; Klein, S.D.; Scholkmann, F.; Wolf, U. Continuous coloured light altered human brain haemodynamics and oxygenation assessed by systemic physiology augmented functional near-infrared spectroscopy. *Sci. Rep.* **2017**, *7*, 10027.

64. Zohdi, H.; Scholkmann, F.; Wolf, U. Individual Differences in Hemodynamic Responses Measured on the Head Due to a Long-Term Stimulation Involving Colored Light Exposure and a Cognitive Task : A SPA-fNIRS Study. *Brain Sci.* **2021**, *11*, 54.

65. Scholkmann, F.; Klein, S.D.; Gerber, U.; Wolf, M.; Wolf, U. Cerebral hemodynamic and oxygenation changes induced by inner and heard speech: a study combining functional near-infrared spectroscopy and capnography. *J. Biomed. Opt.* **2014**, *19*, 017002.

66. Tachtsidis, I.; Leung, T.S.; Tisdall, M.M.; Devendra, P.; Smith, M.; Delpy, D.T.; Elwell, C.E. Investigation of frontal cortex, motor cortex and systemic haemodynamic changes during anagram solving. *Adv. Exp. Med. Biol.* **2008**, *614*, 21–28.

67. Caldwell, M.; Scholkmann, F.; Wolf, U.; Wolf, M.; Elwell, C.; Tachtsidis, I. Modelling confounding effects from extracerebral contamination and systemic factors on functional near-infrared spectroscopy. *Neuroimage* **2016**, *143*, 91–105.

68. Al-Ayash, A.; Kane, R.T.; Smith, D.; Green-Armytage, P. The influence of color on student emotion, heart rate, and performance in learning environments. *Color Res. Appl.* **2016**, *41*, 196–205.

69. Mehta, R.; Zhu, R.J. Blue or red? Exploring the effect of color on cognitive task performances. *Science (80-.).* **2009**, *323*, 1226–1229.

70. von Castell, C.; Stelzmann, D.; Oberfeld, D.; Welsch, R.; Hecht, H. Cognitive performance and emotion are indifferent to ambient color. *Color Res. Appl.* **2018**, *43*, 65–74.

71. Scholkmann, F.; Wolf, U. The Pulse-Respiration Quotient: A Powerful but Untapped Parameter for Modern Studies About Human Physiology and Pathophysiology. *Front. Physiol.* **2019**, *10*, 1–18.

72. von Bonin, D.; Grote, V.; Buri, C.; Cysarz, D.; Heusser, P.; Moser, M.; Wolf,

U.; Laederach, K. Adaption of cardio-respiratory balance during day-rest compared to deep sleep-An indicator for quality of life? *Psychiatry Res.* **2014**, *219*, 638–644.

73. Moser, M.; Voica, M.; Kenner, T.; Lehofer, M.; Egner, S.; Hildebrandt, G. Phase- and Frequency Coordination of Cardiac and Respiratory Function. *Biol. Rhythm Res.* **1995**, *26*, 100–111.

74. Jacques, S.L. Optical properties of biological tissues: a review. *Phys. Med. Biol.* **2013**, *58*, R37–R61.

75. Viola, A.U.; James, L.M.; Schlangen, L.J.M.; Dijk, D. Blue-enriched white light in the workplace improves self-reported alertness, performance and sleep quality. *Scand. J. Work. Environ. Health* **2008**, *34*, 297–306.

76. Tosini, G.; Ferguson, I.; Tsubota, K. Effects of blue light on the circadian system and eye physiology Gianluca. *Mol. Vis.* **2016**, *22*, 61–72.

77. Cowan, R.L.; Frederick, B.D.B.; Rainey, M.; Levin, J.M.; Maas, L.C.; Bang, J.; Hennen, J.; Lukas, S.E.; Renshaw, P.F. Sex differences in response to red and blue light in human primary visual cortex: a bold fMRI study. *Psychiatry Res. - Neuroimaging* **2000**, *100*, 129–138.

78. Lueck, C.J.; Zeki, S.; Friston, K.J.; Deiber, M.P.; Cope, P.; Cunningham, V.J.; Lammertsma, A.A.; Kennard, C.; Frackowiak, R.S.. The colour centre in the cerebral cortex of man. *Nature* **1989**, *340*, 386–389.

79. Labin, A.M.; Safuri, S.K.; Ribak, E.N.; Perlman, I. Müller cells separate between wavelengths to improve day vision with minimal effect upon night vision. *Nat. Commun.* **2014**, *5*, 1–9.

80. Labin, A.M.; Ribak, E.N. Color sorting by retinal waveguides. *Opt. Express* **2014**, *22*, 32208.

81. Clarke, T.; Costall, A. The emotional connotations of color: A qualitative investigation. *Color Res. Appl.* **2008**, *33*, 406–410.

82. Kwallek, N.; Lewis, C.M.; Lin-Hsiao, J.W.D.; Woodson, H. Effects of nine monochromatic office interior colors on clerical tasks and worker mood. *Color Res. Appl.* **1996**, *21*, 448–458.

83. Elliot, A.J.; Maier, M.A. Color Psychology: Effects of Perceiving Color on Psychological Functioning in Humans. *Annu. Rev. Psychol.* **2014**, *65*, 95–120.

84. Alkozei, A.; Smith, R.; Pisner, D.A.; Vanuk, J.R.; Berryhill, S.M.; Fridman, A.; Shane, B.R.; Knight, S.A.; Killgore, W.D.S. Exposure to Blue Light Increases Subsequent Functional Activation of the Prefrontal Cortex During Performance of a Working Memory Task. *Sleep* **2016**, *39*, 1671–1680.

85. Killgore, W.D.S.; Dailey, N.S.; Raikes, A.C.; Vanuk, J.R.; Taylor, E.; Alkozei, A. Blue light exposure enhances neural efficiency of the task positive network during a cognitive interference task. *Neurosci. Lett.* **2020**, *735*, 135242.

86. Krueger, G.; Granziera, C. The history and role of long duration stimulation in fMRI. *Neuroimage* **2012**, *62*, 1051–1055.

87. Bandettini, P.A. Twenty years of functional MRI: The science and the stories. *Neuroimage* **2012**, *62*, 575–588.

88. Perrin, F.; Peigneux, P.; Fuchs, S.; Verhaeghe, S.; Laureys, S.; Middleton, B.; Degueldre, C.; Del Fiore, G.; Vandewalle, G.; Balteau, E.; et al. Nonvisual responses to light exposure in the human brain during the circadian night. *Curr. Biol.* **2004**, *14*, 1842–1846.